Techniques in Broadband Interferometry

A Compilation of Patents 1997-2002

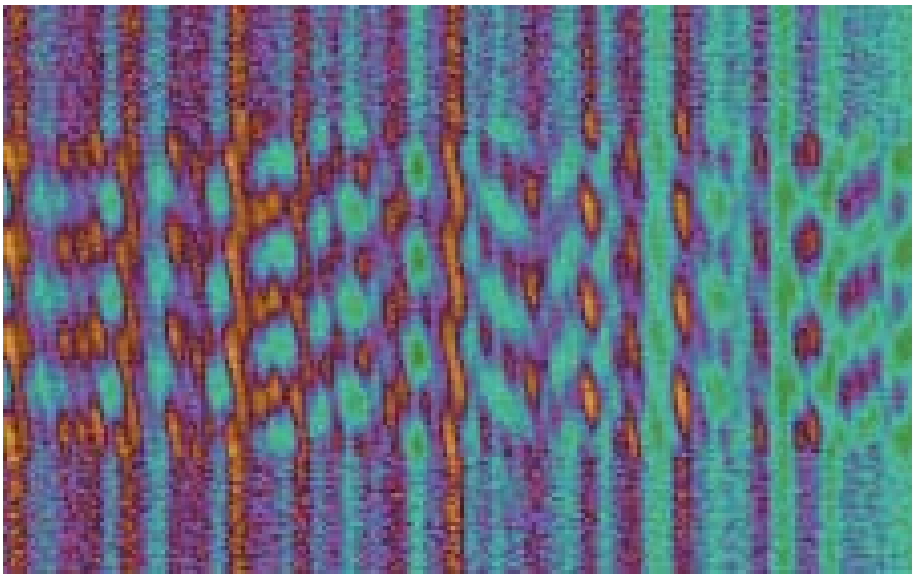

David J. Erskine

Lawrence Livermore National Laboratory

December 2003 UCRL-TR-201695

This work was performed under the auspices of the U.S. Department of Energy by University of California, Lawrence Livermore National Laboratory under Contract W-7405-Eng-48.

Contents

Contents in detail

Preface

This is a compilation of my patents issued from 1997 to 2002, generally describing interferometer techniques that modify the coherence properties of broad-bandwidth light and other waves, with applications to Doppler velocimetry, rangefinding, imaging and spectroscopy.

Patents are tedious to read in their original form. In effort to improve their readability I have embedded the Figures throughout the manuscript, put the Figure captions underneath the Figures, and added section headings. Otherwise I have resisted the temptation to modify the words, though I found many places which could use healthy editing. There may be minor differences with the official versions issued by the US Patent and Trademark Office, particularly in the claims sections.

David J. Erskine

Lawrence Livermore National Laboratory
December, 2003

erskine1@llnl.gov

Introduction

In my shock physics work I measured the velocities of targets impacted by flyer plates by illuminating them with laser light and analyzing the reflected light with an interferometer. Small wavelength changes caused by the target motion (Doppler effect) were converted into fringe shifts by the interferometer. Lasers having long coherence lengths were required for the illumination.

While lasers are certainly bright sources, and their collimated beams are convenient to work with, they are expensive. Particularly if one needs to illuminate a wide surface area, then large amounts of power are needed. Orders of magnitude more power per dollar can be obtained from a simple flashlamp, or for that matter, a 50 cent light bulb. Yet these inexpensive sources cannot practically be used for Doppler velocimetry because their coherence length is extremely short, i.e. their bandwidth is much too wide. Hence the motivation for patents **1** & **2** is a method (**White Light Velocimetry**) for allowing use of these powerful but incoherent lamps for interferometry. The coherence of the illumination is modified by passing it through a preparatory interferometer.

This method developed for light would also work for other wavelengths and kinds of waves– such as microwaves for radar and sound for sonar and medical imaging. In these applications the ability to measure distance, not only velocity, was important. In the prior art, measuring both simultaneously require two kinds of sources, velocity using a long coherence length source and range using very short coherence length source. That is, they could not be measured simultaneously with the same apparatus. Hence patent **3** explored methods of measuring range and Doppler velocity simultaneously with a single short coherence length source. The name "**Noise-Pair Radar**" refers to the use of incoherent illumination that is sent through a preparatory interferometer to generate an echo. Both the original signal and echo illuminate the target.

The above method requires construction of delay lines (i.e. interferometers) for microwave frequencies that are very long compared to the wavelength. To accomplish this with simple cables could be impractical, due large weight and cost. Patent **4** (**Multichannel Heterodyning**) solves this problem by subdividing the wide bandwidth of the signal into smaller chunks and lowering their frequencies through a heterodyning effect to a range where inexpensive electronics can delay them.

The White Light Velocimetry method also requires interferometers and delays lines that are long compared to the wavelength, but in the optical regime. Patent **5** (**Superimposing Interferometers**) describes methods of creating these interferometers. These work with the uncollimated beams characteristic of ordinary lamps, rather than the convenient pencil beams of lasers. The patent also describes several applications which can be done by combinations of interferometers, such as **encrypted communications** (page 5-29).

Excited about the news that astronomers could detect exoplanets by measuring Doppler shifts in white starlight, and having already measured similar magnitude velocities in white light interferometrically, I explored ways of helping their effort. Being an interferometer specialist, my approach was naturally biased toward interferometry rather than the purely dispersive spectrographs of the prior art. Since I had already explored the combination of dispersion with

interferometry in patent 1 (see Fig. 5, page 1-10), that became my approach. The difference was that for astronomical velocimetry the target was not actively illuminated but emitted its own light having identifiable spectral features. Hence the preparatory interferometer of Fig. 5 was eliminated. This led to patent **6**, called a variety of names including Fringing Spectroscopy, **Externally Dispersed Interferometry**, Spectral Interferometry, Dispersive/Interference Vector Spectroscopy.

Developing this technique led to ancillary applications. The ability to precisely measure a white light fringe shift– needed to measure small Doppler velocities– can also measure the angular position of a star, if the interferometer is modified to have two inputs separated by a baseline (**Spectral Astrometry**, page 6-17). The significant spectral dispersion allows a new ability not shared by the prior art– the ability to measure two or more stars simultaneously on the same detecting CCD chip. This allows for the first time differential angular measurements that are dramatically insensitive to drifts in the optical path length of the baseline. This solves a significant engineering problem of the prior art.

Another ancillary application is enabling the spectrograph to detect higher spectral resolution features than when used without the interferometer (spectral mapping or high resolution spectroscopy, page 6-19, also called **Resolution Boosting**). The moiré patterns created in the spectrum are numerically processed to recover high spectral details otherwise blurred by the spectrograph. Hence the interferometer can be added to an existing spectrograph system like "eyeglasses" to improve the system's performance at low cost.

Part 1
White Light Velocity Interferometer

US Patent 5,642,194
Issued June 24, 1997

David J. Erskine*
Lawrence Livermore Nat. Lab.

The invention is a technique that allows the use of unlimited bandwidth and extended illumination sources to measure small Doppler shifts of targets external to the apparatus. Monochromatic and point-like sources can also be used, thus creating complete flexibility for the illumination source. Although denoted white light velocimetry, the principle can be applied to any wave phenomenon, such as sound, microwaves and light. For the first time, powerful, compact or inexpensive broadband and extended sources can be used for velocity interferometry, including flash and arc lamps, light from detonations, pulsed lasers, chirped frequency lasers, and lasers operating simultaneously in several wavelengths. Superimposing interferometers are created which produce delays independent of ray angle for rays leaving a given pixel of an object, which can be imaged through the interferometer.

I. BACKGROUND OF THE INVENTION

A. Field of the Invention

The present invention relates to velocimetry, and more specifically, it relates to the use of a velocity interferometer capable of using unlimited bandwidth illumination.

B. Description of Related Art

Measuring the velocity of an object remotely through the Doppler shift of reflected wave radiation (electromagnetic waves, sound) is an important diagnostic tool in a variety of fields in science and engineering. In shock physics, velocity interferometry is an important optical technique measuring velocities of impacted targets, typically moving 1-10 km/s. In law enforcement and meteorology, other kinds of Doppler velocimeters using microwaves measure velocities of automobiles and raindrops. And in medicine using ultrasound, Doppler instruments detect the motion of blood in vivo. All these velocimeters require coherent quasi-monochromatic illumination, which is generally more expensive and lower power than broadband incoherent sources, for any kind of wave radiation. For example using light, for the single interferometer velocimeter, the illumination was previously restricted to lasers operating in a single longitudinal frequency mode, which reduces their power. For the double interferometer velocimeter (U. S. Patent No. 4,915,499), the illumination was restricted to less than 4 nm for typical laser illumination, and would be even less for an extended source. In comparison, visible light (red to blue) has a bandwidth of approximately 200 nm. (The limited bandwidth was calculated by the authors of that patent in an article "Multiple-line laser Doppler velocimetry" by S. Gidon and G. Behar, Applied Optics Vol. 27, p2315-2319, 1988, on page 2317, below Equation 11, and assumed a typical optical arrangement.)

The invention and the prior art velocimetry discussed here is characterized by a single illuminating beam striking the target. This is distinguished from another widely used velocimetry technique using two intersecting laser beams in a transparent fluid, in which scattering particles carried by the fluid pass through a standing wave grating created by the intersecting beams. That technique is commonly called LDV, for laser Doppler velocimetry. (The title is not helpful in distinguishing the different kinds of prior art, since they all are based on Doppler shifts and almost all on laser illumination.)

1. Superimposing interferometers

The prior art of velocity interferometry (single beam striking the target) can be classified into kinds using a single interferometer, or two interferometers before and after the target. The former is much more common. For use with light, single interferometer velocimeters are distinguished by the kind of interferometer. Those using monochromatic *superimposing* Michelson interferometers are called VISARs (velocity interferometer system for any reflector), and those using non-superimposing Fabry-Perot interferometers are called Fabry-Perot velocimeters. The latter are non-superimposing because of their design, (and their method of use depends on

*erskine1@llnl.gov

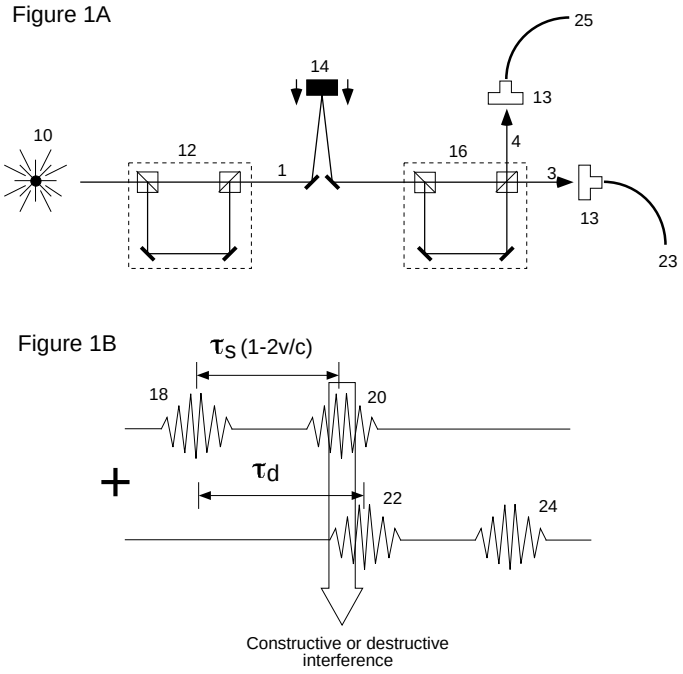

Figure 1A illustrates the white light velocimeter concept of the present invention. Figure 1B shows the waveform after the detecting interferometer when the source is a single wave packet.

the non-superimposing nature through the creation of off-axis fringes which shift in angle with velocity.) The definition of superimposing will be defined later. A double interferometer using two non-superimposing Fabry-Perot interferometers is described in U. S. Patent No. 4,915,499.

The prior art either uses single interferometers, or double interferometers lacking in the proper superimposing quality. The prior art did not recognize that in order to use unlimited bandwidth illumination from an extended source, two achromatic superimposing interferometers are needed, before and after the target. (The two can be optionally conveniently accomplished with one set of interferometer optics by retro-reflecting the light from the target.) Furthermore, the superimposing designs presented in the present invention are achromatic, whereas the prior art of single superimposing interferometers (VISARs) suffered chromatic aberrations which limit their use to monochromatic light.

The distinction between the superimposing quality of the present invention and the non-superimposing quality of the prior art is important to understand, and is crucial in creating many of the beneficial capabilities of this invention. The non-superimposing velocimeter cannot imprint a constant delay on all the light from a non-directional extended source, such as an incandescent lamp, due to the slight dependence of the delay on ray angle. Thus, it cannot form an imaging velocimeter having a constant imprinted delay across the image. For the non-superimposing interferometer, there is a tradeoff between maximum bandwidth and degree of parallelism of the source rays. This in turn prevents many desirable capabilities that come from a wide bandwidth, such as simultaneous multiple velocity detection, unambiguous velocity determination, independence from target and illumination color, and lack of speckle.

2. Velocity sensitivity

The velocity sensitivity of all the velocity interferometers discussed, single or dual interferometer, superimposing or non-superimposing, broad or narrowband, all have the same fundamental relationship between fringe phase shift for a specific color, and target velocity. This will be described now. The additional advantages that come with broadband illumination will be discussed later.

The single interferometer velocimeter consists of a monochromatic source illuminating the target, and an interferometer analyzing the reflected radiation. If the interferometer is a Michelson design, it has a fixed delay τ between its two arms. In the case of a Fabry-Perot interferometer, τ describes the delay between multiple output pulses produced from a single input pulse, if the illumination was considered hypothetically to be a stream of independent pulses. The nonzero value of the delay converts small Doppler shifts of the reflected light spectrum into fringe shifts in the interferometer output. Fringes denote the fluctuations in time-averaged output intensity that are not due to fluctuations in the input intensity. These can vary sinusoidally, or at least periodically, with target velocity v, wavelength λ and delay τ. There is a propor-

tionality η between the target velocity and fringe phase shift for a specific wavelength of illumination described by

$$\eta = \frac{\lambda}{2\tau} \tag{1}$$

and λ is the average wavelength of light. For example, to measure highway velocities in green light, η should be of the order 10 m/s, which requires $c\tau \approx 8$ m, where c is the speed of light. (Delays are conveniently described either by duration τ, or the distance light travels in that time $c\tau$.) Equation 1 neglects dispersion in the glass optics inside the interferometer, assumes $v/c \ll 1$ and that light reflects normally off the target.

If light does not reflect normally off the target, the velocity component being measured can always be defined as half the rate of change of the effective round trip path length from the source to the target to the detecting optics. The effective path length is the integral of the refractive index along the path. This definition accounts for any arrangement of source, target, target motion vector, detecting optics and changes in refractive index of the medium or target, and applies to all Doppler velocimeters.

The velocimeter can measure target displacement or velocity, depending on the time scale of the recording system. If the detector response time is very fast, faster than the interferometer delays, but still slower than a system coherence time Λ_{sys}/c, then the fringe shift $\Delta\phi$ is related to a displacement of the target during the interval τ according to

$$\Delta\phi = \frac{2d}{\lambda} \tag{2}$$

where d is component of the target motion toward the source and detecting interferometers. This is not the typical situation. Typically the detector or recording equipment response time is slower than the delay time τ. In this case, the fringe shift is related to velocity according to

$$\Delta\phi = \frac{2v\tau}{\lambda} \tag{3}$$

The velocity component of the target toward the velocimeter is obtained from the fringe phase shift $\Delta\phi$ by

$$v = \Delta\phi\ \eta = \frac{\lambda}{2\tau}\Delta\phi \tag{4}$$

3. Using sources with higher power

In previous velocimeters, the coherence length (Λ) of the illumination must be as large as $c\tau$ in order to produce fringes with significant visibility. This severely restricted the kind of light source which could be used. The Λ of white light ($\sim$1.5 μm) was insufficient. Previously, lasers were the only light sources used because their coherence length could be made sufficiently long when operated in a single frequency mode. However, in this mode the output power is low.

The low output power restricted the applications of optical velocimetry. Typical laboratory measurements in shock physics were limited to measurement of velocity at a single point on the target. These experiments, and many other laboratory and industrial applications can be greatly improved if sample velocity could be measured simultaneously at more than one point, such as over a line or an area. For example, to measure the velocity field over an area at a single moment in a wind tunnel, or to measure the complex motion of an exploding non-symmetrical object.

However, measuring velocity over a line or an area in a snap-shot requires orders of magnitude more power than what can be provided by single mode lasers. Amplifiers can be used to boost laser power, however, these are expensive and bulky. Furthermore, velocimetry of a remote object through a telescope in the field demands orders of magnitude more power, since reflected light intensity is weak. Previously, the velocity can be measured over an area by scanning a single point measuring beam. However, this is not appropriate for measuring complex dynamic events such as turbulence, which grow on a time scale faster than the scanning can be completed.

In contrast, the invention we describe can measure velocities simultaneously over an area, taking advantage of the velocimeter's imaging capability, and the higher power available from inexpensive and compact broadband extended sources. These sources are not suitable for a conventional velocity interferometer due to their non-parallel rays and broad bandwidth. Even the prior art double Fabry-Perot velocimeter can only use but a fraction of the available power because of the trade-off between maximum bandwidth and degree of parallelism. In contrast, the superimposing interferometers described in this application create a fringe phase which is constant over a range of ray angles.

For the purpose of illuminating a target over a wide area, the directional quality of a laser beam is not a comparative advantage, since the laser light must be dispersed to cover the area, and the target will usually randomly scatter the reflected light in all directions. For example, a $50,000 argon laser operating in single-frequency mode only produces approximately 1 watt of power. In contrast, a flashlamp costing a $1000 dollars can create perhaps a 100,000 watts. If the superimposing interferometers are achromatic and have a large numerical aperture capability, then a large fraction of the ray angles and colors of the flashlamp can be utilized for white light velocimetry. Thus, for illuminating an area, more illuminating power can be obtained from the flashlamp than the laser, and for less expense.

II. SUMMARY OF THE INVENTION

It is an object of the present invention to measure the velocity, or displacement during a short interval, of objects using light, microwaves or sound from sources which may be broadbanded and may be extended in emitting area. This requires two achromatic superimposing interferometers in series, with the target interposed, topologically.

It is another object of the invention to delay the light rays of one interferometer arm in time, yet superimpose them in path, to create a superimposing delay and hence a superimposing interferometer. It is an object to make these delays achromatic, that is, satisfy the superimposing conditions for a wide range of wavelengths and for uncollimated rays.

It is another object of the invention to optionally measure velocity at more than just a single point on the target surface, by forming a line or a 2-dimensional image of the target at the detector which manifest fringes from which the velocity is deduced.

It is another object of the invention to optionally use illumination whose wavelength changes with time (chirped), in conjunction with a spectrally or delay-organized detector, so as to record velocity and reflectivity of objects versus time in analogy to an electronic streak camera.

The first object is achieved only through the simultaneous use of two conditions 1) two delay-matched interferometers in series with the target interposed; and 2) interferometers which are achromatically superimposing. When the interferometer delays match within a system coherence time, partial fringes are produced which shift with target velocity via the Doppler effect. The invention is a generic method for velocity interferometry using any source, broad or narrowbanded, pointlike or extended. The principle is applicable to any wave phenomenon for which superimposing interferometers can be constructed, such as light, sound, and microwaves. Powerful flashlamps, which are extended and broadbanded, can be used for velocity interferometry where they were prohibited before. Impulsive sound created by pulses of laser light communicated to a patients body through optical fibers can now be used for Doppler ultrasound imaging, where previously it was prohibited due to incoherence.

The fourth object will form a device capable of measuring velocities and reflectivities of objects down to 2 ps time resolution when used with chirped illumination. This embodiment is called a chirped pulse velocimeter. "Chirped" light is defined herein as light which instantaneously has an approximately pure wavelength that varies with time. It forms a kind of optical streaking camera, similar to an electronic streak camera, whose time resolution is not affected by the motion of electrons, but by the wave properties of light.

The superimposing requirement for the interferometers is mandatory in the case of waves which travel in media in more than one dimension. If the waves are expressed as a 1-dimensional quantity, such as the voltage in an electrical cable leading from an antenna or a transducer, the superimposing requirement is moot, since there is only one ray path, not a manifold of paths. In that case, the interferometers can use a simple time delay, implemented by electronics or mathematically implemented through software.

The present invention is distinguished from the prior art by the achromatic superimposing quality of the interferometers, which can be constructed to operate on waves of a general nature, not necessarily light. In this application, the term "white" denotes the broadband quality of waves of any kind, not restricted to light, such as microwaves and sound.

III. DETAILED DESCRIPTION OF THE INVENTION

A. Explanation in Time-domain

Figure 1A illustrates the white light velocimeter concept of the present invention. A coherent echo is imprinted on the source light 10 by a superimposing interferometer (denoted the source interferometer 12) having a delay τ_s. The reflected light from the target 14 is observed through a second superimposing interferometer (denoted the detecting interferometer 16) having delay τ_d. This forms complementary outputs 3, 4. Figure 1A is a topological diagram only, the detailed positions of optics internal to the interferometers is not meant to be depicted. The time averaged output intensity is observed by a detector 13 or camera, which could be a single channel or multi-channel device. Partial fringes result when $\tau_s \approx \tau_d$.

Suppose white light is modeled by a series of independent wave packets; then we can follow the result of a single wave packet from the source. The waveform leaving the detecting is shown in Figure 1B. The source interferometer 12 splits the single packet into two identical packets (18, 20). The detecting interferometer does the same to create four of the two (22, 24). Two of those packets (20 , 22) will overlap and interfere if $\tau_s \approx \tau_d$, within a coherence length, contributing fringes to the net detected intensity 23. Target 14 motion during the interval τ_s will change apparent τ_s, so that it appears to be $\tau_s(1 - 2v/c)$ to the detecting interferometer. This is the Doppler effect, which contracts or dilates the waveform, or equivalently dilates or contracts the spectrum, causing a fringe shift in the detecting interferometer output intensity 23. The velocity/displacement is approximately given by the fringe phase shift according to Eq. 4 or Eq. 2, where λ is the average wavelength of the light reaching the detector or specific detecting channel.

The other packets (18, 24) add incoherently and contribute nonfringing components. Thus the visibility of the fringes are always partial (although use of a high finesse Fabry-Perot as the source interferometer 12 can

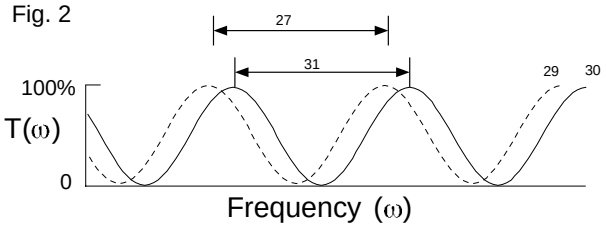

Figure 2 compares $T(\omega)$ for source and detecting interferometers.

arbitrarily increase fringe visibility at the expense of throughput). The fringe visibility can be made 100% by simultaneously recording both complementary detecting interferometer outputs (23, 25) and numerically or electronically subtracting them. This also eliminates extraneous light, which is defined light that has not passed through the source interferometer.

B. Explanation in Frequency-domain

An equivalent explanation of the basis of operation is to consider each interferometer to be a filter which has a periodic power transmission spectrum $T(\omega)$, also called a "comb" filter. This explanation is valid when the detector time response is slower than 2τ, which is the usual case. The angular frequency ω is related to the ordinary frequency and wavelength through $\omega = 2\pi f = c/\lambda$. Figure 2 compares $T(\omega)$ for source and detecting interferometers. For each comb filter 29, 30, the periodicity in frequency 27, 31 is inversely proportional to the time delay. If $\tau_s = \tau_d$ and the target is stationary, then transmission peaks of the source comb filter overlap peaks of the detecting comb filter. This produces a "bright" fringe in the output. If the target moves, the source spectrum is changed (multiplied by $1 + 2v/c$) by the Doppler effect, so that the peaks of the source filter may no longer correspond to the peaks of the detecting comb filter, as depicted in Figure 2. This produces a "dark" fringe in output intensity of the light passing through both interferometers, integrated over all frequencies. (This is similar to the creation of a Moiré pattern from two finely spaced grids.) Depending on the illumination bandwidth, the integrated overlap of source and detecting comb filter peaks goes in and out of phase as the target velocity increases, producing a sequence of light or dark fringes.

The description of the time-averaged detecting interferometer output intensity $\langle I \rangle$ for a target velocity v is given by the overlap integral over angular frequency ω.

$$\langle I \rangle \propto \int_0^\infty d\omega \; S(\omega/D_2)\; T_s(\omega/D_2)\; R_t(\omega/D_1)\; T_d(\omega) P(\omega) \tag{5}$$

where

$$D_2 = (1 + 2v/c) \tag{6}$$

and

$$D_1 = (1 + v/c) \tag{7}$$

are Doppler multipliers, valid when $v \ll c$. $S(\omega)$ and $P(\omega)$ are the power spectra of the illumination and detector sensitivities, respectively. The functions $T_s(\omega)$ and $T_d(\omega)$ are the power transmission spectra of the source and detecting interferometers respectively. These are calculated by the magnitude squared of the Fourier transform of the impulse response in the electric field.

If the detector time response is much shorter than the coherence time for the detecting channel, then the Equations stated here may not apply. If the detector time response is greater than or equal to the coherence time, then the Equations stated here apply, provided the velocity is constant during the observation time. If the target is accelerating, the fringe will shift, and if the fringe shifts more than 90° during the detector response time, the net fringe will wash out.

An idealized dispersionless Michelson interferometer (a 50% reflective beamsplitter is assumed for this discussion) has

$$T(\omega) = \tfrac{1}{2}(1 + \cos\omega\tau) \tag{8}$$

A superimposing Fabry-Perot interferometer has

$$T(\omega) = [1 + \alpha \sin^2(\omega\tau/2)]^{-1} \tag{9}$$

mirror reflectivity R by $\alpha = 4R/(1-R)^2$. Here we assumed both cavity mirrors have the same reflectivity. However, this is not required in general.

For the common case of Michelson source and detecting interferometers, fringes in the output intensity described by Equation 5 will occur when $\tau_s \approx \tau_d$, within a coherence time Λ/c. That is, these fringes will be sinusoidal under an envelope having a width Λ/c. At the center of the envelope, the intensity will vary approximately as

$$\langle I \rangle \propto \cos\left[\frac{2\pi}{\lambda}(c\tau_s - c\tau_d) - \frac{2\pi}{\lambda}(c\tau_s)\,(2v/c) + \phi_0\right] \tag{10}$$

where ϕ_0 is some phase constant. For Michelson interferometers with 50% transmitting/reflecting beamsplitters, the amplitude of the fringes at the peak of the envelope is a visibility of 50%, and less than this on the wings of the envelope.

1. *Velocity sensitivity*

The velocity can be calculated from the shift of any part of the fringe pattern, either the envelope or the phase of the fringes underneath the envelope. If the fringe phase is used, then the velocity/displacement is found from Eq. 4 or Eq. 2. If the shift of the envelope is used, then the shift is first expressed in terms of delay length which could be denoted $c\Delta t$. Then the displacement is found through $d = c\Delta t/2$ and the velocity is found through $v = c\Delta t/2\tau$.

2. Interferometry at multiple wavelengths

Note that the fringes of Equation 10 vary sinusoidally versus velocity, frequency (c/λ), and difference in interferometer delay (τ_s-τ_d). Thus the fringe behavior can be measured and analyzed versus frequency, or delay, or combinations of both. If the fringe behavior is decomposed into components organized by wavelength, each component will have an individual phase shift which can be measured and a velocity value computed from each through Eq. 4 using the specific wavelength associated with each component. These velocity values should all agree if the correct integer order is guessed when measuring the phase. Thus, the use of several wavelength components provides a self-consistency check on the analysis that resolves integer fringe skip ambiguities.

C. Other topics

1. Transverse velocity component

Assuming that the light from illuminating source 10 reflects nearly normally from the target 14, then the term velocity means the component toward the source/detector. However, the source 10 can illuminate laterally, or approximately on the opposite side of the target 14 so that a transverse velocity component is measured. This could be advantageous in fluid flow measurements. The illumination could pass through the target, such as if the target were a region of plasma whose refractive index was being probed. In all cases, the term "2v" in the Equations represents the rate of increase of the round trip effective path length source-target-detector, where the effective path length is the refractive index of the medium integrated along the physical path.

2. Relation to Optical Coherence Tomography

In the sense that the two inner pulses (20, 22) of Figure 1B are being compared by time of arrival, white light velocimetry is related to optical coherence tomography (OCT), which uses incoherent light to measure differences between two interferometer mirror displacements. The distinction is that in OCT, the target plays the role of one of the interferometer mirrors, that is, the target is internal to an interferometer. In white light velocimetry, the target is external to any interferometer. This is a great advantage for uncooperative targets, since strict alignment is not required, as in OCT.

D. Complementary outputs

In Figure 1A, the box-like constructions for source interferometer 12 and detecting interferometer 16 are icons representing generic amplitude-splitting interferometers which satisfy the superposition condition. The complementary outputs are not always drawn, but are implied. Their use is not mandatory, but is usually helpful. Michelson, Mach-Zehnder, Sagnac, or special Fabry-Perot design interferometers can be modified to satisfy the superposing condition and therefore be usable in this velocimeter (the ordinary Fabry-Perot design will not work because it is not superimposing). The source interferometer 12 and detecting interferometer 16 need not be the same design. For example, the source and target may have different numerical aperture requirements, so that optimal designs are different. Also, since the complementary source interferometer output is discarded in the simplest configuration, the source interferometer can have a more streamlined designed, such as an inline superimposing Fabry-Perot.

On the other hand, if it is desired, the role of both interferometers can be performed by the same optics by observing the light retro-reflecting from the target 14 back toward the source. This is accomplished simply by identifying in the single interferometer the output beam coming from the target. This automatically satisfies $\tau_s \approx \tau_d$ and greatly simplifies alignment. However, separate interferometers will be desired for the case of illumination that is very intense relative to reflected light, to avoid the glare from shared optics.

1. Push-pull use of complementary outputs

It is recommended, but not necessary, that both complementary outputs 3 & 4 of the detecting interferometer be recorded. By numerically or electronically subtracting their signals, any background light that has not passed through source interferometer will be eliminated from the signal. This is called "push-pull" processing of the signals. Secondly, the determination of fringe phase will be much more accurate for fluctuating target reflectivity, since the difference signal will be known to be centered about zero. Thirdly, when the velocimeter is used in a single-channel velocity discriminator mode, only the objects having the required velocity will produce a nonzero image in the difference signal. Fourthly, if the complementary signals are added instead of subtracted, then the non-fringing (i.e. ordinary) image will be obtained without speckle. This is useful for the presentation of the data; the velocity map created from interpreting the fringing image can be later graphically overlaid with the non-fringing image.

The summed signal will also give the system spectrum, that is, the combined spectrum of the illumination, target reflectivity and detector power sensitivity. The bandwidth of the system spectrum is represented by $\Delta\lambda_{sys}$, and is important for determining the fringing behavior of the velocimeter.

It will be implied in the descriptions below, although not explicitly shown for clarity, that what ever optical

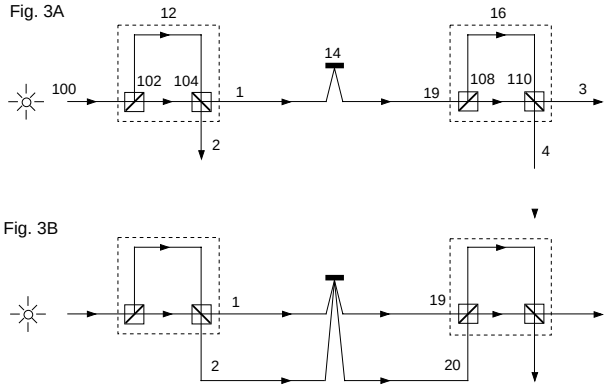

Figure 3A shows a simple white light velocimeter configuration. Figure 3B shows the use of angle of incidence to distinguish the complementary beams reflecting from a target.

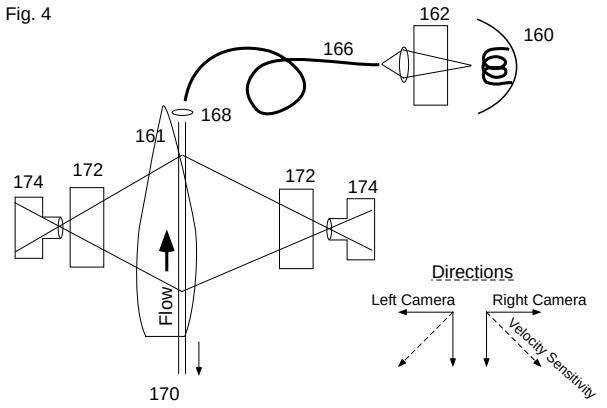

Figure 4 shows an embodiment of the white light velocimeter for measuring fluid flow.

manipulations are done to one detecting output, may also be done simultaneously to the other complementary detecting output, and that these outputs may subsequently be subtracted or summed after conversion to a voltage or digital value. A velocity can be determined using either complementary outputs singly, or both as a difference signal.

Furthermore, many techniques that have been employed for conventional VISAR velocimeters can be utilized for the present invention. For example, the use of a $\lambda/4$ retarder to produce a 90° phase lag between vertical and horizontal polarizations is commonly used to determine the direction (polarity of change) of the fringe shift in conventional VISARs. This technique can also be used in the present invention, although it is redundant in many cases since the use of broadband illumination in a multi-channel mode can determine fringe shift polarity. One situation where it wouldn't be redundant is when the velocimeter is used with chirped pulse illumination.

2. Practicalities using complementary outputs

In the simplest white light velocimeter configuration (Figure 3A), one of the complementary outputs 2 of the source interferometer is discarded. This is fundamentally necessary to produce the valleys in the source interferometer's power transmission spectra. Without the valleys, the changing overlap between source and detecting spectra will not produce fluctuations in the detecting output, and hence no fringes would be produced. Thus in the simplest configuration shown in Figure 3A, which uses a Michelson source interferometer with 50% reflective beamsplitter, 50% of the source power must be discarded.

Figure 3A is a topological diagram only. The beamsplitters 102 and 104 are shown separately for clarity; in actuality, they may simply be a different portion of the same optical piece. Similarly for beamsplitters 108 and 110. Each interferometer (12 and 16) has two complementary outputs (1, 2 and 3, 4). Each also has two complementary inputs (only 19 and 20 are shown). Broadband light from the source enters the source interferometer and is evenly divided between the two source outputs 1 and 2. In the simplest configuration (Figure 3A), only one of these outputs, 1, is used to illuminate the target. In the complex configuration (Figure 3B), both outputs are used. However, the outputs must be distinguished from each other as they reflect off the target. This can be accomplished by polarization or angle of incidence. If polarization is used, then polarizing beamsplitters can be used for all the beamsplitters. Figure 3B shows the case where angle of incidence is used to distinguish the beams reflecting from the target. The two reflected beams enter the two complementary inputs 19 and 20 of the detecting interferometer. Therefore, 100% of the illuminating power is used in the complex configuration.

E. Example application measuring fluid flow

Figure 4 shows an example application of a white light velocimeter measuring fluid flow, such as a gas jet seeded with light scattering particles. The arrangement consisting of a light source 160 (e.g., a flashlamp), whose light passes through a source interferometer 162 and enters a thick illuminating fiber 166. Light leaving the fiber is collimated by a cylindrical lens 168 into a fan-like shape which illuminates a thin slab of the jet volume 170. The light scattered from particles in the jet is observed by one or more camera systems 174, each which observe through a detecting interferometer 172. The detecting interferometer delays are matched to the source interferometer in order to produce fringes. The details of the camera systems are left unspecified. They could be one of a variety of configurations, measuring a point, a line, or an area of the target.

The purpose of Figure 4 is to show that 1) if the source interferometer optics have sufficiently low aber-

rations such that $c\tau_s$ is the same for all rays within $\lambda/8$, a non-imaging system such as a thick multi-mode fiber can be used to communicate the imprinted light from the source interferometer to the target. 2) In order to measure different velocity components, there can be more than one detector and the illumination can be laterally oriented. The velocity component which is sensed by each camera is given by the vector sum of two unit length vectors: target-camera and target-source. By having two cameras on opposite sides of the target and the illumination to the top, the vertical and transverse components can be resolved. With one or more additional cameras mounted out of the plane of Figure 4, the remaining velocity component can be resolved.

1. Range of allowed velocities

Let $\Delta\lambda_{sys}$ be the system bandwidth, which is defined the spectral width of light having passed through all the optical elements and converted to electrical signal by the photodetector, including target reflectivity, photodetector responsivity and illumination color. The system coherence length is $\Lambda_{sys} \sim \lambda^2/\Delta\lambda_{sys}$. Partial fringes result only when $|c\tau_s - c\tau_d| \approx \Lambda_{sys}/2$. Since target velocity causes a change in effective τ_s, the range of velocities which produce visible fringes is controlled by the system bandwidth through

$$\left|\frac{c\tau_s}{1+2v/c}\right| < \tfrac{1}{2}\Lambda_{sys} \tag{11}$$

Equation 11 is for a single detecting channel. Many of the attractive velocimeter features are implemented by a multi-channel velocimeter. The multiple detecting channels can be organized by wavelength or by delay τ_d. In the former case, the individual channel bandwidth is very narrow, and τ_d is the same for every channel. In the latter, the channel bandwidth is very wide, but τ_d is different for each channel. These two modes are described in more detail later.

F. Theory regarding the superimposing condition

The theoretical reason for requiring the superimposing condition for the interferometers is as follows. Let the condition where interference is prevented be called interfereless. (This could be achieved in concept by blocking one of the two interferometer arms in the case of a Michelson, or zeroing the partial reflectivity of the mirrors in the case of a Fabry-Perot.) Let the optical field in the region of an extended incoherent source be $S(t,\mathbf{r})$ and the field at every point "downstream" through an interfereless optical system be $H(t,\mathbf{r})$ where $\mathbf{r}$ is a position vector. Now, restoring the interference, if the output rays of the interferometer beams exactly superimpose, so that the images of the source viewed through the interferometer superimpose both transversely and longitudinally, then we say the superposition condition is satisfied. In the case of a multiple echo interferometer such as a Fabry-Perot, this condition must apply to each echo.

If this condition is satisfied for the source interferometer 12, then the velocimeter can be equivalently be expressed as an interfereless system having an effective source $S(t,\mathbf{r}) + S(t+\tau,\mathbf{r})$, which produces an optical field everywhere downstream $H(t,\mathbf{r}) + H(t+\tau,\mathbf{r})$. If the detecting interferometer 16 also superimposes, then the velocimeter output corresponds to $H(t,\mathbf{r}) + H(t+\tau_s,\mathbf{r}) + H(t+\tau_d,\mathbf{r}) + H(t+\tau_s+\tau_d,\mathbf{r})$. The point is that these expressions are easy to analyze since they all share the same spatial dependence- the same as an interfereless system, which is covered by traditional optics.

Thus in the superimposing case, the spatial dimensions can be ignored and only the temporal behavior need be solved. The problem collapses to 1-dimension, as if the signals were propagating along wires. This greatly simplifies the analysis.

If the superposition condition is violated, then the source is described as $S(t,\mathbf{r}) + S(t+\tau,\mathbf{r}+\delta\mathbf{r})$ where $\delta\mathbf{r}$ is the displacement vector between the source images seen in the beamsplitter. This produces a complicated optical field downstream since the two terms do not share the same spatial dependence. For sufficiently large $\delta\mathbf{r}$, the fringes at the velocimeter output will wash out and therefore fail to give a readable velocity signal. Since some image displacement is inevitable through imperfect optics, an estimate is made of the maximum value of $\delta\mathbf{r}$ which maintains significantly visible fringes. This will tell us the maximum amount of aberrations we can tolerate in the interferometer optics.

1. Distorting elements tolerated

A very practical consequence of the superimposing condition is that the path between the target and velocimeter can contain distorting or dispersive elements, or a non-imaging system such as an optical fiber without effecting the fringe visibility (for a uniform velocity target and constant distortion). In other words, high quality optics are needed only internal to the interferometers. This feature is highly desired for the use of a velocimeter on out of door targets, or communicating light between the velocimeter apparatus and the target through optical fiber, such as in an industrial situation. Once the echoes have been imprinted on the illuminating beam, their phase relationship is maintained, since both echoes propagate over the same path (assuming the distortion changes slowly compared to τ).

Secondly, the superposition argument above shows that an imaging velocimeter can be produced if the interfereless form of the optics produces an image. Each point of the image has a time averaged intensity dependence which is described by the 1-d theory below.

IV. THREE MODES OF MEASURING FRINGES

There are three modes of detecting the fringes and interpreting them into velocity: 1) single-channel; 2) multi-channel delay-distributed; and 3) multi-channel wavelength-distributed. The three are mathematically related. Many of the attractive velocimeter features, such as simultaneous multiple velocity detection, only come from the use of the multi-channel modality. The single-channel modality must be understood to understand the multi-channel modality. All these modalities apply to interpreting the velocity of the target at a single target point. For a line or areal imaging velocimeter, the modalities apply to each pixel of the image.

A. Single detecting channel

In the case of a single detecting channel, broadband illumination will produce a velocimeter with a narrow velocity range. From Equation 11, the center of the velocity range is given by

$$v_{center} = \frac{\tau_s - \tau_d}{\tau_s}\left(\frac{c}{2}\right) \tag{12}$$

and the range width is

$$v_{width} = \frac{\Lambda_{sys}}{c\tau_s}\left(\frac{c}{2}\right) \tag{13}$$

Thus, a broad spectrum produces a narrow Λ_{sys}, which in turn yields a narrow range of velocities that give visible fringes.

This narrowness can be used as a velocity selector or discriminator. By numerically subtracting the complementary detecting interferometer outputs after detection, only the fringing targets will produce a nonzero difference signal. This is particularly useful for an imaging velocimeter, since this means only the objects having a specific velocity component will appear different from the background image. For example in a radar or LIDAR application, if there are a multitude of missiles approaching, and one is only interested in detecting the missiles having a velocity component indicating that they will impact somewhere important, then the operator would set the interferometer delays according to Eq. 12 so that only those velocities produce fringes.

B. Multiple detecting channels

Velocimeters implemented with multiple output channels, organized either by delay or wavelength, offer many attractive features. The advantages include a much greater velocity range for a given overall bandwidth, independence from target and illumination color, an absolute velocity determination, and the ability to detect simultaneous multiple velocities. The latter two abilities are very important, particularly in the field of shock physics where discontinuous accelerations and disintegrating materials create difficult targets. The ability to determine absolute velocity from a target acquired after it has accelerated (suddenly appearing at the horizon) is very important for LIDAR and radar velocimetry, as is being able to discriminate targets against stationary clutter such as chaff.

1. Wavelength distributed system

A wavelength distributed system is shown in Figure 5A. This consists of the white light velocimeter of Figure 1A with the added prism 90 to disperse the output according to wavelength across a set 92 of multiple detecting channels. In a single target-point mode, the point is dispersed into a line which can be shown on the slit of a streak camera to be recorded. In a line-target mode, the line is dispersed into a rectangle which can be recorded by a multi-channel areal detector such as a CCD array, or film. Since a rectangle cannot be dispersed into a third dimension, a two-dimensional image of the target can be measured if one can uses multiple discrete two-dimensional detectors, each with bandpass filters to limit the wavelengths detected. Even a modest number of channels, such as 3 or 4, provide advantages, particularly if the channel center wavelengths are widely separated.

The greatest advantages of this wavelength-organized system will be when there are many channels individually having a very narrow bandwidth $\Delta\lambda_{sys}$, but collectively having a wide bandwidth. When each channel's $\Delta\lambda_{sys}$ is very small, then individually each channel has a very large velocity range according to Eq. 12. That is, for an accelerating target many fringes can pass before their visibility diminishes. This allows a small velocity per fringe coefficient η, which increases the velocity resolution.

Figure 5B shows the simulated spectrum for a single target point versus velocity for a fixed source-detector delay difference. The vertical scale is proportional to $1/\lambda$ or light frequency ω. The dark bands represent fringe maxima or minima, depending on which complementary detecting output is observed. The plot for negative velocities is a reflection of the positive side. For a given target velocity, the number of fringes counting along a vertical slice of the graph will indicate the velocity. This can be mathematically accomplished by taking the Fourier transform of the intensity along the vertical slice. A given spatial frequency component will correspond to a given target velocity. The higher the velocity, the higher the spatial frequency.

If more than one target having different velocities is in the velocimeter field of view, then each target will contribute a different spatial frequency component. These can be resolved if the velocities are sufficiently different compared to η, given by Eq. 1. The greater the amplitude of that Fourier component, the greater the net

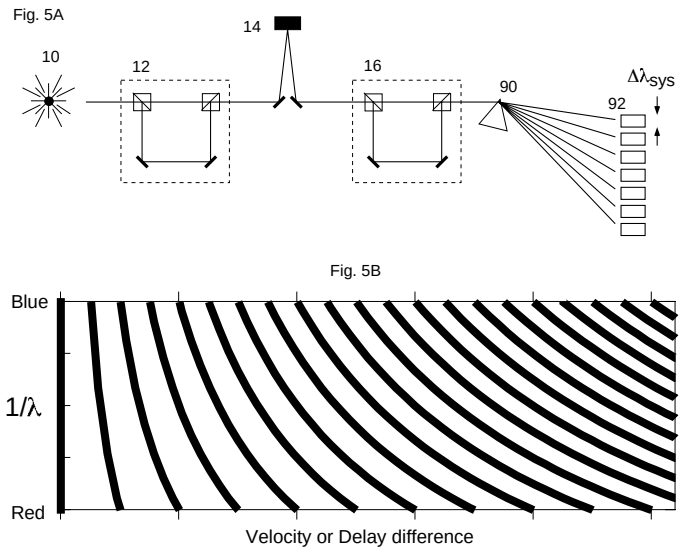

Figure 5A shows a wavelength distributed system. Figure 5B shows the simulated spectrum for a single target point versus velocity for a fixed source-detector delay difference.

target area moving with that velocity.

2. Delay distributed system

In a delay-distributed multi-channel system, each channel has the same system spectrum, which is optimally very wide, but at a different delay difference $(\tau_s - \tau_d)$. This can be accomplished by tilting one of the interferometer mirrors so that delay is a function of the output's transverse position on the camera's film plane. The reason tilting causes this is shown in Figures 7A-7F. Figure 7A shows a Michelson interferometer with perfectly aligned mirrors 402, 403. From the point of view of the detector 405, the reflection of the source 10 appears in the beamsplitter 404 to be at two locations 400, 401. These are superimposed for the aligned Michelson in Figure 7B. In Figure 7C, mirror 402 is tilted out of alignment. This moves apparent position of the source 401 so that it does not superimpose with 400 (Figure 7D). Figure 7E shows a camera lens 406 imaging the two twin source images on to a film plane 407. Different positions along the film correspond to different angle q of ray bundles leaving the source twin, and these have slightly different delay difference Δdelay, shown in closeup Figure 7F.

Position across Figure 6A and 6B perpendicular to the fringe comb corresponds to increasing delay difference $(\tau_s - \tau_d)$. Each resolvable column on the Figure parallel to the fringe comb corresponds to a channel. Just as in the λ-distributed system, the wide bandwidth provides absolute velocity determination, multiple simultaneous velocity detection, and independence from details of the system spectrum.

Since the channel bandwidth is very wide, fringe visibility maximizes for a very specific delay difference satisfying Eq. 12. Integrating over the intensity changes of Figure 6A shows the center of fringe pattern is at a well defined location indicated by the white arrow. For the stationary target (Figure 6A), this corresponds to the location on the image where $(\tau_s - \tau_d) = 0$. For the moving target (Figure 6B), this corresponds to a different location on the image where $(\tau_s - \tau_d) \neq 0$. Thus the shift in center position of the fringe pattern yields the velocity.

The location of the center of the fringe pattern can be determined mathematically by Fourier analysis, from the phase shift of each component. This also determines the system spectrum, because each color produces a fringe comb component with periodic spacing proportional to λ, and amplitude equal to the intensity of the color. Thus, even though this modality does not use a prism or diffraction grating, or a wavelength sensitive detector, the color components and their relative intensities can be resolved. (This is the basis for an existing laboratory spectroscopy technique called Fourier transform spectroscopy). Thus, the wavelength and delay-organized multi-channel systems are mathematically related. Furthermore, this means that the chirped pulse streaking technique described later can be accomplished without a diffraction grating, if the detecting interferometer is operated in the delay-organized multi-channel mode.

3. Narrow-band illumination

Laser and other narrowband illumination can be applied to the white light velocimeter in the same manner as broadband light. However, the attractive features of absolute velocity determination and simultaneous multi-

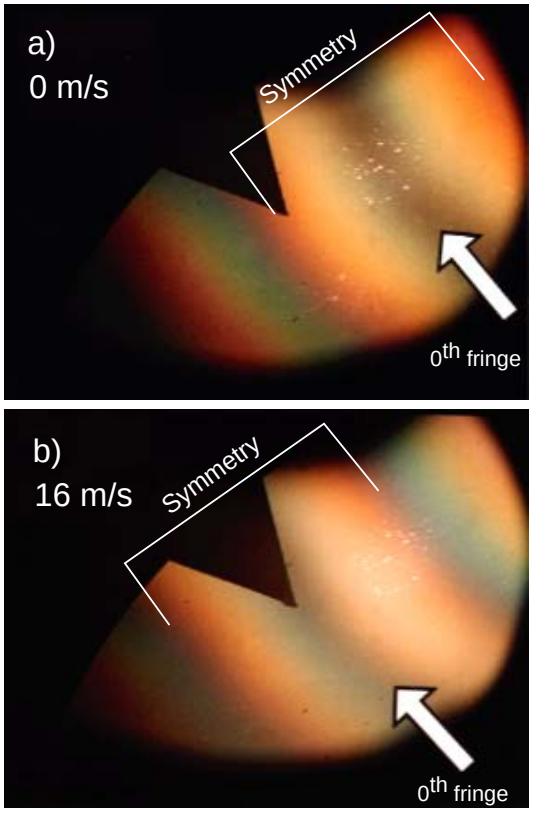

Figure 6A depicts an experimentally measured fringe pattern of a stationary object. Figure 6B depicts a an experimentally measured fringe pattern of a moving target.

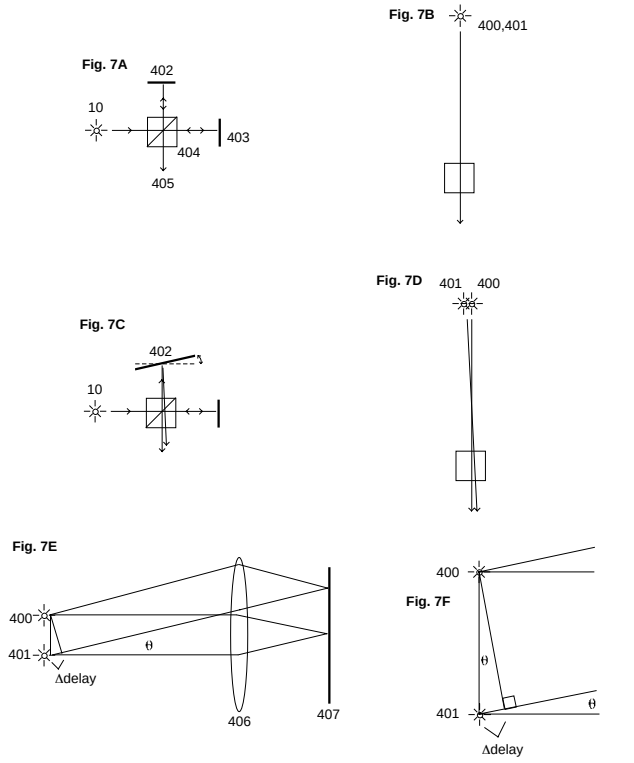

Figures 7A–7F illustrates the effect tilting a mirror has on delay.

ple target detection are not available for monochromatic light. Some degree of these features can be retained if at least 2 or 3 colors are present, such as in a multi-line laser, i.e., Argon or Krypton ion laser. The user should be aware that if $c\tau_s$ is smaller than the laser coherence length, (so that the interferometer free spectral range is larger than the laser bandwidth), slight adjustment of τ_s may cause the power to switch from one source interferometer output to the other. This is particularly relevant when using a multi-line laser, since τ_s should be selected such that the important spectral lines emerge from the same output arm.

4. Chirped illumination

An interesting application of the white light velocimeter is with specially prepared light called chirped light. This embodiment is called a chirped pulse streaking velocimeter and it can measure velocity or reflectivity changes versus time for every place on a line imaged across the target. The device is interesting because it can potentially reach very short time resolutions, down to 2 ps, depending on the amount of chirp on the light. Let us describe "chirped" light as light which instantaneously has an approximately pure color which varies with time. Chirped light is distinguished from incandescent broadband light in that there is never simultaneously two different colors present– the colors arrive in sequence. Chirped light is usually in pulsed form, but it could be a continuous beam if the frequency was scanned in a repetitive fashion. This could be produced by a CW or pulsed laser whose wavelength is caused to sweep by an intracavity electro-optic device, or by taking a very short laser pulse and sending it through a matched pair of diffraction gratings to stretch it. These techniques are common in laser laboratories.

The chirped pulse streaking velocimeter is obtained simply by using the white light velocimeter in a multi-channel mode with chirped illumination. Both the wavelength-organized and delay-organized multi-channel modalities can be used, since they are mathematically related. However, it is easiest to understand the operation of the device when it is in the spectrally organized mode. In that case a line image of the target is imaged to the slit before a prism or grating, which spectrally disperses the output. Because the instantaneous color of the light is changing with time, the output from the grating will sweep across an integrating recording medium such as film or a CCD camera.

The chirped pulse streaking velocimeter of Figure 8 consists of chirped pulse input 120, source interferometer 122, moving target 124, lens 126, detecting interferometer 128, slit 130, dispersive element 132 and film or CCD 134.

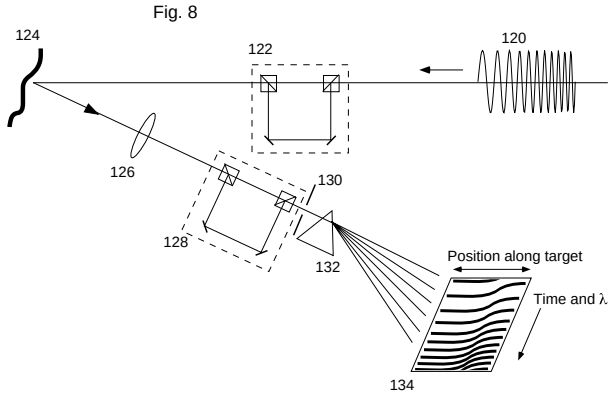

Figure 8 shows the chirped pulse streaking velocimeter.

It is assumed that the instantaneous wavelength versus time is known by an independent measurement. Thus, the position along the streak record in the wavelength direction will correspond to time. The complementary detecting interferometer output can be similarly recorded, and the two signals subtracted or added. Fringe shifts in the difference signal are interpreted into a velocity versus time record using Equation 4. The sum signal yields the reflected target light intensity history.

The reader should note that because chirped light is instantaneously monochromatic, the chirp pulse velocimeter does not have the multiple-target, absolute velocity resolving features of the non-chirped broadband configuration. If these are desired, the user can operate the device in a hybrid configuration simply by using more complex illumination with the same optical apparatus. The complex illumination could consist of, for example, 3 simultaneous colors, which are all being swept across a wavelength range 1/3 as wide as the full spectrum. That is, the illumination may start as red, yellow, and blue, and end up as orange, green and violet.

If the velocimeter detecting channels are organized by detecting delay, such as created by tilting an interferometer mirror, then the output beam will "sweep" in a different manner. (The grating is not used in this case.) As the different colors sequentially pass out the velocimeter, they will create fringe combs having different spatial frequencies. A one-for-one association can be made between a spatial frequency and a moment in time. Thus, in order to analyze the record, a Fourier transform of the recorded intensity is made. The phase shift for a given spatial frequency yields the instantaneous velocity, and the magnitude of the component yields the target reflected light intensity.

The optical streaking concept can be applied to create a much simpler device that measures only target reflectivities and not velocities. This embodiment is called a chirped pulse streaking camera. The two interferometers needed for velocimetry are discarded. The device simply consists of the grating dispersing the chirped output and the detector. The time resolution capability of this device is exactly the same as for the chirped pulse velocimeter. Alternatively, only the source interferometer is discarded, and the detecting interferometer is used in the delay-distributed mode without any grating.

The optical streaking of these inventions is analogous to that in an existing electronic streak camera, except that the sweep speed is not controlled by any electrical behavior inside the camera, but by the degree of chirp of the illumination entering the optics. Electronic streak cameras can suffer from jitter in the triggering time. That is, it takes a finite amount of time from the arrival of the trigger pulse to the beginning of the high voltage ramping (which sweeps the electrons), and this lag time can be unpredictable in single-shot experiments. The advantage of the optical streaking is that there is no jitter in the device's operation. The chirped diagnostic illumination can be synchronized by optical delays to the other laser beams which may drive the experiment being studied (such as studying the expansion of a laser-created plasma). Optical delays are controlled by physical distances, which are extremely reproducible from shot to shot. Secondly, apart from the expense of the chirped illumination, the chirped pulse streaking velocimeter and camera are relatively inexpensive optical devices to build, and an arbitrarily large number can be used to simultaneously observe the same experiment from different angles, all illuminated by the same chirped source.

To estimate the time resolution Δt, the chirped pulse was modeled as a series of transform limited elemental pulses of width Δt concatenated over a duration T_p with a linearly ramping average frequency. Using the uncertainty relationship for the elemental pulse we find that

$$\Delta t = \sqrt{\frac{T_p}{c(1/\lambda_1 - 1/\lambda_2)}} = 1.8\text{ps}\sqrt{\frac{T_p(\text{ns})}{(1/\lambda_1 - 1/\lambda_2)(\mu m^{-1})}} \tag{14}$$

where T_p is the pulse duration in ns and λ_1 and λ_2 are the bracketing wavelengths in μm describing the chirp. For example, with T_p=100 ns and a 10% chirp from λ_1=500 nm to λ_2 = 550 nm, Eq. 14 yields Δt=43 ps. The ratio of record length to time resolution is 100000/43=2300. This is an order of magnitude greater than the ratios ($\sim$200) estimated for the phosphor screens of an electronic streak camera having a $\sim$30 mm diameter screen. For T_p=10 μs and the same 10% chirp as above, Eq. 14 yields Δt=0.43 ns and a record length ratio of 23000. This vastly exceeds the capability of today's electronic streak cameras.

V. INTERFEROMETER DESIGN CLASSES

A. Michelson vs. Fabry-Perot

Interferometer designs can be organized into two classes according to the number of output pulses produced from a single applied pulse. A Fabry-Perot-class

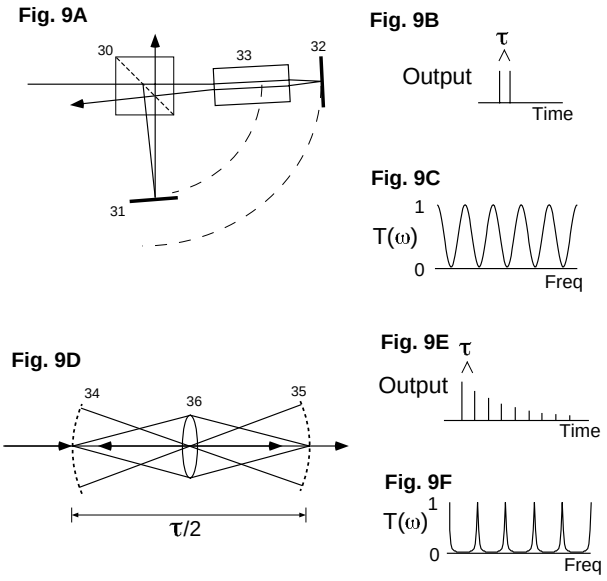

Figure 9A shows a Michelson class interferometer using an etalon delay. Figure 9B shows the impulse response for the Michelson class interferometer. Figure 9C shows the sinusoidal power transmission spectrum for the Michelson class interferometer. Figure 9D shows the Fabry-Perot class interferometer in a superimposing configuration. Figure 9E shows the impulse response for the Fabry-Perot class interferometer. Figure 9F shows the thinner peaks of the Fabry-Perot class power transmission spectrum.

(F-P) interferometer generates an infinite series of output pulses, whereas the Michelson-class generates a finite number (two). It will be shown that the number of output pulses determines the number of fringing sidebands in the intensity versus velocity plot discussed below. There is also a fundamental difference in the fringe visibility and power throughput of the two classes. By increasing the partial reflectivity R of the F-P mirrors, the velocimeter fringe visibility can be increased arbitrarily at the expense of smaller throughput. This is not true of the Michelson-class, where the fringe visibility cannot exceed 50% for a single output. (Push-pull subtraction will increase fringe visibility by eliminating constant components.)

Figures 7A and 7D show these two interferometer classes, distinguished by their impulse responses. The Michelson class shown in Figure 9A consists of a beamsplitter 30, mirror 31, and a superimposing delay, which in this case is the combination of an etalon 33 and mirror 32. Other superimposing delay designs described below can be substituted. Figures 9B and 9C shows that the impulse response for the Michelson class is pair of echos separated by τ.

The Fabry-Perot (F-P) class shown in Figure 9D consists of two partially reflective mirrors 34, 35 separated by a distance $\tau/2$ and having a lens 36 placed in between mirrors 34, 35. The lens must image the surface of one mirror on to the other. The lens is crucial for the superimposing behavior. An ordinary F-P does not have this lens and is not superimposing. For the Fabry-Perot (F-P) class, the impulse response is an infinite number of echos of geometrically decreasing amplitude, as shown in Figure 9E.

Figure 9C shows the power transmission spectrum for the Michelson class interferometer is sinusoidal. The F-P class power spectrum can have thinner peaks, as shown in Figure 9F, depending on mirror partial reflectivity R.

B. Superimposition

Associated with each output pulse of the impulse response is an image of the source. The purpose of the superimposing interferometer is to superimpose these images as closely as possible, for all wavelengths and incident ray angles, while one image is delayed in terms of time-of-flight of the light. This is achieved in practice only for a limited range of wavelengths and incident angles due to ordinary and chromatic aberrations. The greater these ranges, the greater the power available for velocimetry from non-directional broadband sources such as incandescent lamps. Thus the chief design goal for a superimposing delay is to minimize aberrations for the range of wavelengths and ray angles desired.

The dispersion of glass optics affects the interferometer two ways: it chromatically smears the image position which detriments the superposition, and secondly, it causes a wavelength dependence to the time delay. The time delay smear is not a problem. However, the image position smear is a problem since it can seriously reduce the fringe visibility. Any other aberrations, chromatic or ordinary, which smear the images will detriment the superposition.

1. Tolerance for smear

The tolerance for smear will be estimated. Let the smear be modeled by a simple displacement vector $\delta\mathbf{r}$ of twin images seen in the beamsplitter in a Michelson design. The tolerance between the multiply displaced images of a superimposing F-P should be similar. It will be shown that the narrower the numerical aperture of the optics, the greater $\delta\mathbf{r}$ which can be tolerated.

Let the displacement vector $\delta\mathbf{r}$ be

$$\delta\mathbf{r} = \hat{\mathbf{x}}\delta r_x + \hat{\mathbf{z}}\delta r_z \tag{15}$$

with components δr_x and δr_z in the transverse $\hat{\mathbf{x}}$, and longitudinal $\hat{\mathbf{z}}$ (on-axis) directions. By comparing the distances to two point-sources on an entrance pupil from a single third point on an exit pupil, and requiring the difference in the two distances to be constant within a tolerance $\lambda/4$, it can be shown that the maximum displacements in the longitudinal and transverse directions

must be less than

$$\delta r_z < \frac{\lambda}{2}\frac{1}{\theta^2} \tag{16}$$

and

$$\delta r_x < \frac{\lambda}{8}\frac{1}{\theta} \tag{17}$$

where θ is an angle which characterizes the numerical aperture subtended between the entrance and exit pupils, whichever numerical aperture is larger.

Equations 16 and 17 can be used in reverse, to solve for the range of angles θ from an illumination source which produce visible fringes (and therefore suitable for velocimetry) for a known displacement between twin images in the interferometer. The displacement vector $\delta\mathbf{r}$ would be caused either by aberrations, or by use of a non-superposing interferometer.

For example, this can be used to show the disadvantages of a non-superimposing interferometer. A non-superimposing interferometer will not be able to utilize the full power available from a non-directional broadband source such as an incandescent lamp. Either the bandwidth will be limited for all ray angles, or the ray angles will be limited for all bandwidth. An example of this is the non-superimposing double Fabry-Perot of US Patent 4,915,499. In the former case, the patent authors calculated in their aforementioned Applied Optics article that their bandwidth was limited to <4 nm when the interferometer is used to measure off-axis fringes, (and therefore involving a large range of ray angles.) In the latter case, which is when on-axis fringes are measured, by using Equation 16 where δr_z is the mirror spacing of several cm, it can be seen that the range of acceptable angles is very small, of the order $\theta \sim 0.002$ radian. Thus the only a superimposing interferometer (and thus $\delta r_z \approx 0$) will simultaneously allow a large range of angles and large bandwidth, and therefore utilize the full power available from an extended area broad bandwidth source.

C. Fabry-Perot Interferometers

Two kinds of interferometers will be discussed: superimposing Fabry-Perots, and Michelsons incorporating superimposing delays.

The reason the classical Fabry-Perot (F-P) interferometer is not superimposing is illustrated in Figure 10A. An off-axis entrance ray 39 zig-zags between the mirrors 41 and 42, producing output rays 40 that are successively translated transversely, for each round trip. To be superimposing, the output rays must share the same path, for all round trips. For the classical F-P, this only occurs for the on-axis ray.

In a superimposing Fabry-Perot, shown in Figure 10B, echoes for all the round trips exit along the same output ray 44, for each incident ray 43. This condition is satisfied for any incident ray angle, not limited to the on-axis rays as in the classical F-P. Thus, the temporal characteristics of the superimposing F-P is the same as the on-axis classical F-P.

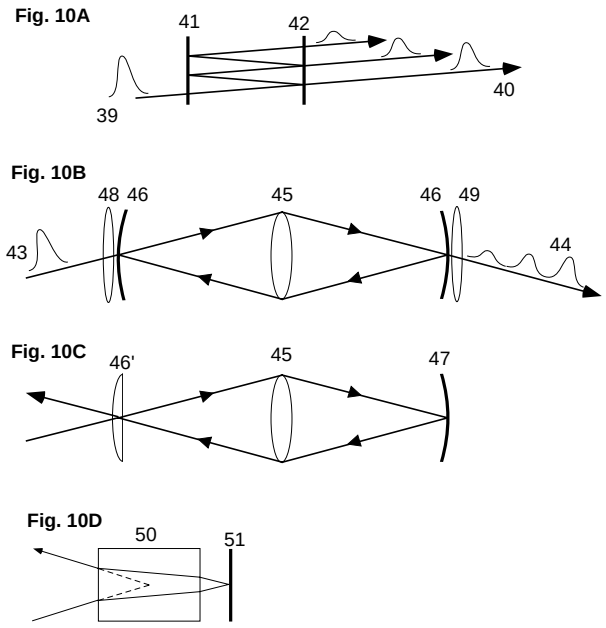

Figure 10A illustrates the nonsuperimposing Fabry-Perot interferometer. Figure 10B illustrates a superimposing Fabry-Perot. Figure 10C shows a superimposing relay delay using real imaging. Figure 10D illustrates the path of a ray through an etalon delay.

The superimposing F-P is achieved by a lens 45 between two partially reflecting spherical mirrors 46 and 47, such that exactly +1 magnification is achieved per round trip. This is achieved when the surface of mirror 46 is imaged to the surface mirror 47 by the lens 45. The radii of curvature of the spherical mirrors are centered at lens 45. Lenses 48 and 49 allow a collimated beam to pass as collimated. The interferometer will be achromatic if an achromatic lens 45 is used.

D. Superimposing delays

Superimposing delays which can be incorporated into one arm of a Michelson interferometers will now be described. Generally, a superimposing delay should act like a plane mirror in terms of how the output ray directions behave, but yet delay the light in time. The created mirror will be called the "effective" mirror. (The term "virtual" is avoided here to prevent confusion with the term virtual imaging, used below to classify the lens arrangement.) The mirror of the other interferometer arm is positioned to superimpose with this effective mirror position, thus creating a delay while satisfying the superposition condition.

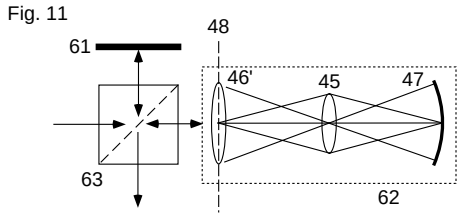

Figure 11 shows how a superimposing delay is used in one arm of a Michelson interferometer.

1. Etalon delay

The simplest superimposing delay is the etalon delay. Figure 10D shows how due to refraction the mirror 51 behind the glass slab 50 appears closer to the slab, yet a pulse is delayed by the slower speed of light through the glass. The etalon delay is used in conventional laser-illuminated VISAR velocimeters, as shown in Figure 9A. The advantage of the etalon is its simplicity of alignment. However, the etalon delay suffers chromatic aberration because of dispersion in the glass. Thus it can only be used in the white light velocimeter for high collimated light, or for sufficiently small delays such as for high velocity measurements.

The other superimposing delays described below are achromatic. The achromatism comes from the use of individually achromatic lenses and mirrors, or the matching of elements having opposite chromatisms. Except where noted, the mirrors are assumed to be first surface reflectors and therefore achromatic. To avoid duplication, the drawings will chiefly show the use of transmissive optics. However, it is implied that reflective optics could optionally be substituted with minor rearrangement of positions to enhance the achromatic quality or reduce cost.

2. Delays using real imaging

The delay designs can be classified according to whether real or virtual imaging is used between a lens and a mirror. This strictly depends on the lens-mirror distance compared to the focal length.

A relay lens delay is a superimposing delay using real imaging related to the superimposing F-P. Referring to Figure 10C, the relay lens delay is obtained from the superimposing F-P optics, by making the exit mirror 47 totally reflective and removing the entrance mirror. Lens 45 images the mirror 47 surface to the plane at lens 46′. The focal point of lens 46′ is at lens 45, and the center of curvature of mirror 47 is at lens 45. These two arrangements allow a collimated beam to pass through the delay as collimated. The optics as a unit act as a plane mirror superimposed at the position of lens 46′, and yet it takes light a finite time to traverse the unit. Lenses 45 and 46′ should be achromatic to produce an achromatic delay.

Figure 11 shows how this delay is used in one arm of

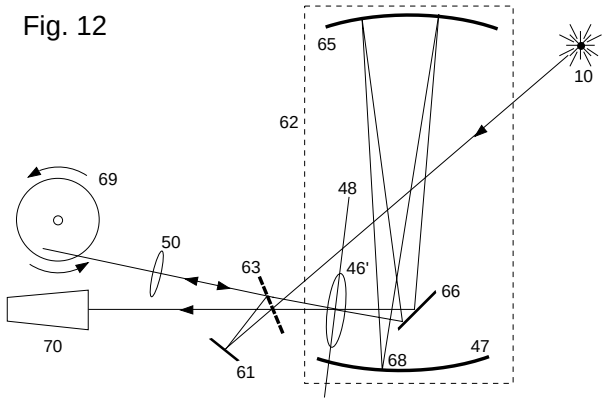

Figure 12 shows an embodiment of a complete velocimeter using retro-reflected light.

a Michelson interferometer, as the group of elements enclosed in the dashed box 62 form an effective plane mirror at 48. The mirror of the other arm 61 is superimposed by beamsplitter 63 at this plane 48. To implement a meter scale delay having f/10 optics, the internal lens 45 can be implemented by a spherical mirror 65, as shown in Figure 12. This shows a complete single interferometer velocimeter including source 10, target 69 and detecting telescope or camera 70. Lens 50 images the target 69 to the interferometer mirror planes 48 and 61. The purpose of this is discussed later. The optics enclosed by the dashed box 62 form an effective plane mirror at 48. The pick-off mirror 66 is needed so that lens 46′ and mirror 47 are the same distance from mirror 65. To minimize astigmatism due to off-axis reflection from the spherical mirror 65, the rays 68 should pass closely to the pick-off mirror 66. On the other hand, the size of the image of the target at plane 48, which is also the size of the image at mirror 47, limits the rays 68 from coming very close to mirror 66. Thus there is a compromise between astigmatism and image size.

3. Lens delays using virtual imaging

Figure 13A shows a virtual imaging delay using a combination of an achromatic transmissive lens 210 and an front surface spherical mirror 212 (which is achromatic). In this design, lens 210 and mirror 212 are separated by a distance less than the lens's focal length F (213), hence, virtual imaging is involved. If the lens is positive, the mirror is convex as in Figure 13A; if the lens is negative, the mirror is concave as in Figure 13C.

Figure 13A and 13C, the focal point of lens 210 is arranged to be at the mirror center of curvature 214 so that the lens 210 images point 214 infinitely far way. For the case of a positive lens 210 in Figure 13B, the surface of the mirror at point 216 is imaged by lens 210 to a position 217. Thus, the effective image of mirror 212 is a plane mirror 213 at a position 217. Similarly for the case

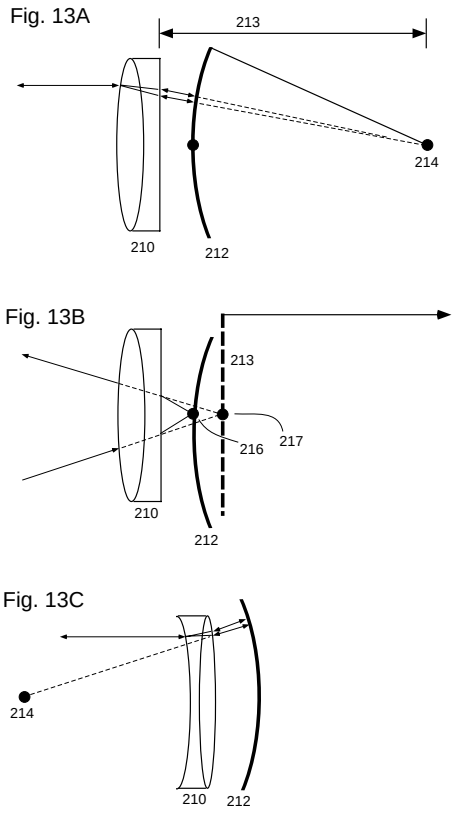

Figure 13A shows a virtual imaging delay using a combination of an achromatic transmissive lens and a front surface spherical mirror. Figure 13B shows the surface of a mirror imaged by a lens to a fixed position. Figure 13C shows the use of a negative lens and a concave mirror.

of a negative lens 210.

4. Minimizing chromatic aberrations

In Figure 14, if an etalon 240 is placed in between the lens 241 and the reflector 242, the chromatic aberration introduced by the etalon is of opposite polarity as that of a simple lens and therefore can reduce or zero the net aberration of the combination lens-etalon. The rays drawn in Figure 14A are drawn for blue and red and the dispersive quality of the etalon is greatly exaggerated. The rays are drawn as if the refractive index for red is 1 (i.e., no refraction) and for blue much larger than 1 (much refraction). An object behind a slab of glass always appears closer to the observer. Since the refractive index is greater for blue than red, the mirror center of curvature 244 will appear closer to the lens for blue rays than red rays. This may help compensate the chromatic aberration of a simple uncorrected lens 241, since that lens will focus the blue closer to lens 241 than for red. Thus, the apparent mirror center of curvature will remain at the focal point of the lens for both blue and red.

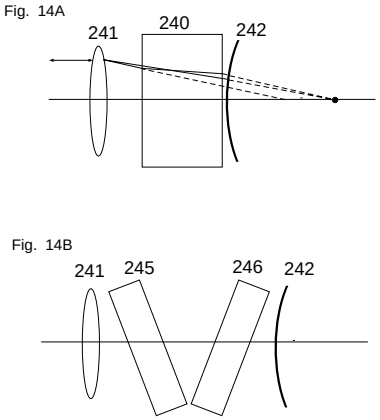

Figure 14A shows the use of an etalon to reduce or zero the net aberration of the combination lens-etalon. Figure 14B shows that tilting glass etalons can adjust the amount of chromatic aberration contributed by the etalons.

Figure 14B shows that tilting glass etalons 245 and 246 can adjust the amount of chromatic aberration contributed by the etalons, so that the net amount for the combination lens-etalons can be zeroed. A pair, instead of a single etalon, may be used to prevent introduction of other aberrations. One may need an additional pair of tilted etalons (not shown) tilted in an orthogonal direction (out of the plane of the Figure) to avoid astigmatism.

5. Creating negative and positive delays

The introduced delay can be positive or negative depending on the total glass thickness in the delay, and the position of the effective mirror 242′. In practice, only the magnitude of the delay is relevant, since moving the delay to the other arm will flip the polarity, or swapping interferometer outputs will have the same effect.

In Figure 15A, a thin achromat 250 and small radius of curvature mirror 252 create a large negative delay, since a photon traveling through the combination will appear sooner than a photon traveling to the apparent mirror and back. This is because the apparent mirror 252′ is far to the right, and the amount of glass small. In Figure 15B, a thick achromat 254 and large radius of curvature mirror 256 create a positive delay. A photon traveling through the combination will emerge later than one traveling to the apparent mirror 256′, because the light travels slower through glass and the apparent mirror is close. Figure 15C shows a design with a negative lens 260 that achieves a wider angle of acceptance then 13A for the same large delay.

Fig. 15A

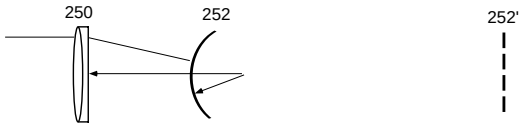

Fig. 15B

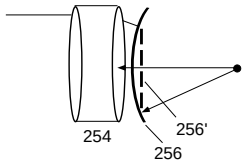

Fig. 15C

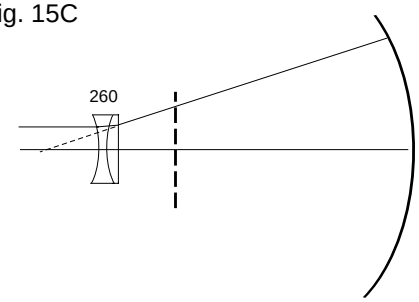

Figure 15A illustrates the use of a thin achromat and a small radius of curvature mirror to create a large negative delay. Figure 15B illustrates the use of a thick achromat and a large radius of curvature mirror to create a positive delay. Figure 15C shows a design with a negative lens that achieves a wider angle of acceptance then 13A for the same large delay.

Fig. 16

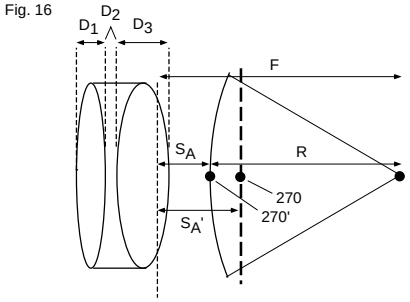

Figure 16 illustrates the variables used to compute net delay.

6. *Computing the net delay*

Figure 16 illustrates the variables used to compute the net delay. We must have $F = R + S_a$ in order for the apparent mirror to be plane (have infinite radii of curvature.) The delay is the sum of two components: delay due to the slower speed through the glass, and delay due to the change in distance between actual 270 and apparent $270'$ mirror positions. Let the former delay be called τ_{glass} and the latter τ_{mirror}.

Fig. 17

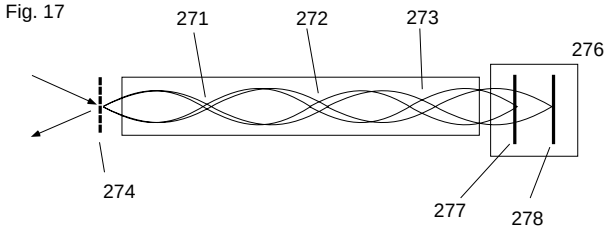

Figure 17 shows the use of an imaging optical waveguide.

The insertion delay of a glass element of thickness D is $(n-1)D$, where n is the refractive index. Each piece of glass contributes a delay, so to sum over all the elements

$$\tau_{glass} = \sum D_i(n_i - 1) \tag{18}$$

where n_i and D_i are the refractive index and thickness at the axis of each element of a compound lens.

The apparent mirror distance is computed from the lens law. Let the distance from the lens' principal plane to the mirror surface at the axis be S_a, and to the imaged mirror surface S'_a. Thus

$$\frac{1}{S'_a} = \frac{1}{S_a} - \frac{1}{F} \tag{19}$$

Equation 19 was written so that S'_a is a positive quantity. Then

$$\tau_{mirror} = S'_a - S_a = \frac{1}{1/S_a + 1/F} - S_a \tag{20}$$

The net delay is

$$\tau = \tau_{glass} - \tau_{mirror} \tag{21}$$

By using telescope mirrors, achromatic superimposing delays of the order several meters long can be constructed, having reasonable large numerical apertures. However, larger delays would require prohibitively large mirrors to maintain the same numerical aperture. One solution is to use single mode fiber optics to create a delay. The delay is superimposing since it only supports one ray direction. Unfortunately, this precludes imaging velocimeters, which are desirable.

7. *Use with optical waveguide*

Another solution is to use an imaging optical wave guide, shown in Figure 17. This consists of a thick (several mm) "fiber" 270 with a refractive index that decreases approximately as the radius squared. In such a wave guide, real images are formed periodically (271, 272, and 273) at specific distances along the fiber, as shown in Figure 17, similar to a relay chain of positive lenses. These wave guides are commercially available. If a single

Fig. 18

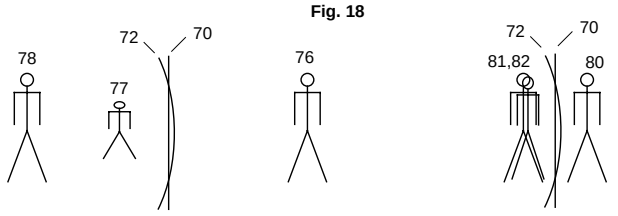

Figures 18A and 18B illustrate why imaging the target to the interferometer mirror plane improves image superposition for aberrated optics.

mirror is placed at the end of the fiber, the mirror is imaged to the front neighborhood 274 of the fiber and thus forms a superimposing delay for monochromatic light. The glass dispersion prevents its use with broadbanded light with a single mirror.

To use the wave guide fiber for broadband light a distributed mirror 276 is needed, where the mirror position for each color (277 for blue, 278 for red) is different so that the image of the mirror at the front of the fiber 274 is superimposed for all colors. The distributed mirror would have a large thickness, of the order $(n_{blue} - n_{red})D$, where $n_{blue,red}$ are the refractive indices at the center of the fiber for blue and red light, and D is the fiber length. For typical glass, $(n_{blue} - n_{red})$ is of the order one percent. Thus for example, if the fiber is 10 meters long, the distributed mirror will be approximately 10 cm.

A distributed mirror could be constructed of a volume hologram. This operates on the principle that a transparent material which has a refractive index which varies sinusoidally will strongly reflect light of the wavelength matching the periodicity of the sinusoidal variation. Standard holographic techniques can be used to construct the hologram such that the effective position of the reflector varies in depth with color.

8. Why put image at mirror plane

In all realistic superimposing delay designs, some aberrations are inevitable and these will cause the effective mirror of the delay to have a slight curvature, instead of being ideally plane. When the plane mirror of the non-delayed interferometer arm and effective mirror are superimposed by the interferometer beamsplitter, any curvature of the effective mirror can detriment fringe visibility. Such a detriment can be significantly reduced if the target is imaged close to the mirror planes, and not in front or behind it. In Figure 12, this is accomplished by the lens 50. The improvement in fringe visibility by the use of this lens can be dramatic.

Figure 18A illustrates why imaging the target to the interferometer mirror plane improves image superposition for aberrated optics. The effective mirror positions of the two arms of the detecting interferometer, delayed and non-delayed, are located at 70 and 72 after being superimposed by the beamsplitter. Suppose the effective mirror at position 72 has curvature due to distortions. Suppose also that a lens images the target to position 76 far from mirror positions 70 and 72. Then any mirror curvature greatly changes the magnification of one reflection 77 of the target image compared to the other 78. This increases the displacement vector $\delta\mathbf{r}$ between the twin images, which needs to be minimized to achieve visible fringes. However, if the target is imaged to position 80 (Figure 18B) near the mirror surfaces, no change in magnification is produced between its twin reflections 81 and 82.

9. Use with sound or microwaves

The delays and interferometers discussed have manipulated waves such as light traveling as rays in more than one spatial dimension. The same 3-dimensional configurations of lenses and reflectors can apply directly to other directional waves, such as sound and microwaves, provided the size of the elements is appropriately large so that diffraction of the waves is not serious. If the element size is small compared to the wavelength so the diffraction is relevant, then the shape of the elements may be slightly different.

10. One-dimensional configurations

If the wave travels along only one path (single-mode propagation), instead of a manifold of paths, then the superimposing requirement is moot. For example for microwaves and sound, an antenna or transducer can sample the 2 or 3-dimensional wavefield and produce a time-varying voltage. The voltage wave then propagates along an electrical cable in a single mode. A lens focusing light onto a single-mode optical fiber is another example.

For a single-mode wave, the superimposing interferometer simply consists of delaying a portion of the wave, and then recombining it. For an electrical wave, this can be implemented by analog delay lines, or done digitally after the voltage is converted to a number by an analog/digital converter. For a single-mode optical fiber, the interferometer can be implemented by fiber loops using appropriate single mode couplers acting as beamsplitters. These 1-D interferometers cannot form prompt imaging velocimeters. However, by scanning the beam from the antenna or transducer, an image can be constructed over time.

A single-mode fiber-optic interferometer can have enormous delay lengths not practical by use of open-air optics. This creates cm/s velocity sensitivity. In order to automatically compensate for fluctuations in fiber length due to temperature and physical vibrations, the reflected light from the target could be retro-reflected so that the

source and detecting interferometers are implemented by the same fiber.

11. For matter waves

Crystals and other structures having periodicity on a small length scale are known to interact with matter (such as electrons, neutrons, other sub-atomic particles, atoms and small molecules) as though they were waves. Thus, in principle it is possible to construct an interferometer for matter waves. Two such interferometers in series topologically and having nearly matched delays could measure the change in energy spectrum of waves reflecting off or transmitting through a target region being probed. Such a device could form a sensitive particle energy meter able to detect very slight energy changes. These could be caused, for example, by gravitational or electric fields, or absorption of energy when the particle beam interacts with the target, or emits other particles. The change in energy spectrum of the matter waves is treated by the invention analogous to the Doppler change in energy spectrum of light previously discussed.

VI. EXAMPLE APPARATUS USING RETRO-REFLECTED LIGHT

Figure 12 shows the apparatus of a demonstration white light velocimeter measuring a 16 m/s target using ordinary incandescent light. The color fringe output of it is shown in Figure 6A and 6B for stationary and moving target, respectively. A single Michelson interferometer with a superimposing relay lens delay (the optics in the dashed box 62) is used. By using the retro-reflected light from the target, the single interferometer accomplishes both source and detecting interferometer functions. This simplifies alignment and automatically insures the source and detecting delays match closely.

In order to measure the 16 m/s speed, the velocity per fringe coefficient was arranged to be $\eta \approx 19$ m/s per fringe, by a delay of $c\tau$=4 m. This delay is notably longer than that of a typical VISAR, which commonly has delays of only a few centimeters. Lens 50 images the target 64 to the interferometer mirror planes. This is important for good fringe visibility, since the effective mirror suffers some astigmatic distortion due to the off-axis reflection from the spherical mirror 52. The illumination source 10 was a 10× microscope objective roughly collimating the output of a 600 μm diameter fiber illuminated by a incandescent lamp. The target 69 is a fan with reflective tape on its blades, and a telescope or camera 70 is placed to receive the exit light traveling from beamsplitter 63. Mirrors 61 and 66 are plane mirrors, and mirrors 65 and 47 have a 1 m radius of curvature and are separated 1 m. Lens 46′ is a 1 m focal length lens. The other interferometer output (not used here) travels toward the source and is accessible by inserting a beamsplitter between beamsplitter 63 and source 10.

Figures 6A and 6B show the fringe output of the interferometer. The beamsplitter or interferometer mirror is slightly tilted to create a comb of fringes, so that the delay difference τ_s-τ_d varies transversely across the film record. The figures compares the fringes obtained for the stationary target to the fringes of the target moving at 16 m/s. The white arrows indicate the central fringe of the pattern. A shift in the fringe pattern is observed that is proportional to the target velocity.

The velocity is determined from the shift measured in terms of fringe spacing, which in turn depends on color. All of the colors are present and each create a fringe comb. Any of them can be used for the velocity determination. Observing through a 500 nm bandpass filter, a shift of $\Delta\phi = 0.85 \pm 0.07$ fringe was observed. For λ=500 nm, η=18.7 m/s from Eq. 4, a interferometrically measured velocity of 15.9± 1 m/s was measured. A stroboscope measuring rotational frequency, and measurement of the range of radii which the beam intercepted the blade yielded a velocity component toward the velocimeter of 15.7± 0.3 m/s.

This demonstration measured the target velocity averaged over an area defined by the illuminating beam cross-section on the target, because the camera was greatly defocused. To create a velocity image of the target, rather than measuring a single value velocity, the camera would be nearly focused, forming an image of the target on the film plane. The camera should not be perfectly focused unless the interferometer is perfectly aberrationless. Given that there is inevitably some displacement $\delta\mathbf{r}_2$ between the twin images of the target on the film plane, the camera must be defocused enough that the focal blur exceeds $\delta\mathbf{r}_2$, so that the two separate focal spots associated with pixels from each target twin image overlap.

Changes and modifications in the specifically described embodiments can be carried out without departing from the scope of the invention, which is intended to be limited by the scope of the appended claims.

Acknowledgments

This work was performed under the auspices of the U.S. Department of Energy by the University of California, Lawrence Livermore National Laboratory under contract No. W-7405-Eng-48.

VII. CLAIMS

(Submitted, not official version)

1. A method for generating partial fringes, comprising:

generating broad bandwidth illumination comprising a plurality of originating rays denoted white waves irrespective of actual wavelength and medium;

imprinting at least one coherent echo on said white waves to produce an imprinted beam, wherein each echo of said at least one coherent echo is superimposed in ray direction and position with the ray from which each said echo originated, wherein each echo of said at least one coherent echo is separated in time by a delay τ_s with respect to each other and to said white waves;

reflecting said imprinted beam from an object to produce a reflected beam comprising a plurality of reflected rays;

imprinting at least one second coherent echo on said reflected beam to produce a second imprinted beam, wherein for each reflected ray of said reflected beam, each echo of said at least one second coherent echo is superimposed in ray direction and position with the reflected ray from which said echo originated, wherein each echo of said at least one second coherent echo is separated in time by a delay τ_d with respect to each other and to said reflected beam; and

detecting the time-averaged intensity of said second imprinted beam; wherein the average is determined over a time at least as long as the coherence time of said white waves; wherein partial fringes occur in said intensity of said second imprinted beam when $\tau_s\tau_d$, within a coherence length.

2. The method of claim 1, further comprising:

repeating the above steps to produce a second set of partial fringes;

taking the phase difference between said partial fringes and said second set of partial fringes to produce a fringe shift; and

multiplying said fringe shift by a proportionality constant to produce a quantity selected from a group consisting of velocity and displacement.

3. A method for measuring the velocity or displacement of an object, comprising:

generating broad bandwidth illumination comprising a plurality of originating rays denoted white waves irrespective of actual wavelength and medium;

imprinting at least one coherent echo on said white waves to produce an imprinted beam, wherein each echo of said at least one coherent echo is superimposed in ray direction and position with the ray from which each said echo originated, wherein each echo of said at least one coherent echo is separated in time by a delay τ_s with respect to each other and to said white waves;

reflecting said imprinted beam from an object to produce a reflected beam comprising a plurality of reflected rays;

imprinting at least one second coherent echo on said reflected beam to produce a second imprinted beam, wherein for each reflected ray of said reflected beam, each echo of said at least one second coherent echo is superimposed in ray direction and position with the reflected ray from which said echo originated, wherein each echo of said at least one second coherent echo is separated in time by a delay τ_d with respect to each other and to said reflected beam;

detecting the time-averaged intensity of said second imprinted beam; wherein the average is determined over a time at least as long as the coherence time of said white waves, wherein partial fringes occur in said intensity of said second imprinted beam when $\tau_s\tau_d$, within a coherence length;

repeating the above steps to produce a second set of partial fringes;

taking the phase difference between said partial fringes and said second set of partial fringes to produce a fringe shift; and

multiplying said fringe shift by a proportionality constant to produce a quantity selected from a group consisting of velocity and displacement.

4. The method of claim 1, wherein the step of detecting the time-averaged intensity further comprises distributing detection of said time-average intensity into multiple detecting channels.

5. The method of claim 4, wherein said multiple detecting channels are organized by wavelength.

6. The method of claim 4, wherein said multiple detecting channels are organized by imprinted delay τ_d.

7. The method of claim 4, wherein said white waves comprise chirped waves having an instantaneous wavelength that changes as a function of time, in conjunction with said multiple detecting channels.

8. The method of claim 4, further comprising measuring the time dependence of target reflectivity with chirped waves comprising illumination having an instantaneous wavelength that changes as a function of time, in conjunction with said multiple detecting channels.

9. The method of claim 1, wherein said broad bandwidth illumination comprises periodic waves.

10. The method of claim 9, wherein said periodic waves are selected from a group consisting of electromagnetic radiation waves, pressure waves, sound waves and matter waves.

11. The method of claim 1, wherein said second imprinted beam comprises complementary output beams, said method further comprising subtracting intensities of said complementary output beams from each other.

12. The method of claim 1, wherein said second imprinted beam comprises complementary output beams, said method further comprising adding intensities of said complementary output beams to each other.

13. The method of claim 4, further comprising forming an image of said object on a detector of said multiple detecting channels.

14. The method of claim 13, wherein said image is selected from a group consisting of a line-image and a real image.

15. An apparatus for generating partial fringes, comprising:

means for generating broad bandwidth illumination comprising a plurality of originating rays denoted white waves irrespective of actual wavelength and medium;

means for imprinting at least one coherent echo on said white waves to produce an imprinted beam, wherein each echo of said at least one coherent echo is superimposed in ray direction and position with the ray from which each said echo originated, wherein each echo of said at least one coherent echo is separated in time by a delay τ_s with respect to each other and to said white waves;

means for reflecting said imprinted beam from an object to produce a reflected beam comprising a plurality of reflected rays;

means for imprinting at least one second coherent echo on said reflected beam to produce a second imprinted beam, wherein for each reflected ray of said reflected beam, each echo of said at least one second coherent echo is superimposed in ray direction and position with the reflected ray from which said echo originated, wherein each echo of said at least one second coherent echo is separated in time by a delay τ_d with respect to each other and to said reflected beam; and

means for detecting the time-averaged intensity of said second imprinted beam; wherein the average is determined over a time at least as long as the coherence time of said white waves; wherein partial fringes occur in said intensity of said second imprinted beam when $\tau_s\tau_d$, within a coherence length.

16. The apparatus of claim 15, wherein said means for generating broadband illumination comprises a source of waves whose bandwidth is greater than $1/\tau_s$, wherein said source comprises a set of individually narrow bands if the overall bandwidth of the set is greater than $1/\tau_s$.

17. The apparatus of claim 16, wherein said source is selected from a group consisting of incandescent lamps, the sun, explosive compression of gases, electric discharges, gas discharge lamps, fluorescence, flames, light emitting diodes, diode lasers, lasers operated simultaneously in more than one wavelength, combinations of lasers which individually are monochromatic, short pulse lasers, chirped lasers.

18. The apparatus of claim 16, wherein said source is selected from a group consisting of vibration and any broad bandwidth sound.

19. The apparatus of claim 16, wherein said source is selected from a group consisting of noise, explosions, impulsive pressures created from laser irradiation and sound created from a transducer.

20. The apparatus of claim 16, wherein said source comprises broad bandwidth electromagnetic waves selected from a group consisting of radio waves, microwaves, ultraviolet lamps, x-rays sources and broad bandwidth matter waves selected from a group consisting of beams of electron, neutrons, alpha particles and atoms.

21. The apparatus of claim 15, wherein each echo of said at least one coherent echo is superimposed in ray direction and position with the ray from which each said echo originated, wherein each echo of said at least one coherent echo is separated in time by a delay τ_s with respect to each other and to said white waves.

22. The apparatus of claim 15, wherein said means for imprinting at least one coherent echo comprise a superimposing interferometer selected from a group consisting of a superimposing Fabry-Perot and a superimposing Michelson, wherein said Fabry-Perot comprises interferometers creating an infinite number of echos of decreasing intensity for a given applied pulse, wherein said Michelson comprises interferometers creating a finite number of echos for a given applied pulse, including variants such as the Twyman-Green, Mach-Zehnder and Sagnac arrangements, wherein said Fabry-Perot further comprises means for imaging the surface of one partially reflective mirror to another imaging lens or spherical mirror internal to the partially reflective mirror cavity, wherein said Michelson further comprises a superimposing delay in one interferometer arm, said superimposing delay comprising optical elements selected from a group consisting of combinations of lenses and curved and plane mirrors, optical fibers with graded refractive index and distributed mirrors.

23. A method for measuring the change in energy spectrum of white waves interacting with a potential-field or matter in a region of the target volume, which could be free-space, comprising:

generating broad bandwidth illumination comprising a plurality of originating rays denoted white waves irrespective of actual wavelength and medium;

imprinting at least one coherent echo on said white waves to produce an imprinted beam, wherein each echo of said at least one coherent echo is superimposed in ray direction and position with the ray from which each said echo originated, wherein each echo of said at least one coherent echo is separated in time by a delay τ_s with respect to each other and to said white waves;

transmitting said imprinted beam through a volume to produce a transmitted beam comprising a plurality of transmitted rays;

imprinting at least one second coherent echo on said transmitted beam to produce a second imprinted beam, wherein for each transmitted ray of said transmitted beam, each echo of said at least one second coherent echo is superimposed in ray direction and position with the transmitted ray from which said echo originated, wherein each echo of said at least one second coherent echo is separated in time by a delay τ_d with respect to each other and to said transmitted beam;

detecting the time-averaged intensity of said second imprinted beam; wherein the average is determined over a time at least as long as the coherence time of said white waves; wherein partial fringes occur in said intensity of said second imprinted beam when $\tau_s \tau_d$, within a coherence length,

repeating the above steps to produce a second set of partial fringes;

taking the difference between said partial fringes and said second set of partial fringes to produce a fringe shift; and

converting said fringe shift into a change in energy spectrum of said white waves.

24. An apparatus for measuring the change in energy spectrum of white waves interacting with a potential-field or matter in a region of the target volume, which could be free-space, comprising:

means for generating broad bandwidth illumination comprising a plurality of originating rays denoted white waves irrespective of actual wavelength and medium;

means for imprinting at least one coherent echo on said white waves to produce an imprinted beam, wherein each echo of said at least one coherent echo is superimposed in ray direction and position with the ray from which each said echo originated, wherein each echo of said at least one coherent echo is separated in time by a delay τ_s with respect to each other and to said white waves;

means for transmitting said imprinted beam through a volume to produce a transmitted beam comprising a plurality of transmitted rays;

means for imprinting at least one second coherent echo on said transmitted beam to produce a second imprinted beam, wherein for each transmitted ray of said transmitted beam, each echo of said at least one second coherent echo is superimposed in ray direction and position with the transmitted ray from which said echo originated, wherein each echo of said at least one second coherent echo is separated in time by a delay τ_d with respect to each other and to said transmitted beam; and

means for detecting the time-averaged intensity of said second imprinted beam; wherein the average is determined over a time at least as long as the coherence time of said white waves; wherein partial fringes occur in said intensity of said second imprinted beam when $\tau_s \tau_d$, within a coherence length.

Part 2
White Light Velocity Interferometer, continued

This is a continuation of US Patent 5,642,194. Only the claims section is different.

US Patent 5,910,839
Issued June 8, 1999

David J. Erskine*
Lawrence Livermore Nat. Lab.

The invention is a technique that allows the use of unlimited bandwidth and extended illumination sources to measure small Doppler shifts of targets external to the apparatus. Monochromatic and point-like sources can also be used, thus creating complete flexibility for the illumination source. Although denoted white light velocimetry, the principle can be applied to any wave phenomenon, such as sound, microwaves and light. For the first time, powerful, compact or inexpensive broadband and extended sources can be used for velocity interferometry, including flash and arc lamps, light from detonations, pulsed lasers, chirped frequency lasers, and lasers operating simultaneously in several wavelengths. Superimposing interferometers are created which produce delays independent of ray angle for rays leaving a given pixel of an object, which can be imaged through the interferometer.

I. CLAIMS

(Submitted, not official version)

1. A method of imprinting at least one coherent echo on a beam, comprising:

creating an apparent mirror by real imaging or virtual imaging of an end mirror, wherein the imaged surface of said end mirror defines the location of said apparent mirror, wherein the imaged center of curvature of said end mirror defines the center of curvature of said apparent mirror;

providing a second mirror optimally having the same curvature as said apparent mirror; and

superimposing the location of said second mirror with the location of said apparent mirror in the reflection of a beamsplitting surface.

2. The method of claim 1, wherein said apparent mirror can be slightly tilted from perfect overlap in order to create a delay time which varies with position across the plane of said apparent mirror, wherein said beam can be any wave kind which travels in 2 or 3 dimensions.

3. The method of claim 2, wherein said wave kind comprises electromagnetic waves selected from a group consisting of microwaves, visible light, infrared light, ultraviolet light and x-rays.

4. The method of claim 2, wherein said wave kind comprises sound waves.

5. The method of claim 1, wherein said beam is uncollimated, wherein said beam comprises a range of ray angles significant enough to prevent a coherent delay if said beam were to propagate in free space over a distance comparable to the distance between said apparent mirror and said end mirror.

6. The method of claim 1, wherein said real imaging is accomplished using at least one elements selected from a group consisting of lenses, curved mirrors, plane mirrors, distributed mirrors and waveguides.

7. The method of claim 6, wherein said real imaging is accomplished using at least one transmissive lens and said end mirror.

8. The method of claim 7, wherein said end mirror comprises a curved mirror.

9. The method of claim 6, wherein said end mirror comprises a plane mirror in combination with a lens which together effectively act as a curved mirror.

10. The method of claim 6, wherein said real imaging is accomplished by a transmissive lens, at least one center curved mirror and said end mirror.

11. The method of claim 10, wherein said end mirror comprises a curved mirror.

12. The method of claim 10, wherein said end mirror comprises a plane mirror in combination with a lens which together effectively act as a curved mirror.

13. The method of claim 1, wherein the optics forming said apparent mirror are achromatic so that the location of said apparent mirror is approximately constant over a significant range of wavelengths.

14. The method of claim 1, wherein at least one of the elements forming said apparent mirror is a distributed mirror comprising an effective reflective surface depth that is a function of wavelength.

15. The method of claim 14, wherein said effective reflective surface depth wavelength dependence compensates for chromatic dispersion of other elements forming said apparent mirror so that the net chromatic abberation of said apparent mirror is reduced.

16. The method of claim 1, wherein said virtual imaging is accomplished using lenses and a curved end mirror.

17. A method of imprinting an infinite series of diminishing amplitude coherent echos on a beam, comprising:

creating an apparent mirror by real or virtual imaging of a first end mirror, which may be partially transmitting;

providing a second end mirror having the same curvature and curvature polarity as said apparent mirror, wherein said second end mirror may be partially transparent;

*erskine1@llnl.gov

superimposing said second end mirror with said apparent mirror so that a recirculating path is created having a magnification of positive unity for a roundtrip along the optic axis, wherein said roundtrip is from said first end mirror to said second end mirror then back to said first end mirror;

introducing said beam to said recirculating path by partial transmission through a partially reflecting surface; and

extracting a portion of said beam from said recirculating path through a partially transmitting surface, wherein the roundtrip travel time along said recirculating path determines the interferometer delay time, wherein said portion comprises an infinite series of diminishing amplitude coherent echos.

18. The method of claim 17, wherein said beam is uncollimated, wherein said beam comprises a range of ray angles significant enough to prevent a coherent delay if said beam were to propagate in free space over a distance comparable to the distance between said apparent mirror and said first end mirror.

19. The method of claim 17, wherein said real imaging is accomplished using at least one element selected from a group consisting of lenses, curved mirrors, plane mirrors, distributed mirrors and waveguides.

20. The method of claim 19, wherein said real imaging is accomplished by at least one lens and said end mirror.

21. The method of claim 20, wherein said end mirror comprises a curved mirror.

22. The method of claim 20, wherein said end mirror comprises a plane mirror in combination with a lens which together effectively act as a curved mirror.

23. The method of claim 20, wherein said real imaging is accomplished using at least one curved mirror and and said end mirror.

24. The method of claim 23, wherein said end mirror comprises a curved mirror.

25. The method of claim 23, wherein said end mirror comprises a plane mirror in combination with a lens which together effectively act as a curved mirror.

26. A method of coherently delaying a beam, comprising;

creating an apparent mirror by real or virtual imaging of an end mirror, wherein the imaged surface of said end mirror defines the location of said apparent mirror, wherein the imaged center of curvature of said end mirror defines the center of curvature of said apparent mirror; and

reflecting said beam off said apparent mirror, wherein the beam is delayed by the interval of round trip travel between said apparent mirror and said end mirror and back to said apparent mirror, wherein the beam can be any wave kind which travels in 2 or 3 dimensions.

27. The method of claim 26, wherein said wave kind is visible light.

28. The method of claim 26, wherein said wave kind comprises electromagnetic waves selected from a group consisting of microwaves, visible light, infrared light, ultraviolet light and x-rays.

29. The method of claim 26, wherein said wave kind comprises sound waves.

30. The method of claim 26, wherein said wave kind comprises matter waves.

31. The method of claim 26, wherein said beam is uncollimated, wherein said beam comprises a range of ray angles significant enough to prevent a coherent delay if said beam were to propagate in free space over a distance comparable to the distance between said apparent mirror and said end mirror.

32. The method of claim 26, wherein said real imaging is accomplished using at least one element selected from a group consisting of lenses, curved mirrors, plane mirrors, distributed mirrors and waveguides.

33. The method of claim 32, wherein said real imaging is accomplished with at least one lens and said end mirror.

34. The method of claim 33, wherein said end mirror comprises a curved mirror.

35. The method of claim 33, wherein said end mirror comprises a plane mirror in combination with a lens which together effectively act as a curved mirror.

36. The method of claim 32, wherein the real imaging is accomplished with a transmissive lens, at least one center curved mirror and said end mirror.

37. The method of claim 36, wherein said end mirror comprises a curved mirror.

38. The method of claim 36, comprises a plane mirror in combination with a lens which together effectively act as a curved mirror.

39. The method of claim 26, wherein the optics forming said apparent mirror are individually or as a group achromatic so that the location of said apparent mirror is approximately constant over a significant range of wavelengths.

40. The method of claim 26, wherein at least one of the elements forming said apparent mirrors comprises a distributed mirror whose effective reflective surface depth is a function of wavelength.

41. The method of claim 40, wherein the wavelength dependence of said effective reflective surface depth compensates for chromatic dispersion of other elements forming said apparent mirror so that the net chromatic abberations of said apparent mirror is reduced.

42. The method of claim 26, wherein said virtual imaging is accomplished by a lens and a curved end mirror.

43. An apparatus for imprinting at least one coherent echo on a beam, comprising:

means for creating an apparent mirror by real imaging or virtual imaging of an end mirror, wherein the imaged surface of said end mirror defines the location of said apparent mirror, wherein the imaged center of curvature of said end mirror defines the center of curvature of said apparent mirror;

providing a second mirror optimally having the same curvature as said apparent mirror; and

superimposing the location of said second mirror with the location of said apparent mirror in the reflection of a beamsplitting surface.

44. The apparatus of claim 43, wherein said wave kind comprises light.

45. The apparatus of claim 43, wherein said wave kind comprises electromagnetic waves selected from a group consisting of microwaves, visible light, infrared light, ultraviolet light and x-rays.

46. The apparatus of claim 43, wherein said wave kind comprises sound waves.

47. The apparatus of claim 43, wherein said beam is uncollimated, which is to say that there is a range of ray angles significant enough to prevent a coherent delay if said beam were to propagate in free space over a distance comparable to the distance between said apparent mirror and said end mirror.

48. The apparatus of claim 43, wherein said real imaging is accomplished using at least one element selected from a group consisting of lenses, curved mirrors, plane mirrors, distributed mirrors and waveguides.

49. The apparatus of claim 48, wherein said real imaging is accomplished by one or more transmissive lenses and said end mirror.

50. The apparatus of claim 49, wherein said end mirror comprises a curved mirror.

51. The apparatus of claim 49, wherein said end mirror comprises a plane mirror in combination with a lens which together effectively act as a curved mirror.

52. The apparatus of claim 48, wherein said real imaging is accomplished by a transmissive lens, at least one center curved mirror and said end mirror.

53. The apparatus of claim 52, wherein said end mirror comprises a curved mirror.

54. The apparatus of claim 52, wherein said end mirror comprises a plane mirror in combination with a lens which together effectively act as a curved mirror.

55. The apparatus of 43, wherein the optics forming said apparent mirror are individually or as a group achromatic so that the location of said apparent mirror is approximately constant over a significant range of wavelengths.

56. The apparatus of 43, wherein at least one of the elements forming said apparent mirror comprises a distributed mirror whose effective reflective surface depth is a function of wavelength.

57. The apparatus of 56, wherein the wavelength dependence of said effective reflective surface depth compensates for chromatic dispersion of other elements forming said apparent mirror so that the net chromatic abberations of said apparent mirror are reduced.

58. The apparatus of claim 43, wherein said virtual imaging is accomplished by one or more lenses and a curved said end mirror.

59. An apparatus for imprinting an infinite series of diminishing amplitude coherent echos on a beam, comprising:

means for creating an apparent mirror by real or virtual imaging of an end mirror, which may be partially transmitting;

a second end mirror having the same curvature and curvature polarity as said apparent mirror, wherein this second end mirror may be partially transparent, wherein said second end mirror is superimposed with said apparent mirror so that a recirculating path is created having a magnification of positive unity for a roundtrip along the optic axis, wherein said roundtrip is from said first end mirror to said second end mirror then back to said first said end mirror;

a partially reflecting/transmitting surface through which said beam can be introduced into said recirculating path;

a partially reflecting/transmitting surface through which a portion of said beam from said recirculating path can be extracted, wherein the interferometer delay time is determined by the roundtrip travel time along said recirculating path.

60. The apparatus of claim 59, wherein said beam is uncollimated, wherein said beam comprises a range of ray angles significant enough to prevent a coherent delay if said beam were to propagate in free space over a distance comparable to distance between said apparent mirror and said first end mirror.

61. The apparatus of claim 59, wherein said real imaging is accomplished using at least one element selected from a group consisting of lenses, curved mirrors, plane mirrors, distributed mirrors and waveguides.

62. The apparatus of claim 61, wherein said real imaging is accomplished by at least one lens and said end mirror.

63. The apparatus of claim 62, wherein said end mirror comprises a curved mirror.

64. The apparatus of claim 62, wherein said end mirror comprises a plane mirror in combination with a lens which together effectively act as a curved mirror.

65. The apparatus of claim 62, wherein said real imaging is accomplished using one or more curved mirrors and said end mirror.

66. The apparatus of claim 65, wherein said end mirror comprises a curved mirror.

67. The apparatus of claim 65, wherein said end mirror comprises a plane mirror in combination with a lens which together effectively act as a curved mirror.

68. An apparatus for coherently delaying a beam, comprising;

an end mirror; and

means for creating an apparent mirror by real or virtual imaging of said end mirror, wherein the imaged surface of said end mirror defines the location of said apparent mirror, wherein the imaged center of curvature of said end mirror defines the center of curvature of said apparent mirror, wherein said beam is reflected off said apparent mirror, wherein the beam is delayed by the interval of round trip travel between said apparent mirror and said end mirror and back to said apparent mirror, wherein the beam can be any wave kind which travels in 2 or 3 dimensions.

69. The apparatus of claim 68, wherein said wave kind comprises visible light.

70. The apparatus of claim 68, wherein said wave kind comprises electromagnetic waves selected from a group consisting of microwaves, visible light, infrared light, ultraviolet light and x-rays.

71. The apparatus of claim 68, wherein said wave kind comprises sound waves.

72. The apparatus of claim 68, wherein said wave kind comprises matter waves.

73. The apparatus of claim 68, wherein said beam is uncollimated, wherein said beam comprises a range of ray angles significant enough to prevent a coherent delay if said beam were to propagate in free space over a distance comparable to the distance between said apparent mirror and said end mirror.

74. The apparatus of claim 68, wherein said real imaging is accomplished using at least one element selected from a group consisting of lenses, curved mirrors, plane mirrors, distributed mirrors and waveguides.

75. The apparatus of claim 74, wherein said real imaging is accomplished by at least one lens and said end mirror.

76. The apparatus of claim 75, wherein said end mirror comprises a curved mirror.

77. The apparatus of claim 75, wherein said end mirror comprises a plane mirror in combination with a lens which together effectively act as a curved mirror.

78. The apparatus of claim 74, wherein the real imaging is accomplished by a transmissive lens, at least one center curved mirror, and said end mirror.

79. The apparatus of claim 78, wherein said end mirror comprises a curved mirror.

80. The apparatus of claim 78, wherein said end mirror comprises a plane mirror in combination with a lens which together effectively act as a curved mirror.

81. The apparatus of 68, wherein the optics forming said apparent mirror are individually or as a group achromatic so that the location of said apparent mirror is approximately constant over a significant range of wavelengths.

82. The apparatus of 68, wherein at least one of the elements forming said apparent mirror comprises a distributed mirror whose effective reflective surface depth is a function of wavelength.

83. The apparatus of 82, wherein the wavelength dependence of said effective reflective surface depth compensates for chromatic dispersion of other elements forming said apparent mirror so that the net chromatic abberations of said apparent mirror is reduced.

84. The apparatus of claim 68, wherein said virtual imaging is accomplished by a lens and a curved said end mirror.

85. The method of claim 2, wherein said wave kind comprises light waves.

86. The method of claim 2, wherein said wave kind comprises matter waves.

87. The apparatus of claim 43, wherein said wave kind comprises matter waves.

Acknowledgments

This work was performed under the auspices of the U.S. Department of Energy by the University of California, Lawrence Livermore National Laboratory under contract No. W-7405-Eng-48.

Part 3

Noise-Pair Velocity and Range Echo-Location System

US Patent 5,872,628
Issued Feb. 16, 1999

David J. Erskine*
Lawrence Livermore Nat. Lab.

An echo-location method for microwaves, sound and light capable of using incoherent and arbitrary waveforms of wide bandwidth to measure velocity and range (and target size) simultaneously to high resolution. Two interferometers having very long and nearly equal delays are used in series with the target interposed. The delays can be longer than the target range of interest. The first interferometer imprints a partial coherence on an initially incoherent source which allows autocorrelation to be performed on the reflected signal to determine velocity. A coherent cross-correlation subsequent to the second interferometer with the source determines a velocity discriminated range. Dithering the second interferometer identifies portions of the cross-correlation belonging to a target apart from clutter moving at a different velocity. The velocity discrimination is insensitive to all slowly varying distortions in the signal path. Speckle in the image of target and antenna lobing due to parasitic reflections is minimal for an incoherent source. An arbitrary source which varies its spectrum dramatically and randomly from pulse to pulse creates a radar elusive to jamming. Monochromatic sources which jigger in frequency from pulse to pulse or combinations of monochromatic sources can simulate some benefits of incoherent broadband sources. Clutter which has a symmetrical velocity spectrum will self-cancel for short wavelengths, such as the apparent motion of ground surrounding target from a sidelooking airborne antenna.

I. INTRODUCTION

A. Field of the Technology

The present invention relates to the simultaneous measurement of target velocity and position by microwaves (radar), sound (sonar and ultrasound) and light, and more specifically, it relates to the use of long delay interferometric techniques, short coherence length illumination and the Doppler effect to measure velocity and range.

B. Description of the Background

Measuring the velocity and range of an object remotely by the response of reflected waves (microwaves, light and sound) is an important diagnostic tool in a variety of fields in science and engineering. In many cases, the velocimetry and range finding are accomplished by opposite kinds of illuminating waves. Traditionally, highly coherent and therefore narrowbanded illumination is used for velocimetry, so that the Doppler frequency shift in the reflected waves is larger than the illumination bandwidth β. This allows the Doppler frequencies of moving targets to be easily distinguished from those of stationary objects by the use of narrowbanded filters. In contrast, for range finding a short coherence length Λ is desired, since half the coherence length defines the range resolution. A short coherence length implies broadband illumination because of the reciprocal relationship $\Lambda \sim c/\beta$, where c is the speed of the waves. Thus, illumination optimized for conventional velocimetry is very different from that optimized for range finding.

For example, monochromatic laser illumination is conventionally used for optical velocimetry, whereas broadband and incoherent light such as white light is used for rangefinding, which in optics is called optical coherence tomography. Pulse Doppler radars are used for velocimetry having monochromatic waves enveloped into $\sim$1 μs pulses. The range resolution of these is limited by the $\sim$300 meter pulse envelope length. In contrast, range finding or mapping radars use illumination having a much shorter coherence length. This is often achieved by increasing the bandwidth of the waveform through frequency modulation or the repetitive use of a coded pulse to simulate randomness.

A theoretical optimum waveform for many range find-

*erskine1@llnl.gov

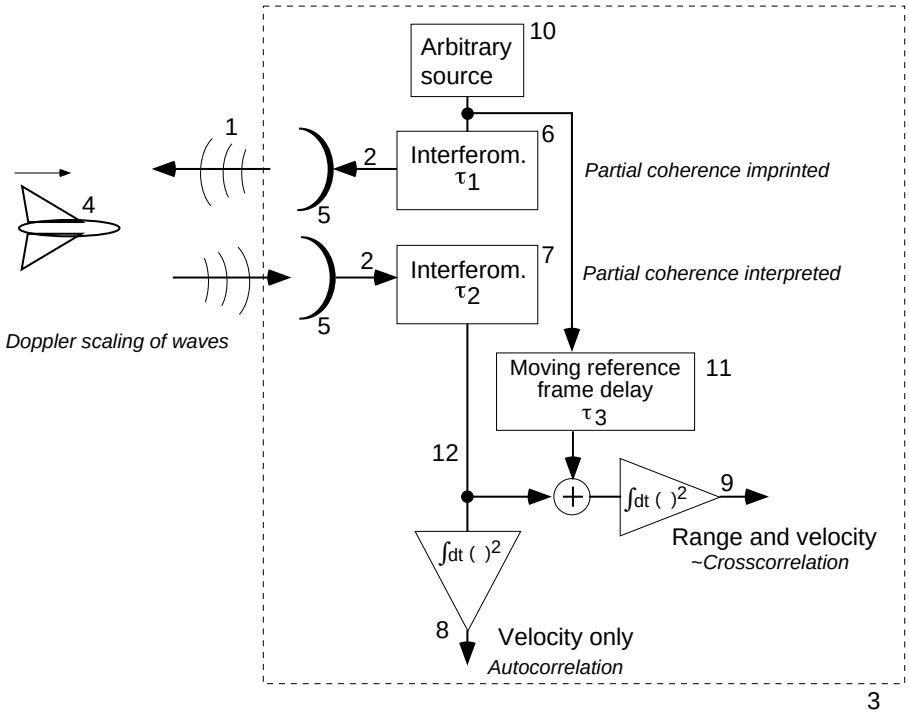

Figure 1A illustrates a block diagram of the invention.

ing applications is wideband and incoherent, analogous to white light generated by incandescence. For radar and sonar this could be generated by an electronic noise source. A truly incoherent waveform is random and therefore never repeats. This is an advantage because any speckle or temporary coherences in the echolocation target image is blurred away, improving the observation of detail. Incoherent illumination will not suffer the interference effect between the transmitted beam and parasitic reflections from the Earth, thus minimizing the lobed characteristics of antennas in the altitude direction. A further advantage of incoherent illumination over a short pulse or frequency modulated pulse having the same coherence length is that a random waveform can be arbitrarily long without repetition. That is, its time-bandwidth product can be arbitrarily large. The longer pulse carries correspondingly more energy to the target, which increases the maximum range of detection.

An important desirable trait of echolocation systems is the ability to measure velocity and range simultaneously to high resolution. In radar, the velocity resolution is used to separate moving targets from ground clutter. Once detected, the range and if possible, the size of the target is desired to be known. In medical ultrasound, the motion of the blood can distinguish blood vessels from surrounding tissues. A map of the vessels having high spatial resolution and color coded by velocity is the goal of these devices.

Measuring the velocity and range simultaneously to high resolution is possible by measuring the range to high resolution at two different, but well defined times and finding the rate of change. This is accomplished in some radars using short coherence waves and by cross correlating the reflected and transmitted signals. A disadvantage with a cross-correlation is that distortions in the waves suffered anywhere between the transmitter and receiver can broaden the cross-correlation peak, and hence can blur the velocity determination. Such distortions could include distortions in the final stages of the transmitting amplifier, the effect of propagation through the atmosphere, the target albedo spectrum such as resonances, and reverberations from previous pings.

A different method for determining velocity is the autocorrelation. This is a comparison of the received signal with itself delayed by a time τ_2. For those waveforms which produce an autocorrelation peak, the peak shifts with velocity v by an amount $\Delta\tau_2 = 2\tau_2 v/c$. The advantage of the autocorrelation is that it will not broaden by slowly varying distortions, which includes many practical distortions. Thus the autocorrelation will give an accurate velocity under distortions that would cause a cross-correlation to blur.

The problem is that autocorrelations cannot be used with the most desirable illumination, perfectly random and ever changing waveforms, because these waveforms are by definition incoherent over all delay scales. The method of the present invention is a solution to this problem. In addition to velocimetry using incoherent illumination, the invention is capable of measuring range and velocity simultaneously to high resolution, providing a way to discriminate moving targets from background clutter.

II. SUMMARY OF THE INVENTION

It is an object of the present invention to use an arbitrary waveform, which may be incoherent, to measure the range and velocity of a target by autocorrelating and cross-correlating the waves reflected from the target.

It is also an object of the present invention to provide a method to produce partially coherent illumination from arbitrary waveforms which could be incoherent.

Properties of the target which produce a dilation or contraction of the illuminating waveform can be measured by this method, where the illuminating beam can either reflect or pass through the target. For example, if the target consists of a region containing plasma, the time rate of change of the plasma density will dilate or contract the waveform of the reflected or transmitted illumination similar to the Doppler effect of a moving reflector.

A transmitter comprises a wave source, an interferometer having a delay τ_1, and an antenna or transducer for sending the waves toward the target. The transmitting interferometer imprints the source with partial coherence for a very specific delay τ_1, and uses this for illuminating the target. A receiver comprises an antenna or transducer for detecting the waves reflected from the target, and a second interferometer of delay τ_2 nearly identical to τ_1. The output of the receiving interferometer is converted to a time-averaged intensity which constitutes an autocorrelation. The autocorrelation can be interpreted to yield target velocity. The output of the receiving interferometer is also added to a copy of the source waveform, copied prior to the transmitting interferometer, and delayed in time by τ_3 to form a combined signal. The time-averaged intensity of this combined signal versus τ_3 constitutes a cross-correlation which gives range information. By slightly dithering the value of $(\tau_1 - \tau_2)$, the portions of the cross-correlation associated with a target moving at a specific velocity will fluctuate synchronously with the dither. Thus the range of targets having specific velocities can be identified in the cross-correlation apart from other targets having different velocities. This allows a moving aircraft to be detected even though its radar reflections are overlapped by reflections from stationary ground clutter.

The transmitting interferometer allows the use of a incoherent source by imprinting a partial coherence to it, for a very specific delay value of τ_1. On other lengths scales, the illumination sent to the target appears incoherent. Without the transmitting interferometer, the autocorrelation at the receiver would not produce a peak which can be interpreted into velocity, and the cross-correlation would not depend on the dither of $(\tau_1 - \tau_2)$, so there would be no velocity discrimination in the range measurement.

By the use of a incoherent wideband source waveform, high range and velocity resolutions are achieved simultaneously due to the short illumination coherence length. Most of the randomness of the source is preserved in the imprinted waveform used for illumination. This randomness blurs any speckle in the cross-correlation due to temporary coherences. A random waveform delivers a large energy to the target without repeating. Repetition is avoided to reduce range and velocity ambiguities.

It is an object of the interferometers to produce from an applied waveform an output waveform consisting of an undelayed waveform and a finite number of delayed waveforms, called echos. The time separation between the undelayed and each of the delayed waveforms is defined the interferometer delay. The delayed and undelayed waveforms must be coherent replicas of each other. However, it is allowed that the undelayed and delayed waveforms differ from the applied waveform. That is, distortion is allowed in the interferometer mechanism provided the distortion affects undelayed and delayed waveforms equally. This allows inexpensive schemes to create the interferometer delays which may not treat all fequency components equally.

III. DETAILED DESCRIPTION OF THE INVENTION

A. Overview

Figure 1A shows an overview of the invention, consisting of a means for performing interferometry, autocorrelations and cross-correlations, called the apparatus 3, and a means 5 such as an antenna or transducer for converting the waves 1 propagating between the target 4 and apparatus into the waves 2 which will carry the information through the apparatus. The source 10 generates a waveform which can be nearly arbitrary, the exception described later. The preferred embodiment is for a wideband waveform having a very short coherence length Λ and which is incoherent on all other length scales, and which is ever evolving in a random way so that speckle in the correlations are washed out over time.

The source passes through an interferometer 6, called the transmitting interferometer, which has a very long delay τ_1 compared to Λ. A second interferometer, called the receiving interferometer 7 has a delay τ_2 very nearly matched to τ_1. The time averaged intensity 8 of the receiving interferometer output is equivalent to an autocorrelation. The transmitting interferometer imprints a partial coherence on the source waveform that allows the subsequent autocorrelation of the received signal to produce a peak at delays τ_2 near τ_1. The peak's shift determines the velocity. A cross-correlation 9 of the receiving interferometer output and the source yields range and velocity information. By dithering τ_2, the portions of the cross-correlation corresponding to a moving target of a particular velocity can be distinguished from other objects having different velocities. Thus output 9 can be called a velocity discriminated range signal.

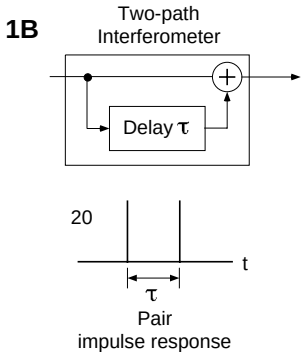

Figure 1B illustrates a two-path interferometer concept and its impulse response.

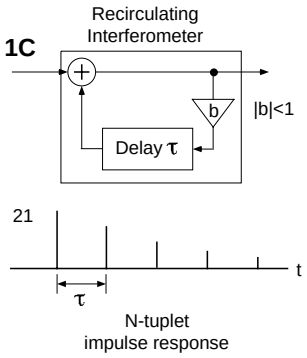

Figure 1C illustrates a recirculating interferometer concept and its impulse response.

B. About the interferometers

The partial coherence is imprinted on the source waveform by the transmitting interferometer by creating from the original waveform a pair or N-tuplet of waveform replicas, where N is not infinite, and the replicas are separated in time by τ_1. Without this imprinting, an incoherent source would not create an autocorrelation peak near τ_1, because that is the definition of incoherence. The preferred embodiments use either a two-path interferometer (Fig. 1B) or a recirculating interferometer (Fig. 1C). The two-path interferometer creates two equal strength pulses in its impulse response separated by τ. The recirculating interferometer creates an infinite number separated by τ having a geometrically decreasing strength. The number of pulses having at least 50% of the original amplitude is approximately N. Other interferometer impulse responses are permissible, provided the spacing of output pulses is a uniform τ.

As the recirculating gain coefficient $|b|$ approaches unity, the N approaches infinity. An infinite value for N is not preferred because then it is impossible for the output waveform to change. An evolving waveform is preferred so that speckle (temporary coherences) is removed by averaging. On the other hand, increasing N increases the robustness of the autocorrelation to statistical noise somewhat. The optimum N may depend on the noise environment, but is likely to be N=2 to 4.

The term "replica" in the definition of the interferometer should be qualified. The undelayed and delayed components of the interferometer output must be coherently identical to each other. However, these are allowed to differ from the waveform applied to the interferometer. This is equivalent to allowing a distortion 322 or 320 in the interferometer mechanism, as shown in Fig. 1E, provided the distortion affects delayed 321 and undelayed 325 portions of the waveform equally.

C. Measuring a Doppler Shift

The process that allows a slight Doppler shift to be measured from a short coherence length waveform can be explained by Figures 2A-E. Fig. 2A shows an optical embodiment of the invention that measures only the velocity and not the range, corresponding to output 8 of Fig. 1A. This apparatus is described in U. S. Patent Application Serial Number 08/597,082, incorporated herein by reference. Although the waveform in general can be of arbitrary length, the explanation is simplest by modeling the source 21 as a single very short pulse 36 having the same duration as the coherence time Λ/c. The source waveform passes through a transmitting interferometer 22, reflects off a target 24, and passes through a receiving interferometer 23. The interferometer delays τ_1 and τ_2 are approximately equal, their gross value is denoted τ where $\tau = \tau_1 \approx \tau_2$. For example, in one embodiment of Fig. 2A $\tau \approx 10^{-8}$ s and τ_1 and τ_2 may differ by 10^{-14} s, which is a million times smaller than τ. The time averaged intensity of the receiving interferometer complementary outputs $\langle I^+ \rangle$ 26 and $\langle I^- \rangle$ 27 are detected by detectors 38 and 39. The integration time of the detectors is longer than the coherence time Λ/c.

Figure 2B shows a hypothetical single source pulse. Fig. 2C shows the pair of identical pulses created by the transmitting interferometer. Fig. 2D shows the pair after reflection from the target 24 moving with velocity v toward the apparatus. The pulse separation has changed from τ_1 to $\tau_1 D$ due to the Doppler effect, where D is the Doppler scaling factor $D = (1 - 2v/c)$. That is, during the interval τ_1, the target has closed its range by $2v\tau_1$ and hence shortened the arrival time of the second pulse by $2v\tau_1/c$. (This assumes the illumination reflects normally from the target. For other angles, the term $2v$ should be replaced be the time rate of change of the combined distance between the transmitter to target to receiver.)

The receiving interferometer creates a pulse pair for each of the two pulses applied to it, creating a total of four pulses, shown in Fig. 2E. The two inner pulses 33, 34 overlap if $\tau_1 D \approx \tau_2$ within the coherence length Λ, interfering constructively or destructively depending on the exact time difference. Suppose the total energy of these four pulses are integrated by the detector. The two pulses 32, 35 on the early and late ends contribute con-

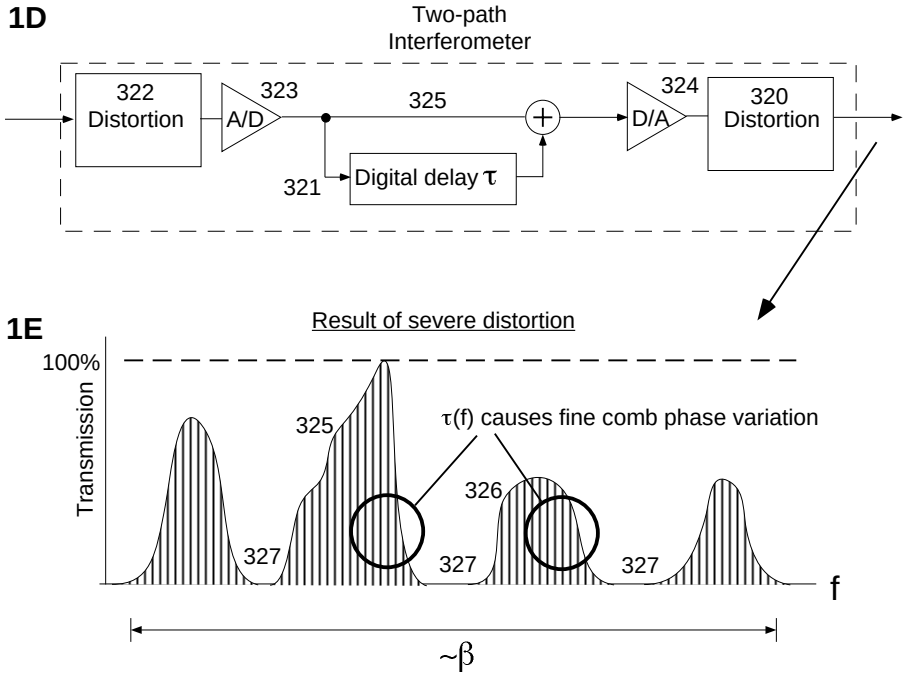

Figure 1D illustrates a digital embodiment of a two-path interferometer. Figure 1E illustrates the transmission spectrum of an interferometer with severe distortion.

stant energy, independent of the Doppler multiplier. The two inner pulses 33, 34 contribute a fluctuating amount of energy, depending on whether there is constructive or destructive interference. That is, their contribution depends on the Doppler multiplier. These fluctuations are called fringes. Since 2 of 4 pulses contribute to the fluctuating portion, the fringe visibility is 50%. The target velocity is determined from the phase of the fringes.

Since long incoherent waveforms can be modeled as a superposition of many short pulses of duration Λ/c, this explanation also applies to a source of random waves having arbitrary length. It is not required that the detector be so slow that it integrates over all 4 pulses, it is only necessary to integrate over the inner two 33 and 34, and thus time average over approximately Λ/c. Thus, after an initial dwell time of τ_2, the receiver becomes sensitive to Doppler shifts, and can detect them as rapidly as on the time scale of Λ/c. Practical embodiments however will use a much slower averaging time to reduce statistical fluctuations present in incoherent sources.

The apparatus of Fig. 2A used so-called two path interferometers that create a pair of replica waveforms from the source. The method also works for so-called recirculating interferometers that generate an N-tuplet of replicas.

D. Velocity from Phase Shift

The fringes are only formed for a specific range of delays, when $|\tau_1 D - \tau_2| = \Lambda/c$. Thus short coherence length sources produce the best velocity discrimination. This is relevant when there is more than one target contributing to the reflected signal. For a single target, any coherence length can be used. The term clutter denotes an undesired target, usually of small velocity such as the ground, that also contributes reflections.

The velocity is determined by the shift in phase of the fringes. During the interferometer delay τ, the target range has changed by $2v\tau$, and this divided by the average wavelength $\langle\lambda\rangle$ yields the number of fringes shifted from the zero velocity point. Thus, velocity is the fringe shift times $\langle\lambda\rangle/(2\tau)$. For the optical example of Fig. 2A when τ=13 ns and $\langle\lambda\rangle$=500 nm, each fringe represents ≈20 m/s.

E. Equivalence to an Autocorrelation

The fringe phase can be determined from either $\langle I^+\rangle$ or $\langle I^-\rangle$ singly, or from the difference $\langle I^+\rangle - \langle I^-\rangle$. The latter is called the pushpull signal 29. The subtraction improves the fringe contrast in the output, because non-interfering constant components are eliminated. The pushpull signal versus delay is equivalent to an autocorrelation signal $\mathrm{AC}(\tau_2)$. This can be seen by considering that if the undelayed wave is A, and the delayed B, then because the intensity detectors are square law devices, the push-pull signal is $(A+B)^2-(A-B)^2 = 4AB$, which after time averaging yields a value proportional to the autocorrelation $\mathrm{AC} = \int AB\ dt$.

Thus when a square law detector is used after the in-

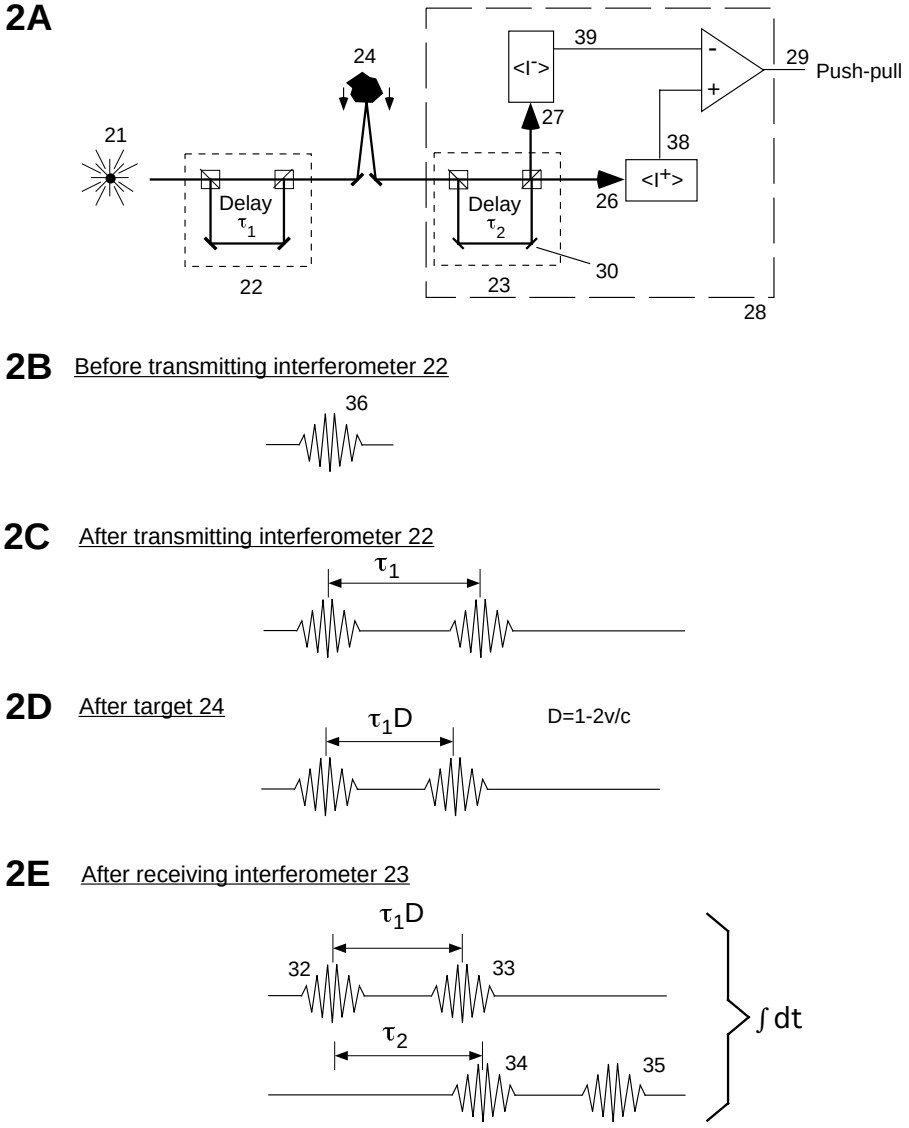

Figure 2A shows an optical embodiment of the invention for measuring velocity. Figure 2B models the source as a single short pulse. Figure 2C shows the waveform after the transmitting interferometer. Figure 2D shows the Doppler contracted waveform after reflection from the target. Figure 2E show the four replica pulses created by the receiving interferometer.

terferometer 23 or 7, it is equivalent to an autocorrelation signal, as in 8. Note that if the signal to noise ratio is favorable, the push-pull subtraction is not required and either single interferometer output $\langle I^+ \rangle$ 38 or $\langle I^- \rangle$ 39 can determine the shape of $\mathrm{AC}(\tau_2)$, since they differ only by a constant.

Figure 3A shows that $\mathrm{AC}(\tau_2)$ is a localized group of sinusoidal fringes having an envelope width of Λ/c. The fringes underneath the envelope are sinusoidal and are proportional to

$$\langle I \rangle \propto \cos\left[\frac{2\pi}{\langle\lambda\rangle}(c\tau_1 - c\tau_2) - \frac{2\pi}{\langle\lambda\rangle}(c\tau_1)\left(\frac{2v}{c}\right) + \phi_0\right] \quad (1)$$

where ϕ_0 is some phase constant. Equation 1 depends on both delay difference $(\tau_1 - \tau_2)$ and target velocity v. The envelope 50 and the phase of the fringes underlying the envelope shift together with velocity by an amount $2v\tau/c$ (52) along the delay axis from the zero velocity point, which is $\tau_2 = \tau_1$. The velocity can be calculated from either the envelope shift or the phase shift, since they are locked together.

F. Targets Separated from Clutter

Figure 3B shows that the presence of two targets having different velocities creates two fringe groups 54 and 56. One group 54 is due to clutter, presumed at zero velocity. The two groups can be resolved if their delay separation is greater than Λ/c. Thus the velocity ambiguity is $\Lambda/2\tau$. Hence, short coherence length illumination

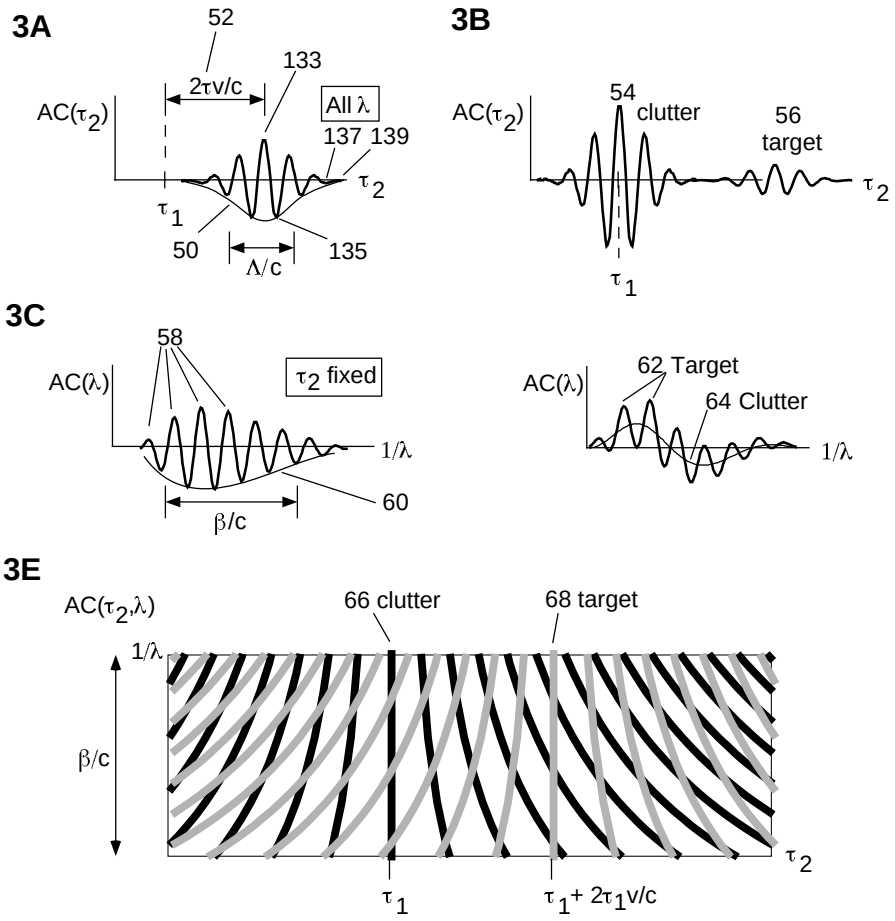

Figure 3A shows the autocorrelation signal for the full bandwidth versus receiving interferometer delay. Figure 3B shows the autocorrelation signal for the full bandwidth for two targets having different velocity. Figure 3C shows the autocorrelation at fixed delay versus frequency. Figure 3D shows the autocorrelation at fixed delay versus frequency for two targets having different velocity. Figure 3E shows a 2-D map of the maxima in the autocorrelation versus essentially frequency and delay for two targets having different velocities.

improves both the velocity and range resolution. As an example, for the radar embodiment if τ=2 ms, and an aircraft traveling at 45 m/s is to be resolved from stationary clutter, then Λ should be 18 cm. This implies a bandwidth $\beta = c/\Lambda$ of 1.6 GHz.

If the clutter and target are widely separated, then the presence of a target at an anticipated velocity can be detected by measuring AC at a single delay value. However, it is more useful to measure AC(τ_2) over a range of τ_2, so that unanticipated target velocities can be detected, and to aid in distinguishing the clutter and target fringe groups. The known symmetry of the envelopes can be used to help distinguish the components having different velocities.

Measuring AC(τ_2) over a range of τ_2 can be done in the apparatus of Fig. 2A either promptly, or by slowly scanning τ_2. If an interferometer mirror such as 30 in the receiving interferometer is tilted slightly out of alignment, then the delay difference $\tau_1 - \tau_2$ can be made to vary transversely across the output beam. This allows AC(τ_2) to be determined promptly for a single source pulse by photographing the output fringe pattern or using some other multi-channel detector. Alternatively, the interferometer can be aligned to produce the same delay uniformly across its output and a single detecting channel used. Then τ_2 can be scanned slowly compared to Λ/c to accumulate AC(τ_2) over a range. This latter method is only appropriate if the target velocity changes slowly.

If the radar/sonar observes a set of targets that are unresolvable in range and possess a distribution of velocities, then if the velocity spread exceeds 1/2 fringe shift, the fringe amplitude for the group will begin to blur away. This is an advantage, since it means that clutter such as weather and the seas which have a distribution of velocities can self-cancel, aiding separation of target from clutter.

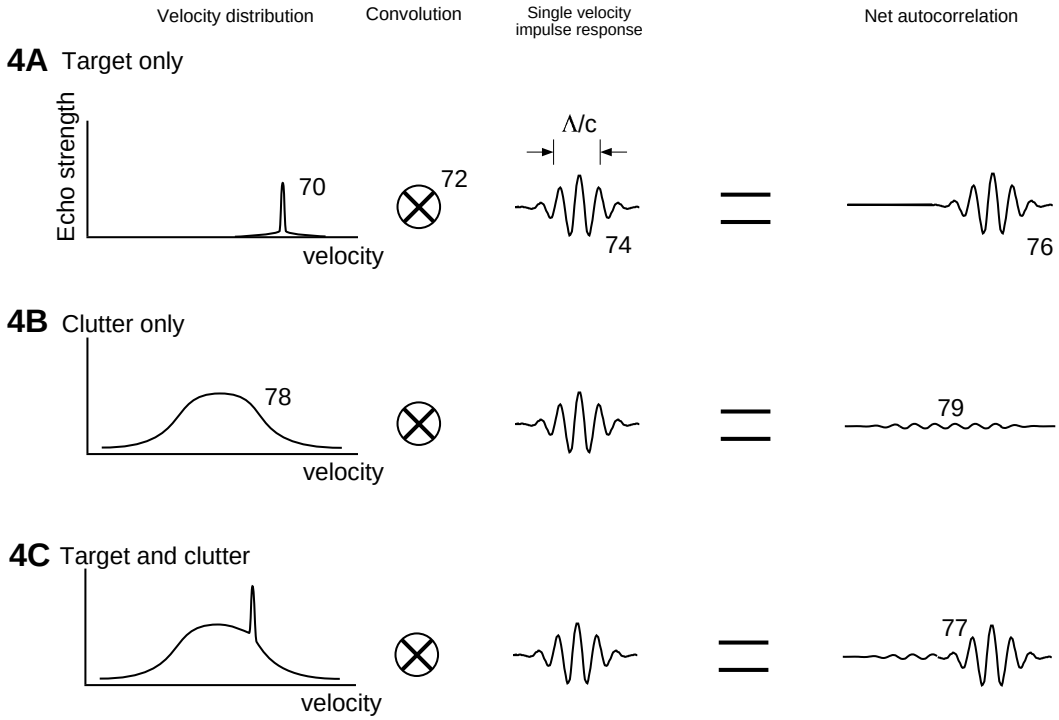

Figure 4A shows the convolution between a narrow velocity distribution and a single velocity fringe impulse response. Figure 4B shows the convolution between a broad velocity distribution and a single velocity fringe impulse response. Figure 4C shows the combination of a narrow and broad velocity distribution and a single velocity fringe impulse response.

G. Clutter Cancellation

Figures 4A-C illustrate that the process of computing the net autocorrelation fringe pattern is a convolution, indicated by symbol 72, between a velocity distribution and the fringe pattern 74 from a single target having a distinct velocity. The shape 74 could be called a single velocity impulse response. Fig. 4A shows that the velocity distribution for a single target having a well defined velocity is a spike 70. The convolution between the spike and 74 is a shape 76 very like 74. Fig. 4B shows the velocity distribution of hypothetical clutter 78. If the distribution is approximately symmetric and has a width which is greater than 1/2 the fringe wavelength inside 74, then the convolution will be a very weak set of fringes 79, much less than what would be implied by the area underneath the velocity distribution curve 78. Fig. 4C shows that the combination of clutter and a single velocity target can produce a fringe pattern 77 where the clutter partially self-cancels and contributes a diminished amplitude, allowing the target to be identified.

The self-cancellation effect for clutter is enhanced as $\langle\lambda\rangle \rightarrow 0$. Therefore, as long as the desired target does not self-cancel, then it is advantageous to use as short of average wavelength as possible. This is in addition to the benefit of using short Λ for improved velocity ambiguity.

The self-cancellation effect can be used advantageously in a moving antenna platform, such as an airborne platform, to lessen the contribution of ground clutter and

Figure 5A

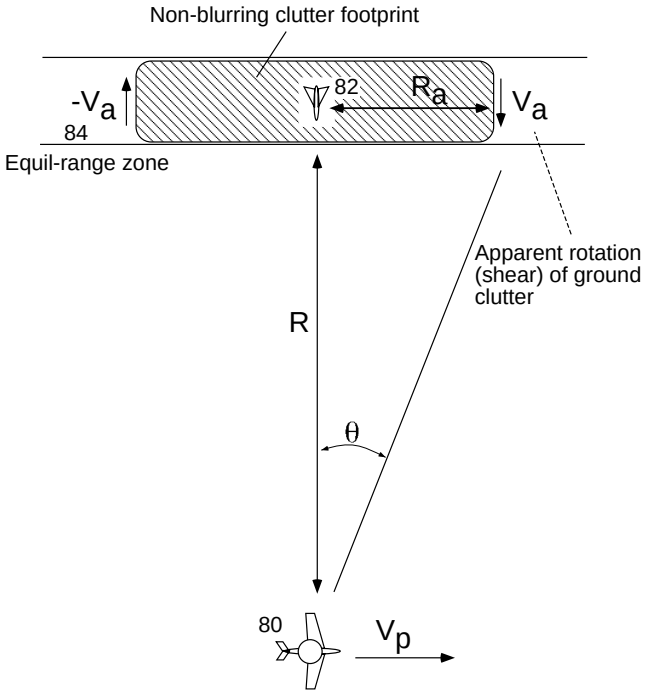

Figure 5 shows the footprint of ground clutter that will remain after blurring due to a moving antenna.

effectively narrow the angular resolution of the radar similar to the principle in synthetic aperture radar (SAR). Fig. 5 shows that from the point of view of the antenna aircraft 80, which is moving transversely at a velocity V_p, the ground on either side of the target 82 is rotating. Only the strip of ground 84 within the range resolution of the radar around the target needs to be considered. The rotation generates a symmetrical velocity distribution for the ground clutter which self-cancels for large azimuth values. The magnitude of the apparent velocity due to rotation at an azimuth distance R_a is $V_a = R_a V_p/R$. For azimuth distances below $R_a = \langle\lambda\rangle R/(4\tau V_p)$ the apparent rotation does not exceed 1/2 a fringe. Thus there will effectively be a residue amount of ground clutter represented by the footprint that has an azimuth size of R_a. The angle θ in radians that this subtends from the point of view of the airborne platform is $\theta = \langle\lambda\rangle/(4\tau V_p)$. For example, if V_p=300 m/s, τ=2 ms and $\langle\lambda\rangle$ =1 cm then θ=0.24°. This is a similar value as that computed from a SAR radar when 2 pulses are considered. That is, in both the present invention and in SAR, the effective transverse size of the antenna is given by the distance the platform moves during the observation time of the radar.

In SAR, successive received waveforms are added, after offsetting by the repetition time of the emitted pulse train, so that a correlation is accumulated. A changing slight phase shift is usually added to mimic the curvature of a giant curved antenna along the airborne platform's line of flight, to effectively focus the synthetic antenna at distances other than infinity. Figures 6A and B help illustrate how the present invention differs from SAR and other prior art. 1) The purpose of SAR (Fig. 6A) is radar mapping, that is, range finding instead of velocimetry, and thus the arrival time of successive reflections are referenced to the emission time of the transmitted pulse to determine range. In the present invention (Fig 6B); however, to perform velocimetry there is no reference to the emission time of the transmitted pulse. 2) The present invention is able to form correlations 92 from an incoherent source by passing the source through a transmitting interferometer 90. This imprints a partial coherence. The individual pulses in the source pulse train 94 in Fig. 6B are labeled alphabetically to indicate their individuality and that they would have no correlation between them. Because the interferometer delay is set to be approximately the pulse repetition period (PRP), each pulse of the transmitted pulse train 96 contains components of at least two individual pulses from the source train 94 (more if a recirculating interferometer is used). Thus, when they are superimposed in the autocorrelation process 92, the two similar components can correlate. For example in 92, "A,B" will partially correlate with "B,C" because of the common B component.

In the prior art however, if an incoherent source is used, there will be no correlation in the receiver at 98. Even though pulses "A", "B" and "C" are added so that they superimpose in time, there is no coherent correlation between them because they are random and unrelated. Any correlation would be of an incoherent kind, that is, related to the envelope of the pulses and not the underlying phase.

H. Plotting the Autocorrelation vs Wavelength

In the velocimeter apparatus of Fig. 2A, prisms (wavelength dispersive elements) could be placed in between the receiving interferometer 23 and the detectors 26 and 27. These would create a spectrum that would be recorded by multi-channel detectors. This spectrum, and therefore the autocorrelation would have fringes, as shown in Fig. 3C and 3D for the case of $\tau_2 = \tau_1$. Equation 1 shows that the fringes plotted versus $1/\lambda$ are sinusoidal, with a spatial "frequency" along the $1/\lambda$ axis of $[c(\tau_1 - \tau_2) - 2\tau_1 v]$. If $\tau_2 = \tau_1$, then the target velocity is proportional to this spatial frequency 58. Fig. 3D shows that the clutter 64 can be distinguished from the target 62 by its much lower spatial frequency. The plot is versus the variable $1/\lambda$, which is proportional to wave frequency and should not be confused with the term spatial frequency discussed above.

The autocorrelation can therefore can be plotted versus both τ_2 and $1/\lambda$, in a 2-dimensional map as shown in Fig. 3E, where AC maxima are displayed as black or gray fringes. The gray 68 fringe network associated with a target can be easily distinguished from the black fringes 66 of stationary clutter. The networks are the same shape, just translated in delay. The amount of translation yields the velocity. This flexible method of signal presentation may be useful for distinguishing target from clutter in a noisy environment. For example, if an enemy is jamming a radar with quasi-monochromatic waves, these can be ignored most easily in the AC(λ) presentation. If the enemy is jamming with short pulses, then these can be most effectively isolated by the AC(τ_2) presentation.

I. Sensing Target Albedo

If the complementary outputs $\langle I^+\rangle$ and $\langle I^-\rangle$ are added instead of subtracted, then the envelope 60 of the AC is obtained. This is the power spectrum of the reflected signal. Thus the target albedo spectrum can be measured, after dividing by the known spectrum of the transmitted illumination. Changes in the resonances of the target albedo can yield information about the structure and orientation of the target, in addition to shape information that comes from the range signal, discussed later.

J. Pulse Repetition and Echolocation

Figure 1A shows the transmitting and receiving antennas to be separate, to indicate that in general the source waveform can be arbitrarily long. However, because reflections from distant targets are very weak, a practical

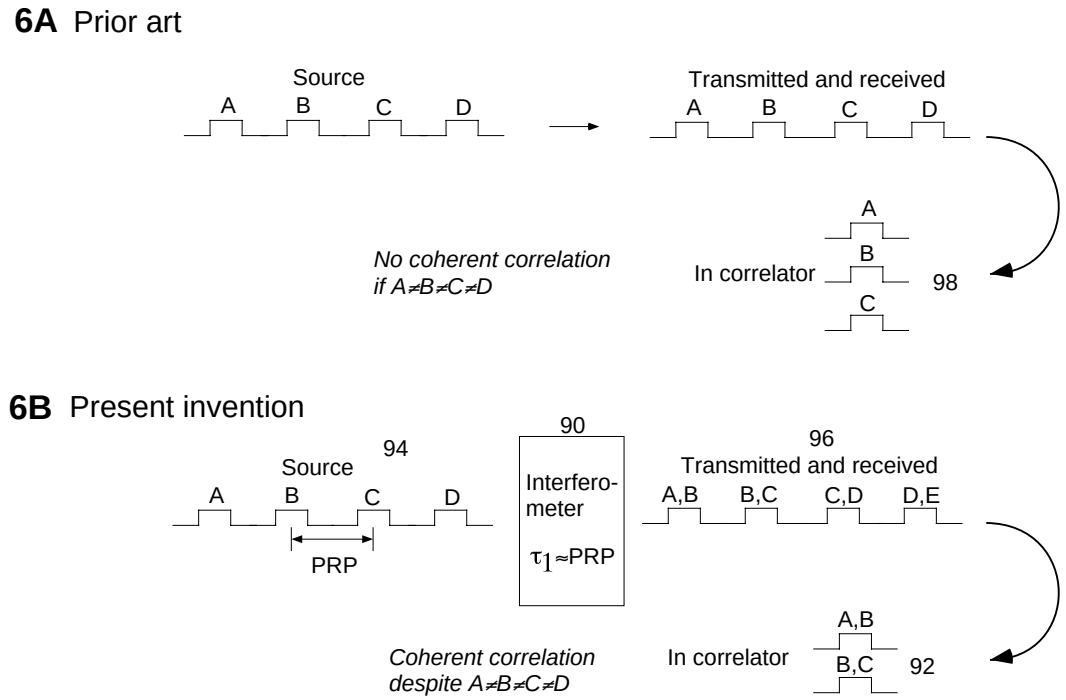

Figure 6A shows the scheme in prior art for correlating pulses. Figure 6B shows the scheme of the present invention for correlating pulses.

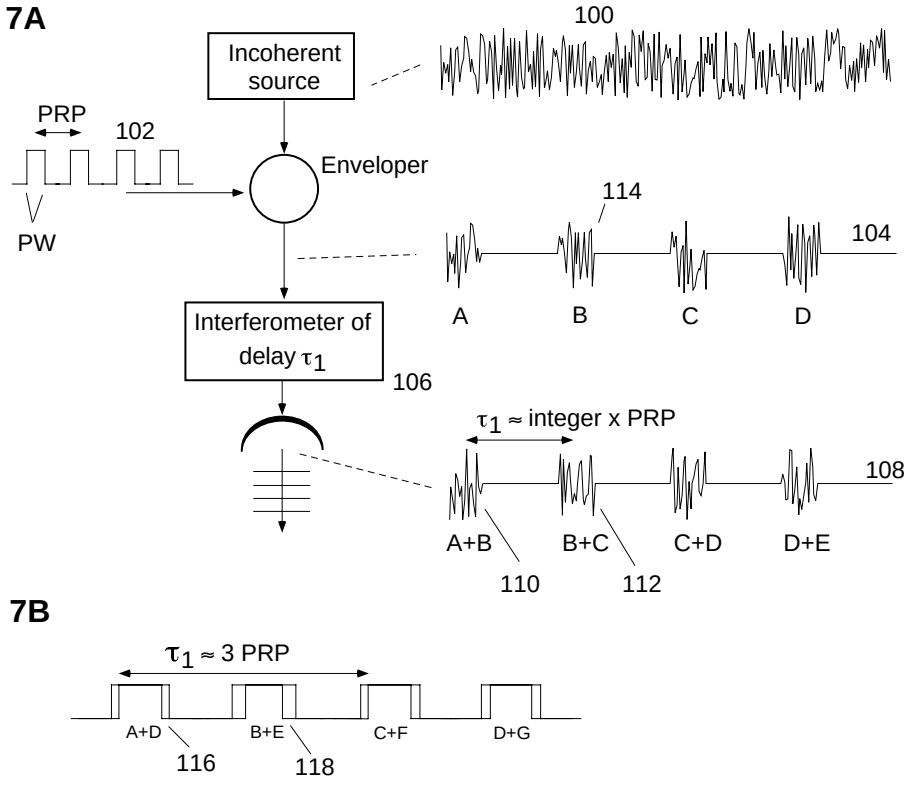

Figure 7A shows the enveloping of an incoherent waveform into periodic pulses. Figure 7B shows the effect of jiggering the interferometer delay relative to the pulse envelope period.

echolocation system will usually operate in a pulsed mode so that strong and immediate reflections from short range clutter do not swamp the distant weak signals, and so that a time dependent gain can be used on the receiving amplifier. Conventionally, the same antenna is used for transmission and reception, through the use of a duplexer switch. Fig. 7A illustrates that the expected best radar and sonar embodiment of this invention is to envelope the source waveform into broad pulses of duration PW, repeated in a train with a pulse repetition period PRP. The PW would be determined by the minimum target range and the PRP from the maximum target range. For a radar example, for a minimum and maximum range of 5 km and 150 km respectively, the PW and PRP would be 33 μs and 1 ms, respectively.

To maintain the approximate pulse envelope, the transmitting interferometer delay τ_1 should be nearly equal to an integer multiple of the PRP. However, τ_1 is not required to be exactly proportional to PRP. Fig. 7A shows the random source signal 100, the enveloping signal 102, and the signal after the enveloper consisting of individual and uncorrelated pulses of a train 104 labeled alphabetically. When τ_1 is nearly a multiple of PRP, then the pulse train 108 after the interferometer 106 is a pulse train where each pulse is an additive combination of at least two of the individual pulses of the previous train 104, (more than 2 for a recirculating interferometer, Fig. 1C). This generates the partial coherence that allows autocorrelation. For example, pulses 110 and 112 both contain a component of the source pulse "B" 114, and thus there can be interference in the subsequent receiving interferometer. Fig. 7B shows the transmitted pulse train if τ_1 is approximately 3 times PRP. To prevent the enemy from rapidly determining τ_1, then it is advantageous to randomly change τ_1 after each source pulse of 104. Such a random jitter in τ_1 relative to PRP is indicated in Fig. 7B by the variation in overlap in the edges of the pulses 116, 118. The enemy cannot determine τ_1 without waiting for the later pulse to arrive. However by then both pulses have reflected from the target and useful information about the target range and velocity has been obtained.

K. Explanation in Frequency Domain

A useful analysis of the invention is in the frequency domain. Fig. 8A shows two replicas of a incoherent source waveform pulse separated in time by τ, as the waveform would appear after a two-path transmitting interferometer. Each individual replica 120 has a hypothetical power spectrum shown in Fig. 8B, having a bandwidth β. The two-path interferometer has a transmission spectrum shown in Fig. 8C. It can be described as a comb filter, since it consists of a periodic array of peaks and valleys having a periodicity $1/\tau$. For the particular case of a two-path interferometer the transmission function is sinusoidal. A recirculating interferometer generating

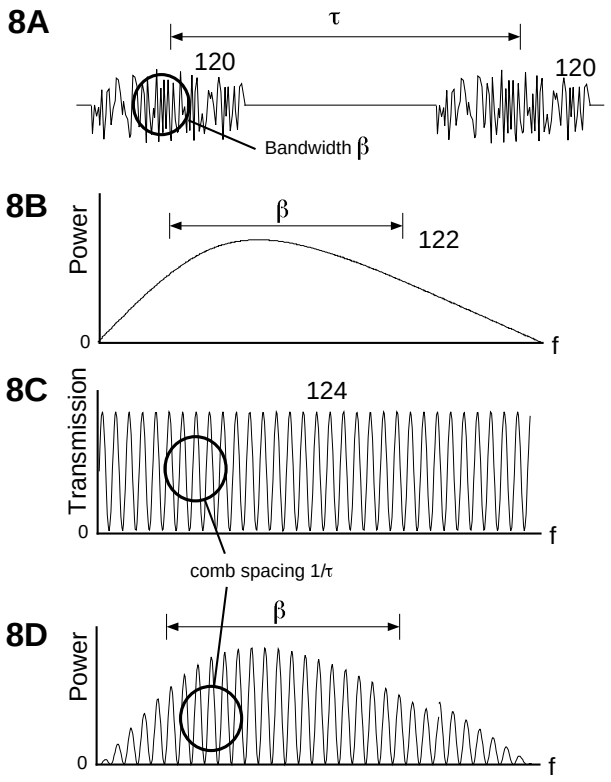

Figure 8A shows a pair of identical replicas of a pulsed incoherent waveform. Figure 8B shows the power spectrum of the incoherent waveform before being paired. Figure 8C shows the fine comb filter nature of an interferometer. Figure 8D shows the power spectrum of a pair of identical replicas of a pulsed incoherent waveform.

a N-tuplet of replicas would produce a comb filter with the same comb periodicity, but with thinner and non-sinusoidal comb peaks. The overlap between the single pulse spectrum 122 and the interferometer spectrum 124 is the power spectrum of the pulse pair of Fig. 8A.

The fineness of the comb is what allows detection of small Doppler shifts, much smaller than β, and yet the large gross spectrum bandwidth β produces a short coherence length Λ which allows high range resolution. For example, if τ=2 ms and β=1.6 GHz, then the comb spacing is 6 million times smaller than the gross bandwidth.

The velocimetry aspect of the invention can be considered to be two nearly matched comb filters in series. (Matched in comb periodicity, but not matched in the conventional usage of that term in radar. The second interferometer is not a time-reversal of the first.) The output of the receiving interferometer is the intensity that passes through overlap of both filters integrated over all the frequencies of the source. When $\tau_2 = \tau_1$ and v=0, then the power spectra perfectly overlap and large power is passed. Target motion causes the power spectrum of the pulse pair reflected from the target to scale by the factor $D = (1 + 2v/c)$. This scaling causes large fluctuations in the overlap which are manifested as fringes in

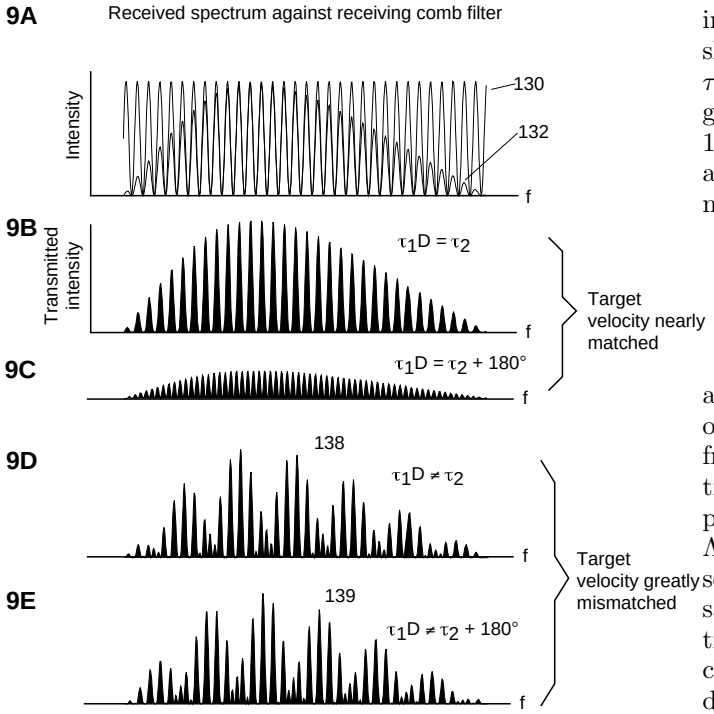

Figure 9A shows the receiving comb filter compared against spectrum of wave from target. Figure 9B shows spectrum passing through receiving comb filter when receiving delay is set to anticipate target Doppler shift. Figure 9C shows spectrum passing through receiving comb filter when delay is incremented by half a fringe over Figure 9B. Figure 9D shows spectrum passing through receiving comb filter when receiving delay is very mismatched to anticipated target Doppler shift. Figure 9E shows spectrum passing through receiving comb filter when delay is incremented by half a fringe over Figure 9D.

the output power of the receiving interferometer. This effect is analogous to the Moiré fringes seen when two meshes of slightly different pitches are overlapped. This allows detection of pitch changes too slight to be observed directly in a single mesh.

Figure 9A shows the receiving interferometer spectrum 130 and the reflected signal spectrum 132 from a pulse pair when the two periodicities are perfectly matched, when $\tau_2 = \tau_1 D$. Fig. 9B is the resulting overlap intensity spectrum. The integration of this over frequency is the detector time averaged signal $\langle I^+ \rangle$ which yields the autocorrelation. This would correspond to point 133 of Fig. 3A. As the velocity changes, or if τ_2 changes, the periodicity becomes mis-matched. Fig. 9B shows the overlap under the slight mismatch equivalent to half a fringe, that is, when $c(\tau_1 D - \tau_2) = \langle \lambda \rangle / 2$. The integrated power is much reduced and corresponds to point 135 of Fig. 3A. The large fluctuations in power generate the large fringes at the center of the fringe group envelope 50.

If τ_2 is set to be greatly mismatched to the target velocity, then weak or no fringes are produced. This can be seen because there is little difference in the overlap integral when τ_2 is dithered by half a fringe. Fig. 9D shows the overlap when τ_2 is greatly mismatched from $\tau_1 D$. Fig. 9E shows the overlap when τ_2 is a half fringe greater. The areas under the two overlap curves 138 and 139 are nearly equal and correspond to the portions 137 and 139 of Fig. 3A where the AC does not fluctuate significantly.

1. *Undesired Kind of Illumination*

For a single target (no clutter), the invention can operate using source waveforms of any kind of coherence, high or low, and still generate fringes, and the phase of the fringes will yield the correct velocity according to Equation 1. However, one specific kind of waveform is not preferred for this invention. That is a waveform where $\Lambda \approx \tau_1 c$ and which Λ fluctuates, because in that case the source will already have a fine comb spacing nearly the same as the transmitting interferometer, and thus the transmitted intensity will fluctuate strongly with small changes in source Λ. These fluctuations do not prevent determination of the velocity, because they do not affect the fringe phase in the receiving interferometer output. However, they may be a nuisance because the signal level and therefore the fringe amplitude will vary erratically. Because of this, it is recommended that the source should not be a repeating pattern with a repetition period close to τ_1, unless the period is carefully stabilized to be constant.

2. *Comparison to Matched Filters*

The double interferometers of this invention should not be confused with the matched filters of pulse compression radar. The filters of the two techniques have different purposes and behaviors. Furthermore, the pulse compression technique will not detect a Doppler shift of 1 part in 10^6 using the same source bandwidth as this invention. In pulse compression, the first filter stretches the pulse by a factor of 100 to 1000 to lower the peak power by this same factor. A single pulse is outputted for a single pulse inputted. In the present invention, two identical pulses are outputted, not one, and each are not significantly broadened from the original. Consequently the peak power is only reduced by a factor of 2. In pulse compression, the second filter is a time reversal of the first, so that in the receiver the single broad reflected pulse is compressed to its original narrow width. In the present invention, the second interferometer is not a time reversal of the first, since it does not output a single pulse for two input pulses.

In pulse compression, the intensity transmission spectrum does not contain valleys which completely eliminate some frequencies. This is because spectral components are merely moved around in time, not eliminated. Without these narrow valleys it is not possible for the pulse

compression scheme to measure a Doppler shift that is 1 part in 10^6 narrower than the source bandwidth.

L. Expected Practice for Radar

The expected practice of a radar embodiment would be to initially use the velocity-only signal 8 (of Fig. 1A), or this signal with simple range gating, to search for the presence of a moving target and measure its velocity. Once the velocity is known, the velocity discriminating cross-correlation signal 9 can be used to determine the range and size of the target. This is done by setting $\tau_2 = \tau_1 D$ for the expected target velocity, and setting the moving reference frame delay 11 to move at the expected velocity. Then τ_2 is dithered by a slight amount, equivalent to 1/2 of a fringe, to cause the portion of the cross-correlation representing the target to fluctuate in synchronism with the dither.

The cross-correlation signal 9 is formed by adding the receiving interferometer output 12 to a delayed copy of the source waveform, which is delayed by the moving reference frame delay τ_3 11. This sum is then squared and time averaged over duration at least as long as Λ/c by element 9.

1. Moving Reference Frame

The purpose of the moving reference frame delay τ_3 is to reduce the motion of the target in the output cross-correlation signal 9 so that slow electronics after the time integration at 9 can display it without blurring its position. Secondly, the delay is set so that if the source was a short pulse, the copied source waveform correlates with the inner two pulses 33, 34 and not the outer pulses 32, 35 of the output of the receiving interferometer. Thus, the gross value of τ_3 is set to $\tau_3 = \tau_1 + 2R/c$, where R is the expected range. The rate of change of τ_3 is set to the expected target range rate, $d\tau_3/dt = -2v/c$.

The cross-correlation aspect of the present invention can be explained by considering the output at 12 to be the source waveform 10 passing through a single filter having the same impulse response as the combination of interferometers 6 and 7 in series. This effective impulse response has the form shown in Fig. 10A and 10B. If $\tau_1 D = \tau_2$, then the two interferometers are exactly matched and their combined impulse response has a central peak 150 formed from the constructive interference of the two inner pulses 33, 34. If τ_2 is increased by half a fringe, that is if $\tau_1 D = \tau_2 + \lambda/2c$, then the central peak disappears 152 because of destructive interference between the inner two pulses. The outer two lobes 154, 156 are independent of the dither. Thus the signal 12 to be cross-correlated contains portions identified with the target that fluctuate synchronously with the dither applied to τ_2, provided the target velocity matches the anticipated velocity.

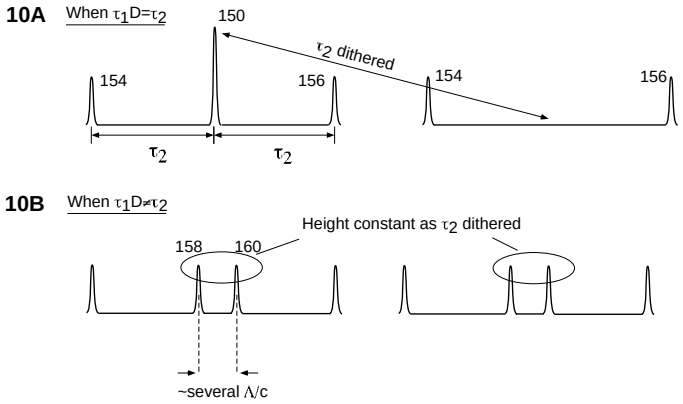

Figure 10A shows net impulse response of the transmitter and receiver interferometers in series when delays are matched for the target Doppler shift and one delay is dithered by half a fringe. Figure 10B shows net impulse response of the transmitter and receiver interferometers in series when delays are grossly mismatched for the target Doppler shift and one delay is dithered by half a fringe.

For clutter having velocity that does not cause a match between interferometers 6 and 7, the combined impulse response is insensitive to dither in τ_2. Fig. 10A shows that in this case the combined impulse response has two peaks 158, 160 instead of one in the center, and the height of these does not fluctuate with τ_2 dither because they do not overlap. Thus, the portions of the signal at 12 associated with clutter does not vary synchronously with dither.

If there is no distortion anywhere in the signal path between the source and signal 12, then the width of the peak 150 in the combined impulse response is infinitely narrow. In this case, for the target having its velocity exactly matched the cross-correlation signature will not be any wider than it would be without the interferometers. The presence of distortions will cause the cross-correlations signatures to blur. However, the velocity discrimination will remain sharp with respect to the velocity parameter because it depends on autocorrelation.

The cross-correlation signal plotted versus range and τ_2 would have the schematic character indicated by Fig. 11. The data could be processed to present only the portions of the signal fluctuating synchronously with the dither in τ_2. The target 170 would stand out from clutter 172 at the same range because it would have a sinusoidal dependence on τ_2. The projections 174 of the data integrated along the range axis would be similar in appearance to AC(τ_2) shown in Fig. 3B.

M. Several Embodiments

Figure 12 shows the invention embodied for radar, sonar or ultrasound or any wave which can be transduced into an electrical signal by the antenna or transducer 180.

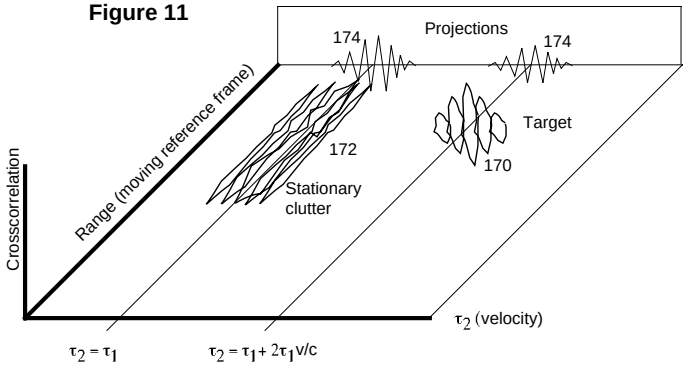

Figure 11 shows a 2-dimensional plot of cross-correlation signal versus receiving interferometer delay and the delay corresponding to range in the moving reference frame.

A source of electronic noise 182 is enveloped at 184 into pulses of width PW and repetition period PRP, consistent with conventional usage of a single transducer and duplexer 187.

1. Ultrasound

For ultrasound, separate transmitting and receiving transducers can be used effectively. The transducer must respond to or actuate the field of the wave, such as pressure in the case of sound, and not a time averaged quantity such as sound intensity. The transducer must be coherent so that the same waveform always produces the same response. For example, Fig. 13 shows a possible medical embodiment of the transducers. Laser light 200 propagating through an optical fiber 202 vaporizes tissue inside a medical patient's body at 204 and generates sound, which reflects off a target 206 and is detected by a transducer 208. This embodiment will work provided the vaporization is not so intense during the undelayed waveform component that the tissue responds differently for the delayed waveform component.

2. General Operation

In all the preferred embodiments, simple range gating can be performed in the conventional manner on the received signal to reduce clutter signal from range areas known to not contain the target. This is shown in Fig. 12 at 185. There is no advantage to having the range gate width less than PW. This range gating is an incoherent process, as opposed to the coherent cross-correlation at 188, because the gate width is much longer than $\langle\lambda\rangle$.

To form correlations, the signals must pass through a non-linear device 192 that creates a squared component that is time averaged over at least Λ/c. This squared component corresponds to the intensity of the signal. The receiving interferometer 190 is shown duplicated only for clarity. The outputs 194 and 196 can generated once and then used in several spots to form the various kinds of cross-correlations and autocorrelations. The prompt formation of the autocorrelation AC(τ_2) over a range of τ_2 can be accomplished by multiple autocorrelators 181 having slightly different delays, but an easier method is to use Fourier transforms, as in Fig. 14. After the waveforms have been Fourier transformed by 220, the cross-correlation is produced by multiplying one signal at 221 with the complex conjugated of the other 226 and taking the inverse Fourier transform of the product 222. The autocorrelation is produced by squaring the magnitude at 223 before taking the inverse Fourier transform. This automatically produces the spectral dependence of these correlations as an intermediate step before they are inverse transformed. By masking the undesired spectral components at 224, the AC spectrum is obtained 225.

N. Simultaneous Multiple Banded Operation

Some of the benefits of incoherent illumination can be achieved by sets of simultaneous monochromatic sources that cover roughly evenly but sparsely the bandwidth range β. This may be a less expensive way to generate somewhat incoherent illumination. Secondly, this can be used in conjunction with a filter before the receiver to thwart jamming by the enemy, as shown in Fig. 15A. The source 230 generates multiple narrowbands whose configuration changes randomly rapidly, as shown in Fig. 15B. The spectral information is passed to a multiband narrowband filter 232, which prevents harmful jamming signals from entering the sensitive receiver. The spectral information is delayed at 234 by the same delay as the transmitting interferometer, (except for differences in arrival time due to different target range), so that the filter 232 anticipates the correct narrow bands to pass when the legitimate signal from the target arrives. This system can also be used to perform a kind of range gating, since if the spectral content is changed more rapidly than PRP, the filter 232 can exclude signals from other than the desired range.

1. Means for Achieving Long Delays

A means for implementing a long delay high bandwidth interferometer for electrical signals is shown in Fig. 16. The idea is that different sections of the signal spectrum can be heterodyned to a set of lower bandwidth channels by mixing with a set of local oscillators. Multiple parallel channels are used that preferably cover the complete original spectral bandwidth β contiguously. A less-preferred embodiment uses channels that sparsely cover the spectrum. The bandwidth requirements of an individual channel are proportionately less than the original signal. For the example of Fig. 16, a 1600 MHz bandwidth received input signal 340 is split by a spectrome-

Figure 12

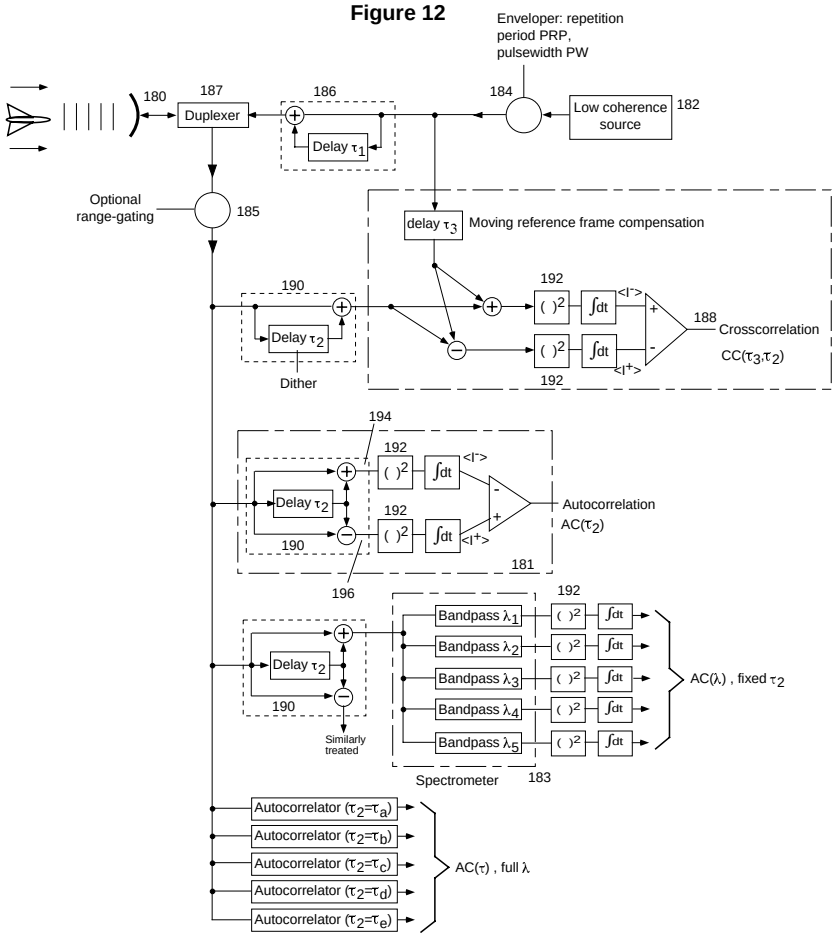

Figure 12 shows an embodiment for radar, sonar or ultrasound using essentially analog electrical devices.

Figure 13

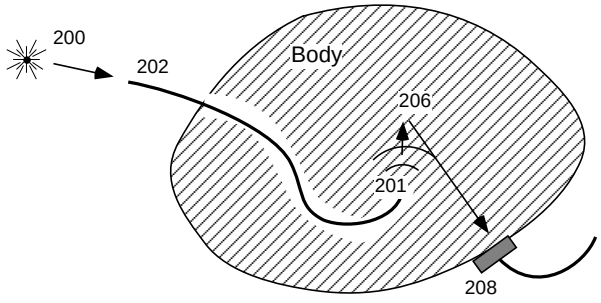

Figure 13 shows an embodiment for biomedical ultrasound where light through a fiber generates sound.

ter 342 into 16 channels of 100 MHz bandwidth spaced every 100 MHz. The spectrometer could be constructed of a collection of bandpass filters. The set of local oscillators 344 heterodyne the different bands to a common 100 MHz bandwidth. From this point, all the channels are identical. The autocorrelation or cross-correlation is accomplished on the individual channels, and then the combined output signal formed by reheterodyning with the same set of local oscillators and summing at 346 or 348. An analogous process occurs in the transmitter.

The advantage of this scheme is that less expensive electronics can be used to implement the delays and analog to digital conversions when the bandwidth is low. The average frequency of the local oscillators are not required to be exactly locked in a mathematical relation to the other local oscillators, provided the same local oscillator set is used for the transmitting and receiving interferometers. Their frequency can wander in the long term. Over the delay $\sim 3\tau$, the local oscillator must be stable to $\pm 1/4$th a cycle, so that for a given channel the signal in the transmitter interferometer encounters the same delay within 1/4th fringe as in the receiving interferometer, including the time traveling to the target and back. For the example of a 10 GHz average frequency and delay of 2 ms, this is a stability requirement of 0.01 part per million per 6 millisecond, which is readily achievable.

If the local oscillator frequencies are not locked in a regular mathematical relationship, or if the bands do not cover the original bandwidth contiguously and evenly, then this is equivalent to a signal distortion 322 or 320 in Fig. 1D prior to the analog-to-digital conversion 323 or af-

Figure 14

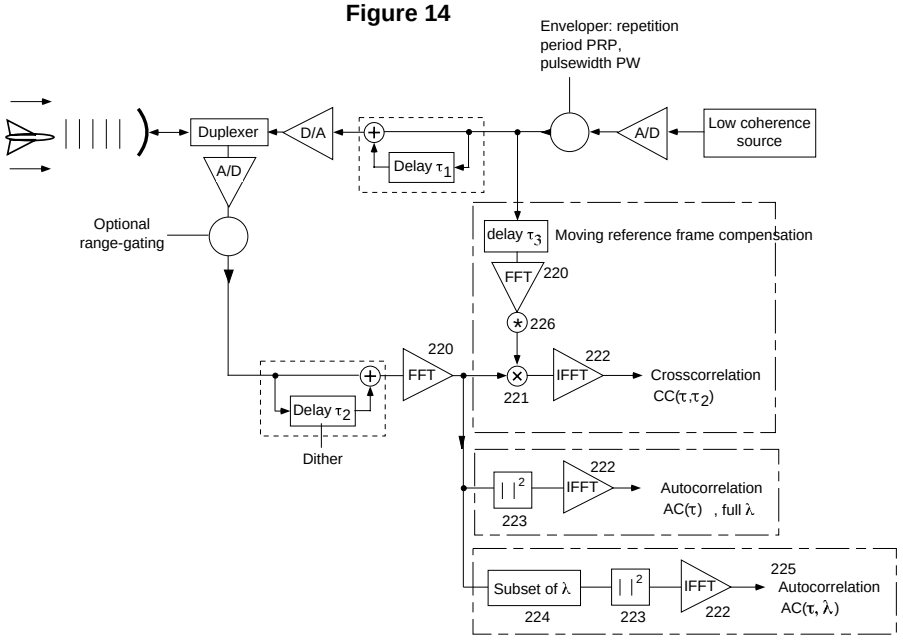

Figure 14 shows an embodiment for radar, sonar or ultrasound using numerical processing to perform correlations.

15A

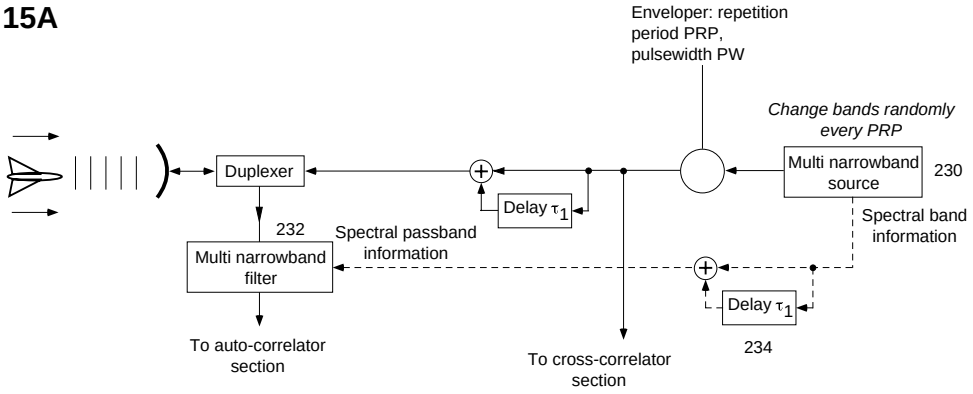

Figure 15A shows a scheme for using a randomly changing multiband narrowband source and filter to defeat enemy jamming.

ter the digital-to-analog conversion 324. This could produce a hypothetical distorted interferometer spectrum Fig. 1E which contains stop bands 327. Since this distortion is applied equally to delayed 321 and undelayed 325 signal paths, this distortion will not prevent the formation of a useful autocorrelation.

The presence of a dispersion in the time delay, that is, a frequency dependence to τ, will cause the phase of the fine fringe comb to be incoherent from pass band 325 to pass band 326. However, this will not blur (disperse) the full bandwidth autocorrelation if the delay dispersion characteristics of the transmitting and receiving interferometers are the same. If they are not exactly the same, any residual dispersion in the autocorrelation can be corrected mathematically after the time averaging has been performed (where it is less computationally expensive), since it corresponds to a systematic tilting or curving of the network of fringes in $\mathrm{AC}(\lambda, \tau_2)$ shown in Fig. 3E.

A long delay interferometer can be constructed of a single mode optical fiber or an acoustical delay line. If the other portions of the apparatus use electrical signals, the electrical signal modulates an optical beam or a sound wave which travels through the fiber or acoustical delay and is demodulated at the end of the delay back into an electrical signal. The undelayed signal could also be converted to and from light or sound so that the same distortions are imparted to it by the conversion process. This way the delayed and undelayed paths have the same distortion. The dispersion in the delay should be matched between transmitting and receiving interferometers.

15B

Randomly varying multispectral source

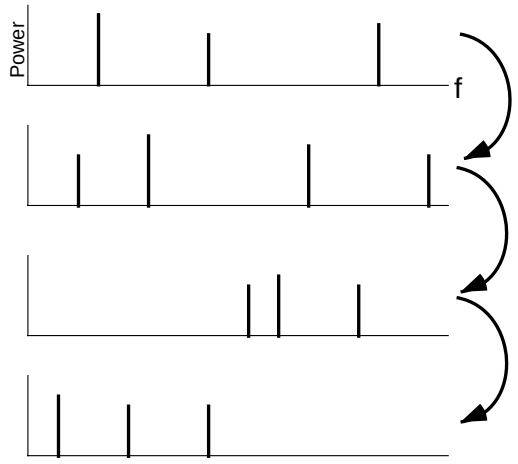

Figure 15B shows an example sequence of spectra for the scheme of Figure 15A.

Figure 16A

Source and transmitting interferometer

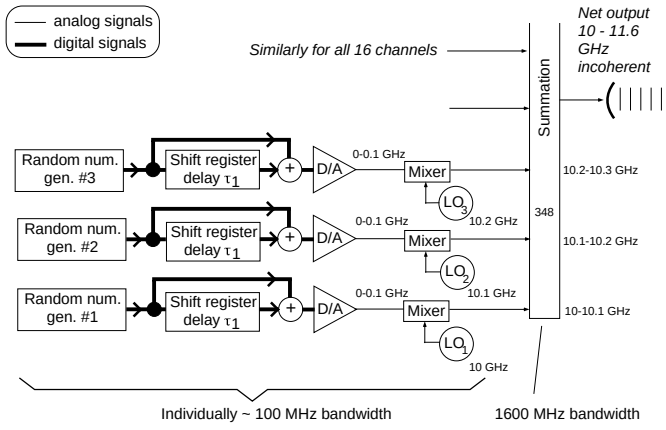

Figure 16 shows a means for creating a high bandwidth long delay interferometer using parallel heterodyning. (A) shows the transmitting portion.

Figure 16B

Receiving autocorrelator

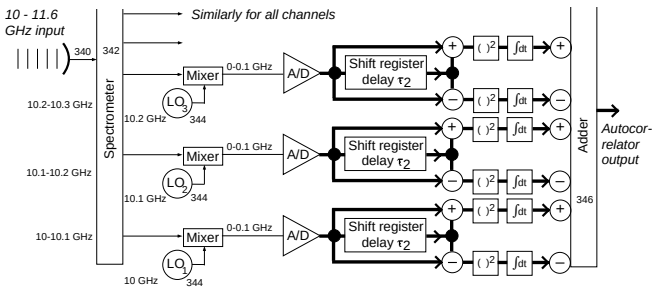

Figure 16B shows the receiving portion for a means for creating a high bandwidth long delay interferometer using parallel heterodyning.

O. Optical Embodiments

An optical embodiment for invention which measures range while discriminating velocity is shown in Fig. 17. The optical embodiment for the velocity-only signal has already been discussed in Fig. 2. The interferometers 240 and 242 are constructed similarly and are image superimposing interferometers. The image superimposing condition is required of any interferometer in this invention working with an image or using an unparallel rays, including interferometers using sound or microwaves that propagate in 3-dimensions as opposed to being converted to 1-dimensional electronic signals or 1-dimensional optical signals along a single mode fiber. (It is possible to construct lenses, mirrors and beamsplitters and thus interferometers analogous to light for sound and microwaves.) Practical sources of incoherent broadband light emit light over a range of angles or emit over an area. To select only exactly parallel rays by use of an infinitely small pinhole at a distance would in the mathematical limit of zero aperture diameter produce zero power. Thus all velocimeters intending to use practical white light sources must satisfy the superimposing condition, otherwise vanishingly little power can be utilized from them.

The image superimposing condition states that for each of a plurality of output rays generated by a given input ray, the ray position and angle must superimpose. That is, the multiple images created by an interferometer must superimpose longitudinally, transversely, and in magnitude. This creates an interferometer delay which is independent of ray angle passing through each pixel image and is preferred to be achromatic. When this condition is satisfied, the 3-dimensional interferometer behaves as a 1-dimensional interferometer, and the details concerning the imaging can be separated from the details concerning the temporal and spectral behavior of the velocimetry and range finding.

Embodiments of superimposing interferometers for light are shown in Fig. 18A-C. More embodiments of superimposing interferometers and a more detailed mathematical description of the temporal and spectral behavior of the velocimetry aspect of the invention are described in U. S. Patent Application Serial Number 08/597,082. Fig. 18A shows an example of an interferometer of the prior art, called a Fabry-Perot, which does not satisfy the image superimposing requirement and therefore cannot be used with broadband sources that emit non-parallel light in this invention. The input ray 280 bounces between two partially reflecting mirrors 288 to produce several output rays 282, 284, 286 which are displaced translationally from each other, not superimposing.

Figure 18B shows a recirculating interferometer which has the same temporal properties of the Fabry-Perot, but satisfies the image superimposing condition. The lens 272 images the surface of partially reflecting spherical mirror 274 to the other partially reflecting spherical mirror 276 with positive unity magnification. The lenses 278 focus

Figure 17

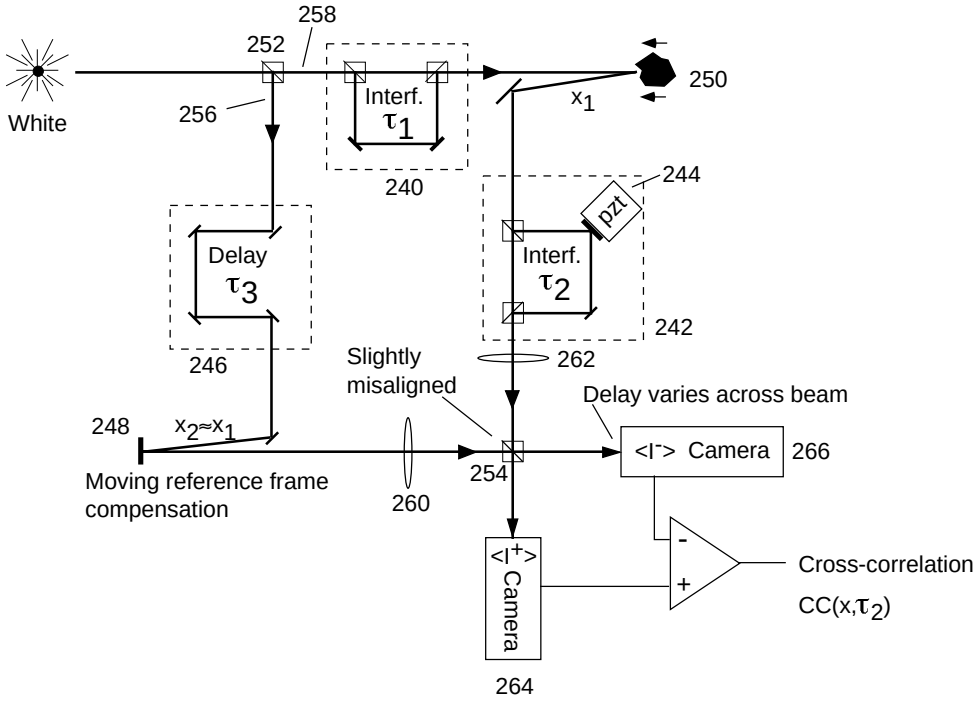

Figure 17 shows an open-beam optical embodiment of the invention.

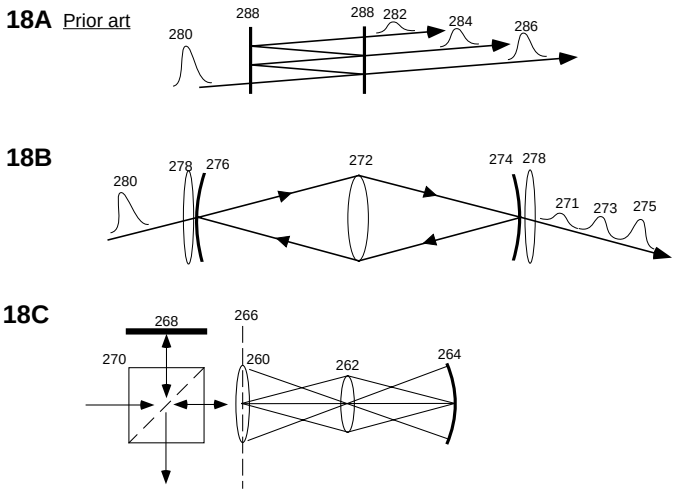

Figure 18A illustrates the non-superimposing nature of a Fabry-Perot interferometer. Figure 18B illustrates an optical recirculating interferometer satisfying the superimposing condition. Figure 18C illustrates an optical two-path interferometer satisfying the superimposing condition.

approximately to the center of lens 272 so that collimated light applied to the system emerges as collimated. Mirror reflectivity of 66% would produce an approximate 3-tuplet impulse response, similar to 21 of Fig. 1C For an input pulse 280, the output rays 271, 273, 275 superimpose in position and angle.

Figure 18C shows a two-path (called a Michelson) interferometer that satisfies the image superimposing condition. Lenses 260 and 262 form a relay system which images the spherical mirror 264 to the dashed plane 266. The dashed plane superimposes with the image of the plane mirror 268 of the other arm seen in the 50% beamsplitter 270. This will produce a pair impulse response shown at 20 in Fig. 1B.

In Fig. 17, the PZT 244 dithers the delay τ_2 by half a fringe. The compensating delay τ_3 (246) approximately equals τ_1 so that a short pulse from the source will interfere with the inner pulses 33, 34 of Fig. 2E. The mirror 248 position and velocity compensates for the position and velocity of the target 250 so that path length from beamsplitter 252 to beamsplitter 254 for the inner two pulses 33, 34 changes little. Lenses in the delay 246 superimpose the image of the beamsplitter 252 to the beamsplitter 254. The two paths 256 and 258 emerging from beamsplitter 252 and recombining at beamsplitter 254 must form a superimposing two-path (Michelson) interferometer. That is, lenses 260 and 262 must cause an image located in the region near 252 to superimpose in the region near 254. The beamsplitter 254 is optionally misaligned slightly so that the cross-correlation delay varies across the beam. By recording the image of the beam by multi-channel cameras 264 and 266 the cross-correlation over a range of delays can be recorded promptly. A push-pull signal obtained by subtracting the complementary

outputs yields the cross-correlation.

Figure 19 shows an embodiment using single-mode optical fibers which is analogous to Fig. 17. The delays are accomplished by differing lengths of fibers, such as 291. The superimposing condition is moot because images are not propagated along the single-mode fiber. The beamsplitters of Fig. 17 are replaced by fiber-splitters 290, except for the final beamsplitter 254. This remains an open-beam beamsplitter so that it can be slightly misaligned and cause a delay between beams 296 and 298 which varies across the image at 293. This allows the cross-correlation to be recorded over a range of delays promptly. Lenses 292 at the fiber ends couple between 3-dimensional waves interacting with the target 294 to 1-dimensional signals in the fibers. The delay τ_2 is dithered by some means such as straining the fiber spool so that the length changes by $\langle\lambda\rangle/2$.

Acknowledgments

This work was performed under the auspices of the U.S. Department of Energy by the University of California, Lawrence Livermore National Laboratory under contract No. W-7405-Eng-48.

Figure 19

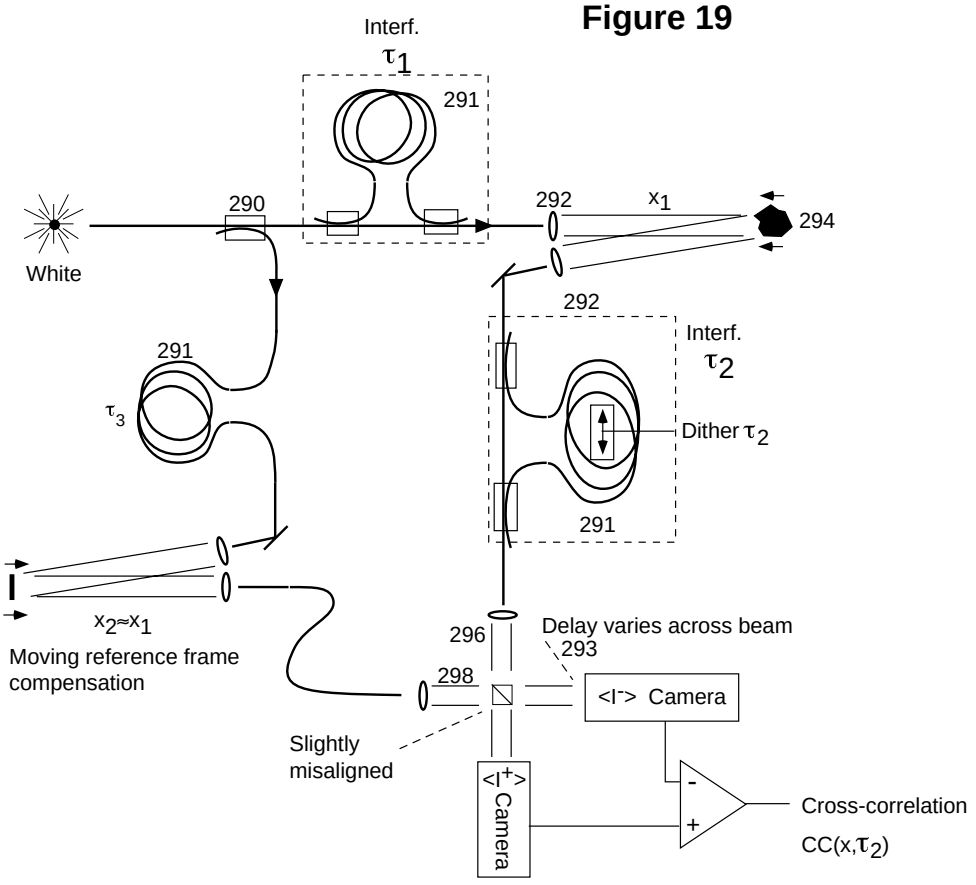

Figure 19 shows a fiber-optical embodiment of the invention.

IV. CLAIMS

(Submitted, not official version)

1. An apparatus, comprising:

a source of arbitrary waves;

means for imprinting a finite number of coherent echos onto said arbitrary waves to produce imprinted waves;

means for propagating said imprinted waves onto a target, wherein said imprinted waves are either transmitted through or reflected from said target to produce reflected/transmitted waves;

means for imprinting a finite number of coherent echos onto said reflected/transmitted waves to produce a combined signal; and

means for time averaging the square of said combined signal to calculate the velocity of said target.

2. The apparatus of claim 1, further comprising means for producing a velocity discriminated range value comprising means for cross-correlating said combined signal with said wide bandwidth waves from said source before said imprinted waves are produced.

3. The apparatus of claim 1, wherein said arbitrary waves comprise any waveform.

4. The apparatus of claim 1, wherein said arbitrary waves comprise wide bandwidth waves.

5. The apparatus of claim 1, wherein said arbitrary waves comprise waves which over the illumination time of the target behave incoherently or randomly.

6. The apparatus of claim 1, wherein said arbitrary waves comprise sets of narrowband waves where the maximum and minimum frequency bands are widely separated.

7. The apparatus of claim 1, wherein said arbitrary waves comprise

narrowband waves whose instantaneous frequency changes significantly with time, continuously or discontinuously (chirped waves).

8. The apparatus of claim 1, wherein said arbitrary waves comprise waves whose smallest coherence time is comparable to or less than the interferometer delay time.

9. The apparatus of claim 1, wherein said arbitrary waves comprise waves whose smallest coherence length is comparable to or less than the change in round trip distance between target and apparatus during the interferometer delay time.

10. The apparatus of claim 1, wherein said arbitrary waves comprise waves selected from a group consisting of waves whose smallest coherence time is comparable to or less than the interferometer delay time and waves whose smallest coherence length is comparable to or less than the change in round trip distance between target and apparatus during the interferometer delay time, wherein said waves are non-repeating waves.

11. The apparatus of claim 1, wherein said arbitrary waves comprise waves selected from a group consisting of waves whose smallest coherence time is comparable to or less than the interferometer delay time and waves whose smallest coherence length is comparable to or less than the change in round trip distance between target and apparatus during the interferometer delay time, wherein said waves are repeating waves.

12. The apparatus of claim 1, wherein said arbitrary waves comprise waves selected from a group consisting of waves whose smallest coherence time is comparable to or less than the interferometer delay time and waves whose smallest coherence length is comparable to or less than the change in round trip distance between target and apparatus during the interferometer delay time, wherin said waves are produced by a noise source.

13. The apparatus of claim 1, wherein said arbitrary waves comprise waves selected from a group consisting of waves whose smallest coherence time is comparable to or less than the interferometer delay time and waves whose smallest coherence length is comparable to or less than the change in round trip distance between target and apparatus during the interferometer delay time, wherein said waves are produced by a digital algorithm or read from a memory device.

14. The apparatus of claim 1, wherein said means for imprinting a finite number of coherent echos onto said arbitrary source of waves to produce imprinted waves comprises delayed and undelayed components that are coherently identical, wherein all components are separated by a delay t1, wherein said delayed and undelayed components can differ from said waves from said source, wherein slight dispersion of the delay with wavelength is tolerated if matched by the same dispersion in the imprinting process of the reflected/transmitted waves, wherein there could be one delayed component and one undelayed component, and wherein there could be one undelayed component and many delayed components of gradually decreasing intensities for increasing time.

15. The apparatus of claim 1, wherein said means for imprinting a finite number of coherent echos onto said arbitrary source of waves to produce imprinted waves, wherein said coherent echos comprise a wave kind in the imprinting process that is any wave kind for which constructive or destructive interference occurs in the combined intensity in an interferometer when a delayed replica is combined to the undelayed wave, and the said wave kind in the imprinting process can be 1-, 2- or 3-dimensional, and wherein if said wave kind is 2- or 3- dimensional, the imprinting process must satisfy the superposition condition where each output ray associated with an input ray must superimpose in position and angle.

16. The apparatus of claim 1, wherein said means for imprinting a finite number of coherent echos onto said arbitrary source of waves to produce imprinted waves, wherein said coherent echos comprise a wave kind in the imprinting process that can be an electrical signal, a numerical value processed by digital circuits or by mathematical techniques such as Fourier transforms, or represented by modulating another kind of wave such as the intensity, color or polarization of an optical wave.

17. The apparatus of claim 1, wherein said means for imprinting a finite number of coherent echos onto said arbitrary source of waves to produce imprinted waves, wherein said coherent echos comprise a wave kind in the imprinting process that can be heterodyned to a different average frequency, called the intermediate frequency signal (IF), wherein said wave kind can be split into several components which are individually heterodyned to a set of parallel IF signals which are individually imprinted and then recombined by a reverse heterodyning process.

18. The apparatus of claim 1, wherein said imprinted waves can be converted to another wave kind by an antenna or transducer, wherein said wave kind may be electromagnetic waves such as light, microwaves, infrared waves, or vibrations of pressure or strain such as sound, and could be 1-, 2- or 3-dimensional, and wherein said wave kind may be any kind for which the target activity being measured produces a dilation or contraction of the waveform returned to the apparatus.

19. The apparatus of claim 1, wherein said reflected/transmitted waves can be converted by an antenna or transducer to a second wave kind before imprinting, wherein said second wave kind comprises delayed and undelayed components that are coherently identical, wherein all components are separated by a delay t1, wherein said delayed and undelayed components can differ from said waves from said source, wherein slight dispersion of the delay with wavelength is tolerated if matched by the same dispersion in the imprinting process of the reflected/transmitted waves, wherein there could be one delayed component and one undelayed component, and wherein there could be one undelayed component and many delayed components of gradually decreasing intensities for increasing time.

20. The apparatus of claim 1, wherein for 2- and 3-dimensional waves, imprinted delay can be a function of position across the image.

21. The apparatus of claim 1, further comprising a wavelength dispersive device to organize the channels detecting the output intensity versus wavelength.

22. A method, comprising:

imprinting a finite number of coherent echos onto a wide bandwidth source of waves to produce imprinted waves;

propagating said imprinted waves onto a target, wherein said imprinted waves are either transmitted through or reflected from said target to produce reflected/transmitted waves;

imprinting a finite number of coherent echos onto said reflected/transmitted waves to produce a combined signal; and

time averaging the square of said combined signal to calculate the velocity of said target.

23. The method of claim 22, further comprising producing a velocity discriminated range value further comprising the step of cross-correlating said combined signal with said wide bandwidth waves from said source before said imprinted waves are produced.

Part 4

Multichannel Heterodyning for Wideband Interferometry, Correlation and Signal Processing

US Patent 5,943,132
Issued Aug. 24, 1999

David J. Erskine*
Lawrence Livermore Nat. Lab.

A method of signal processing a high bandwidth signal by coherently subdividing it into many narrow bandwidth channels which are individually processed at lower frequencies in a parallel manner. Autocorrelation and correlations can be performed using reference frequencies which may drift slowly with time, reducing cost of device. Coordinated adjustment of channel phases alters temporal and spectral behavior of net signal process more precisely than a channel used individually. This is a method of implementing precision long coherent delays, interferometers, and filters for high bandwidth optical or microwave signals using low bandwidth electronics. High bandwidth signals can be recorded, mathematically manipulated, and synthesized.

I. INTRODUCTION

A. Field of the Technology

The present invention relates to interferometry, correlation and autocorrelation of wide bandwidth signals, and more specifically the coherent conversion of wide bandwidth signals to a set of many lower frequency signals and subsequent parallel signal processing.

B. Description of Related Art

Electromagnetic waves such as microwaves and light, and ultrasound waves are widely used for echolocation, velocimetry and imaging. These techniques involve signal processing such as correlation, interferometry, time delaying, filtering, recording and waveform synthesis. Currently, many of these applications use fairly monochromatic waves having a long coherence length. If instead wide bandwidth waves are used, an increased precision of the location and velocity of the target results due to the illumination's shorter coherence length.

U.S. Patent No. 5,642,194, titled "White Light Velocity Interferometer" and U.S. Patent Application Serial No. 08/720,343, titled "Noise Pair Velocity and Range Echo-Location System", both incorporated herein by reference, describe how two interferometers nearly matched in delay can be used with wide bandwidth illumination to measure target velocity using processes of interferometry and autocorrelation (Fig. 2A). The wideband illumination can be used to measure target range using the process of correlation (Fig. 2B). These processes of interferometry, correlation and autocorrelation require coherent delays. For microwave radars, the delays are chosen to be several milliseconds to match radar pulse repetition rates, which in turn are set by the desired maximum target range of hundreds of kilometers. Several milliseconds is a long delay compared to the period of the wave, which could be 30 picoseconds. Electronics, and particularly digital electronics, is the most attractive method of creating long delays, as well as for performing general signal processing. The challenge is that the bandwidths found in microwave and optical signals can greatly exceed the capability of easily available electronics.

For example, suppose we wish to construct a device using 10-30 GHz microwaves having a bandwidth of 20 GHz, using interferometers of 2 ms delay. (This could provide meter/sec velocity measurement and ∼1 cm range resolution.) It is impractical to create such a

*erskine1@llnl.gov

Figure 1 **Multiheterodyning Signal Processor**

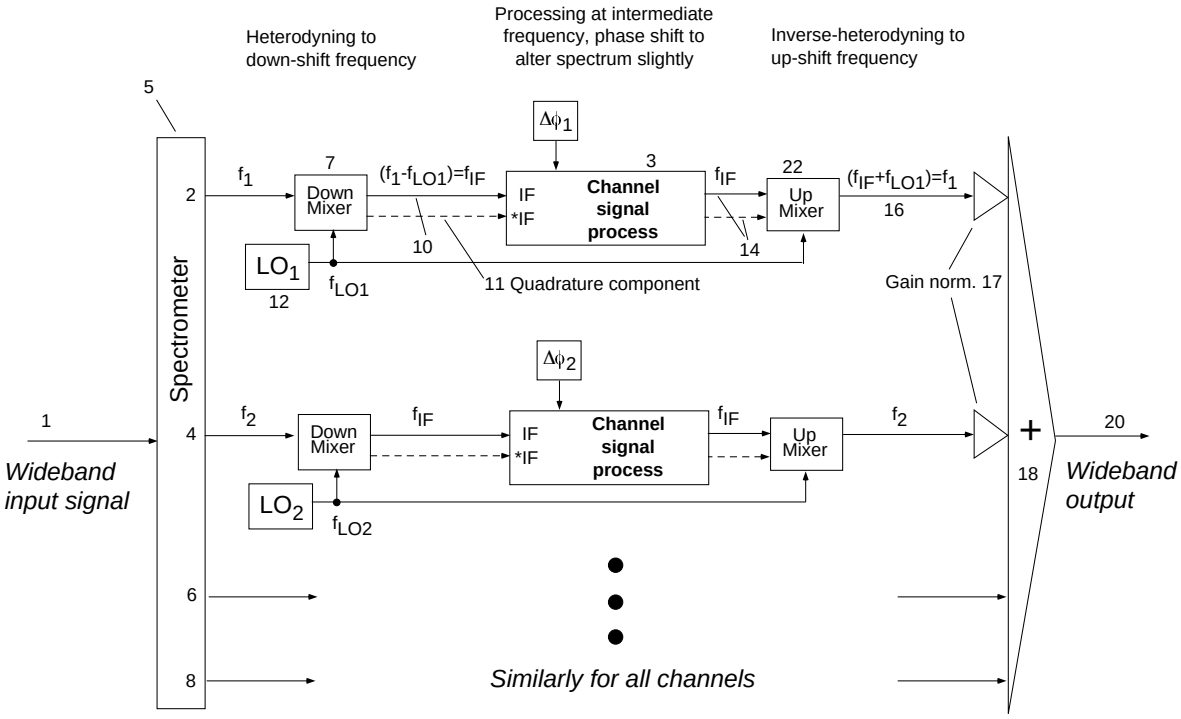

Figure 1 is a schematic of multiheterodyning signal processor.

Figure 2

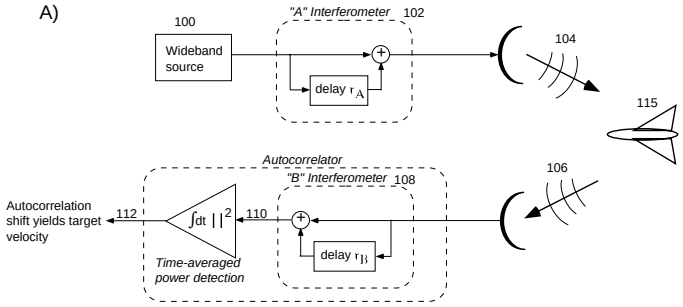

Figure 2A shows a double interferometer velocimeter using wideband illumination.

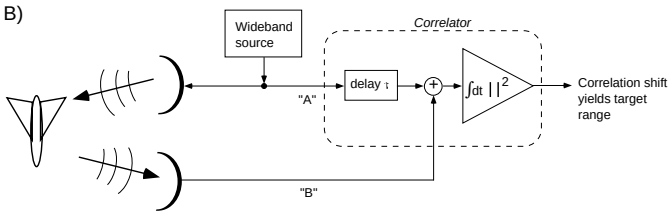

Figure 2B shows the use of correlation and wideband illumination to find the range of a target.

long delay by analog cable, because the cable length required is hundreds of km, and serious attenuation and dispersion of the signal would result, in addition to the impractical weight and cost of the cable. A digital delay line consisting of an analog-digital converter (A/D), shift register, and digital-analog converter (D/A) can easily create a 2 millisecond delay. However, the 20 GHz input signal bandwidth greatly exceeds the bandwidth capability of commonly available digital electronics, which may be closer to 0.2 GHz.

The bandwidth of optical signals can be even much higher than microwaves and thus even further beyond the capability of current electronics. (Optical velocimeters having long delays are useful for measuring extremely slow velocities.) In spite of lower weight of optical fiber, a spool of fiber hundreds of km long is still large and expensive, and the attenuation and dispersion through such a length would force the use of repeaters, further increasing cost and weight.

In addition to velocimetry, applications for correlating wide bandwidth optical signals abound in astronomy, for creating long baseline optical telescopes analogous to radio telescope arrays. These could increase the angular resolution by orders of magnitude over current optical telescopes. The challenge here is to correlate two or more optical signals received many hundreds of kilometers apart. Propagating a weak optical signal through long optical fibers brings severe attenuation and dispersion, losing the phase information required for correlations. Digitally encoding the time varying optical field

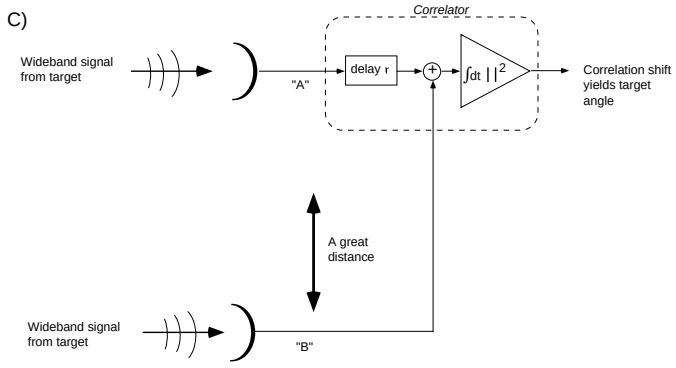

Figure 2C shows the use of correlation to find angular position of a wideband emitting target.

(amplitude and phase) was not feasible previously.

A high bandwidth requirement can also come from the use of multiple input data streams which need to be correlated to form a 2-dimensional image. Such is the case of an ultrasound imaging device using multiple detectors (transducers) and using wideband illumination (to reduce speckle). While a single detector produces a 1 to 10 MHz bandwidth signal, which is low enough to be processed by a single channel of electronics, a matrix of 100 such detectors requires calculating a large number of correlation combinations. This can exceed real-time processing capacity.

Figures 2A, 2B, and 2C show applications for interferometry, autocorrelation and correlation. Figure 2A shows a double interferometer velocimeter, which is also called a "white light" velocimeter for optical waves (see U.S. Patent No. 5,642,194) and a "noise pair" radar for microwave waves (See U.S. Patent Application Serial No. 08/720,343). Waves from a wideband source 100 pass through an interferometer 102 labeled "A" having a delay τ_A. This imprints a coherent echo on the source to form an illumination beam 104, which is sent to a target 115. The presence of the coherent echo causes a comb-filter shape to the power spectrum of waves 104. The waves 106 reflected from the target are Doppler shifted by the target velocity, which dilates the comb-filter spectrum slightly. The reflected waves pass through a second interferometer 108 labeled "B" having a delay τ_B and which imposes its own comb-filter pass spectrum. This creates a detected wave 110. The time-averaged power 112 of the detected wave is measured versus delay τ_B to form an autocorrelation. The autocorrelation will have a peak for delays $\tau_B \approx \tau_A$. This is because the maximum amount of power will pass through the "B" interferometer when its spectrum matches the Doppler shifted spectrum of the "A" interferometer. Let the position of the peak be τ_p. For target velocity v, and for a target reflecting light 180° back toward the apparatus, the autocorrelation peak shift is proportional to velocity, $\tau_p - \tau_A = (2v/c)$, where c is the wave speed. Thus very long delay times produce sensitive velocity detection. The advantage of high bandwidth for the source 100 is a smaller coherence length, which makes the autocorrelation peak narrower, reducing velocity ambiguity. This allows resolving velocities of multiple targets.

An interferometer is a device that coherently sums an applied signal with a delayed replica. It is a filter with a power transmission spectrum which is sinusoidal, as shown in Fig. 3A, ideally given by $T = (1/2)[1 + \cos(\omega\tau + \text{const})]$, where "const" is a constant, $\omega = 2\pi f$ is the angular frequency, and τ the interferometer delay. This kind of spectrum is also called a "comb-filter". Figure 3B shows a close-up of the sinusoidal peaks having a periodicity $1/\tau$ in frequency units and 360° in phase units. (The periodicity of the sinusoids in these Figures is exaggerated for clarity. For example, a 2 ms delay interferometer would have 2 ms × 20 GHz = 40 million peaks from 10 GHz to 30 GHz.)

Note that it is the structure of the comb-filter on the scale $1/\tau$ which produces the velocity measuring effect. Spectral changes much broader and much narrower than $1/\tau$ do not significantly affect the phase of the fringes. Thus a less-than-ideal interferometer that broadly modifies the spectrum of the applied signal can still be used, as well as one having slightly non-uniform spacing (phase) of comb peaks, provided both "A" and "B" interferometers share the same non-uniformity.

Figure 2B shows an application of high bandwidth signals to find the range of a target, and Fig. 2C to measure the angle of a target by the difference in arrival times of a wave at two antenna spaced well apart (such as in radio astronomy). These applications both create a correlation between two signals "A" and "B". The position (in delay-space) of the correlation peak yields the range or angle information. Again, the advantage of using a high bandwidth source is to create a narrow correlation peak, which reduces ambiguity of the measurement.

In addition to correlations and interferometry, other signal processes which benefit from high bandwidth are the recording and synthesis of waveforms. The time resolution of these processes is given by the reciprocal of the bandwidth, so high bandwidth allows for the shortest time resolution.

II. SUMMARY OF THE INVENTION

It is an object of the present invention to provide techniques for coherently combining a set of low bandwidth signal processing channels to form a collective high bandwidth signal processing device.

A high bandwidth reference signal, which in many embodiments is provided by a set of oscillators conventionally called local oscillators (LO), but could also be a single mode-locked signal having many harmonics, provides the synchronization that preserves the coherence between channels. The phase relationship between the multiple channels is set to precisely define the temporal response of the net device. In this way, for the cases of interferom-

Figure 3

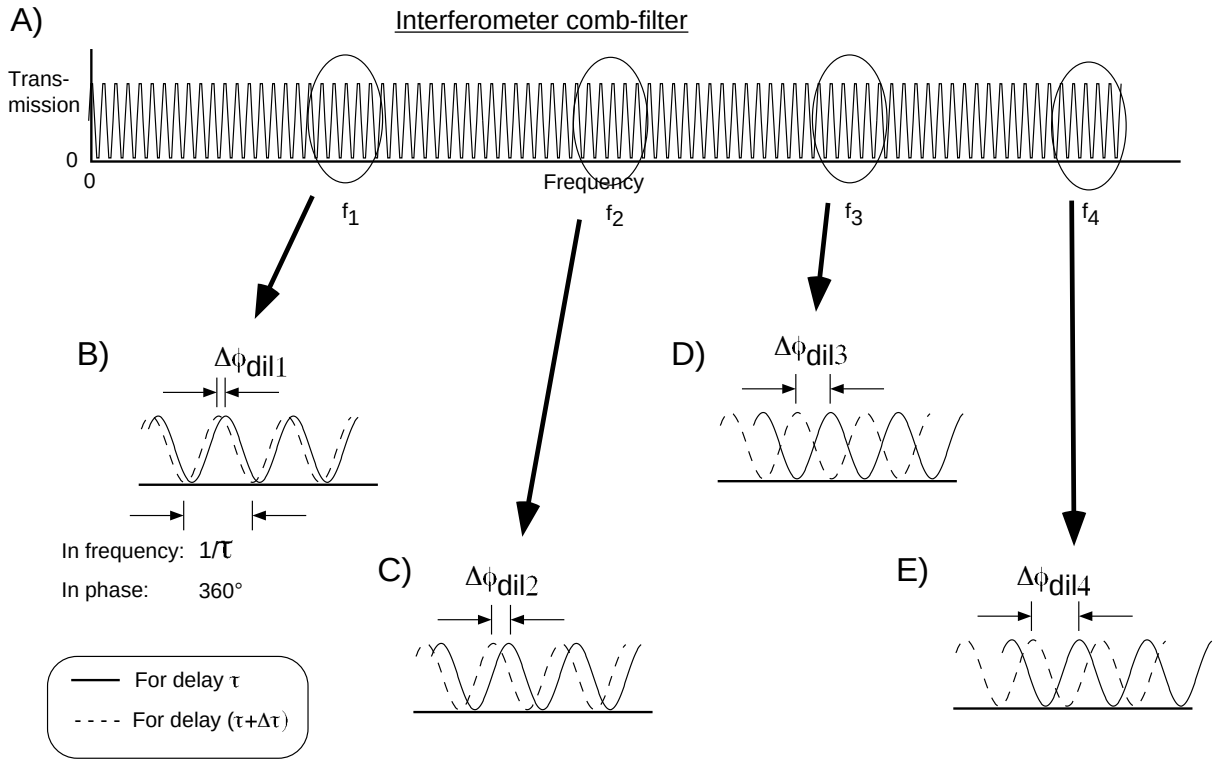

Figure 3A shows the comb-filter transmission spectrum of a phase-linear interferometer. Figure 3B shows a detail of the interferometer transmission spectrum having sinusoidal peaks of period $1/\tau$. Figures 3C through 3E show that the effect of slightly changing the interferometer delay is to locally shift the spectrum by an amount proportional to frequency.

eter, filter, autocorrelator, correlator, or delay-line signal processes which involve a characteristic delay time τ, the effective value of τ can be controlled with much higher precision than by a single channel used alone.

The method of the invention could be called "multichannel heterodyning", or "multiheterodyning", and can be used to interfere, correlate, autocorrelate, delay, filter, record and synthesize waveforms, as well as combinations of those processes. The philosophy is to subdivide the input signal spectrum into many narrow bands (channels) which are shifted to a lower frequency (called an intermediate frequency, (IF)) by heterodyning against a set of reference frequencies (f_{LO}), one per channel. Both the phase and amplitude information of the original input frequency components can be preserved in the heterodyning. The overall signal process desired for the input signal is applied individually to each channel. The channel spectra are spectrally re-assembled by a second heterodyning process which shifts the frequencies upward to form a net high bandwidth output signal, or in the case of correlation and autocorrelation processes the net time-averaged power is computed and summed over all channels, omitting the up-heterodyning step. In autocorrelation, correlation, interferometry, or delay, each channel process spectra (Fig. 4A) is similar for all channels. Then the net spectrum (Fig. 4B) comprises a set of these 200, 201, 202, translated upward in frequency via heterodyning to fill the input bandwidth. The channel spectra could also be individualized to create a non-periodic spectrum (Fig. 4C).

Since the phase and amplitude of the input frequency components can be determined through the down-heterodyning process, the entire Fourier spectrum of the input signal (real and imaginary parts across the full input bandwidth) can be recorded, by recording each individual channel and re-assembling the spectral information at a later time. (Optimal recording desires the channel bandshapes to contiguously fill the input bandwidth shoulder-to-shoulder). Knowledge of the full-band Fourier spectrum is a complete description of the input signal.

For real-time processes, any arbitrary filtering process that can process each frequency component independent of the others can be implemented by the invention. (An example of a process that is inappropriate is a non-linear process where widely separated high and low frequency components are expected to mix and form sum or difference frequency output terms. Such pairs are not easy to form in real-time for the invention because the high and low input frequencies are segregated into separate channels.) However, the combination of recording an input signal, manipulating its recorded Fourier spectrum

Figure 4

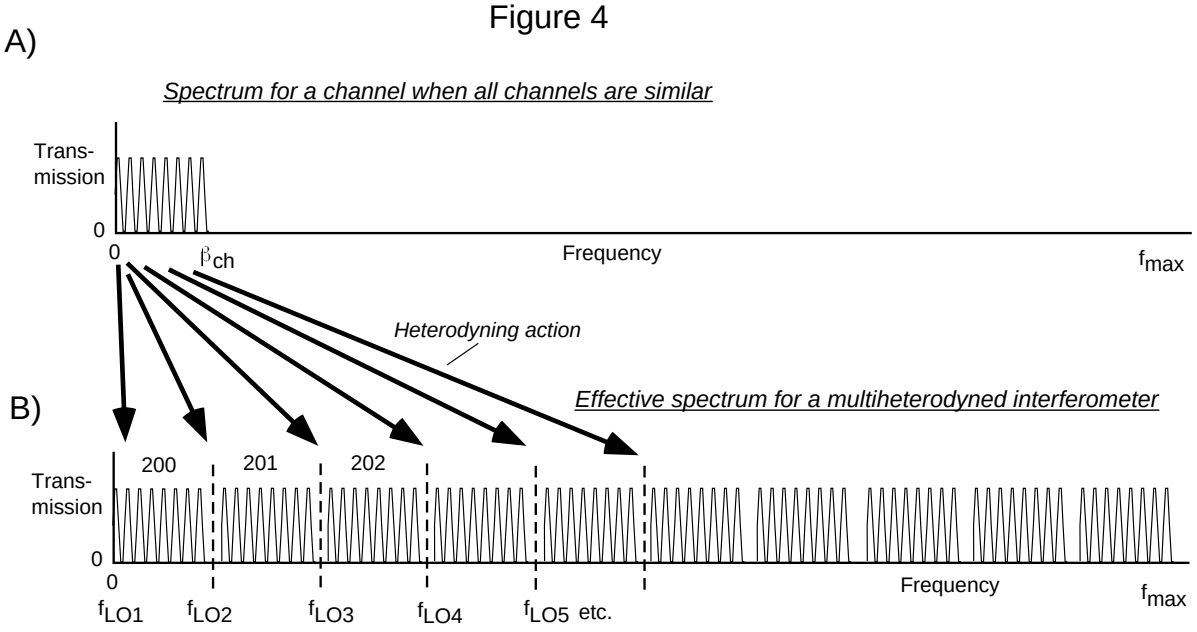

Figure 4A shows a channel interferometer transmission spectrum. Figure 4B shows the effective transmission spectrum of a multiheterodyning interferometer formed from many similar channels contiguously filling the input bandwidth.

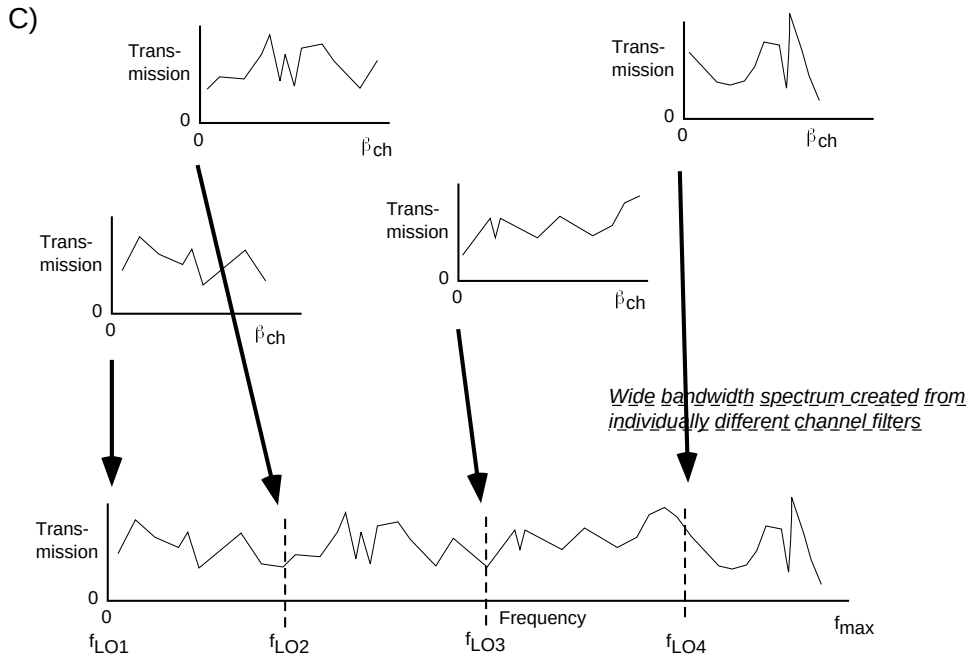

Figure 4C shows a non-periodic wideband spectrum formed from many individualized channel spectra.

mathematically in any arbitrary way, and then synthesizing the output signal provides powerful flexibility in creating a wide variety of signal processes, including the aforementioned non-linear processes which require mixing of widely separated frequency components.

The advantage of the invention is that it allows the use of inexpensive, low bandwidth and low frequency signal processing components such as digital electronics, to manipulate signals having much higher bandwidth and frequency. This is especially important for the creation of very long coherent time delays for high bandwidth microwave and optical signals. Such long time delays are needed to construct velocimeters and range-finders using short coherence length illumination, which offer advantages of simultaneous unambiguous velocity and range determination, and lack of confusing speckle.

A great practical advantage of the invention occurs for applications involving comparison of two signals when a set of reference frequencies can be shared between two multiheterodyning apparatuses. This comparison can be a correlation between two received signals to determine angle of a radar or optical target, or the correlation of a transmitted and reflected signal to determine range, or the autocorrelation of a reflected signal previously imprinted with an echo by an interferometer to determine target velocity. When two multiheterodyning apparatuses share the same reference frequencies the comparison process is insensitive to the detail values of those frequencies. This allows the reference frequencies to drift slowly with time, such as due to thermal drift. This can dramatically reduce cost of the apparati by reducing need for stabilization. Secondly, the channel bandshapes can have slightly irregular shapes. This reduces the cost of the spectrometer.

III. DETAILED DESCRIPTION OF THE INVENTION

Figure 1 shows an embodiment of the invention appropriate for signal processes that create a wideband output from a wideband input, such as delay, interferometry, and filtering with an arbitrary impulse response. Portions of Fig. 1 are also appropriate for other signal processes. For the processes of correlation and autocorrelation, the up-mixing step is omitted and an integral signal summed over all channels forms a net integral output. For the process of recording, the real-time up-mixing step is also omitted. Instead, it is performed essentially mathematically at a later time. For waveform synthesis, the input spectrometer 5 and down-mixing steps are omitted.

The multiheterodyning process can be described by following a signal through Fig. 1. The wideband input signal 1 having bandwidth β_{net} is subdivided by the spectrometer 5 into many separate signals 2, 4, 6, 8 and so on, called band signals. These have smaller bandwidth of about β_{ch} and different average frequencies. Each band signal is processed by a channel in a overall parallel manner. Only two of many possible channels are drawn, with the other channels being analogous. Let f_x represent the frequencies of a generic band signal, and f_1, f_2 etc. those of specific channels. The term "bandshape" refers to the power transmission versus frequency curve of signals sent into a particular channel by the spectrometer. It is given by the output signal power spectrum divided by the input signal spectrum so that the transfer function of all the components along the signal path are included, including those of the input spectrometer, down-mixer, amplifiers in the channel signal processor, and up-mixer and output spectrometer, if used. Thus β_{ch} is not necessarily set by the spectrometer, but could be set by other components further along the channel, whatever is more limiting.

A. Spectrometer

The spectrometer 5 could comprise a diffraction grating or prism, which disperses the signal versus frequency into different physical output paths, or a parallel arrangement of bandpass filters. It is optimal for the tightest correlations and for the most accurate preservation of the input signal character that the channel bandshapes fill the input bandwidth contiguously (shoulder-to-shoulder), so that there are N_{ch} channels, N_{ch}=β_{net}/β_{ch}. However, sparsely arranged channel bandshapes can be tolerated in many applications, such as correlations. The correlation so obtained is less precise than one obtained with contiguous bands, but it may still be sufficiently precise to be useful, and is cheaper to achieve. Sparsely filled bandshapes will be the usual case for optical input signals, since the optical bandwidth (10^{14} Hz) is 5 orders of magnitude larger than typical electronics bandwidth (10^9 Hz), and N_{ch} will usually be quite less than 100,000.

The path of a signal through a generic channel will be described, while sometimes referring to items in the Figures specific to the first channel, for concreteness. The band signal 2 from the spectrometer is heterodyned to a lower frequency by the down-mixer 7 to form an intermediate frequency (IF) signal 10, and a quadrature version 11, called *IF. The heterodyning is done by mixing the band signal 2 with a frequency f_{LO1}, which is optimally located at the edge of the band. (Our analysis assumes $f_{LO} < f_x$. If $f_{LO} > f_x$, the polarities of the required channel phase shifts to achieve a given effect will be flipped.) Thus the IF signal could have frequency components ranging from 0 to $\sim \beta_{ch}$. Let f_{IF} represent the frequency of a generic component of IF. Let f_{LO} represent the generic reference frequency and f_{LO1}, f_{LO2} etc. represent one specific to a particular channel.

In Fig. 1, f_{LO1} is shown generated by an oscillator 12 (typically called a "local oscillator"). However, instead of having separate signals f_{LO1}, f_{LO2} etc., the reference frequencies could be components of a single reference signal, such as provided by a mode-locked oscillator having many harmonics. In this case the reference signal could be added to the input signal prior to the spectrometer, as shown in the optical embodiments of Fig. 5 and Fig. 6, rather than after the spectrometer. Since f_{LO} and f_x are close together in frequency, the spectrometer could route both of these to the same channel where heterodyning is subsequently performed.

B. Down-mixer

Heterodyning is well established in the art. Down-heterodyning can occur if two signals both illuminate an intensity (power) detector or are presented together to a non-linear device (Fig. 7A). Suppose the input signal (band signal) 751 is represented by $E_x e^{i\omega_x t}$ and the reference signal component 753 by $E_{LO} e^{i\omega_{LO} t}$, then the power ($P$) at a detector 754 is $|E_x e^{i\omega_x} + E_{LO} e^{i\omega_{LO} t}|^2$, which be-

Figure 5

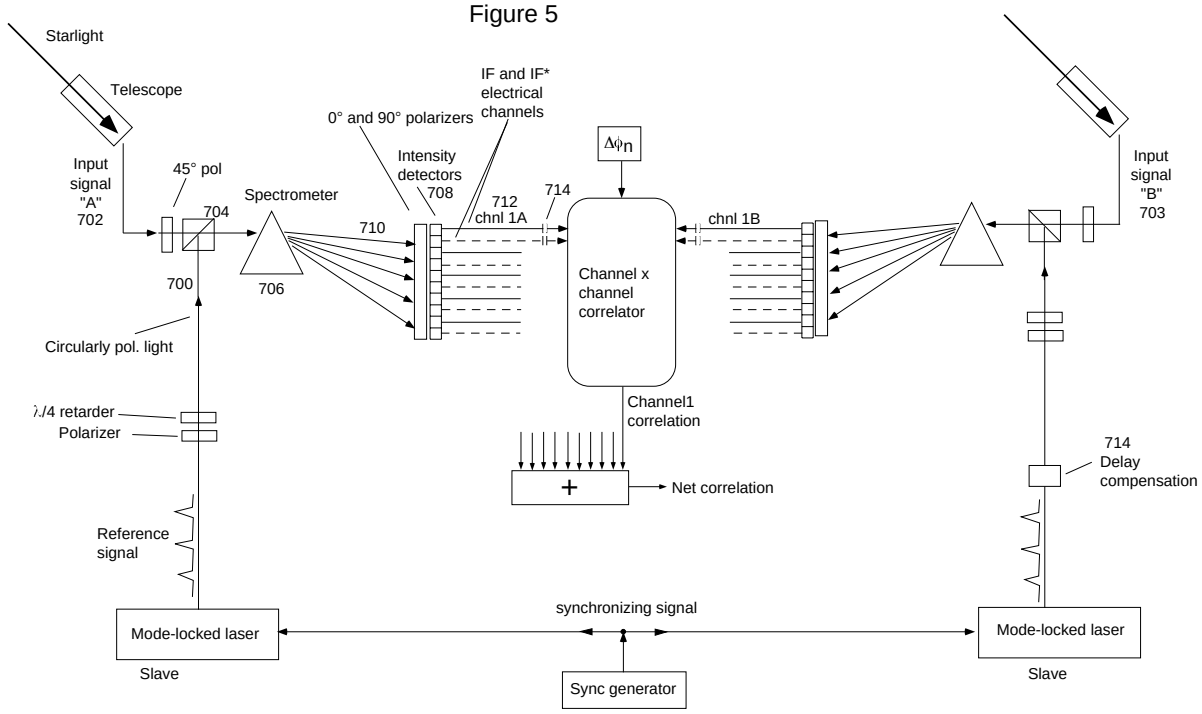

Figure 5 shows an optical embodiment of a multiheterodyning correlator.

Figure 6

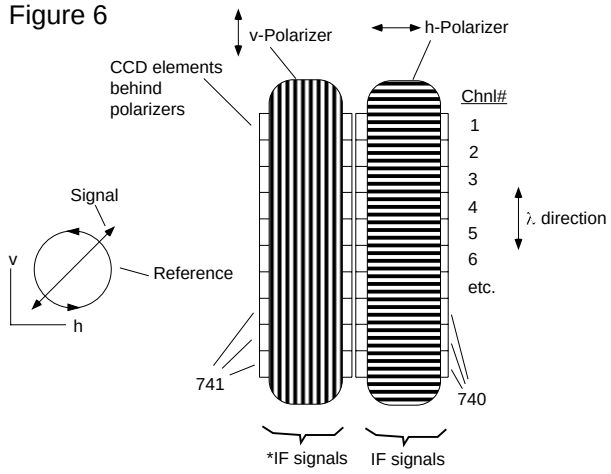

Figure 6 shows the orientation of polarizers before the intensity detectors of the spectrometer in the optical correlator of Fig. 5.

Figure 7

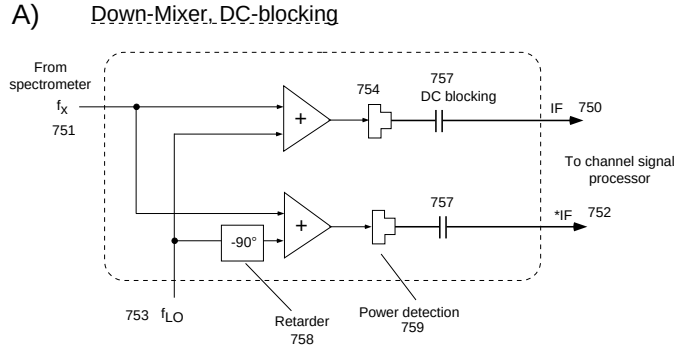

Figure 7A shows a down-mixer creating a down-heterodyned signal using intensity detection and using a DC-blocking capacitor.

comes

$$P_{IF} = |E_x|^2 + |E_{LO}|^2 + 2\mathrm{Re}[E_x E_{LO}^* e^{i(\omega_x - \omega_{LO})t}] = \text{constant} + \sim \cos(\omega_x - \omega_{LO})t. \quad (1)$$

The last term of Eq. 1 is the difference frequency term which forms the IF output 750 and has cosine-like character. The first two terms of Eq. 1 are DC (zero frequency) terms and they need to be excluded from the IF output, otherwise they will masquerade as a legitimate DC term produced from band signal components having frequencies near f_{LO}. In Fig. 7A, the DC terms are blocked by capacitors 757 from the mixer outputs.

In Fig. 7A a quadrature output 752 is formed by heterodyning the input signal 751 against the reference signal 753 retarded at 758 by -90° (advanced by 90°). Then the power at detector 759 is $|E_x e^{i\omega_x t} + E_{LO} e^{i90^\circ} e^{i\omega_{LO} t}|^2$, which becomes

$$P_{*IF} = |E_x|^2 + |E_{LO}|^2 + 2\mathrm{Re}[E_x E_{LO}^* e^{-i90^\circ} e^{i(\omega_x - \omega_{LO})t}] = \text{constant} + \sim \sin(\omega_x - \omega_{LO})t. \quad (2)$$

The last term of Eq. 2 is the difference frequency term which forms the *IF output 752 and has sine-like behav-

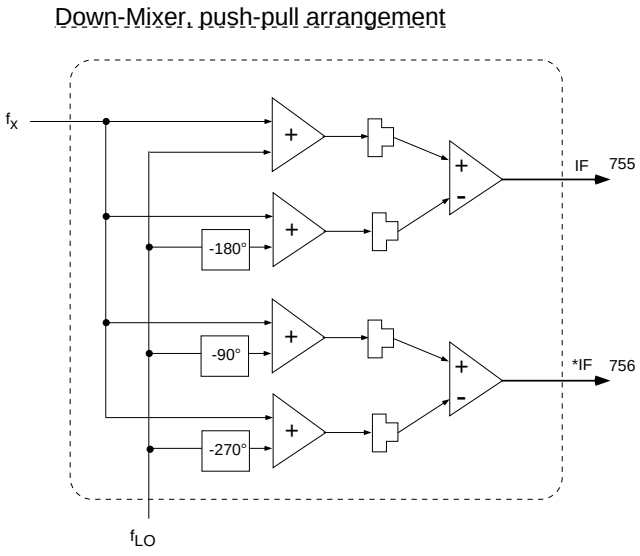

Figure 7B shows a down-mixer creating a down-heterodyned signal using intensity detection and using push-pull subtraction to eliminate the DC component.

ior. These two mixer outputs 750, 752 (IF, *IF) form a so-called "vector" intermediate frequency signal which is sent to the channel signal processor (3 in Fig. 1).

In general, the quadrature output (*IF) is produced by heterodyning against a reference signal phase shifted by 90° relative to the input signal. The relative phase shift can be +90° or -90° depending on whether *IF is intended to lead or lag IF. A lagging *IF is produced by retarding the input signal, or advancing (retarding by a negative amount) the reference signal, or a combination of both so that the difference in retardations is 90°. A leading *IF is produced by the opposite arrangement. (In this specification, the term "retardation" generically can have either polarity, and whether a positive or negative retardation is called for needs to be taken from the context.)

The choice of whether to retard the input signal or reference signal depends on practical details. For example, for a weak input signal it may be undesirable to insert a retarding element into the input signal path because it may attenuate the signal, whereas the reference signal is usually strong.

Secondly, it is arbitrary whether to have *IF lead or lag IF, provided the operator is aware that this choice will flip the polarity of vector rotation $\Delta\theta$ required to apply to the channel signal process to produce the desired frequency shift. The retardation in Fig. 7A is chosen so that *IF lags IF, so that the *IF signal is analogous to the imaginary part and not the negative imaginary part of a complex number, and IF represents the real part.

Because it is easy to make a polarity mistake in the mathematics that describes vector rotations and channel phase shifts, the reader should use the following operational guideline: the correct polarity of phase shift and IF rotation to increase the effective delay of the net signal process is that which causes the spectrum of the channel signal process, as mapped to the input spectrum by the heterodyning, to appear to shift to lower frequencies.

It is acceptable that *IF lags or leads IF by an angle different than 90°, provided it is not a small angle, say not less than 45°. For this non-orthogonal case, the sinusoidal coefficients used for the vector rotations are different than that stated by Eq. 9 and Eq. 10. The correct rotational transformation can be found through straightforward vector mathematics by re-expressing the non-orthogonal direction vectors in terms of orthogonal direction vectors.

A drawback of the down-mixer circuit in Fig. 7A is that the DC blocking capacitors 757 also block the legitimate DC components. Figure 7B shows a preferred down-mixer embodiment using a "push-pull" scheme that preserves legitimate DC components while eliminating the illegitimate DC components. By retarding the reference frequency by two amounts 180° apart, such as -90° and -270°, or 0° and -180°, and by subtracting the associated intensities, the differences 755 and 756 contain only legitimate DC terms. The push-pull schematic is analogous to the algebraic expression $(A+B)^2-(A-B)^2=4AB$.

Down-heterodyning can also be achieved by replacing the power detectors in Fig. 7A and Fig. 7B by a non-linear device such as a diode that has a quadratic term in its output versus input behavior.

The heterodyning process can confuse $(f_x - f_{LO})$ signals with $(f_{LO} - f_x)$ signals. This confusion is called "aliasing" and is usually unwanted. To avoid aliasing, f_{LO} can be chosen to be on the edge of the band rather than in the middle of it. Our analysis assumes f_{LO} is on the lower edge of the band.

C. Vector signals

The expression of the down-heterodyned signals as a pair of signals (IF, *IF), one of which is in quadrature, could be called a *vector* signal, as opposed to a single IF signal which could be called *scalar*.

The vector signals are symbolized in the Figures by a pair of lines, one of which is dashed, such as the pair 10, 11 in Fig. 1. The vector expression is useful for expressing phase information for near-DC components of IF. For example, it is not possible to communicate the both the phase and amplitude of a DC component of IF by only one signal path. Secondly, even if DC components are not used, the vector expression of the IF signal allows simple methods for phase shifting all IF frequency components by the same amount, independent of intermediate frequency. This is desired to translate uniformly the spectral behavior contributed by each channel relative to the overall spectral behavior. This is useful for simulating a dilating net spectrum and hence a dilating temporal response for the net device.

This later discussion of phase shifting will center

Figure 8

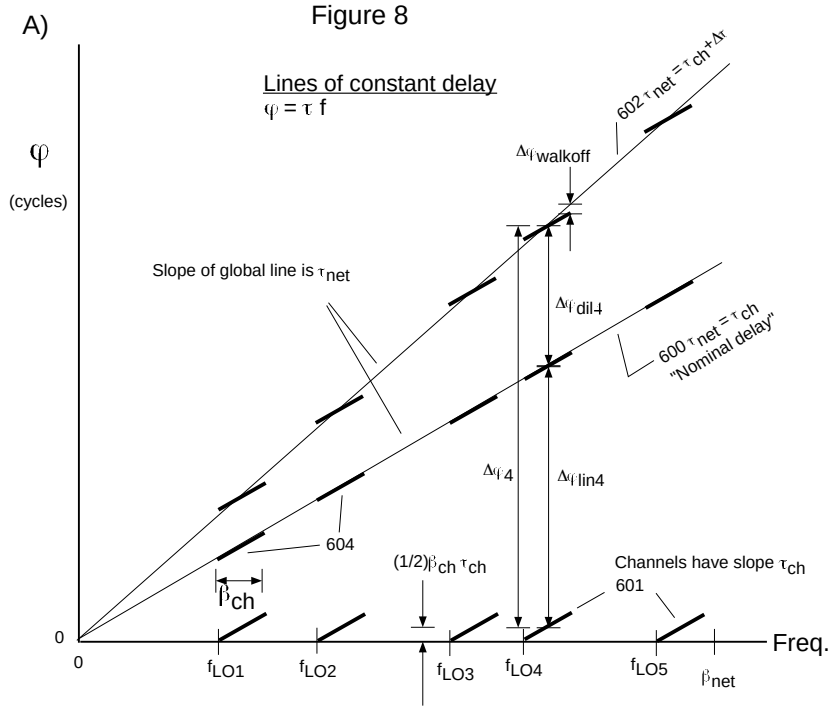

Figure 8A shows a plot of phase versus frequency of a signal from a signal process having characteristic delay τ.

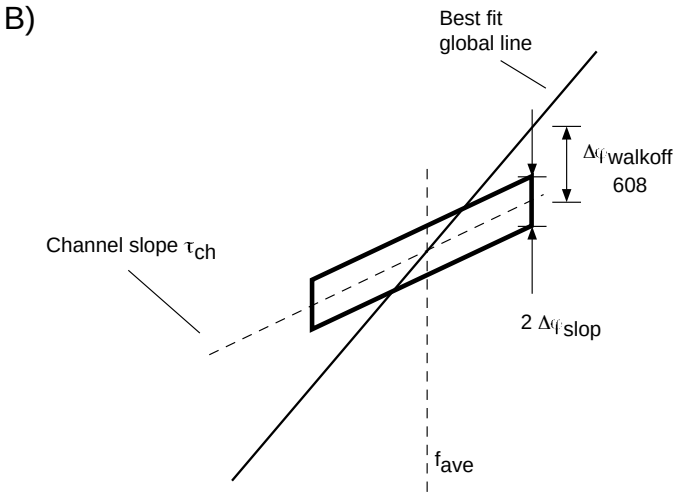

Figure 8B is a close-up of Figure 8A where the segment representing a phase-shifted channel meets a global line representing behavior of the net multiheterodyning device.

around Fig. 8A, and a IF phase shifting process that is independent of IF frequency has the effect of translating the bold line segments 601 called "channel segments" vertically without changing their slope. In point of fact, small changes in the slope can be tolerated, and depending on their polarity they can even help reduce dephasing due to "walkoff error". We can call the phase shift nonuniformity over the channel bandwidth an error $\Delta\phi_{slop}$, and generally we desire it to be less than 0.25 cycle in order to avoid dephasing effects.

To achieve a phase-linear process, it is optimal that the channel segments match the best fit global line as much as possible, such as within 0.25 cycle. In some applications phase-linearity is not required. For example, to compare two signals being sent through two multiheterodyning apparatuses, it is the *difference* in phase error between channels "A" and "B" being compared and not the absolute phase error which is relevant.

D. Channel signal processors

For each channel, the vector signal (10, 11 in Fig. 1) from the down-mixer is applied to a channel signal processor, such as 3. For processes which will produce a high frequency output signal for the net device, such as interferometry, filtering, time delay or waveform synthesis, the channel signal processor outputs a vector signal 14 which is sent to the up-mixer 22 to be raised in frequency to form a channel high frequency signal 16. These are then summed over all channels by 18 to form the net wideband output 20. For processes such as correlation and autocorrelation, the signal processor output is a slowly varying scalar (also called a time-averaged or integral signal). These are summed over all channels omitting the up-heterodyning step to form the net correlation or net autocorrelation. For the process of recording, the (IF, *IF) vector channel input is stored for subsequent analysis at less than real-time and the real-time up-heterodyning step is omitted. (More pre-

cisely, the up-heterodyning step is performed essentially mathematically during the Fourier reconstruction of the input signal.)

Each channel signal processor has a phase shift parameter ($\Delta\phi$) input chosen by the user. This causes the spectral behavior for that channel to shift by $\Delta f = -\Delta\phi\tau_{ch}$, where τ_{ch} is the delay characterizing the channel signal process. Let $\Delta\phi_n$ be the $\Delta\phi$ for the nth channel. The choice of the set $\Delta\phi_n$ allows the temporal behavior of the overall multiheterodyning device to be adjusted precisely.

This phase shifting can be implemented by inserting a retarder into the IF path that delays the IF signal by a phase shift $\Delta\theta \propto \Delta\phi$ which is ideally independent of f_{IF}. The allowed range of f_{IF} may be restricted to those frequencies (such as by excluding DC components) where the error in $\Delta\theta$ is tolerable, such as less than 0.25 cycle. Alternatively, the phase shifting may be implemented by expressing the intermediate frequency signal as a (IF, *IF) vector and rotating that vector through sinusoidal linear combination by a rotation angle $\Delta\theta$, where $\Delta\theta \propto \Delta\phi$. This has the advantage of working for all frequencies, including DC components. Portions of the channel signal processor responsible for rotations include "vector rotators" and "rotating delays". Another method called "post-average weighting" uses unrotated IF, *IF signals as inputs and applies the sinusoidal weighting to signals formed at the *end* of a process, such as *after* instead of before the time-averaging that occurs in a channel correlation process. Another phase shifting method is to adjustably retard the reference or input signal arriving at the down-mixer.

In single delay processes $\Delta\theta = \Delta\phi$. In multiple delay (multiple echo) processes $\Delta\theta = \Delta\phi(\tau_m/\tau_{ch})$, where τ_m is the delay associated with the mth echo. If the *IF leads instead of lags IF, then the polarities of $\Delta\theta$ are flipped from those stated above. If $f_{LO} > f_x$ instead of $f_{LO} < f_x$, then the polarities are flipped again.

In cases where channel outputs are summed over channels, the channel outputs are adjusted in gain prior to summing, to normalize them. This is indicated in the Figures by amplifiers such as 17 in Fig. 1. The normalization takes into account the loss of signal through the entire signal path from spectrometer, down-mixer, channel signal processor, and up-mixer and final combiner, if applicable. Suppose the signal process was a perfectly neutral process where the (IF, *IF) vector channel input directly formed the vector channel output. Then optimally the gains of the channels would be adjusted so that the output of the multiheterodyning device would be a coherent replica of the input, as much as possible.

E. Up-mixing

Figure 9A shows an up-mixer, which is responsible for shifting the frequency of the channel output signal upward from f_{IF} to, or near to, its original value prior to down-heterodyning. It does this by heterodyning against

Figure 9

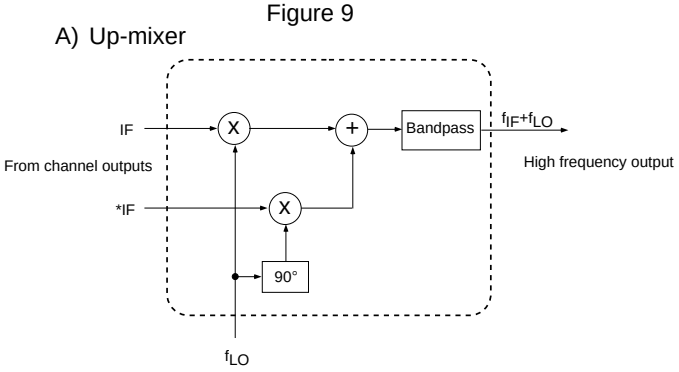

Figure 9A shows an up-mixer creating an up-heterodyned output using amplitude modulation.

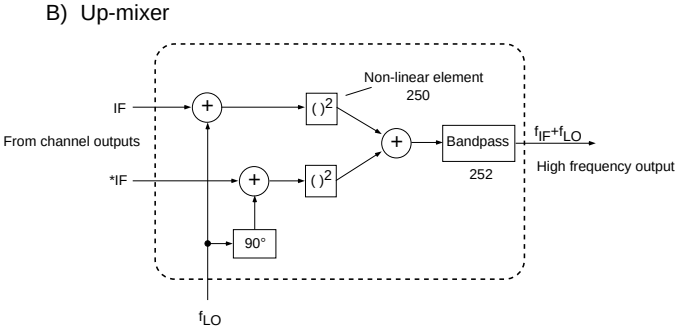

Figure 9B shows an up-mixer creating an up-heterodyned output using passage of signal and reference through a non-linear device.

f_{LO} (or other reference frequency) and bandpass filtering to allow the sum frequency component $f_{IF} + f_{LO}$ to pass. (If $f_{LO} > f_x$, then the difference frequency $f_{IF} - f_{LO}$ is used.)

The quadrature intermediate frequency signal is up-heterodyned against the reference signal retarded or advanced by 90°, depending on whether *IF lags or leads IF. This way the original phase of the input signal can be restored in the net output.

Usually it is desired to up-heterodyne with the same reference frequency as was used in the down-heterodyning process, so that spectral components of the input signal are restored to their original values in the net output signal, and phase coherence is easy to maintain. Also, this obviates the problem of stabilizing the frequency of a second reference frequency relative to the first. Practically, it is simplest to use the same reference frequency for up and down mixing. If it is desired to create a wholesale shift of frequencies between net input and net output, such as to compensate for Doppler effects in moving targets, then this is more practically done by dynamically changing channel phases $\Delta\phi$ at a desired beat frequency.

If it is important to have a phase coherent wide bandwidth output, then the difference in phase of the reference

signal at the up-mixer compared to at the down-mixer should optimally be zero or uniform across all channels. For some applications, such as imprinting a comb-filter power spectrum on a noise source, channel to channel phase coherence is not needed.

Heterodyning is fundamentally a multiplication of the LO signal by the IF signal, and could be accomplished by using IF to modulate the gain of an amplifier passing LO. Alternatively, the multiplication can be created in effect by passing the sum signal (IF+LO) through a non-linear device 250 which has a quadratic term in its behavior, as shown in Fig. 9B.

The bandpass filter 252 blocks the carrier (f_{LO}) and difference frequency signals ($f_{LO} - f_{IF}$). The difference frequency signals are an aliased signal having a spectral shape which is reversed compared to the un-aliased signal ($f_{IF} + f_{LO}$). That is, its spectrum is reflected about an axis at f_{LO}. The aliased signal is usually undesired because any frequency shifts created by the channel phase shifting will shift the aliased signals in the opposite direction. These may form a "ghost" signal which has a different spectral character than intended.

In some cases of a pair of multiheterodyning units "A" & "B", the aliased up-heterodyned signal components can be allowed to remain in the net output signal of unit "A", thereby reducing the cost of the apparatus by omitting a filtering step. These cases include when the detecting unit "B" has more sparsely arranged bandshapes that do not sense the aliased versions of the signals outputted by illuminating "A" unit.

F. Summation over channels

The last step is to sum the contributions from all the channels to form the net output. Either the high frequency channel signals from the up-mixer are summed to form a net wideband output, or in the case of correlations, the channel correlation outputs are summed to form a net correlation.

Figure 10 shows how a spectrometer can be used in a reverse orientation from the conventional usage to combine many high frequency channel outputs 50 into one summed output beam 52 having the sum frequency ($f_{IL} + f_{LO}$) while simultaneously excluding the carrier 53 and difference frequencies 54. A slit 56 excludes the unwanted frequencies. If the spectrometer uses a prism made of a normally dispersive material, then the sum frequencies will be refracted by a greater angle than the other components, and so the slit should be on the side as shown in Fig. 10. If instead a diffraction grating is used, high frequencies are diffracted less and the slit should be on the opposite side of the carrier beam 53 as shown in Fig. 10.

G. Phase Linearity

To discuss the need for channel phase shifting we must introduce the concepts of phase-linearity, and temporal/spectral dilation. These concepts are most easy to visualize for an interferometer. However, they apply to the other signal processes as well.

Figure 3A shows the ideal power transmission spectrum of an interferometer $T = (1/2)[1+\cos(\omega\tau + \text{const})]$ where "const" is a constant. The value inside the brackets is the phase ϕ, so that $T = (1/2)[1 + \cos(\phi)]$, and $\phi = \omega\tau + \text{const}$, where phase is in units of radians. Note, $\omega = 2\pi f$, so when phase is in units of cycles we have

$$\phi = f\tau + \text{const}/2\pi. \tag{3}$$

The factors of 2π are often omitted from the language for brevity, and the symbols ω and f used interchangeably. The appropriate units for phase is either radians or cycles, depending on the symbol used.

The ideal interferometer is said to be "phase-linear" because ϕ is a linear function of frequency. If instead $\phi = \omega\tau + \text{const}(\omega)$, where const is a non-linear function of ω, then the interferometer (or other process) is said to be phase-nonlinear. This concept applies to any process that can be mathematically expressed in Fourier terms $e^{i\omega t}$.

A multiheterodyning process is not phase-linear for random values of f_{LO}. However, it can be made phase-linear by setting the channel phases $\Delta\phi$ to a set of values $\Delta\phi_{lin}$ approximately given by

$$\Delta\phi_{lin} = f_{LO}\langle\tau_{ch}\rangle, \tag{4}$$

where $\langle\tau_{ch}\rangle$ is the average of τ_{ch} over all channels, and τ_{ch} is the delay characterizing each channel. (The subscript "ch" helps distinguish this value from the delay characterizing the net device.) These $\Delta\phi_{lin}$ phase shifts raise the channel segments 601 of Fig. 8A so they fall along a global line 600 having slope $\langle\tau_{ch}\rangle$.

It is implied that only the fractional part of a phase shift expressed in units of cycles need be used, since phase is periodic. That is, if $\Delta\phi$=234.563 cycles, we could use $\Delta\phi$=0.563 cycles = 202.68°.

H. Temporal and Spectral Dilation

When the phase ϕ is plotted versus frequency, as in Fig. 8A, the slope of a line is the delay τ characterizing the device or process. Slight changes in τ are called a "temporal dilation" and cause a concomitant spectral dilation of opposite polarity. Because of Eq. 3, $f \sim \phi/\tau$, so increases in τ at constant ϕ cause a decrease in f, and increases in τ holding f constant increases ϕ. Thus positive $\Delta\tau$ is associated with positive $\Delta\phi$ and negative Δf.

Lines extending from zero to β_{net} in frequency are called "global lines". The global line slope can obviously be changed by directly altering τ. Alternatively,

Figure 10

Up-mixer using a spectrometer

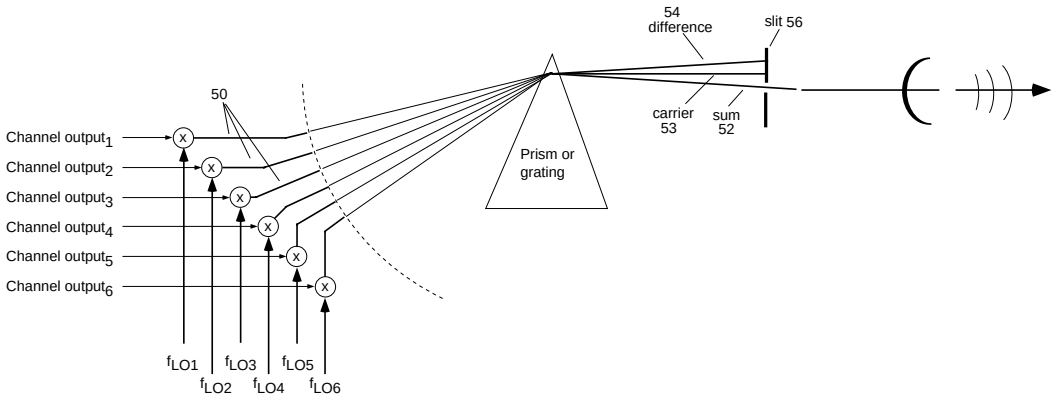

Figure 10 shows an up-mixer constructed from a spectrometer which combines heterodyned signals from many channels and passes only the sum frequency components.

and what is interesting about this invention, is that the average slope can also be changed by dividing it into segments which are moved as blocks, while preserving their original, local slopes, which are given by τ_{ch}. This is what occurs in a multiheterodyning processor through channel phase adjustment, where each block represents the region of input frequencies handled by a channel. Moving the segments as blocks upward is equivalent to shifting the spectra within each channel lower (leftward) in frequency. (This can be remembered by noting that for lines sloping from bottom left to upper right in Fig. 8A, a line lying above another line also lies to the left.)

This is illustrated by Fig. 3B through Fig. 3E. These show closeups of different segments of the interferometer comb-filter spectrum of Fig. 3A when the interferometer delay is dilated from τ [solid curve] to $(\tau + \Delta\tau)$ [dashed curve]. The spectrum contracts, which locally shifts segments to lower frequencies by different amounts $\Delta f = -f(\Delta\tau/\tau)$, proportional to segment average frequency. The frequency shift can also be expressed as a phase shift called $\Delta\phi_{dil}$. According to Eq. 3,

$$\Delta\phi_{dil,n} = f_{ave,n}\Delta\tau, \tag{5}$$

in units of cycles, where $f_{ave,n}$ is the bandshape's average frequency f_{ave} for the nth channel.

Thus the net temporal behavior of the invention can be precisely altered by an amount $\Delta\tau = \Delta\phi_{dil}/f$ by phase adjustments coordinated over many segments (channels). When the device is phase-linear the global line can be considered a best fit line through the channel segments weighted by the detailed shape of the bands. Because this averages the slope over many channels, $\Delta\tau$ can be more precisely determined than for a single channel used alone.

Small delays are achieved by small phase shifts. For example, a 10° shift at a 30 GHz channel corresponds to 0.9 ps. Such small delays are needed to resolve shifts of the autocorrelation peak in a velocimeter for small velocities. For example, a 2.5 m/s target for a τ=2 ms delay velocimeter produces a round-trip Doppler shift of $(2)(2.5\text{ m/s})(2\text{ ms})/(3\times10^8\text{ m/s}) = 33$ ps.

Although it is easiest to visualize the channel phase shift induced dilation effect on a phase-linear device, the dilation effect also works on a nonphase-linear device. It also applies not only to interferometry, but all channel signal processes, because it is rooted in the expression of signals as Fourier components $e^{i\omega t}$, where ω refers to input frequencies and does not change significantly across a band (because $\beta_{ch} \ll \beta_{net}$).

I. Purpose of Channel Phase Shifting

Thus, two purposes for slightly translating the spectrum of each channel are: 1) to simulate the dilation of the overall signal process spectrum so that the effective characteristic time τ of the net device is altered in a very precise manner; and 2) to make the net device phase-linear, if desired. The phase shift applied to each channel is a sum of two contributions

$$\Delta\phi = \Delta\phi_{lin} + \Delta\phi_{dil} \tag{6}$$

where a term $\Delta\phi_{lin}$ brings the net device into phase-linearity, and a term $\Delta\phi_{dil}$ dilates the effective delay of the net device by $\Delta\tau$. Approximately,

$$\Delta\phi_{dil} = f_{ave}\Delta\tau \tag{7}$$
$$\Delta\phi_{lin} = f_{LO}\langle\tau_{ch}\rangle. \tag{8}$$

The effective delay can be dilated *regardless* of whether the device is phase-linear or not. This is a key point that allows the use of reference frequencies that, on a detail level, have no special relationship to each other and can be arbitrary. (On a coarse level, it is optimal to evenly distribute f_{LOn} across the input bandwidth β_{net}.)

It is interesting to point out that for many useful applications a phase-linear device is not required, and in this case $\Delta\phi_{lin} = 0$. A phase-nonlinear device is acceptable for circumstances where two signals are being compared through multiheterodyning devices sharing the same reference frequencies f_{LOn}. On the other hand, a phase-linear device is desired whenever a signal is to be subsequently treated by an external apparatus which expects phase-linearity or cannot share the reference frequencies, e.g., to make a stand-alone delay line which is to output a coherent replica of the input signal.

Applications needing phase-linearity will also probably need channel bandshapes contiguously filling the input bandwidth. Contiguous filling is also optimal for producing the least ambiguous and narrowest correlation and autocorrelation peaks. However, sparsely filling the input bandwidth is more economical, and can be tolerated by multiheterodyning apparatuses sharing reference frequencies.

J. Rotation of the IF Vector

The channel processor is designed to shift its spectrum by an amount $\Delta f = -\Delta\phi/\tau_{ch}$. That is, positive phase shifts produce negative frequency shifts. In general, a signal process may use delayed and undelayed components of the (IF, *IF) signal vector. A spectral shift can be created by using, for the delayed components, a rotated version of the (IF, *IF) vector rotated by an angle $\Delta\theta$. This is called (IF′, *IF′) and given by a rotational transformation

$$IF' = IF\cos\Delta\theta +^* IF\sin\Delta\theta \quad (9)$$

$$^*IF' = -IF\sin\Delta\theta +^* IF\cos\Delta\theta. \quad (10)$$

Note, this method works even for the DC components of (IF, *IF).

If the (IF, *IF) vector is represented by $\sim e^{i\omega t}$, then the rotation specified by Eq. 9 & Eq. 10 is the same as multiplying that term by a phasor ($e^{-i\Delta\theta}$), a clockwise rotation in the complex plane, or a retardation. (To test this, set $\Delta\theta$=90° and we see that IF becomes *IF, which agrees with our assumption that *IF lagged IF.)

Figures 11A through 11F show how rotation of the IF vector works for the case of an interferometer. The simple interferometer shown in Fig. 11A uses IF for both the undelayed 630 and delayed 632 branches and has the power transmission spectrum shown in Fig. 11B, $T = (1/2)[1 + \cos(\omega\tau)]$. Figure 11C shows an interferometer using for the delayed branch the lagging quadrature *IF signal instead of IF. The corresponding spectrum $T = (1/2)(1 - \sin\omega\tau)$ shown in Fig. 11D is shifted to lower frequencies by an amount equivalent to 90° in phase. Thus to translated the spectrum by an adjustable amount, the delayed branch should use an IF signal rotated by an adjustable amount.

This is accomplished by the circuit Fig. 11E, which implements the first equation of the rotational transformation Eq. 9. The corresponding spectrum is shown in Fig. 11F. The mathematical derivation of the spectrum is as follows. Let the undelayed branch be $E(t) = e^{i\omega t}$ and the delayed branch $E(t-\tau) = e^{-i\Delta\theta}e^{-i\omega\tau}e^{i\omega t}$, where the phasor $e^{-i\Delta\theta}$ represents the adjustable rotation. Then the power spectrum is $|E(t) + E(t-\tau)|^2$ and hence $T = (1/2)[1 + \mathrm{Re}(e^{i\Delta\theta}e^{i\omega\tau})] = (1/2)[1 + \cos(\omega\tau + \Delta\theta)]$, where "Re" means "real part of". Hence positive values of $\Delta\theta$ shift the spectrum (dashed) to the left (lowering frequencies). Thus we want $\Delta\theta = \Delta\phi$.

K. Channel Interferometer with Vector Output

The channel interferometer of Fig. 11E produces a scalar output. This is sufficient for phase insensitive applications, which care only about the power spectrum, such as velocimetry. However, to be mathematically complete and for applications where the accurate propagation time of the undelayed portion of the signal through the interferometer matters, a vector output should be provided, so that the correct complex description of the input signal can be propagated through the channel signal processor. For example, in a combination process where correlation follows interferometry, such as to determine range as well as determine velocity, a vector channel output is desired from the channel interferometer.

Figure 12A shows a channel interferometer producing a vector output. This could be called a "vector interferometer". The circuit inside the bold oval 650 could be called a "Rotator" and is responsible for rotating the IF vector signal by $\Delta\theta$, to produce a rotated vector (IF′, *IF′). Nominally we would use $\Delta\theta = \Delta\phi$. The value of τ used in the delays 651 is the parameter τ_{ch} used in the phase shift analysis.

An interferometer is a special case of an arbitrary filter where there is either a constant spacing between echos or a small number of distinct spacings. A spacing value is called the interferometer delay τ, and it is the most important parameter controlling the interferometer behavior. For purposes of forming autocorrelations, it is optimal to have as few distinct τ values as possible, ideally a single value. Otherwise there could be a dilution and confusion of autocorrelation peaks, since there will be a peak associated with each distinct τ value. Multiple τ values can be tolerated if they are significantly different than each other (separated by more than several times the coherence time, $1/\beta_{net}$).

The most common type of interferometer is a two-path interferometer analogous to the Michelson interferometer, where one echo of equal amplitude to the undelayed signal is produced. This echo could have a positive or negative polarity amplitude compared to the undelayed signal, producing complementary outputs analogous to the two complementary arms of a Michelson interferometer. Another useful kind is a recirculating interferometer which generates an infinite number of equally spaced echos having geometrically decreasing amplitudes.

Figure 11

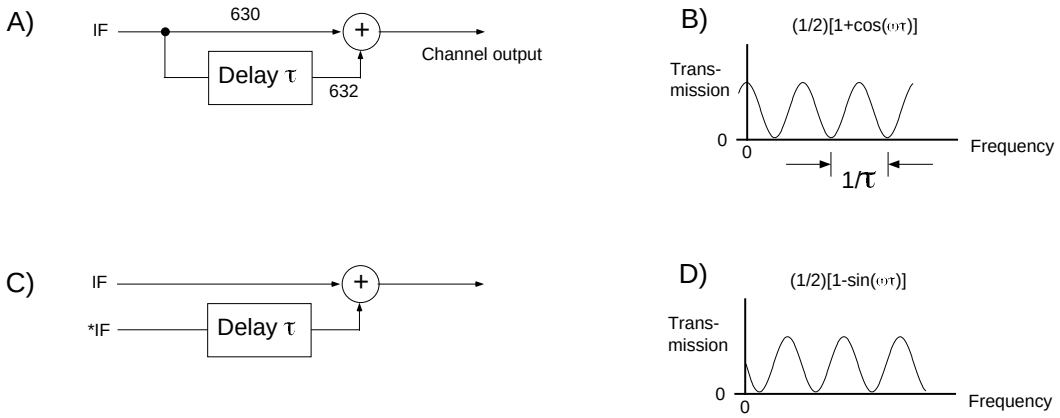

Figure 11A shows an interferometer without phase shift. Figure 11B shows the power transmission spectrum of the interferometer of Fig. 11A. Figure 11C shows a 90° phase-shifted interferometer using quadrature IF signal for the delayed branch. Figure 11D shows the power transmission spectrum of the interferometer of Fig. 11C.

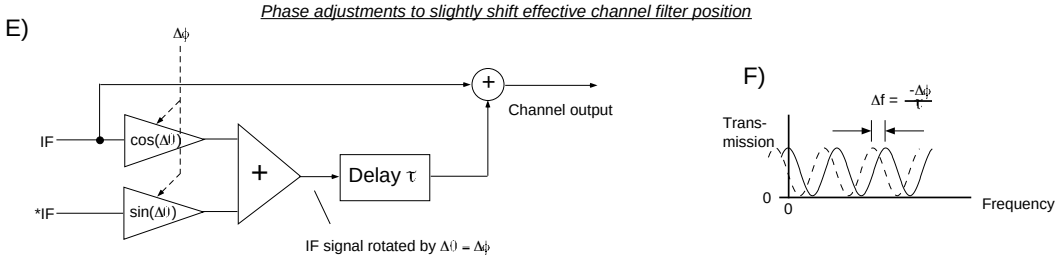

Figure 11E shows an interferometer phase-shifted by an adjustable amount. Figure 11F shows the spectrum associated with the interferometer of Fig. 11E having an adjustable frequency shift.

Figure 12

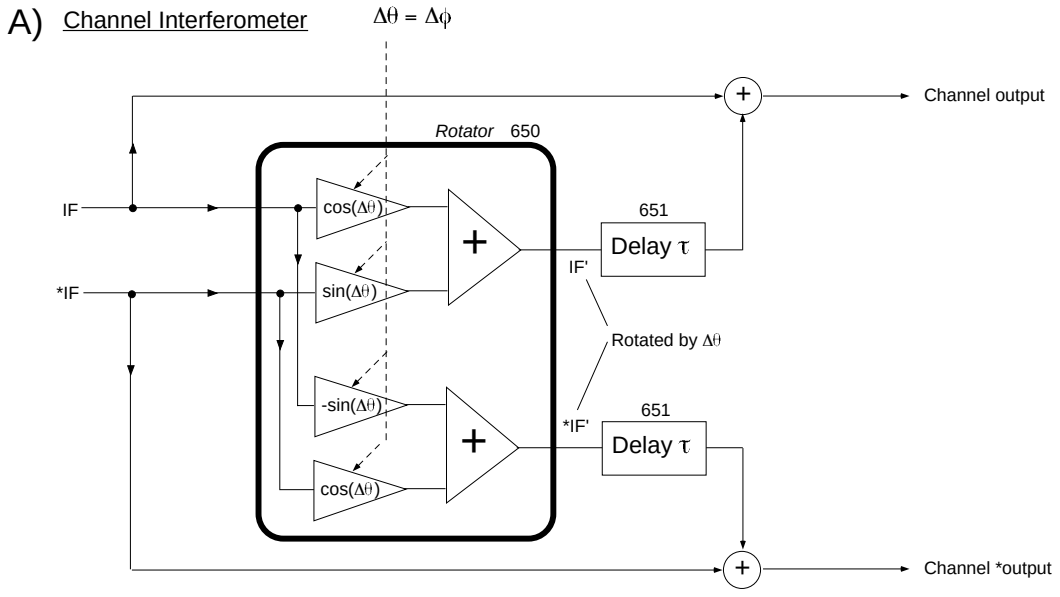

Figure 12A shows a channel signal processor which is an interferometer having delay τ, vector rotation $\Delta\theta$, and forming a vector output.

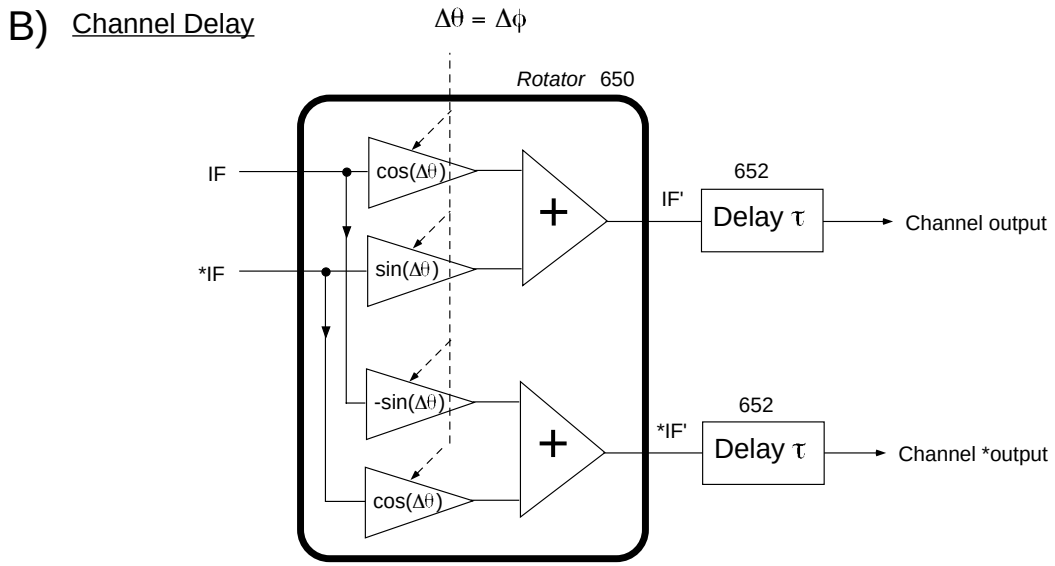

Figure 12B shows a channel signal processor which is a delay of duration τ and vector rotation $\Delta\theta$.

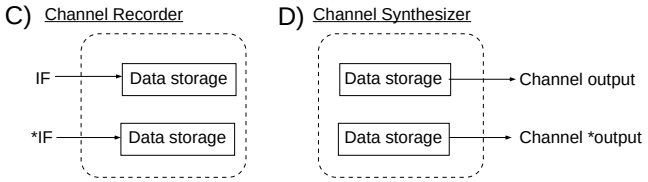

Figure 12C shows a channel signal processor which records the IF and quadrature IF signals. Figure 12D shows a channel signal processor which synthesizes the channel and quadrature channel outputs.

An interferometer can be used to form an autocorrelator, when the time-averaged power passing through the interferometer is measured versus characteristic delay. For this purpose it is optimal that all the echos be equally spaced. A two-path interferometer is the optimal interferometer to use because it can yield a single-peak autocorrelation. In contrast, multiple echo interferometers yield autocorrelations having multiple peaks. These are still useful in situations (such as where small velocity changes are being measured) where the central peak can be distinguished from the other peaks.

A pair of matched interferometers can be used for velocimetry using wideband illumination (Fig. 2A and Fig. 18). The "A" interferometer imprints a comb-filter spectrum on a wideband source 100, which is to say it imprints echos having characteristic delay τ_A. This imprinted beam 104 can illuminate a target. A second interferometer ("B") having nearly identical characteristics observes the waves 106 reflected from the target. The time-averaged power passing through the second interferometer is measured versus "B" interferometer delay to essentially form an autocorrelation. The peak location of this autocorrelation shifts with target velocity (and is proportional to τ_A).

Strictly speaking, for this velocimetry purpose other kinds of matched filters could be substituted for the two interferometers. However, compared to a two-path interferometer these may produce weaker autocorrelations, or the behavior may be more complicated to analyze mathematically. The two-path and recirculating interferometers are the two most useful kinds of filters for wideband velocimetry.

L. Channel Delay Line

A channel delay unit that produces a vector output and has the signal rotation property is shown in Fig. 12B. This could be called a "rotating delay" or a "vector delay". Delay units are fundamental building blocks for constructing filters. Nominally $\Delta\theta = \Delta\phi$.

A method of implementing the actual delaying of the IF or *IF signal, indicated by the boxes such as 652 used throughout the Figures labeled "Delay τ", include digital and analog methods. A digital delay line consisting of an analog-digital converter (A/D), shift register, and digital-analog converter (D/A) can easily create several millisecond delays. These would have a bandwidth roughly half the clock frequency used to drive the shift registers. Analog methods include conversion of IF signal to an acoustic wave which propagates a distance and then is detected, or use of the IF signal to modulate the intensity, color, phase or polarization state of an optical signal sent through a long fiber.

Figure 18

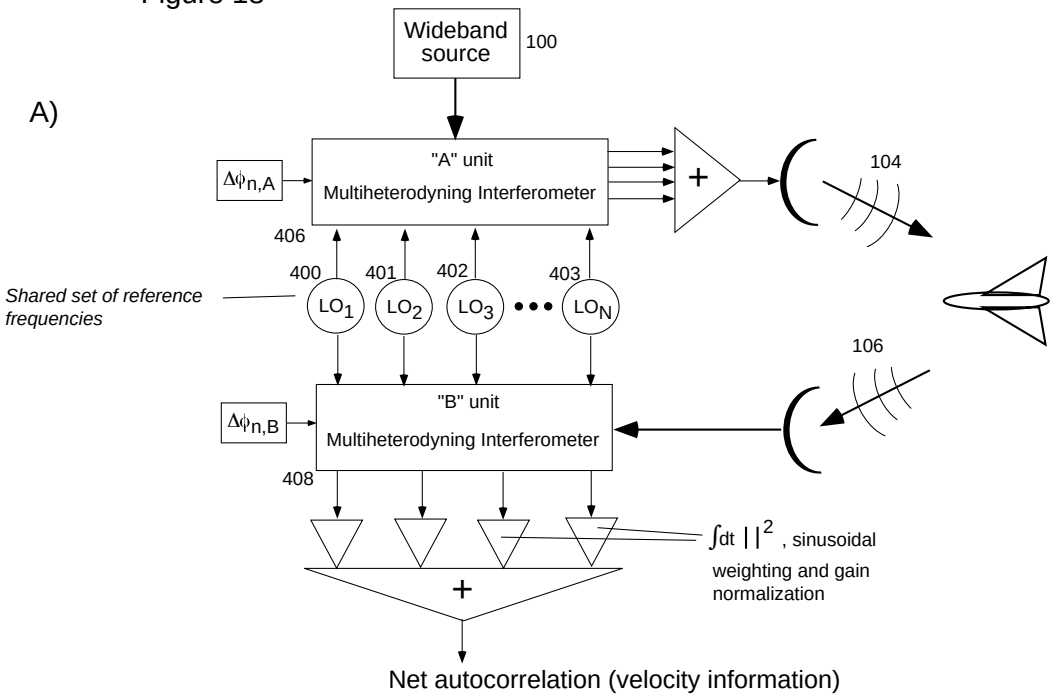

Figure 18A shows a double interferometer velocimeter using two matched multiheterodyning interferometers sharing reference frequencies.

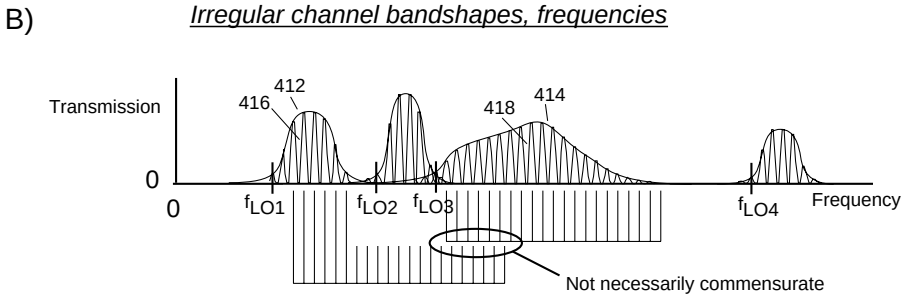

Figure 18B shows irregular channel bandshapes, frequency locations and non-commensurate comb-filter peaks.

M. Channel Recirculating Interferometer

Figure 13A shows a circuit which creates a recirculating interferometer, which is a kind of filter analogous to an optical Fabry-Perot interferometer. This has the impulse response shown in Fig. 13B, an infinite series of geometrically decreasing echos 671, 673 etc. separated by interval τ. The amplitude of each subsequent echo is R times the preceding echo. The Fourier power transform of the impulse response Fig. 13B is the transmission spectrum Fig. 13C. This has the same periodicity $1/\tau$ as the sinusoidal comb-filter but has narrower peaks. The closer R is to unity, the narrower the peaks are relative to the spacing between peaks. The circuit Fig. 13A recirculates the vector IF signal. For each round trip around the circuit and through the block 672, the vector signal 676 is delayed by τ, rotated in phase by $\Delta\theta$, and its amplitude multiplied by factor R (which must be <1 to avoid oscillation). Nominally $\Delta\theta = \Delta\phi$.

N. Channel Arbitrary Filter

To create an arbitrary filter one defines its impulse response, since the impulse response and spectral response are Fourier transforms of each other. Let the first spike 300 of an impulse response (Fig. 14B) define unity amplitude. Subsequent spikes 301-304 are called echos and have user-chosen amplitudes and arrival times. The arrival times are not restricted to be uniformly spaced and can have any time value. Then one constructs a circuit (Fig. 14A) using one or more rotational vector delays 306, 307 etc., shown in bold ovals, having τ_m and R_m

Figure 13

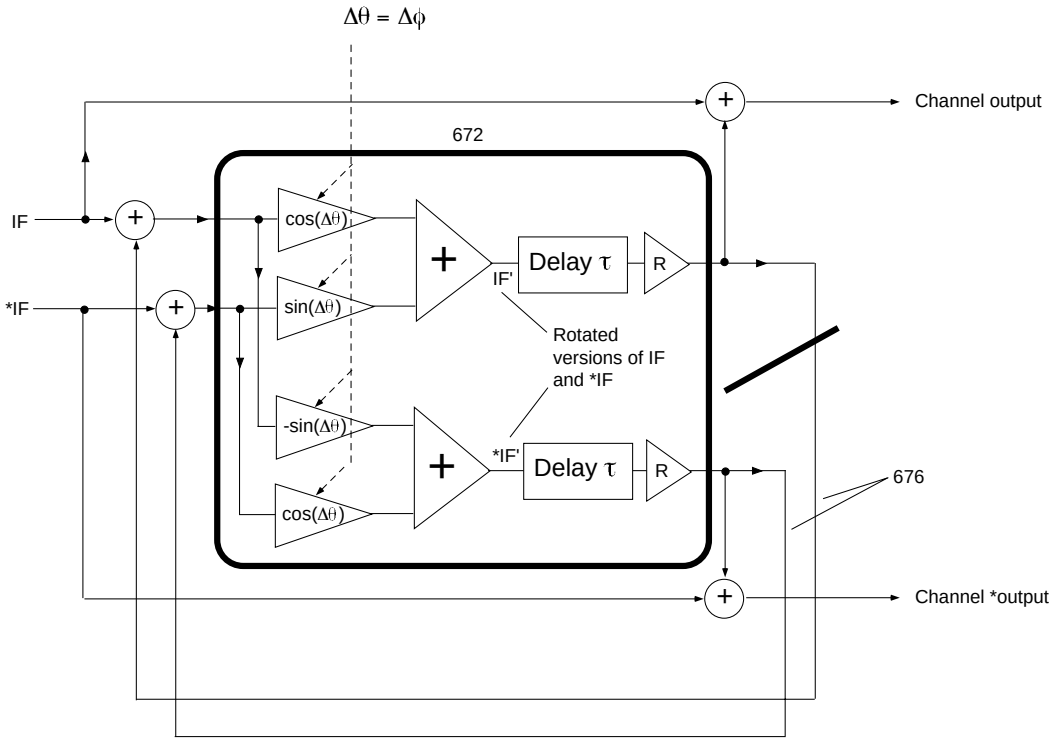

Figure 13A shows a channel signal processor which is a recirculating interferometer having a set amount of signal rotation, delay and attenuation per circuit.

B) Impulse response

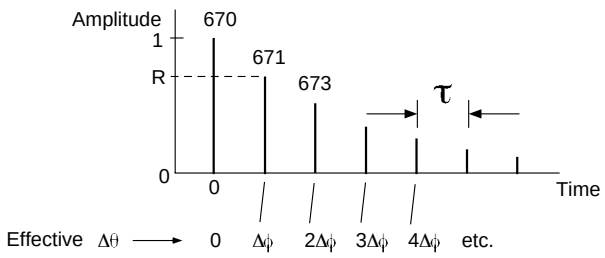

Figure 13B shows the impulse response for a recirculating interferometer.

C) Transmission Spectrum

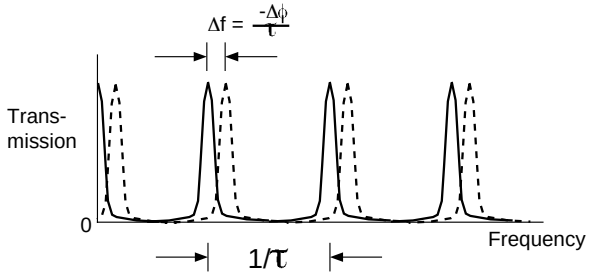

Figure 13C shows the power transmission spectrum for the recirculating interferometer.

values for the mth echo which will create the set of echos in the output described by the impulse response. Each rotational delay 306, 307 etc. represents the circuit 672 shown in the bold oval of Fig. 13A.

Figure 14A shows an example circuit which would create the impulse response Fig. 14B having 4 echo spikes subsequent to the first spike. The paths comprising a dashed and undashed pair of lines represent vector signals. The manipulations (delay, addition, subtraction) act analogous to vector arithmetic in that they are performed on IF and *IF in parallel. Figure 14C shows a more complicated channel filter using interwoven recirculation.

In order to slightly shift a channel filter spectrum in frequency, the phases $\Delta\theta_m$ associated with the mth spike of a filter impulse response Fig. 14B must be changed proportional to the arrival time of the spike in the impulse response. That is, $\Delta\theta_m = \Delta\phi(\tau_m/\tau_{ch})$, where $\Delta\theta_m$ is the phase shift of the mth rotating delay unit having delay τ_m, and τ_{ch} is the characteristic delay of the channel filter. This can be set to one of the τ_m values, such as the echo having the largest amplitude.

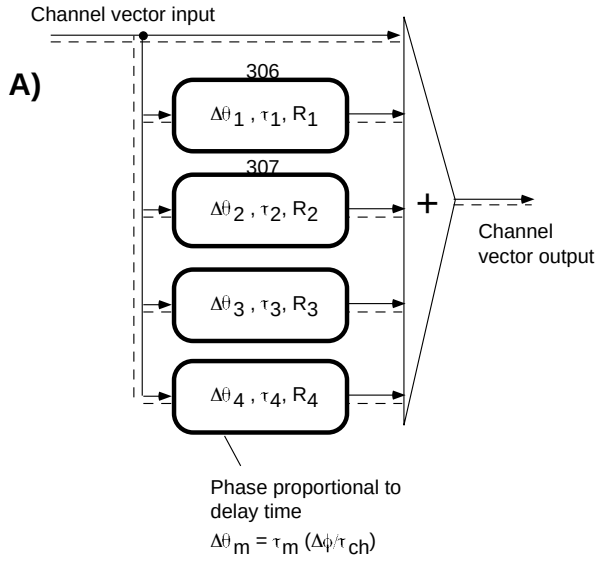

Figure 14A shows a channel signal processor constructed of vector delays that realize a four-echo impulse response.

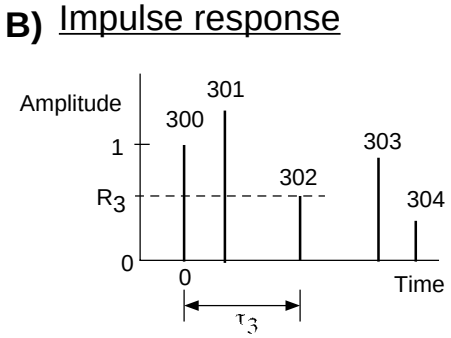

Figure 14B shows a four-echo impulse response.

O. Channel Autocorrelator

An autocorrelation is a correlation of a signal with itself. It is useful to define an autocorrelation AC evaluated at τ of a function $f(t)$ as

$$\mathrm{AC}(\tau) = \mathrm{Re} \int dt\ f(t) f^*(t-\tau). \tag{11}$$

The integral represents time averaging, which occurs over a duration much longer than $1/\beta_{ch}$. Time averaging can be performed by the invention either before or after up-heterodyning. However, practically it is simplest to do it before heterodyning and thereby eliminate the up-mixing step. This is done by summing the channel outputs produced by each channel autocorrelator to form the net autocorrelation output.

A channel autocorrelator is shown in Fig. 15A. Its output 776 is a sum of two separate autocorrelations, which could be called intermediate outputs or intermediate autocorrelations, one (777) from the IF signal, and a quadrature version 778 from *IF. Note, in some applications the quadrature intermediate output 778 can be omitted because signals which show correlations for the real part of the their Fourier spectrum often show the same correlation in the imaginary part. For example, in velocimetry applications, the illuminating interferometer ("A" in Fig. 2A or Fig. 18) creates the same comb-filter power spectrum for the real and imaginary parts of signal sent to the target.

It is convenient to implement the multiplication function 789 by passing a sum or difference of the two signals to be multiplied through a squaring function, or nonlinear device, or power measuring device. Figure 16C shows a simple ("lopsided") circuit that does this, analogous to the formula $(A+B)^2 = 2AB + (A^2+B^2)$. When this is done, essentially the autocorrelation comprises measuring the time-averaged power passing through a vector interferometer 781, as shown in Fig. 15C, and ignoring any delay independent constants. That is, the time-averaged power of a signal $f(t)$ passing through a two-path interferometer of delay τ is

$$P_1(\tau) = \int dt\ |f(t) + f(t-\tau)]|^2 = 2|f(t)|^2 + 2\mathrm{AC}(\tau) \tag{12}$$

where $|f(t)|^2$ is the undesired constant, and the second term is the desired autocorrelation.

A method which automatically deletes the undesired constant term is the push-pull method. This can be applied either before or after time-averaging. When applied before, it comprises a method of multiplication at 789 analogous to the formula $(A+B)^2 - (A-B)^2 = 4AB$. This form of push-pull is shown in Fig. 16B. When applied after, two separate interferometers analogous to Fig. 15C are required, except one of the interferometer subtracts the echo at 785 instead of adding it at 785 to the undelayed branch. Then in addition to the time-averaged power P_1 of the first interferometer, the time-averaged power P_2 of the second interferometer is found. This is

$$P_2(\tau) = \int dt\ |f(t) - f(t-\tau)]|^2 = 2|f(t)|^2 - 2\mathrm{AC}(\tau). \tag{13}$$

Then the two time-average power signals are subtracted and divided by four to form the autocorrelation

$$\mathrm{AC}(\tau) = (1/4)[P_1(t) - P_2(t)]. \tag{14}$$

This method automatically suppresses the $|f(t)|^2$ term. For clarity, circuits using the lopsided method are shown in the Figures, but it is implied that the push-pull method can be substituted wherever the lopsided method is used.

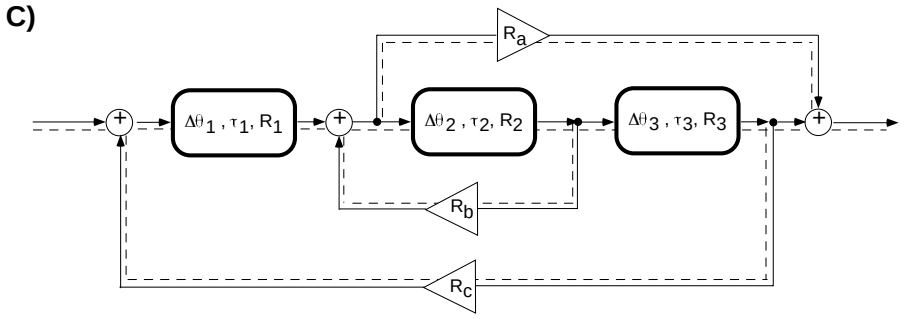

Figure 14C shows a channel signal processor constructed of many recirculating paths which will produce a more complicated impulse response.

Figure 15

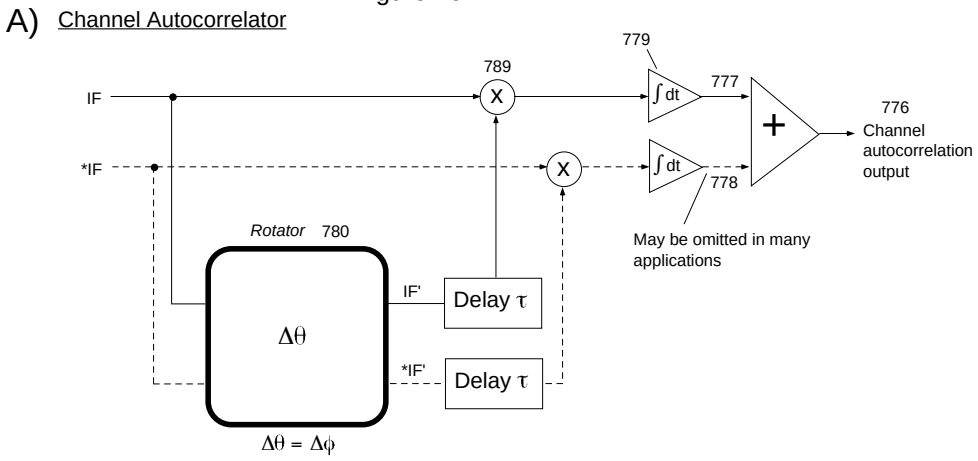

Figure 15A shows a channel signal processor which is an autocorrelator having delay τ and signal rotation $\Delta\theta$.

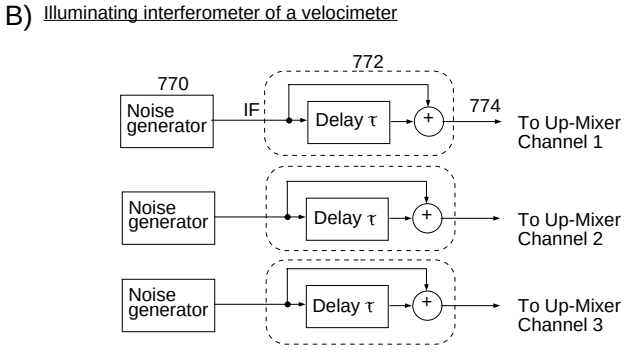

Figure 15B shows channel waveform synthesis using multiple channel noise generators instead of spectrometer-produced signals.

P. Sinusoidal Weighting After Time-averaging

For processes such as correlations that output a time-averaged signal, there is another way of phase shifting the channel spectrum that avoids having to rotate the (IF, *IF) vector. Instead the unrotated IF and *IF are used as inputs. This could be called the "post-average weighting" technique. In this technique the sinusoidal linear combinations are applied after and not before the time-averaging. Therefore they operate on very low frequency, which reduces cost of components performing the arithmetic and makes it economical to calculate them for a variety of $\Delta\theta$ values in parallel. This allows economical evaluation of the correlation over a range of delays, in a snapshot, on the same set of IF vector data.

The mathematical basis for this is now given, for the general case of two-signal correlation. Let the two functions to be correlated be

$$f(t) = f_r + if_i \tag{15}$$

$$h(t) = h_r + ih_i \tag{16}$$

where f_r, f_i, h_r, h_i are the real and imaginary parts of $f(t)$ and $h(t)$ and are directly analogous to the intermediate signals and their quadratures IF_A, $^*\mathrm{IF}_A$, IF_B and $^*\mathrm{IF}_B$, shown in Fig. 17 and as 813-816 in Fig. 16A. Then a correlation between $f(t)$ and $h(t)$ is

$$\mathrm{Cor}(\tau) = \mathrm{Re} \int dt\ f(t)h^*(t-\tau). \tag{17}$$

Figure 15

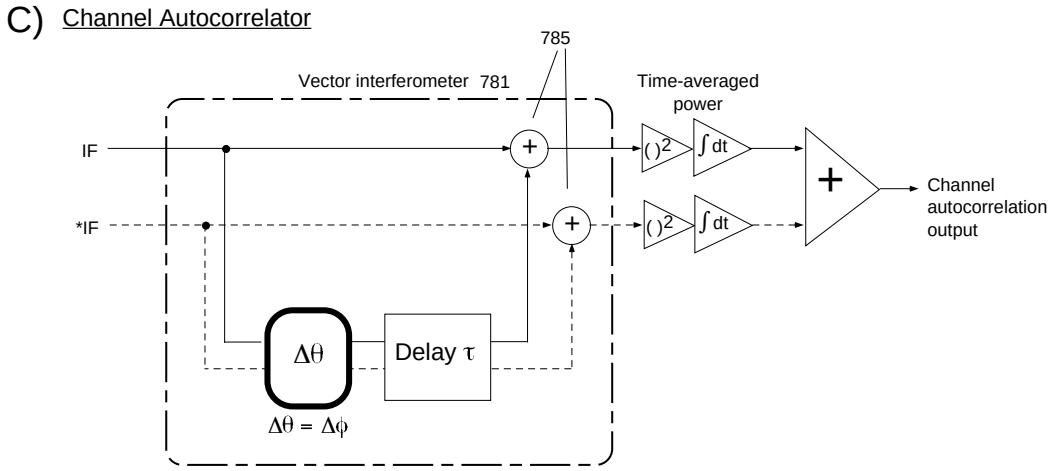

Figure 15C shows a channel autocorrelator formed by measuring the time-average power passing through a vector interferometer.

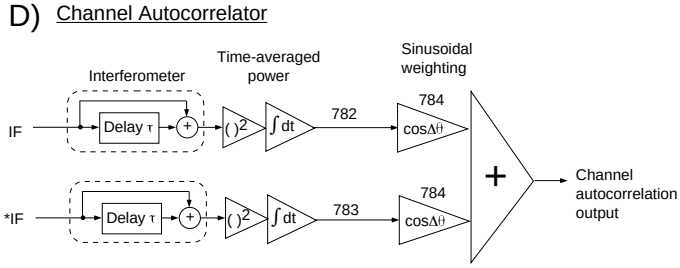

Figure 15D shows a channel autocorrelator where the phase shifting is applied after the time averaging.

Suppose we want to evaluate $\mathrm{Cor}(\tau)$ for small deviations around τ=0 (for this demonstration it is immaterial what the coarse value of τ is). Then let τ be $\Delta\tau$. Then because we can express a complex function in terms of Fourier components, we have

$$h(t-\Delta\tau) \rightarrow e^{-i\omega\Delta\tau}h(t) = e^{-i\Delta\theta}h(t) \qquad (18)$$

where we used the assumption that $\beta_{ch} \ll \beta_{net}$ so that the frequency ω in Eq. 18, which refers to frequencies of the input signal, is almost constant across a given channel. Thus $\omega\Delta\tau$ can be approximately represented by a single value $\Delta\theta$, for each channel. Equation 202 becomes

$$h(t-\Delta\tau) \rightarrow e^{-i\Delta\theta}h(t) = h'_r + ih'_i \qquad (19)$$

where

$$h'_r = h_r\cos\Delta\theta + h_i\sin\Delta\theta \qquad (20)$$
$$h'_i = -h_r\sin\Delta\theta + h_i\cos\Delta\theta. \qquad (21)$$

This is the rotational transformation previously discussed to rotate the IF, *IF vector. Thus we have

$$\mathrm{Cor}(\Delta\tau) = \mathrm{Re}\int dt\ f(t)h'*(t) \qquad (22)$$

where $h'(t)$ is the rotated form given by Eq. 20 and Eq. 21. Equation 206 is what is evaluated by the correlation circuit Fig. 16A, and by the autocorrelation circuit Fig. 15A (when $h(t) = f(t)$).

Now we will re-express Eq. 22 in another form that places the sinusoidal linear combinations Eq. 20 and Eq. 21 *outside* the time integrations instead of inside. Substituting Eq. 20 and Eq. 21 into Eq. 22 yields

$$\mathrm{Cor}(\Delta\tau) = \mathrm{Re}\int dt\ (f_r + if_i)(h_r\cos\Delta\theta + h_i\sin\Delta\theta) - i(-h_r\sin\Delta\theta + h_i\cos\Delta\theta) \qquad (23)$$

which, after taking the real part of, becomes

$$\mathrm{Cor}(\Delta\tau) = \cos\Delta\theta\int dt\ f_rh_r + \cos\Delta\theta\int dt\ f_ih_i + \sin\Delta\theta\int dt\ f_rh_i - \sin\Delta\theta\int dt\ f_ih_r. \qquad (24)$$

Equation 206 shows that the channel correlation can be computed *without* rotating the IF vector, by first com-

Figure 16

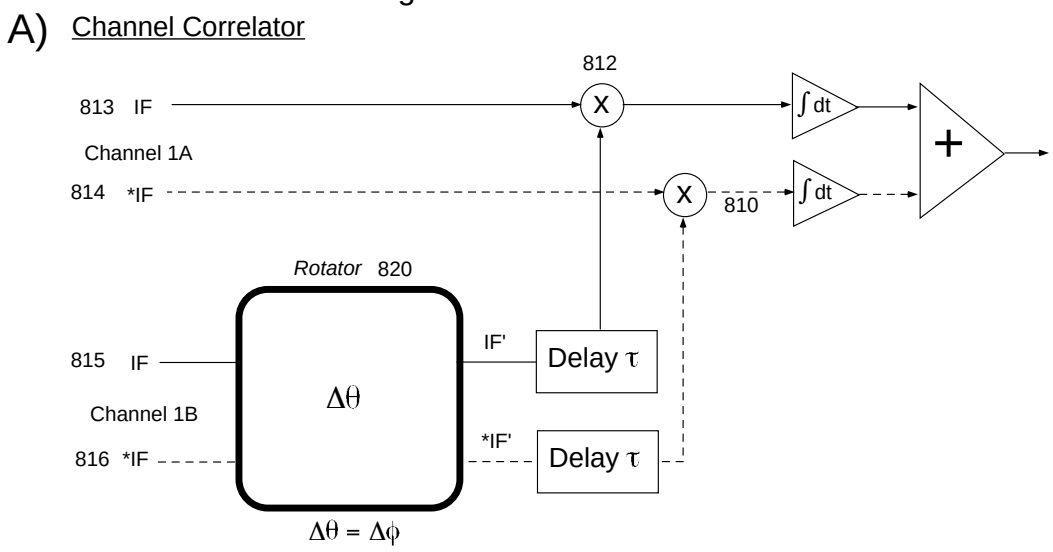

Figure 16A shows a channel signal processor which is a correlator between A & B channels, having delay τ and signal rotation $\Delta\theta$.

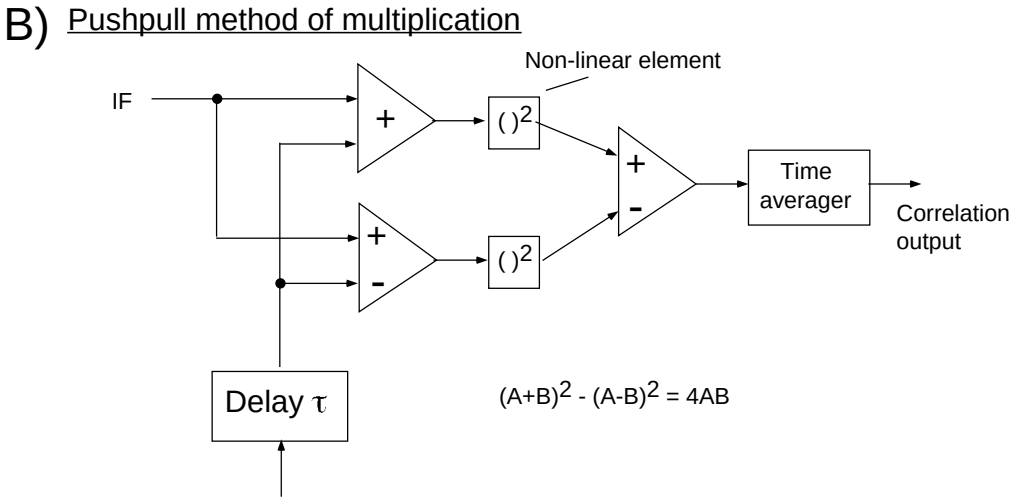

Figure 16B shows that the multiplication function used in Figure 16A can be accomplished by a push-pull arrangement of a non-linear element.

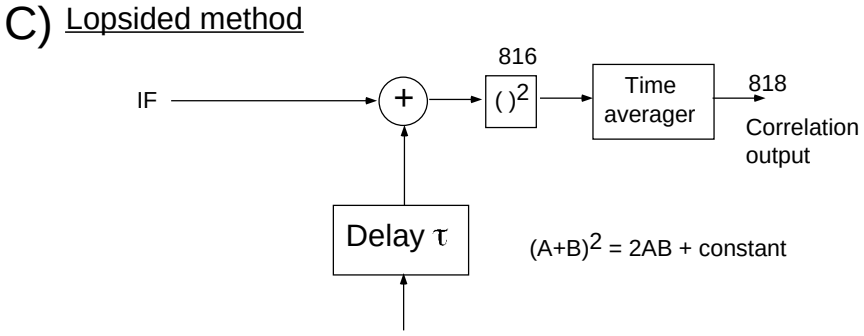

Figure 16C shows the simple use of a non-linear element to create a correlation signal having an offset.

Figure 16

D) Channel Correlator

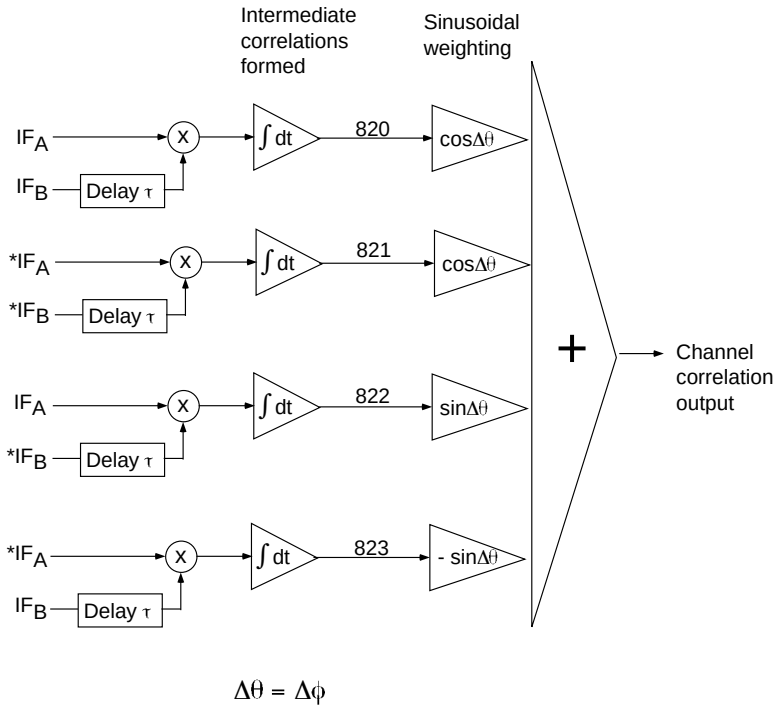

Figure 16D shows a channel correlator where the phase shifting is applied after the time averaging.

puting the intermediate correlations

$$\begin{aligned} \mathrm{Cor}_1 &= \int dt\ f_r h_r \\ \mathrm{Cor}_2 &= \int dt\ f_i h_i \\ \mathrm{Cor}_3 &= \int dt\ f_r h_i \\ \mathrm{Cor}_4 &= \int dt\ f_i h_r \end{aligned} \tag{25}$$

that only involve the IF and its quadrature. That is using various combinations of IF against IF, IF against *IF, *IF against *IF etc.. Then forming sinusoidal linear combinations of these intermediate correlations to produce the channel correlation.

Now for the case of an autocorrelation, $f_r = h_r$ and $f_i = h_i$, and the last two terms of Eq. 24 cancel, leaving

$$\mathrm{AC}(\Delta\tau) = \cos\Delta\theta \int dt\ f_r f_r + \cos\Delta\theta \int dt\ f_i f_i \tag{26}$$

The circuit of Fig. 15D embodies Eq. 26, showing the autocorrelation calculated from a sum of two intermediate autocorrelations 782 and 783, with a sinusoidal coefficient 784. Note that in many situations, an input signal will show the same autocorrelation behavior in its real part as in its imaginary part. Thus, for economy the $\int dt\ f_i f_i$ term, which is calculated from *IF, can be omitted, and the *IF term does not have to be produced. This simplifies the down-mixer apparatus by eliminating the quadrature portion of it, and eliminating the need for retardation 758.

A important advantage of applying the sinusoidal linear combination after the time averaging is that it makes it economical to calculate the autocorrelation or correlation for a range of delay values τ, without having to actually scan τ in real-time. Since the sinusoidal arithmetic is being performed on a very low frequency signal (a time-average), the arithmetic can be easily and rapidly evaluated for many values of $\Delta\theta$. This can produce a snapshot evaluation of $\mathrm{AC}(\tau)$ or $\mathrm{Cor}(\tau)$ over the range of τ accessible by coordinated channel phase shifting, a range $\tau \pm \Delta\tau_{max}$, where $\Delta\tau_{max}$ is defined in a later discussion and is limited by walkoff errors. This is much more rapid than actually scanning the channel delay, which would require dwelling on each delay value long enough for the time-averaging to occur.

Q. Channel Correlator

Figure 17 shows a multiheterodyning correlator which correlates two wideband input signals #A and #B. Ap-

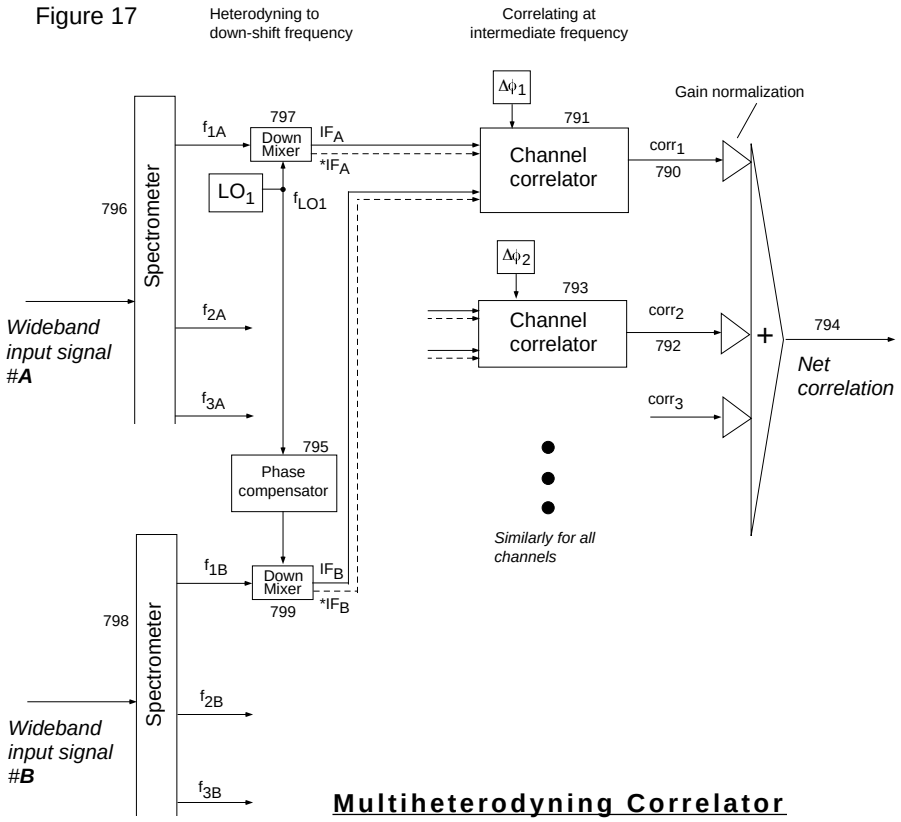

Figure 17 is a schematic of a multiheterodyning correlator.

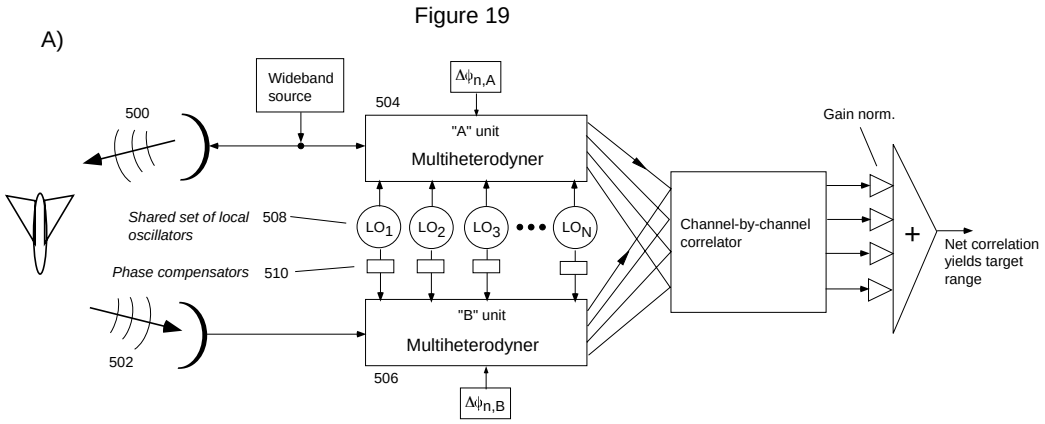

Figure 19A shows a correlator using two matched multiheterodyning units sharing reference frequencies.

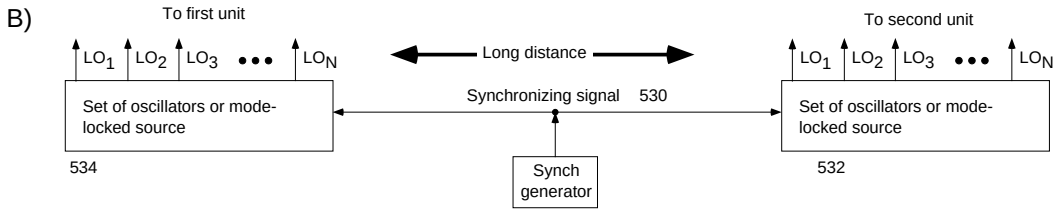

Figure 19B shows synchronization of reference signals for two widely separate multiheterodyning units.

plications include correlating natural wideband signals such as starlight (Fig. 5), radio emitting stars, and artificially created signals such as illumination created a range finding radar, sonar or lidar (Fig. 2B and Fig. 19), or illumination from the "A" interferometer of a velocimeter (Fig. 2A and Fig. 18). Each channel pair 1A and 1B, 2A and 2B etc., are correlated separately by the channel correlator units 791, 793 etc. to produce channel correlation outputs 790, 792 etc. These outputs are summed to form the net correlation output 794. The same reference frequency f_{LO1} is shared between channel 1A and 1B, and similarly for the other reference frequencies. The bandshapes produced for the A and B versions of each channel should optimally be as similar as possible. It may be possible in some embodiments to use the same physical spectrometer to implement spectrometers 796, 798 by having the A inputs and outputs displaced from the B input and outputs, displaced perpendicular to the wavelength direction.

The phase compensator 795 allows adjustment of the difference in arrival time of the reference signal between the down-mixers 797 and 799. This could correct for differences in propagation times in the cables routing the reference signal. These also provide an alternative method implementing the channel phase shifts, by providing another method of rotating the intermediate frequency signals, either rotating IF alone or the vector (IF, *IF). This method can be applied for all the signal processes, not limited to correlations. Equation 1 shows that a phase shift imparted to the reference or input signals will manifest that same phase shift for the corresponding down-heterodyned (IF) signal, and similarly for Eq. 2 and *IF. (The retardations could be applied to either input signal or reference signal, but for concreteness let us assume they are applied to the reference signals). Hence retarding the arrival time of the reference signal at "B" down-mixer 799 relative to "A" down-mixer 797 causes a phase shift equivalent to changing $|\Delta\theta|$ and hence $|\Delta\phi|$. In an interferometer process, for example, instead of obtaining the rotated vector (IF′, *IF′) from a rotator block (650 in Fig. 12A), the rotated (IF′, *IF′) signals could be obtained from a down-mixer unit having an adjustably retarded reference signal. In order to rotate by a positive $\Delta\theta$, the retardation of the reference signal would be negative $\Delta\theta$. In optical embodiments of the multiheterodyning processor, the adjustable retardance of the reference beam or input beam can be implemented electro-optically. Collectively (for all channels) changing the arrival time of the reference signal to the down-mixer, such as by changing a path length, is a method of changing the net delay of the correlating device.

Figure 16A shows a channel correlator. It comprises two independent correlators whose outputs are summed, one from the IF signal and one from the *IF signal. The multiplication function 812 could be implemented by a coincidence gate, such as when photon-counting detectors are used. Nominally $\Delta\theta = \Delta\phi$.

Correlating more than two inputs (such as A, B, C, D, E) can be done by constructing a circuit analogous to Fig. 16A that has multiple vector inputs and implements whatever mathematical definition of a multi-variable correlation the user desires. This includes finding the time average of the square of the sum of the inputs.

Figure 16D shows how the correlation can be performed using the post-averaging weighting method, by forming a sinusoidal linear combination of intermediate correlations 820, 821, 822, 823, as described by Eq. 24. Each intermediate correlation is a correlation between combinations of IF and *IF. This method is advantageous when the down-heterodyned signal is detected by a photon-counting system, and a coincidence gate used for the multiplication function of the correlator. This way, the sinusoidal linear combination can be applied to cumulative output of the coincidence gate, which is a slowly changing signal, rather than the higher bandwidth pulses constituting the IF signals.

R. Channel Recorder

Figure 12C shows a channel recorder which stores the IF vector signals for later use. At the time of measurement, the frequencies f_{LOn}, relative phases, and amplitudes of the reference signal are also measured. The input signal can be recreated from this stored information by Fourier reconstruction.

S. Channel Waveform Synthesizer

For the process of waveform synthesis, vector channel outputs sent to the up-mixer are ersatz and can be taken from stored data, or from some real-time channel process not based on a high frequency ($\sim \beta_{net}$) input. For example, Fig. 15B shows how to generate a high bandwidth noise signal having a comb-filter power spectrum , such as for use in velocimetry (Fig. 2A). Each channel 774 could have a noise generator 770 that passes through a channel interferometer 772. That is, instead of using a single high bandwidth noise generator as a high frequency input (1 in Fig. 1) passing through a spectrometer 5, the noise could be generated at the channel level in a parallel manner by many lower bandwidth noise generators. Thus a spectrometer is not needed. Furthermore, this random signal 770 does not have to be vectorized for velocimetry applications, since the phase of the signal 104 leaving the first interferometer 102 is immaterial.

T. Combination Signal Processes

A combination of channel signal processes can be applied to the channelized intermediate frequency signals in an overall parallel manner to implement a combined wideband signal process. The combinations can include

the channel signal processes already discussed, and arithmetic operations such as adding and subtraction of input signals. Let s_1, s_2, s_3, etc. be channel signal processes, called component processes, and $f(s_1, s_2, s_3, \dots)$ be a network of these, where outputs of any component process s_x could be used as part of the input of any other component process s_y. That is, we are not restricted to simple sequences s_1 to s_2 to s_3 etc. Then this will form a multiheterodyning device that acts on the wideband input signal analogous to $f(S_1, S_2, S_3 \dots)$, where S_1, S_2, S_3 etc. are the individual effect on a wideband signal by s_1, s_2, s_3.

In other words, going from the output of one multiheterodyning apparatus to the input of another we can omit the steps of up-heterodyning, summation over channels, then spectral decomposition into the same channels, and down-heterodyning. This is because there is no point to up-heterodyning and then immediately down-heterodyning, and no point to summing over channels and then immediately decomposing into the same channels. Effectively we can move these steps to outside the network $f(s_1, s_2, s_3, \dots)$. Generally, it is advantageous to keep the wideband signal information expressed as a parallel set of intermediate frequency signals as long as possible, postponing the steps of up-heterodyning and summation over channels.

U. Calculating Desired Channel Phase Shifts

1. Plotting phase versus frequency

The most important parameter describing the behavior of a signal process is the phase $\phi = f\tau$. Thus it is extremely useful to refer to Fig. 8A, which plots ϕ versus f. A phase-linear device having delay τ is represented by a line $\phi = f\tau$. The long thin lines 600 and 602 are "global" lines $\phi = f\tau_{net}$ representing the effective net delay τ_{net} of a multiheterodyning device. (The difference in slopes between lines 600 and 602 has been greatly exaggerated relative to their absolute slope for clarity.) The delay created by an individual channel is a bold short line (such as 604) of horizontal extent β_{ch}, having slope τ_{ch}, and called a "channel segment". These τ_{ch} values can have individually different values ($\tau_{ch,n}$) from channel to channel. The global lines are best-fit lines through all the channel segments, weighted by the detailed shape of the channel bands.

Since phase is periodic with periodicity of 1 cycle or 2π radians, the channel segment and global lines can be equivalently translated vertically any integer number of cycles on Fig. 8A.

2. An Initially Phase-nonlinear Device

When no channel phase shifts are applied, the channel segments initially lay on the horizontal axis, with their left (low frequency) ends at coordinates (f=f_{LOn}, ϕ=0), and having slopes $\tau_{ch,n}$. However, due to the periodicity of phase, the channel segments can be raised vertically by adding any integer number of cycles. Then a global line which is a best-fit line through all the channel segments is attempted to be found. However, for arbitrary values of f_{LOn}, it is unlikely that there will be a very good fit, as there will be random phases, some too high and some too low. Thus, a non-phase linear device will probably result from arbitrary choice of f_{LOn}.

3. Bringing it into Phase-linearity

Bringing the net device into phase-linearity is equivalent to raising each channel segment by an amount $\Delta\phi_{lin}$ so that the "center of mass" of the channel segment at f_{ave} falls along a global line. The global line 600 has a "nominal" delay $\tau_{net} = \langle\tau_{ch}\rangle$. Global line 602 describes a slightly larger delay, $\tau_{net} = \langle\tau_{ch}\rangle + \Delta\tau$, created by altering the channel phase shifts by an additional amount $\Delta\phi_{dil}$.

V. Creating Small Changes in Delay

The $\Delta\phi_{dil}$ phase shifts can be used to create small changes $\Delta\tau$ in τ_{net} while holding τ_{ch} constant for all channels. Phase shifts cannot be used to create large changes in τ_{net}, because then the slope of the channel segments becomes too different from τ_{net}, creating walkoff errors $\Delta\phi_{walkoff}$ (608 in Fig. 8B). The walkoff error is approximately

$$\begin{aligned} \Delta\phi_{walkoff} &= (1/2)\beta_{ch}(\tau_{net} - \tau_{ch,n}) \\ &\approx (1/2)\beta_{ch}\Delta\tau. \end{aligned} \tag{27}$$

When the walkoff errors grow beyond approximately $\pm 1/4$ cycle, de- phasing of the channels makes the multiheterodyned output incoherent, and thus no-longer useful for double interferometer velocimetry or correlation measurements. Thus the maximum practical dilation is

$$\Delta\tau_{max} \approx (1/2)/\beta_{ch}. \tag{28}$$

To create a larger delay change than $\Delta\tau_{max}$ requires changing τ_{ch}, in addition to re-adjusting the channel phasing.

Note that this result assumes $\Delta\theta$ and hence $\Delta\phi$ is independent of intermediate frequency. A positive frequency dependence to $\Delta\theta$ and $\Delta\phi$ would increase the slope of the segment and change the walkoff error. This would reduce walkoff and raise $\Delta\tau_{max}$ for positive $\Delta\tau$, and increase walkoff and reduce $\Delta\tau_{max}$ for negative $\Delta\tau$.

IV. MASTER PHASE EQUATION

To achieve a coherent delay, we find the phase shifts $\Delta\phi_n$ that put the "center" (located at f_{ave}) of each chan-

nel segment along a global line having a slope τ_{net}. Thus

$$(1/2)\beta_{ch}\tau_{ch,n} + \Delta\phi_n = [f_{LOn} + (1/2)\beta_{ch}]\tau_{net} \quad (29)$$

which becomes

$$\Delta\phi_n = [f_{LOn} + (1/2)\beta_{ch}]\tau_{net} - (1/2)\beta_{ch}\tau_{ch,n}. \quad (30)$$

This is a master equation from which we can derive other results. The subscript n denotes that the value is individual to a particular channel #n. For clarity, let us redefine β_{ch} so that given f_{LO} and f_{ave} we always have

$$[f_{LOn} + (1/2)\beta_{ch,n}] = f_{ave,n}. \quad (31)$$

This way, the Eq. 30 will also be valid for asymmetrical bandshapes.

Let us suppose that all the channel delays are the same within a given multiheterodyning unit, so that $\tau_{ch,n} = \langle\tau_{ch}\rangle$ in Eq. 30. (We will allow them to be different between units A and B, but same within A, and within B). This is reasonable if the delays are implemented by shift registers driven by a shared clock frequency. Let us describe the net delay as a deviation from a nominal delay $\tau_{net} = \langle\tau_{ch}\rangle + \Delta\tau$. Then Eq. 30 becomes

$$\begin{aligned} \Delta\phi_n &= f_{LOn}\langle\tau_{ch}\rangle + f_{ave,n}\Delta\tau \\ &= \Delta\phi_{lin,n} + \Delta\phi_{dil,n}. \end{aligned} \quad (32)$$

The first term is the phase shifts $\Delta\phi_{lin,n}$ required to bring the net device into phase-linearity, the second term is the additional phase shifts $\Delta\phi_{dil,n}$ required to change (dilate) the delay. Hence

$$\Delta\phi_{lin,n} = f_{LOn}\langle\tau_{ch}\rangle \quad (33)$$

$$\Delta\phi_{dil,n} = f_{ave,n}\Delta\tau. \quad (34)$$

A. When Using a Pair of Devices Sharing f_{LO}

Now suppose we have a pair of multiheterodyning units "A" & "B" that are being compared, such as to form a correlator or a double interferometer velocimeter, and which share the same reference frequencies f_{LOn}. Since it is only a relative measurement, we need only change one of the unit's τ_{net}, say unit B's. The analysis below assumes the channel delays and phases of unit A will remain the same, while we adjust the channel delays and phases of unit B. From Eq. 32 we have for the A and B channel phases

$$\Delta\phi_{n,A} = f_{LOn}\langle\tau_{ch}\rangle_A \quad (35)$$

$$\Delta\phi_{n,B} = f_{LOn}\langle\tau_{ch}\rangle_B + f_{ave,n}\Delta\tau. \quad (36)$$

Because a correlation or velocimetry measurement only cares about a comparison between A and B within each channel, we are allowed to add an arbitrary constant $\mathrm{Con_n}$ to both A and B that could change from channel to channel.

$$\Delta\phi_{n,A} = f_{LOn}\langle\tau_{ch}\rangle_A + \mathrm{Con}_n \quad (37)$$

$$\Delta\phi_{n,B} = f_{LOn}\langle\tau_{ch}\rangle_B + f_{ave,n}\Delta\tau + \mathrm{Con}_n. \quad (38)$$

Now suppose we make the delays of A and B units the same, $\langle\tau_{ch}\rangle_A = \langle\tau_{ch}\rangle_B = \langle\tau_{ch}\rangle$. This is fairly easy to do if the delays are implemented by shift registers driven by the same clock frequency. Now Eq. 37 and Eq. 38 proves that it is permissible to ignore the $\Delta\phi_{lin}$ terms for a correlator or velocimeter when the f_{LOn} are shared between the units, because that is equivalent to having $\mathrm{Con}_n = -f_{LOn}\langle\tau_{ch}\rangle_A$ so that

$$\Delta\phi_{n,A} = 0 \quad (39)$$

$$\Delta\phi_{n,B} = f_{ave,n}\Delta\tau. \quad (40)$$

Thus the simplest application of a correlator or velocimeter sharing reference frequencies is to set all the channel phases to zero for both A and B units, and the channel delays the same for A and B units. This is sufficient to adjust τ_{netB} over a small range $\langle\tau_{ch}\rangle \pm \Delta\tau_{max}$. For a larger range, we need to change both $\Delta\tau$ and τ_{ch}. The analysis below shows how.

Note that the net delay for this invention is more precise than possible from a single channel used alone, because the slope of the global line is based on the average of many channel segments. Furthermore, if all the channel delay values $\tau_{ch,n}$ drift in the same direction, such as if they are shift registers driven by the same clock frequency, then τ_{net} does not change because that is equivalent to translating the global line vertically without changing its slope. Thus the temporal behavior of the multiheterodyning device is more precise and stable than a single channel used alone.

In order to increase τ_{netB} further than $\Delta\tau_{max}$ we must increase $\langle\tau_{ch}\rangle_B$. In a shift register implemented channel delay, τ_{ch} will be naturally quantized in increments of a clock period, which we will call $\Delta\tau_{ch}$. So let

$$\langle\tau_{ch}\rangle_A = \langle\tau_{ch}\rangle \quad (41)$$

$$\langle\tau_{ch}\rangle_B = \langle\tau_{ch}\rangle + k\Delta\tau_{ch}, \quad (42)$$

where k is an integer which describes which delay *range* we are in. Then we could have

$$\Delta\phi_{n,A} = 0 \quad (43)$$

$$\begin{aligned} \Delta\phi_{n,B} &= f_{LOn}\Delta\tau_{ch}k + f_{ave,n}\Delta\tau \\ &= \Delta\phi_{lin,n} + \Delta\phi_{dil,n} \end{aligned} \quad (44)$$

for $k = 0, 1, 2\ldots$, and

$$\tau_{netB} = \langle\tau_{ch}\rangle + k\Delta\tau_{ch} + \Delta\tau \quad (45)$$

$$\tau_{netA} = \langle\tau_{ch}\rangle. \quad (46)$$

These four equations describe the configuration to use in a two unit correlator or velocimeter when reference frequencies are being shared, and when some simplifying assumptions where used. For any circumstances, the exact result can be computed from the master equation Eq. 30.

If the channel delays are not exactly the same between A and B units, this can be compensated for by adding a

phase adjustment to the B channels of $(1/2)\beta_{ch}(\tau_{ch,n,B} - \tau_{ch,n,A})$.

Fig. 8B shows a close-up of Fig. 8A where a channel segment intersects a global line. The channel segment is shown as a rectangle of vertical thickness $2\Delta\phi_{slop}$ to represent uncertainties in τ_{ch}, $\Delta\theta$, and variation of $\Delta\theta$ with intermediate frequency. Instead of assuming a constant $\Delta\theta$, the most accurate analysis of Fig. 8A would include the actual frequency dependence of $\Delta\theta$. This could make the channel segment curved. For shift register delays driven by the same clock frequency, $\Delta\phi_{slop}$ could be insignificant compared to $\Delta\phi_{walkoff}$.

B. Numerical Example of Choosing Phase Shifts

Let us give a numerical example using a 100 channels of β_{ch}=200 MHz, filling an input bandwidth from 10 GHz to 30 GHz so that β_{net}=20 GHz. Each channel has a shift register delay driven by a clock frequency which must be greater than 400 MHz (according to the Nyquist criteria) in order for β_{ch}=200 MHz. Thus we can increment the shift register delay in quanta of $\Delta\tau_{ch}$=1/(400 MHz) = 2.5 ns. Let the starting value of the shift register delay be τ_{ch} = 2 ms = 2000000 ns. We can set $\Delta\tau$ in Eq. 44 to any value from zero to a maximum value of $\Delta\tau_{max} \sim (1/2)/\beta_{ch}$ ∼2.5 ns, which is when dephasing begins. Note that conveniently, $\Delta\tau_{max} \approx \Delta\tau_{ch}$, so that just as dephasing begins we can jump to a new delay range by increasing $\tau_{ch,B}$ by $\Delta\tau_{ch}$, from 2000000 ns to 2000002.5 ns etc.

We start with all shift register delays set to τ_{ch}= 2000000 ns, $k = 0$, and $\Delta\tau = 0$, and we set all the phase shifts to zero according to Eq. 43 and Eq. 44. The net delay is the nominal value τ_{net}= 2000000 ns. We are in the lowest delay range, and we can adjust τ_{net} from 2000000 ns to 2000002.5 ns by adjusting channel phases according to Eq. 44, by increasing $\Delta\tau$, up to $\Delta\tau$=2.5 ns. At this point we jump to a new delay range by incrementing k to 1 and reseting $\Delta\tau$ to zero. That is, now all the B-units shift register delays will be at 2000002.5 ns. The channel phases are nonzero because of the first term. The second term is zero. Now we can increase τ_{net} from 2000002.5 ns to 2000005 ns by increasing $\Delta\tau$ from 0 to 2.5 ns and adjusting phases according to Eq. 44. And so on. Thus by the combination of changing the delay on a fine level with phases and on a coarse level by the shift registers, we can create any delay with very fine resolution.

C. Practical Advantages of Sharing Reference Frequencies

The invention is very practical because in some embodiments it is not necessary to assign the reference frequencies f_{LO1}, f_{LO2}, f_{LO3}, etc. to any precise set of values. They and their associated channel bandshapes can be approximately scattered across the bandwidth β_{net}. This is a great practical advantage because it allows the use of inexpensive oscillators that may drift in frequency over time. (The frequency must not drift significantly over the delay time, but this is easily achieved.) Secondly, the detailed shape of the bandshape does not critically affect the autocorrelation or correlation in many embodiments (provided it is the same for all channels A, B, etc. sharing a given reference frequency). Thus inexpensive spectrometers and electrical components can be used. Thirdly, for many situations a variance in τ_{ch} among channels is acceptable because channel phase adjustment can compensate for it. This reduces cost of components creating the channel delay.

D. Tolerance for Reference Frequency Drift

The tolerance to frequency drift for the reference frequencies can be estimated. The peak to peak spacing of the comb-filter is $1/\tau$. Suppose we want the drift in frequency to be less than 10% of a comb-filter peak-to-peak spacing $(1/\tau)$, and this drift occurs over a duration of τ or the round trip time of the signal from apparatus to target and back, whichever is greater. For radars, the latter and former could be about the same, and be about 2 ms. Thus we desire (10%)(1/[2 ms])=50 Hz stability over a 2 ms interval, or 25 kHz per second stability for a frequency that may be about 30 GHz. This is about 1 part per million per second stability, which is achievable.

E. An Autocorrelator Sharing Reference Frequencies

Figure 18A shows an embodiment of the invention forming a double interferometer velocimeter analogous to Fig. 2A. The set of local oscillators 400, 401, 402, 403 etc. supply reference frequencies shared between two multiheterodyning interferometer units "A" and "B" (406 and 408). Phase compensators analogous to 510 in the correlator (Fig. 19A) are not necessary in this velocimetry application because the detecting interferometer ("B") only cares about the power spectrum and is not phase sensitive.

The sharing of reference frequencies causes the velocimetry measurement to be insensitive to the choice of specific values for reference frequencies. Furthermore, the detailed band shapes are not critical provided "A" and "B" units have similar shapes within each channel. Figure 18B shows a hypothetical set of channel bandshapes for one of the units, suggesting arbitrary placement and shape. The lack of commensuration between the comb-filter peaks 416 and 418 inside bands 412, 414 suggests lack of phase-linearity. Provided both "A" and "B" units deviate from phase-linearity in the same manner, lack of phase-linearity is acceptable. Also note that it is not critical for the channel bands to contiguously fill the input bandwidth β_{net} in this application, although it is optimal

to do so to produce the least ambiguous autocorrelation peaks.

F. A Correlator Sharing Reference Frequencies

Figure 19A shows an embodiment of the invention performing correlation, where a set of reference frequencies f_{LOn} are shared. This application correlates two wide bandwidth input signals 500, 502 for the purpose of range-finding, analogous to Fig. 2B. Each input signal is spectrally decomposed into channels and heterodyned by the set of reference frequencies in the multiheterodyner units 504, 506. When a set 508 of reference frequencies are shared, as shown in Fig. 19A, this creates the practical advantage that the detailed value of the reference frequencies is immaterial, analogous to the case with the double interferometer velocimeter discussed above. Thus the bandshapes (for each channel pair A, B) and reference frequencies could be arbitrarily arranged. On a coarse scale it is optimal to avoid overlapping channel bandshapes, and optimal to fill the input bandwidth β_{net} contiguously. But on a detail level the particular frequencies chosen do not matter.

Phase compensators 510 placed in series with the reference signals are analogous to 795 in Fig. 17, and control differences in arrival time for reference signals from the sources 508 to each apparati 504, 506.

G. Synchronizing Widely Spaced Correlator Units

If the separate multiheterodyning apparati 504, 506 of a correlator are spaced far apart, such as in radio astronomy or long-baseline optical interferometry, then it may not be practical to communicate the set of reference frequencies via a set of numerous cables. And even if the reference frequencies are combined into a single reference signal, such as produced by a mode-locked oscillator, frequency dependent attenuation or dispersion may make it difficult to communicate a wideband reference signal over long distance. A solution is to use two sets of local oscillators that are synchronized by cable 530, as shown in Fig. 19C. The synchronization signal could have a narrow bandwidth to accommodate the best frequency for the long distance cable. The synchronizing signal also could be expressed as an optical signal in the infrared where optical fibers have a minimum attention. The synchronizing signal could be used to synchronize two mode-lock oscillators, one at station 532 and one at 534, providing the two sets of reference frequencies. Alternatively, the synchronizing signal could be from an external source that is accessible to both stations, such as a satellite or similar distant source.

H. Correlator for Optical Signals

Figure 5 shows a multiheterodyning correlator for optical signals "A" 702 & "B" 703. Reference signal 700 is added to the input signal A (702) with a beamsplitter 704 prior to the spectrometer 706, symbolized by the prism. The spectrometer could comprise a prism or a grating. The input angle of the reference beam into the prism or grating may have to be slightly different than that of the input beam so that the reference and beam fall upon the same intensity detector element 708 when the reference frequency is lower or higher than the portion of the input signal it will heterodyne. The intensity detector produces an electrical signal 712 in response to the difference frequency component between the input signal 710 and f_{LO} contained in reference beam 700. (The terms "power" and "intensity" can be interchanged because the area of the intensity detecting device is constant.)

Figure 6 shows a detail of the intensity detectors in the spectrometer of Fig. 5. The intensity detectors could be elements of a CCD detecting array. A column 740 of elements would be responsible for detecting the IF signals and another column 741 responsible for the quadrature signal *IF. Rows of detectors would be associated with specific channel and with a specific range of wavelengths (frequencies). Let there be two polarization directions "h" and "v" also called horizontal and vertical. The input signal 702 is arranged to be polarized at 45° to "h" so that there is intensity in both the "h" and "v" components, and the reference signal is arranged to be circularly polarized (or vice versa). A horizontal polarizer precedes the IF intensity detectors and a vertical polarizer before the *IF detectors. This way the *IF detectors see a combined beam where the reference component lags 90° behind relative to the IF beam. The DC component of the intensity signal can be blocked by capacitor-like elements 714, analogous to those labeled 757 in Fig. 7A.

Acknowledgments

This work was performed under the auspices of the U.S. Department of Energy by the University of California, Lawrence Livermore National Laboratory under contract No. W-7405-Eng-48.

V. CLAIMS

(Submitted, not official version)

1. A method for applying a signal process to a high bandwidth signal to produce an output signal, comprising:

decomposing said high bandwidth signal into a plurality of spectral bands, wherein each spectral band of said plurality of spectral bands has a smaller bandwidth than said high bandwidth signal;

down-heterodyning each said spectral band to create an intermediate frequency signal by beating each said spectral band against a reference signal or against a component of said reference signal, wherein said reference signal comprises a plurality of reference frequency components, wherein each reference frequency component of said plurality of reference frequency components comprises a unique frequency with respect to every other reference frequency component, wherein for each said spectral band there is a specific reference frequency component having a frequency close to said spectral band, wherein the set of said intermediate frequency signals and their subsequent processing path is called a set of channels;

applying a signal process to each said intermediate frequency signal to produce a set of channel output signals; and

summing said channel output signals to produce said output signal, wherein this method is called "multichannel heterodyning" or "multiheterodyning".

2. The method of claim 1, further comprising up-heterodyning the frequency of said channel output signals prior to the step of summing said channel output signals to produce said output signal.

3. The method of 2, wherein the step of up-heterodyning is performed using the same said reference frequency components.

4. The method of claim 1, wherein the effective spectrum of said signal process applied to said intermediate frequency signal is shifted in frequency by an amount individual to said channel and said amount can be expressed as a phase shift and is called a channel phase shift, wherein said channel phase shift is applied in a coordinated manner to many channels to modify the effective temporal behavior of said output signal.

5. The method of claim 4, wherein said coordinated manner includes having a component of said channel phase shift that causes the effective temporal behavior of said output signal to change by amount Δt, wherein said component is given by approximately the product of the average frequency of said spectral band associated with said channel times said amount Δt.

6. The method of claim 4, wherein said coordinated manner includes having a component of said channel phase shift that brings said output into phase-linearity, wherein said component for said channel is given by approximately the product of said reference signal frequency component for said channel times an average over all said channels of the delay time characteristic of said signal process for said channel.

7. The method of claim 4, wherein said channel phase shift is accomplished by phase shifting said intermediate frequency signal by an amount which is independent of frequency and called a rotation angle to produce a phase shifted intermediate frequency signal, wherein said phase shifted intermediate frequency signal is called a rotated signal, wherein said channel output is formed from combinations of undelayed and delayed replicas of said intermediate signal having user-selected amplitudes, delay values and said rotation angles, wherein said rotation angle is proportional to said channel phase shift and proportional to said delay values.

7B. The method of claim 7, wherein said intermediate frequency signal is phase shifted by retarding said intermediate frequency signal.

7C. The method of claim 7, wherein said intermediate frequency signal is phase shifted by retarding said input signal in spectral band relative to said reference signal component.

8. The method of claim 4, wherein said channel phase shift is accomplished by expressing said intermediate frequency signal as a vector signal comprising said intermediate frequency signal and a quadrature manifestation of said intermediate signal, wherein said quadrature manifestation of a signal is defined as that having a phase approximately 90 degrees different from said signal for all its component frequencies, wherein said vector signal is rotated in its vector space by an angular amount called a rotation angle; wherein said channel output is formed from combinations of undelayed and delayed replicas of said vector signal having user-selected amplitudes, delay values and said rotation angles, wherein said rotation angle is proportional to said channel phase shift and proportional to said delay values.

8B. The method of claim 8, wherein rotation of said vector is accomplished by retarding said input signal in spectral band relative to said reference frequency component.

9. The method of claim 8, wherein said vector rotation is produced from a linear combination of said quadrature and non-quadrature vector components using coefficients which are sinusoidal functions of said rotation angle in analogy to a mathematical rotational transformation.

10. The method of claim 4, wherein said phase shift is achieved for a given said channel by substituting for said intermediate frequency signal in said signal process said intermediate frequency signal or quadrature version of said intermediate signal in different combinations to form a set of intermediate outputs, wherein said channel output is formed from linear combinations of said set of intermediate outputs using coefficients which are sinusoidal functions of an angular amount which is proportional to said phase shift.

11. The method of claim 4, wherein said input signal is an optical wave, wherein said reference signal and said input signal in said spectral band comprise two beams, wherein one of said two beams is circularly polarized relative to the other of said two beam, wherein both beams are detected by a first intensity detector sensitive to linear polarization, wherein both beams are passed through a first polarizer preceding said intensity detector, wherein said non-quadrature component is obtained by passing both beams through a second polarizer oriented orthogonal to said first polarizer.

12. The method of claim 1, wherein said signal process is any process which can be Fourier decomposed and widely separated frequency components are independent of each other, wherein said independence means that the relationship between detailed phases of said widely separated frequency components does not affect said signal process.

13. The method of claim 1, wherein said signal process is selected from a group consisting of a time delay process, a filtering process, an interferometry process, an autocorrelation process and a recording process, wherein said intermediate frequency signal is called an input signal and said channel output signal is called an output signal, wherein said output signal of said time delay process is a delayed replica of said input signal, wherein said output signal of said filtering process comprises one or more delayed replicas of said input signal with an undelayed replica of said input signal, wherein said interferometry process is said filtering process, wherein said one or more delayed replicas of said input signal are optimally spaced with the same interval, wherein said output signal of said autocorrelation process includes time averaging the product of said input signal with a delayed replica of said input signal and includes time averaging the square of the output of said interferometry process, wherein said output signal of said recording process includes storage and less than real-time manifestation of said input signal which may be in vector form, wherein the phase and amplitude of said input signal is stored while simultaneously measuring the relative phase and amplitudes of said multiple frequency components of said reference signal.

14. The method of claim 1, wherein said signal process is a waveform synthesis process, wherein said channel output signal is an ersatz form of said input signal, wherein said ersatz form includes stored data, noise generators, and real-time signals having bandwidth comparable to typical said intermediate frequency signal.

15. The method of claim 1, wherein said input signal comprises at least two separable signals which are to be processed by a multiple input signal process, wherein said multiple input signal pro-

cess includes correlation, wherein said spectral decomposition and said down-heterodyning occur using separate apparatus to produce separate intermediate frequency signals, wherein each said separate apparatus shares said reference signal frequency components, wherein said separate intermediate frequency signals are correlated in a channel-by-channel parallel fashion organized by said reference frequencies.

16. The method of claim 1, wherein said signal process is a correlation of at least two intermediate frequency signals, called input signals, derived from said spectral bands having similar average frequencies and said down-heterodyning performed using the same said reference signal component frequency, wherein a correlation for two said input signals is based on the time averaged product of said two input signals, wherein a correlation for more than two input signals includes a user-defined function that maximizes when all said input signals are replicas of each other, wherein a multiple input correlation includes time averaging the square of the sum of all said inputs.

17. The method of claim 1, wherein said signal process is a combination of signal processes selected from a group consisting of interferometry, filtering, autocorrelation, correlation, delay, recording, waveform synthesis, and arithmetic summing and subtraction of signals.

18. The method of claim 1, wherein the precise value of said reference signal component frequencies may be arbitrary and unrelated to each other, wherein it is optimal that the coarse value of said reference signal components frequencies and average frequency of said spectral bands be evenly positioned across the bandwidth of said input signal.

19. The method of claim 1, wherein said spectral bands are sparsely placed across the bandwidth of said input signal.

20. The method of claim 1, wherein said input signal includes electromagnetic waves and sound.

21. The method of claim 20, wherein said input signal includes visible and invisible light.

22. A method of comparing at least two wideband signals, comprising:

passing each wideband signal of said at least two wideband signals through a multiheterodyning unit, wherein reference frequency components are shared between said multiheterodyning units.

23. The method of claim 22, wherein one of said multiheterodyning units outputs a wide bandwidth illuminating wave having at least one echo, wherein at least one of said multiheterodyning units receives said illuminating wave,

24. The method of claim 23, wherein said at least one receiving unit performs a signal process which includes correlation and autocorrelation.

25. The method of claim 22, wherein said multiheterodyning units correlate said at least two wideband signals.

26. The method of claim 22, wherein said reference frequency component sharing is achieved by synchronizing at least two separate reference signal generators which create reference frequency components for said multiheterodyning units.

27. A method of creating at least two matched wideband filters, comprising:

creating a filter with a multiheterodyning process using a first set of reference frequencies,

creating a second filter with a multiheterodyning process using a set of reference frequencies which are the same as or synchronized to said first set of reference frequencies.

28. The method of claim 4, wherein said input signal is an optical wave, wherein said reference signal and said input signal in said spectral band comprise two beams, wherein for a first polarization direction one of said two beams is retarded by a quarter wave relative the other said beam and relative to a second polarization direction orthogonal to said first polarization, wherein intensity of said two beams in said first polarization direction is detected to form said intermediate frequency signal, wherein intensity of said two beams in said second polarization direction is detected to form said quadrature intermediate frequency signal,

29. The method of claim 10.5, wherein one of said two beams is circularly polarized relative to other beam of said two beams, wherein said other beam is linearly polarized at 45 degrees to said first polarization direction.

30. The method of claim 14, wherein said signal process is the generation of a wideband signal having echos, wherein for each said channel a waveform is generated which then passes through an interferometer to form said channel output.

31. A method for producing an output signal, comprising:

decomposing a high bandwidth signal into a plurality of spectral bands;

down-heterodyning each said spectral band of said plurality of spectral bands to create an intermediate frequency;

applying a signal process to each said intermediate frequency signal to produce a set of channel output signals; and

summing said channel output signals to produce said output signal.

Part 5

Single and Double Superimposing Interferometer Systems

US Patent 6,115,121
Issued Sept. 5, 2000

David J. Erskine*
Lawrence Livermore Nat. Lab.

Interferometers which can imprint a coherent delay on a broadband uncollimated beam are described. The delay value can be independent of incident ray angle, allowing interferometry using uncollimated beams from common extended sources such as lamps and fiber bundles, and facilitating Fourier Transform spectroscopy of wide angle sources. Pairs of such interferometers matched in delay and dispersion can measure velocity and communicate using ordinary lamps, wide diameter optical fibers and arbitrary non-imaging paths, and not requiring a laser.

I. BACKGROUND OF THE INVENTION

A. Field of the Invention

The present invention relates to the design of interferometers, and more specifically, it relates to the design of single interferometers and pairs of interferometers which can use broadband uncollimated light from an extended source.

B. Description of Related Art

Interferometers in single and in double arrangements are very useful devices in a variety of applications in optics, metrology and communications. These interferometers have a delay τ between their arms which can produce fringes in the output intensity. Single interferometers having zero or near zero delay can be used with short coherence illumination to compare distances between one arm containing a sample and a reference arm. Single interferometers having larger delays can be used to measure the spectrum of a source, or to measure Doppler shifts of laser illuminated targets to measure motion, since slight differences in wavelength (λ) cause changes in fringe phase. Double interferometers having non-zero delays are useful in optical communications and measurement of velocity of targets illuminated by broadband radiation.

1. Superimposing Interferometers and Uncollimated Light

Prior art interferometers have a design which requires parallel light, or which is not optimized for very broadband usage, or was impractical for very long delays. Consequently, these interferometers are impractical for many applications involving white light and light from an extended source, such as from a common lamp, which produces non-parallel (uncollimated) beams. This is a serious handicap, because the majority of inexpensive compact sources are then excluded.

The present invention includes the use of interferometers, in single or in pairs, which are capable of working with broadband uncollimated light. These are called achromatic "superimposing" interferometers because they superimpose the images or ray paths associated with each interferometer arm. A similar concept has been discussed previously by others and called "field compensation." However, previous interferometer designs may have been superimposing only for a very limited wavelength range, or are impractical to create large delays, or are impractical to scan the delay.

2. Coherent Delays

Generally, the goal in a superimposing interferometer is to split an input beam into two or more separate beams, coherently delay one beam relative to the other, and recombined them to form an output beam. (Usually just two beams are split and recombined in the case of a Michelson-type interferometer, or an infinite number in the case of a recirculating Fabry-Perot type interferometer). The separate, splitted beams are also called interferometer "arms," and the arms can have different lengths

*erskine1@llnl.gov

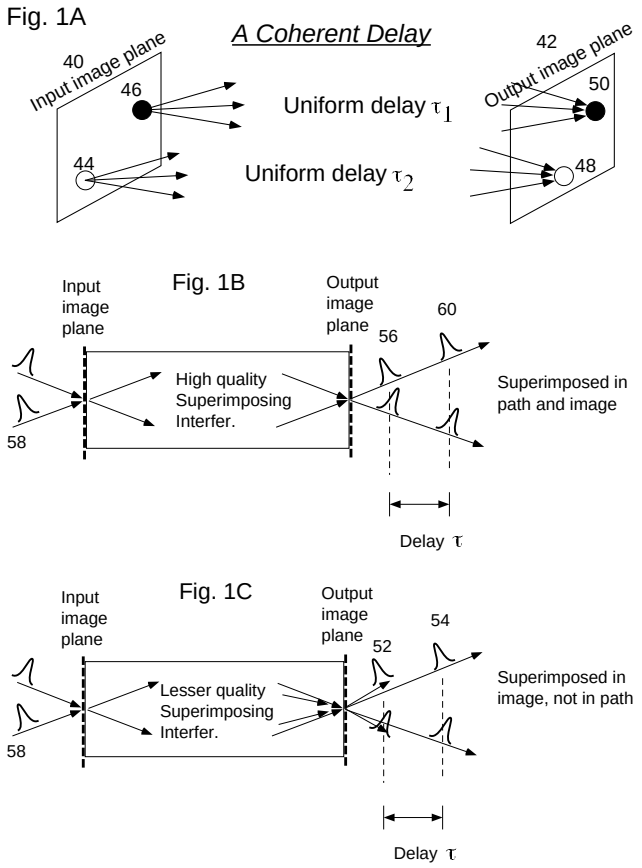

Figure 1A shows a coherent delay between pixels of input and output planes. Figure 1B shows the echo and undelayed signal superimposed in path (and also image). Figure 1C shows the echo and undelayed signal superimposed in image but not path.

which create a relative delay. For each input pulse, two or more pulses are outputted. The earliest output pulse, from the shortest arm, could be called the "undelayed" signal. The later pulses, from the longer arms, are called "echos." The interval between the undelayed signal and the echo is the interferometer delay τ.

The term "coherently delayed" is explained in Fig. 1A. A pattern of light (which could be called an image) may be presented to the input image plane 40, and the interferometer transports the pattern to an output plane 42 by imaging optics, so that there is a correspondence between input and output pixels 46 and 50, and between 44 and 48. The pattern appears for each instance of the output pulses discussed above. We are interested in the delay between instances. The term "coherently" delayed means that the time delay τ_1 for rays of light arriving at output pixel 50 is the same for all the rays of the bundle arriving at 50, within a tolerance of a quarter wave (a time interval of $\lambda/4c$, where c is the speed of the wave). The delay associated with another output pixel 48 could be called τ_2, and this may be different or the same as τ_1. Thus, even though the delay τ may change from output pixel to pixel, within the bundle of rays associated with each pixel the delay is very uniform. This uniformity is necessary to create fringes having significant contrast (visibility).

In some applications it is desired that τ have the same value for all pixels of the input beam. This will produce an infinitely wide fringe on output of the interferometer. In other applications it may be desired that τ vary linearly across the output beam. This will generate an evenly spaced and parallel fringe "comb," where the phase of the fringe varies linearly transversely across the beam. (This is usually easily accomplished by tilting an interferometer arm end mirror.) Only superimposing interferometers can produce infinitely wide or evenly spaced parallel fringe combs. (Conventional Michelson interferometers produce rings of fringes which are not linear or evenly spaced, except very far off axis). A superimposing interferometer could also be called angle-independent or solid-angle independent, because τ is independent of the angle of each ray within the bundle associated with a given image pixel.

A note on terminology: the delay value can be specified several ways, by single-trip path length D, by the round trip path length $c\tau$, or by a time interval τ. Strictly speaking, the units of τ should be time, but for convenience τ is sometimes specified in terms of length units, in which case it is implied that the length should be first divided by c to yield the equivalent time value. Secondly, these delay values usually refer to the difference in path lengths or travel times between interferometer arms, except when an isolated means for creating a delay is discussed, in which case it could refer to the propagation time through this means. When an optical element or assembly is inserted into an optical path, the increase in the propagation time τ causes over the original time is called an "insertion" delay. For example, a 20 mm thick glass etalon having a refractive index of n=1.5 would have an insertion delay of $\Delta D = (n-1)20 = 10$ mm, due to the slower propagation of light through glass compared to vacuum or air. Thirdly, the term "delay" has dual meanings in this document. It may refer to a value, such as τ, $c\tau$ or D, or it may refer to the means for creating the delay value, such as "an etalon delay" or a "relay lens delay".

3. Angle Dependence of Classic Michelson and Fabry-Perot Interferometers

Figure 2A shows a common Michelson consisting of a beamsplitter 24 and two end mirrors 20 and 22. This interferometer is not superimposing because mirrors 20 and 22 do not superimpose in view of the beamsplitter. This has the consequence that τ depends on incident ray angle. The single-trip path lengths between the beamsplitter and end mirrors differ by an amount D for rays parallel to the optic axis. This causes a round trip delay time of $\tau = 2D/c$ between the two arms, where c is

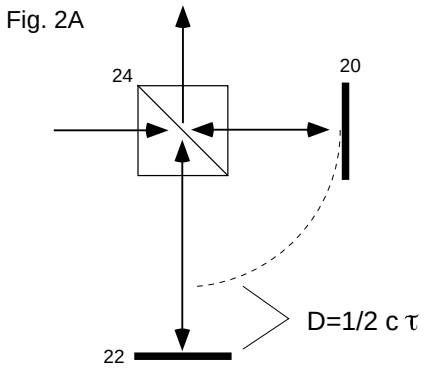

Figure 2A is a conventional Michelson interferometer.

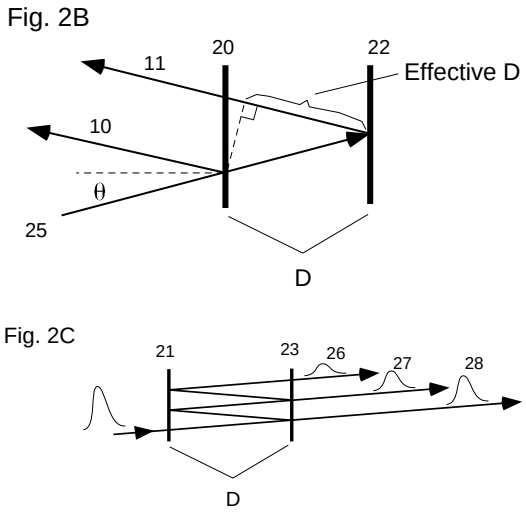

Figure 2B is the optical equivalent of Fig. 2A and shows the angle dependence of delay and lack of superposition of output paths. Figure 2C shows the lack of superposition for a conventional Fabry-Perot interferometer.

the speed of the illumination (which is spoken of as light, but can be any radiation that travels as rays, such as microwaves, sound, x-rays). Figure 2B shows the optical equivalent of Fig. 2A, because the partial reflection off the beamsplitting surface 24 puts the two mirrors 20 and 22 apparently in the same path, but longitudinally displaced. When a ray of light 25 enters with an angle θ to the optic axis, it encounters a path difference which depends on angle as $2D\cos\theta$. Thus the delay deviates from its nominal value of τ by $\tau(1-\cos\theta)$, which is of the order $(1/2)\tau\theta^2$, for small angles with θ in radians. This deviation can smear the delay which reduces fringe visibility. Note also that the ray 10 reflecting off mirror 20 does not overlap the path of ray 11 from the other mirror 22. For the same reason, an object seen in reflection of the two mirrors 20 and 22 will be seen as two images that are longitudinally displaced. Thus, the Michelson having a nonzero delay does not superimpose ray paths nor images, except for perfectly parallel incident light. The non-superposition and the angle-dependence of the interferometer are related.

The common Fabry-Perot interferometer (Fig. 2C) consisting of two flat partially reflecting mirrors 21, 23 separated by a distance D, is non-superimposing and suffers an angle dependence to the delay analogous to the Michelson example. The output rays 26, 27, 28 for a single given input ray 29 do not superimpose in path. Furthermore, the multiple images of an object observed through the interferometer will be longitudinally displaced from each other. Thus this interferometer does not superimpose paths nor images.

The angle dependence of these non-superimposing interferometers creates practical difficulties, because the fringe visibility is small unless the incident light is very parallel. An illumination source producing rays having a range of cone angles up to θ will smear the delay by $\sim (1/2)\tau\theta^2$, which destroys the fringe visibility if this is more than a quarter wave ($\lambda/c4$). This puts a limit of

$$\theta \sim \sqrt{(\lambda/2c\tau)} \qquad (1)$$

for the maximum cone angle. In order to produce this degree of parallelism from an ordinary lamp, which is an extended source, a small pinhole must be used a far distance from the interferometer. This greatly reduces the amount of power available from the lamp. For example, for a 4-meter delay (such as used to measure Doppler velocities typical of automobiles) and green light (λ=500 nm), θ must be less than 0.00025 radian. This limits the numerical aperture of the illumination source to $f/2000$, which greatly reduces the amount of power available from a filament. Secondly, this restriction on parallelism also applies to the reflected light from the target as it enters the detecting interferometer in a velocity interferometer application. This severely reduces the depth of field of the target motion, so that when the optics imaging the target into the interferometer become slightly out of focus, visibility of the fringes is diminished.

Single interferometers (Fabry-Perot and Michelson) are used as for spectroscopy, such as Fourier Transform spectroscopy. The small cone-angle tolerance of these non-superimposing interferometers limits the spectral resolution. A book by R. Beer shows that for conventional Michelson interferometers there is a reciprocal relationship between the solid angle $\Omega = \pi\theta^2$ of a source and the best spectral resolution ($\lambda/\Delta\lambda$) achieved with a single channel detector, so the higher the spectral resolution the smaller the signal power. (Reinhard Beer, "Remote Sensing by Fourier Transform Spectrometry", John Wiley & sons, NY 1992, QD96.F68B43, page 17). The limit on Ω for a given spectral resolution severely limits the etendue or light gathering power (beam area times Ω), and prevents high spectral resolution on diffuse sources such as the aurora, plasmas, light from speckling images of stars, or light communicated through large diameter optical fibers.

In contrast, with a superimposing interferometer the delay is independent of ray angle and all the light can

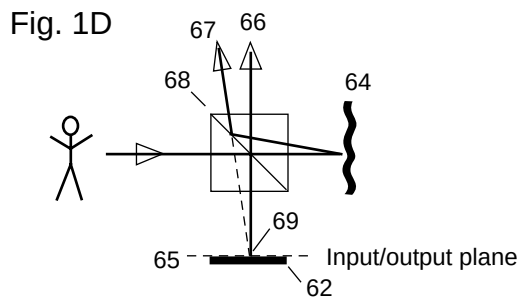

Figure 1D is an example interferometer that superimposes images but not ray paths.

be accepted from an extended source and have the same delay imprinted on it coherently. This can dramatically increase signal power. For the above example where the numerical aperture of a conventional Michelson was limited to $f/2000$, for a superimposing Michelson the numerical aperture could be, say $f/10$. It is not limited by anything having to do with the delay time, but instead by the diameter of the optics used in its construction. The amount of light power is increased by the ratio $(2000/10)^2$ or 40,000. This is a tremendous advantage.

4. Superposition Creates Angle Independence

A method of making an angle-independent delay is to superimpose the ray paths (Fig. 1B) associated with each interferometer arm. This is the best solution. A less desirable method, but still useful, is to superimpose images associated with each interferometer arm (Fig. 1C). Figure 1B shows the rays for a single pulse 58 that enters a pixel at the input image plane will appear at a pixel at the output plane, and there will be at least one echo 56 to the main signal 60, and that the ray paths for the echos superimpose the paths of the main signal. In Fig. 1C the rays for the echos 52 and signal 54 do not share the same path, but still intersect at the output pixel. Note that superimposing paths automatically superimposes images, but not vice versa. Superimposing paths is preferred because then the detector can be placed anywhere along the output optical path. If only images are superimposed, then the detector must be placed at the output plane or a re-image of this plane, otherwise the rays from all the arms do not intersect properly at the appropriate pixels and the fringe visibility is poor. Devices that are ideally designed to superimpose paths may in practice have slight aberrations that cause the paths of one arm to deviate from the intended path, so that strictly speaking only a superposition of images is achieved. Thus there is not a black-and-white distinction between the two kinds, it is a matter of degree.

Figure 1D shows an example, using a Michelson interferometer having zero delay. The interferometer has a plane mirror 62, and an irregular mirror 64 superimposed

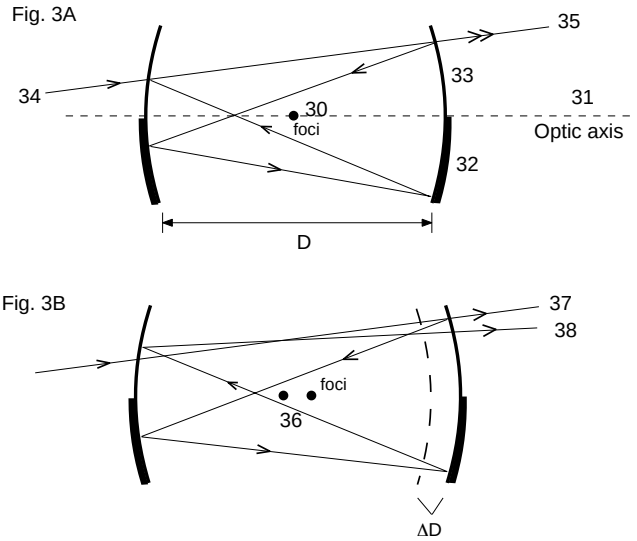

Figure 3A shows a Spherical Fabry-Perot interferometer. Figure 3B shows the effect of changing the mirror separation of a Spherical Fabry-Perot interferometer.

longitudinally in reflection of the beamsplitting surface 68. Let both the input and output planes 65 be at these mirrors. Then the irregular surface of mirror 64 will cause the output ray 67 to have a different angle and hence path than output ray 66 from the flat mirror, yet both rays appear to come from the same pixel 69 of the output plane. Thus images are superimposed while paths are not. In these cases, it is very important that the detector be at the output image plane or a re-image of that plane. This discussion is meant to illustrate the utility of defining input and output planes for realistic interferometers, that is, those having slight aberrations.

5. Superimposing Fabry-Perot

The ray path superposition principle has been discussed in the design of the spherical Fabry-Perot (Fig. 3A) [Pierre Connes, "L' Etalon de Fabry-Perot Spherique", Le Journal De Physique et le Radium 19, p262-269 (1958)], and the wide-angle Michelson interferometer [R.L. Hilliard and G.G. Shepherd, "Wide-angle Michelson Interferometer for Measuring Doppler Line Widths", J. Opt. Soc. Am. 56, p362-369 (1965)], where it was called "field compensation". These interferometer designs have properties that discourage or prevent their use in applications where broadband illumination is used, or long delays are needed, or adjustability of delay is desired.

Figure 3A shows a Spherical Fabry-Perot, consisting of two spherical mirrors spaced such that the two mirror focal points 30 coincide in the middle of the distance separating the mirrors. Each mirror has a half 32 which is totally reflective, and a half 33 which is partially reflective. A ray 34 entering the cavity recirculates between

the left and right mirrors, emitting a series of output pulses with geometrically decreasing intensities. The interval between output pulses is called the interferometer delay τ. Because of the overlap of foci, τ is independent of input ray path and the output rays for a given input ray 34 superimpose in output path 35.

The bottom half 32 of each mirror must be totally reflecting to allow only rays that have made an *even number* of round trips between the left/right halves to emerge. If both halves (32, 33) of the mirror were partially transparent, then output rays would be emitted which would not superimpose with rays 35. Another way to think about it is that if both halves were partially transparent, then an image plus an upside down version of that image would be outputted. The presence of the upside image would spoil the fringe visibility. Note that the edge between the totally 32 and partially reflective halves 33 lies on the optic axis 31. This is inconvenient because it prevents full use of the circular region of the output image around the optic axis where aberrations, such as spherical aberration, are smallest. The spherical Fabry-Perot must therefore be used slightly off-axis.

For the Spherical Fabry-Perot it is not possible to adjust τ and maintain the superimposing condition because the focal lengths are fixed. Figure 3B shows that when the separation of the mirrors is changed, the two mirror foci 36 come out of overlap. Then the undelayed 37 and first echo output ray 38 for a given input ray no longer superimpose and the delay τ becomes dependent on input ray path.

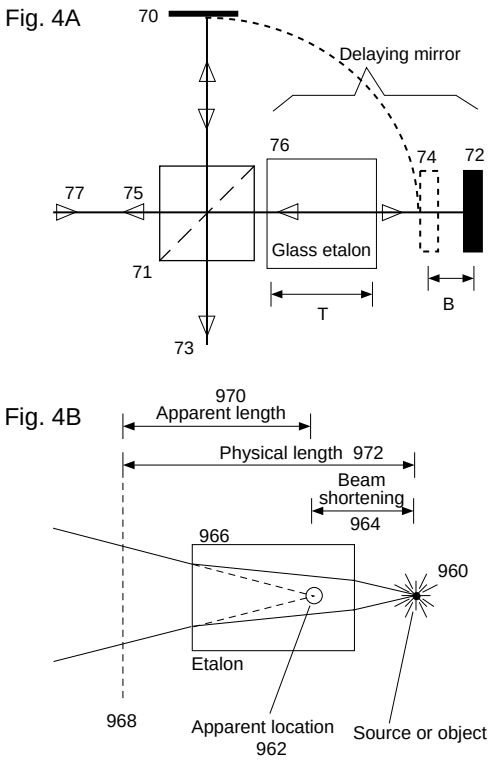

Figure 4A is a Michelson using an etalon to achieve superposition. Figure 4B shows what is meant by the term "beam shortening".

6. *Virtual Imaging by an Etalon*

The wide-angle Michelson discussed by R.L. Hilliard achieves path superposition for monochromatic light by use of a glass etalon, as shown in Fig. 4A. Due to refraction through the glass etalon 76, the mirror 72 behind the etalon appears at 74, closer to the beamsplitter 71 by a displacement B given by $T(n-1)/n$, where T is the etalon thickness and n is the refractive index of the etalon. Mirror 70 of the other arm is arranged to superimpose with the apparent mirror position 74. This creates a time delay between the two arms due to the sum of two effects: the actual mirrors are at different distances from the beamsplitter, and secondly, light travels slower through glass by the factor n. The net delay is

$$c\tau = 2[T(n-1)/n + T(n-1)]. \qquad (2)$$

Due to glass dispersion the apparent mirror position 74 is different for different wavelengths. This prevents the superposition condition to be achieved for all the wavelengths of white light, so that this interferometer is inappropriate for a white light velocity interferometer. Secondly, long delays such as $c\tau = 4$ meters, are not practical. (These long delays are useful for measuring meter/sec velocities found in industry). Thirdly, the delay value cannot be adjusted by a significant amount. (Tilting the etalon adjusts it slightly, but introduces astigmatism).

These disadvantages are not important when the etalon Michelson (Fig. 4A) is used as a velocity interferometer with monochromatic laser illumination. However, there is great utility in being able to use cheap ordinary white light sources for illumination instead of an expensive laser, and these call for a different kind of interferometer.

7. *Double Interferometers for White Light Velocimetry*

Recently, an interferometric method of using broadband illumination to measure target motion has been invented by the present author. The theory of operation is described in patent 5,642,194 by David J. Erskine, which is included herein by reference. In concept, it uses two interferometers in series, with the target interposed. In order to use white light, and uncollimated light from extended sources, the interferometers must be superimposing for a wide range of wavelengths. Furthermore, in order to measure slow velocities, of order meter/second, long delays of several meters in length are needed. In this white light velocity interferometer, the two interferometer delays must match. This requires adjustability of

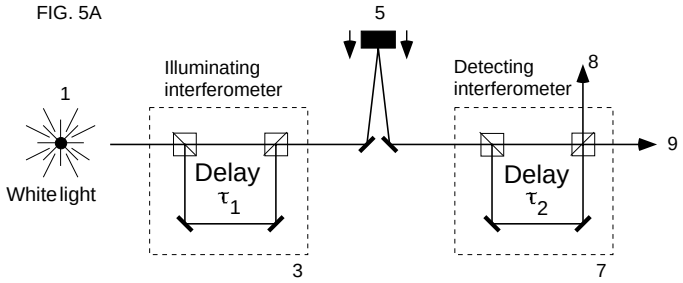

Figure 5A is a topological diagram of a double interferometer configuration able to measure velocity.

the second interferometer delay. All these requirements hinder practical use of the prior art interferometers in the white light interferometer, or in other double interferometer applications, such as communication, where incoherent lamps or multimode fibers are desired for illumination sources.

The topology of a double superimposing interferometer configuration used for broadband velocimetry is shown in Fig. 5A. (The configuration for optical communication is similar, except the target 5 is omitted.) Two superimposing interferometers (3 & 7) are in series with an interposed target 5 and illuminated by a broadband source 1. When the delays τ_1 and τ_2 match within a coherence length of the source illumination, fringes are created in the intensity of the outputs 8, 9, which are complementary in phase. In some embodiments, a single actual interferometer is used to implement the first and second conceptual interferometers by using retro-reflected light from the target. This automatically matches $\tau_1 = \tau_2$, in spite of gross mechanical vibration of the instrument that may change τ. This makes the retro-reflecting configuration attractive for industrial environments, and reduces weight and cost of the optical platform, since this does not have to be as rigid.

Target displacement or refractive index along the round trip path to the target during the interval τ cause a proportional shift $\Delta\phi$ in the fringe phase, where ϕ is in units of fringes. (One fringe is 1 revolution, 360° or 2π radians.) Thus, this is essentially a radial velocity measurement, as opposed to some other systems which measure transverse velocity (such as those involving the intersection of two incident laser beams to create standing waves, through which a particle to be measured travels). However, the combination of several simultaneous radial velocity measurements taken at different angles to the target can provide all 3 components of the velocity vector if desired.

When the light reflects normally off the target so that it approximately doubles back on itself, the displacement Δx during an interval τ is

$$\Delta x = (\lambda/2)\Delta\phi \tag{3}$$

and the average velocity v over that interval is

$$v = (\lambda/2\tau)\Delta\phi \tag{4}$$

so that the velocity per fringe proportionality is $(\lambda/2\tau)$. The phase shift produced by a moving target is $\Delta\phi = v(2\tau/\lambda)$. Hence, in order to produce a significant fringe shift to detect a slow moving target, long delays are desired. A $c\tau = 4$ meter delay produces a fringe shift proportionality of ∼20 m/s per fringe. Since fractional fringe shifts down to $\lambda/100$ can be easily measured, a 4-meter delay can have a velocity resolution of 0.2 m/s, suitable for industrial settings. Now the challenge is to build a 4-meter superimposing interferometer that is achromatic. Clearly, a 4-meter thick glass etalon is not practical due to its cost and chromatic aberration. Some of the designs presented below are a solution to this challenge.

8. Broad Bandwidth Illumination

There are different ways of detecting and interpreting the interferometer output. The output light can be detected by a single detector that is sensitive to a wide bandwidth, in which case an average λ is used. Alternatively, the output can be spectrally resolved into multiple channels. In this case, the velocity can be computed for each channel using the λ specific to each channel. These will give redundant velocity answers which can be used to check for consistency.

One advantage of using wide bandwidth illumination is the unambiguous velocity determination. That is, the lack of integer fringe skips when the velocity jumps more rapidly than the detecting electronics can follow. Essentially, the velocity measurement taken in different colors, such as red, green, blue, can be combined to determine the absolute velocity unambiguously, even though individually each color channel may have an integer fringe ambiguity. This is because each channel has a different velocity per fringe proportionality.

In contrast, in the conventional monochromatically illuminated systems, the fringe phase is ambiguous to an integer due to the periodicity of monochromatic fringes. This creates a great uncertainty in the gross value of the velocity when the target is first acquired (such as a car coming over the horizon) or if the signal drops out temporarily. This fringe skip uncertainty hinders the use of these monochromatic systems in applications where there is no other confirming method of velocity measurement, or where theoretical prediction of velocity is poor.

9. Velocimetry with a Double Fabry-Perot

A similar velocimetry method using two Fabry-Perot interferometers and laser illumination was described in a journal article by S. Gidot and G. Behar, "Multiple-line laser Doppler velocimetry", Appl. Opt. 27, p2316-

2319 (1988). However, since the Fabry-Perot is not a superimposing interferometer, this method is not practical with uncollimated illumination. Uncollimated rays passing through the Fabry-Perot will blur the delay value, which can cause a loss of fringe visibility. This produces a severe trade-off between degree of non-parallelism and maximum source bandwidth which precludes practical use of common white light sources such as lamps.

10. Beam Shortening

Figure 4B shows what is meant by the term "beam shortening", which is an important part of creating a superimposing interferometer. When real or virtual imaging by an optical element 966 causes an object or source 960 to appear by ray tracing to be at a different location 962 than the actual physical location 960, then the difference 964 is called a beam shortening or beam length shortening. The beam length could be measured from some reference plane 968. The apparent beam length 970 is from plane 968 to the apparent object location 962. The physical beam length 972 is from plane 968 to the physical object location 960. Figure 4B shows a positive beam shortening, when the apparent beam length is less than the physical beam length. Negative beam shortenings are also possible.

In those interferometers where the beam reflects off an end mirror, such as 72 in Fig. 4A, and nearly doubles back on itself, the beam shortening changes the position of the end mirror 72 from its physical position 72 to an apparent position 74. The roundtrip beam shortening would be twice B. When beam shortening involves an end mirror, the combination of the end mirror and the optical element performing the imaging could be called a "delaying mirror". In Fig. 4A, the delaying mirror would be etalon 76 and end mirror 72. The term "delaying mirror" replaces the term "superimposing delay" used in the previously mentioned patent 5,642,94 by the present author.

A delaying mirror is a set of optics that acts like a mirror in terms of ray tracing, but delays the waves in time compared to an actual mirror. Delaying mirrors are useful elements in forming a superimposing interferometer. This document present designs of delaying mirrors and designs of superimposing interferometers that may be useful because of their achromatic character, their possible long delay times, adjustability, or wide image field.

II. SUMMARY OF THE INVENTION

A superimposing interferometer involves beam shortening so that two paths appear to have the same length by ray tracing, but may have different propagation times. Many interferometers involve beams that reflect off an end mirror, so that the path nearly doubles back on itself. When beam shortening is applied to such configurations, a virtual mirror is formed that appears to be in a different location than its actual location. This could be called a "delaying mirror".

A delaying mirror is a name for an apparent mirror (A.M.) created by real or virtual imaging of an actual mirror, called an end mirror. The rays incident the A.M. surface leave the surface in a direction as if they reflected from an actual mirror located at the A.M. surface, except they are delayed in time compared to if an actual mirror were located at the A.M. surface. The delay time is controlled in part by the distance between the A.M. and the end mirror, and the amount of glass thickness used in the optics that performs the imaging. The A.M. can be curved or flat, but is usually flat. The position of the A.M. is calculated by imaging the surface of the end mirror. The center of curvature of the A.M. is calculated by imaging the center of curvature of the end mirror. The A.M. is optimally independent of illumination wavelength. Delaying mirror kinds can be classified by the method of imaging used, real or virtual, the arrangement and number of elements performing the imaging, and the kind of end mirror.

A superimposing interferometer is a kind of interferometer that superimposes the path of each of at least two output rays produced by a given input ray. There may be a delay between each of these output rays, and this delay could be zero. The superimposing interferometer has the desirable property that the delay is independent of incident ray angle, for a given location of the ray where it intersects a so-called input plane. (This location is also called a pixel of an input image.) This allows a coherent delay to be imprinted on an uncollimated beam, and allows the use of extended illumination sources in interferometry. The superimposing interferometer is most useful when the superposition is maintained over a range of illumination wavelengths (and thus is called achromatic), so that interferometry may be performed with uncollimated beams of white light, from ordinary lamps that are extended sources.

If the exact superposition of path is not achieved, a lesser, but still useful, kind of superimposing interferometer can be formed by requiring that the at least two output rays associated with each input ray superimpose in location at a so-called output plane. This could be called superposition of images, where each interferometer arm has an image associated with it. The images must superimpose longitudinally, transversely, in magnification. (Note that the superposition of path is a more stringent requirement equivalent to superposition of images while also matching wavefront curvatures.) By placing the detector that records the fringes at the output plane or some relayed image of it, fringes with significant visibility are still observed. An interferometer that satisfies the superposition of paths is more useful than one that satisfies only superposition of images because when paths are superimposed, the detector can be placed anywhere to record visible fringes.

Superimposing interferometers can be formed by superimposing one or more mirror-like elements by the partial reflection of surfaces such as a beamsplitters. The mirror-like elements may be actual mirrors or apparent mirrors (delaying mirrors). The interferometer kinds can be classified by how the superposition is configured, and by the kind of delaying mirror involved. If the mirrors face generally in the same direction as seen in the beamsplitters, then a finite number of output pulses is emitted for each pulse incident on the interferometer, and an N-path interferometer is formed. A superimposing Michelson is a kind of 2-path interferometer. If the mirrors face each other so that a beam bounces back and forth in a recirculating path, then an infinite number of geometrically decreasing intensity pulses is emitted for each input pulse. Then the interferometer is of the recirculating class. A Fabry-Perot interferometer is a member of this class.

Superimposing interferometers can be formed without delaying mirrors, by explicitly routing the beams so that there are more than one path between input and output planes, and by requiring that for each path the input and output planes are superimposed. Both N-path and recirculating classes (kinds) can be formed this way.

Single superimposing interferometers are useful for spectroscopy, especially from extended or wide angle sources. Series pairs of superimposing interferometers with matched delays and dispersions are useful for velocity interferometry and communication using illumination which can be broadbanded and extended, such as from common lamps. A procedure for matching the delays and dispersion between interferometers while individually maintaining the superposition condition for each interferometer involves iteration. The superimposing condition is optimized for one interferometer by temporarily using the interferometer in a retro-reflective mode by observing a retro-reflective target. The second interferometer is then matched in delay, and then in dispersion while holding the delay constant.

In some applications, having a coherent delay which varies across the output plane is useful, since this measure a range of delays in a single moment. This is called an inclined delay. Tilting a mirror is a method of achieving an inclined delay. However, only small values of inclination are practical by this method before the fringe visibility diminishes. A large inclination can be achieved by the use of wedges. Furthermore, by use of more than one wedge having different dispersive powers, an achromatic inclined delay can be achieved. In an analogous fashion, achromatic delays using etalons of different dispersive powers can be achieved. This removes a previous limitation of etalon delays in broadband interferometry.

When a single interferometer is used to observe as well as illuminate the target, this arrangement is called using the interferometer in a retro-reflective mode. The advantage is that the delay and dispersion matching conditions are automatically approximately satisfied, in spite of severe change in the delay such as due to vibration of the mounts holding the optics. However, in order to use this configuration, a method of preventing illuminating light from reaching the detector before reflecting off the target must be found. Several methods are described, including having the beams travel at an angle to the optic axis, offsetting the images of the target for incoming and outgoing beams, and using orthogonal polarizations.

A superimposing interferometer can be constructed that outputs more than two pulses for each input pulse, so there could be two or more delay values between the first output pulse and its echos. This would be an N-path interferometer with N greater than two. When the delays values are different, this is useful for generating simultaneous fringe patterns characterized by different delays. This is useful, for example, in velocimetry for reducing velocity ambiguity and in spectroscopy for measuring different portions of a Fourier Transform fringe record simultaneously, to make the measurement more robust to a fluctuating source. The different delays could also be distinguished by polarization by incorporating polarization elements in the interferometer.

A superimposing interferometer can be combined in series with a prism or diffraction grating to make a spectrum that has uniformly spaced fringes on it, with an adjustable spacing. This is useful, for example, for increasing the fringe visibility in Fourier Transform spectroscopy or velocity interferometry.

Methods of using a delaying mirror to coherently delay a beam are shown, where it is desirable to separate the incoming from outgoing beams.

III. DETAILED DESCRIPTION OF THE INVENTION

A superimposing interferometer can be made by superimposing a delaying mirror with an ordinary mirror, or with another delaying mirror. The different kinds of interferometers can be classified by how the superposition is configured, and by how the delaying mirror is formed. If the delaying mirror and other mirror are superimposed facing the same direction, such as by using partial reflection/transmission from a beamsplitting cube, then the interferometer formed is a kind of Michelson interferometer. If the delaying mirror and other mirror face each other so that light is reflected back and forth, then a recirculating interferometer is formed, similar to the Fabry-Perot (F-P).

A delaying mirror is a set of optics that acts like a mirror in terms of ray tracing, but delays the waves in time compared to an actual mirror located at the same place. In Fig. 6A the delaying mirror assembly is the set of optics 82, 84 and 86 that act as a mirror for one arm of a Michelson class interferometer. The “business” end of the delaying mirror assembly is the apparent mirror (A.M.) surface 80. This is where the delaying mirror appears to be. In general, the A.M. is created by real or virtual imaging of an actual mirror 86, which is called

Fig. 6A

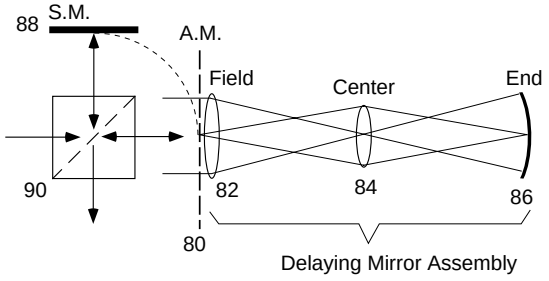

Figure 6A shows a superimposing interferometer using a relay lens delay with a spherical end mirror.

Fig. 6B

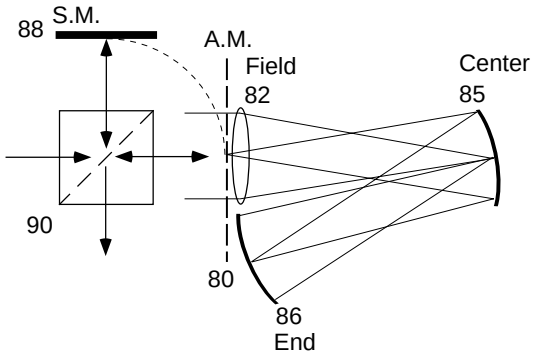

Figure 6B shows the center lens of the relay delay implemented by a spherical mirror.

Fig. 6C

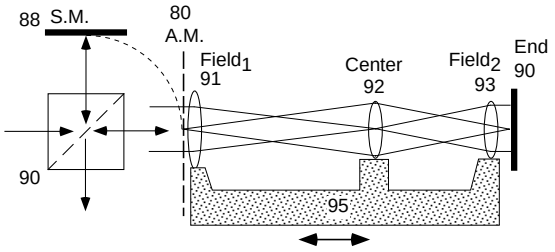

Figure 6C shows the relay delay implemented by transmissive lenses and a plane end mirror.

the end mirror, located a distance away. In Fig. 6A real imaging is used, and this is accomplished by the center lens 84. The field lens 82 is used to flatten the A.M. surface, which would otherwise be curved. The delay time of the delaying mirror assembly is controlled by the distance between the A.M. and the end mirror and the net amount of glass along the optic axis.

Michelson-class interferometers usually are considered to have just two arms. The arm containing the delaying mirror could be called the long arm, and the other arm the short arm. The mirror 88 could be called the short arm mirror (S.M). In general, the S.M. 88 could be an actual mirror, as in Fig. 6A, or a second delaying mirror assembly, as will be discussed in the section on differential interferometers.

To create the superimposing interferometer, the A.M. surface is superimposed with the S.M. This creates an interferometer that for ray tracing purposes acts like a zero-delay interferometer, and is therefore independent of ray angle. By time-of-flight however, there is a non-zero delay time because it takes a finite amount of time for light to pass through the delaying mirror assembly and leave out the A.M. Thus, the spectral properties of a non-zero delay interferometer are achieved while having angle independence.

Optimally, the overlap between the A.M. and the mirror-like elements of the other arms is as perfect as possible everywhere across the A.M. The greater the deviation of the A.M. from the S.M., the greater the loss of fringe visibility for uncollimated beams. Since usually the S.M. is a flat mirror, usually the A.M. should be flat. When the S.M. is a curved mirror, the A.M. should be curved with the same radii of curvature. For concreteness, we will generally assume the S.M. is flat and thus a flat A.M. is desired.

If the A.M. surface is perfectly superimposed with the S.M. surface, then superposition of paths has been achieved (as in Fig. 1B), which is ideal. In this case, the input and output image planes for the interferometer can be anywhere. However, due to aberrations of the optics, the A.M. surface curvature may not perfectly match the S.M. curvature. In this case, it is possible to overlap the location of the A.M and S.M. for some sections of the beam, while the angles of the surfaces are slightly different. This superimposes images but not paths (as in Fig. 1C). This can still produce visible fringes provided the detecting device is placed at a relayed image of the A.M. surface. That is, the input and output image planes should be located at the A.M. (This assumes that the beamsplitting surface is flat. Generally, the input and output planes should be optimally placed closest to the optics that generates the most wavefront irregularities, whether this be the beamsplitter or A.M.).

A description of different interferometer kinds using different delaying mirror kinds follows.

A. Michelson-class interferometers using real imaging

Superimposing Michelson-class interferometers are shown in Fig. 6A, 6B and 6C. These have delaying mirrors that use real imaging to form the A.M. This delaying arrangement is also called a relay lens delay. The A.M. is superimposed with the mirror 88 of the other arm by partial reflection in the beamsplitter 90. In Fig. 6A, the delaying mirror is a relay lens system comprising a field lens 82, a center lens 84, and a spherical end mirror 86. In Fig. 6B the transmissive center lens is replaced by

Fig. 7A

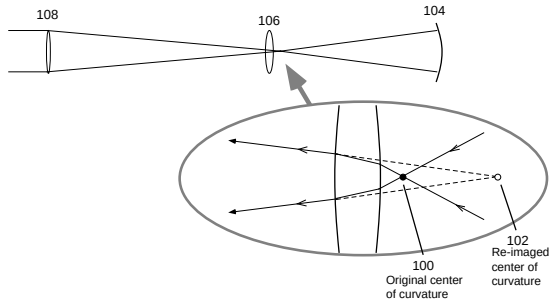

Fig. 7B

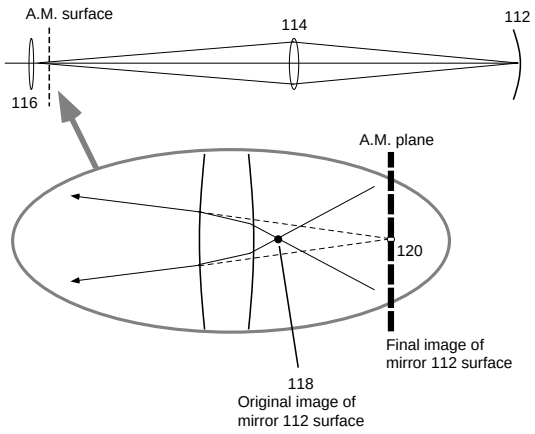

Figures 7A shows calculation of the center of curvature of the apparent mirror for a delaying mirror assembly. Figures 7B shows calculation of the apparent mirror location for a delaying mirror assembly.

equivalent spherical mirror 85. This minimizes the number of glass elements to reduce dispersion and chromatic aberration. In Fig. 6C the spherical end mirror is substituted by a plane end mirror 90 and a transmissive lens 93. This introduces another degree of adjustment which can be an advantage. Then the three lenses 91, 92 and 93 form a telescope and can be moved as a group 95.

The A.M. is formed by real imaging of the end mirror surface (86 or 90). The imaging is mostly accomplished by the center lens (84, 85 or 92). The primary purpose of the field lens (82, 91) is to make the A.M. appear flat, but it may also contribute to the imaging of the A.M. surface if the field lens is not exactly at the A.M. Usually the A.M. is desired to be flat, so that in general the center of curvature of the end mirror should be imaged to infinity by the optics of the delaying mirror assembly. If the center lens 84 lies near the center of curvature of the end mirror 86, then most of the responsibility for imaging the center of curvature lies with the field lens 82. Typically, the center lens is approximately midway between end mirror and A.M., and the field lens is near the A.M. However it is optimal if the center lens is not *exactly* in the middle, because this reduces focusing adjustability.

Figure 7A and 7B shows how to calculate the A.M. curvature and position. The center of curvature 100 (CC) of the end mirror 104 is re-imaged by the optics 106 and 108 to form the CC of the A.M. The inset to Fig. 7A shows that the center lens may slightly shift the initial CC location 100 to an intermediate point 106. This slight displacement must not be ignored in the calculation. Then to make a flat A.M., the focal point of the field lens 108 is arranged to coincide with the intermediate point 102 so that the final CC is at infinity. To calculate the A.M. location, the image of the end mirror surface 112 is first re-imaged by the center lens 114 to an intermediate point 118. The inset of Fig. 7B shows the field lens 116 re-images point 118 to point 120, which then defines the apparent mirror location. This slight shift from 118 to 120 must not be ignored.

The interferometer delay time is given by $\tau = 2D/c + \tau_{glass}$, where D is the difference in single-trip lengths of the two arms measured from the beamsplitter where it intersects the optic axis to the end mirrors 88 and 86. The term τ_{glass} is the insertion delay contributed by glass components measured down the optic axis, given by $\tau_{glass} = 2T(n-1)$, where T is the glass thickness and n is the refractive index. This glass term is much smaller than the $2D/c$ term, but can add dispersion due to the wavelength dependence of n. Thus, the glass term must be considered when discussing dispersion matching between two interferometers. Otherwise it can usually be ignored.

It is preferred that the delaying mirror be as achromatic as practical. This can be achieved by having the lenses and mirrors in the assembly be individually achromatic, by using first surface mirrors and standard multi-element achromatic lenses. In some cases, non-achromatic elements having chromatic effects of opposite polarity can be combined so that the net chromatism is reduced. For clarity, the multi-element nature of the lenses are not drawn in some of the Figures. However it is implied that achromatic lenses be used where-ever possible, unless explicitly stated that the lens need be a simple lens.

Spherical mirrors have superior achromatism over lenses, and when used at a 1:1 conjugate ratio, can have less spherical aberration than a transmissive lens for large numerical apertures. However, the use of a curved mirror as the center lens 85 requires an off-axis reflection which introduces undesired astigmatism. (This astigmatism and other irregularities can be greatly reduced by using a differential configuration described later.)

Delaying mirrors made from real imaging optics such Fig. 6A, B and C are useful because they provide a practical way of generating long achromatic delays, such as several meters in length, having a reasonably large numerical aperture, and having an adjustable delay value. The numerical aperture (f/number) is approximately set by that of the center lens and could be $f/10$, for example. In contrast, glass etalons longer than 30 centimeters and having a sufficient diameter to achieve a similar numerical aperture are impractically expensive, and have prohibitively large dispersion for broadband use. Furthermore, their delay time can't be adjusted practically.

The end mirror of either the short or long arms (88 or 86) can be tilted so that the A.M. is inclined relative to the S.M., by a small enough amount that the superposition is not significantly degraded. This generates a delay value τ which is a function of transverse location across the beam at the input/output plane. This is called an *inclined* delay. When fringes are present in the output, this creates an evenly spaced fringe comb of parallel fringes. This is useful for determining fringe phase, because all portions of the sinusoidal fringe shape can be observed simultaneously, allowing separation from any constant component. In contrast, in a non-superimposing Michelson, the fringes are rings due to the dependence of τ on ray angle. Methods of creating large values of inclination without sacrificing A.M. overlap are discussed in a later section.

B. Manifold of element positions for a relay delay

There are a large variety of lens/mirror spacings, choice of number of elements, selection of focal lengths/mirror curvatures which will produce a flat A.M. by real imaging. This variety produces freedom to adjust the A.M.-to-end mirror spacing while maintaining a constant curvature A.M.. Including more lenses/mirrors yields even more degrees of freedom. The freedom to adjust can be used either to modify the delay time τ while maintaining the superposition condition, or to adjust the overlap quality while maintaining a constant delay τ.

Two example calculations are given, one for the configuration of Fig. 6A, and one for Fig. 6C. A calculation for Fig. 6B would be similar, with the exception that movement of the center mirror changes the total path length as well as the spacing between elements. The configuration of Fig. 6C has an extra degree of freedom allowed by substituting two elements (lens and plane mirror) for the single curved end mirror. The focal lengths for the Fig. 6C example were chosen to be asymmetrical, that is, the center lens is decidedly more asymmetrically placed between the end mirror and A.M. than in the calculation of Fig. 8A.

The calculation for configuration Fig. 6A are shown in Fig. 8A and 8B. These are the manifold of possible positions of the optics which produce a flat apparent mirror, calculated for the specific example of field lens 82 focal length = 100 cm, center lens focal length 50 cm, and end mirror radius of curvature 100 cm. In both Fig. 8A and B, the A.M. to end mirror distance is plotted versus center lens position. However, Fig. 8A the A.M. is fixed, and in Fig. 8B the end mirror is fixed. Figure 8A would be more useful for when the superimposing overlap must be maintained while the delay time τ is being changed, such as in a Fourier Transform spectrometer with a scannable delay. Figure 8b would be more useful in a double interferometer application where the overlap quality of a second interferometer is being adjusted while trying to maintain a specific delay, (such as the delay value defined by the first interferometer).

Stagnant configurations should be avoided, since they have no adjustability. The stagnant configurations are when the derivative of the A.M.-end mirror distance is zero. These configurations are indicated in Fig. 8A & B by the thick arrows. Generally, they occur when the optics is in, or near to, a symmetrical configuration. For this reason, the magnification performed by the center lens should usually be arranged to be something other than exactly unity.

Figures 9A and 9B show the manifold of configurations producing a flat A.M. when the spherical end mirror is replaced by a plane mirror 132 and a second field lens 136. The additional element 136 introduces another degree of freedom, so that the complete manifold must be represented by a 3-dimensional chart showing configuration versus two parameters, which could be the center lens position and one of the field lens positions. For simplicity, only a subset of the possible configurations are shown in Fig. 9A and 9B, using 2-dimensional charts.

Since both ends 130, 132 of the cavity are intended to be flat, the positions of the A.M. and end mirror could be interchanged. Secondly, partially reflecting mirrors could occupy both the A.M. and the end mirror so that a recirculating cavity is formed. This is also true of the configurations in Fig. 8A and 8B. Thus this or analogous calculations could apply to recirculating cavities, which will be discussed later.

In Fig. 9A, 9B the focal lengths were chosen to asymmetrically place the center lens between the two field lenses, to illustrate that this avoids stagnation points. Field_1 136 focal lengths = 30 cm while field_2 lens focal length = 90 cm. Center lens 134 focal length = 30 cm. The A.M-end mirror separation with the A.M. position fixed is plotted versus center lens position. Figure 9A shows the case where the Field_1 lens 130 is fixed at the A.M.

Figure 9B shows the case where the three lenses 130, 134, 136 are moved together as a group. This is an easy method of adjusting the relay delay length while keeping the A.M. constant. The three lenses are mounted on a platform 95 (Fig. 6C) which can be moved relative to the end mirror. The three lenses form a telescope. The three lenses are first spaced properly amongst themselves so that collimated light incident to the telescope is outputted from the telescope as collimated. This can be accomplished by illuminating the interferometer with HeNe light and obtaining a fringe comb of parallel fringes instead of rings. The parallelism of the fringe comb indicates that the A.M. is flat. Once the A.M. is flat, the telescope 95 can be translated relative to the end mirror in the fashion indicated by Fig. 9B to adjust the A.M.-end mirror spacing.

Displacement of the telescope 95 only affects the A.M.-end mirror spacing if the telescope comprises lenses with asymmetrical focal length values ($\text{field}_1 \neq \text{field}_2$ focal length). The greater the asymmetry, the greater the change of the A.M.-end mirror separation per telescope

Fig. 8A

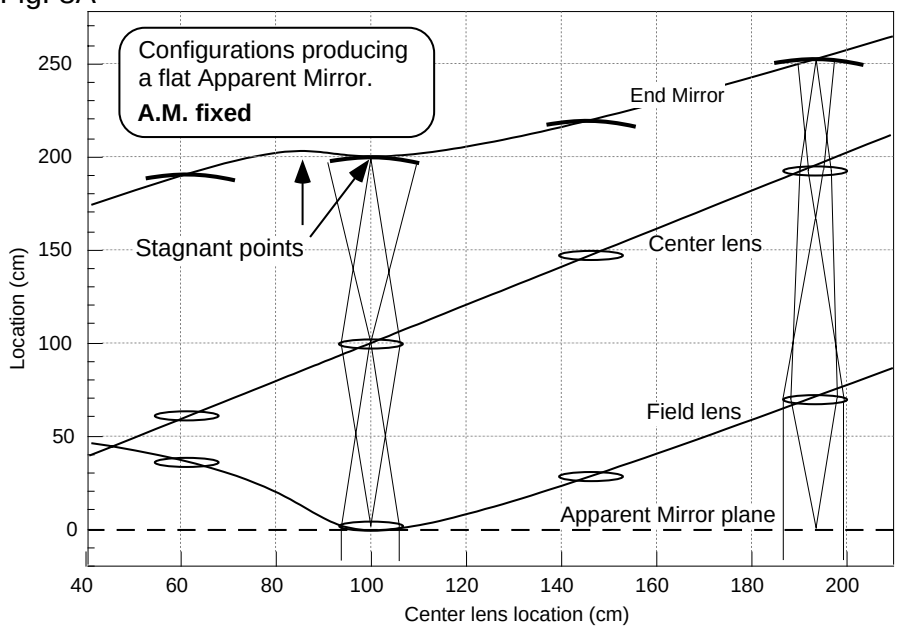

Fig. 8B

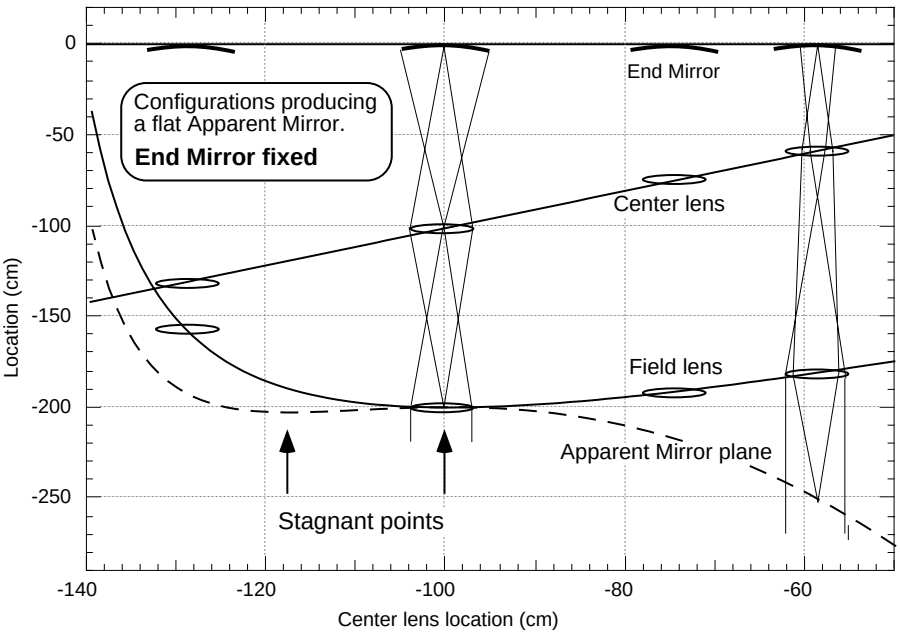

Figure 8A shows a manifold of configurations for a flat delaying mirror, when positions are measured from the apparent mirror. Figure 8B shows the same manifold of configurations as Fig. 8A, when positions are measured from the end mirror.

displacement. For example, in the symmetric case where field$_1$=field$_2$ focal length, there is zero such adjustability.

C. Applications for an adjustable delay superimposing interferometer

An interferometer with an adjustable delay time is useful in Fourier Transform (FT) spectroscopy, or as one interferometer in a pair of matched interferometers for white light velocimetry or communications. The FT spectroscopy application requires scanning the delay over a significant range. The matched-pair interferometer application requires adjusting the second interferometer to match the delay of the first, while preserving the superimposing overlap condition. Previous superimposing interferometers (spherical F-P or etalon delayed Michelson) did not have a practical method to adjust the delay

Fig. 9A

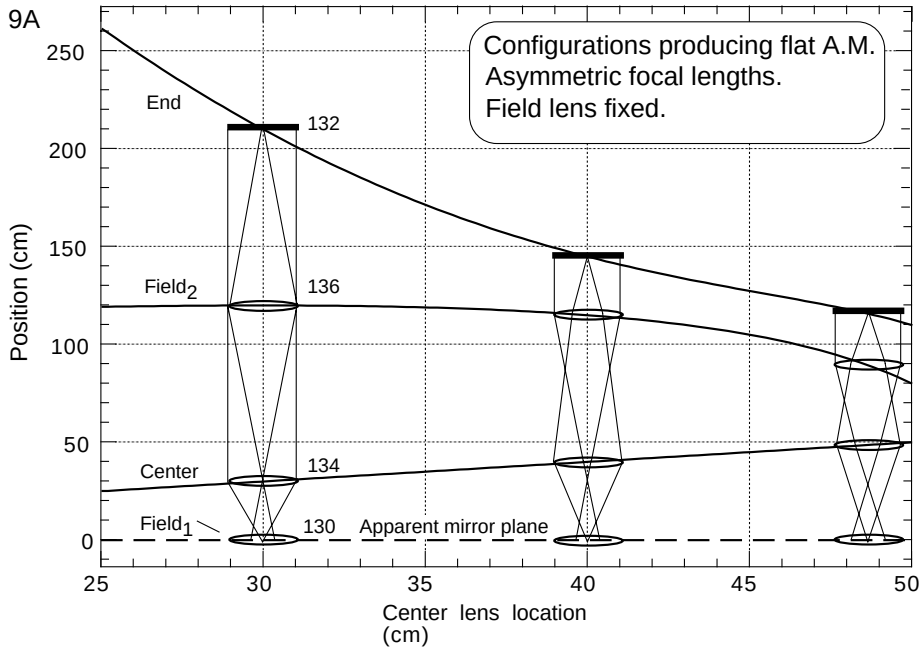

Fig. 9B

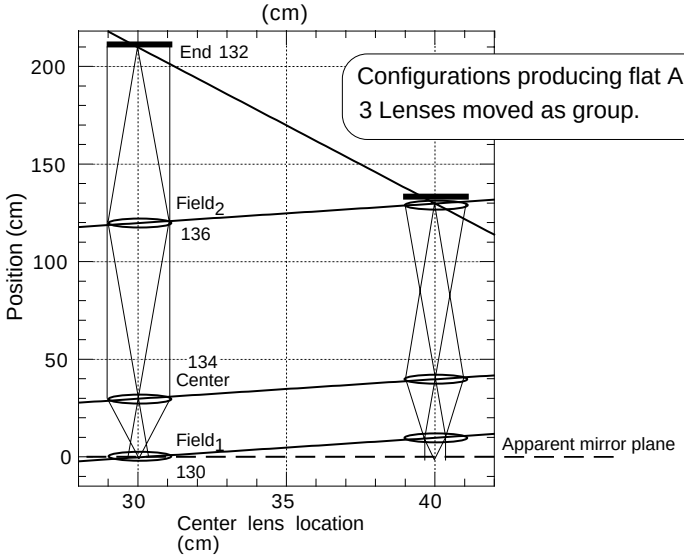

Figure 9A shows a manifold of configurations for a flat delaying mirror, for an asymmetrical group of lenses and when one field lens is stationary. Figure 9B shows a manifold of configurations for a flat delaying mirror, when 3 lenses are moved as a unit.

over a significant range. Consequently, the interferometer commonly used for FT spectroscopy is the conventional Michelson, and because this is non-superimposing it has a limited solid angle over which it can produce a uniform phase fringe. Now the superimposing interferometer using a relay delay can be used for FT spectroscopy. This increases the available solid angle at high spectral resolutions (which require long delays), so that wide angle sources such as aurora can be viewed).

It is advantageous to use a superimposing interferometer for FT spectroscopy of wide-angle sources because then fringe rings are not produced. Instead, a single infinitely wide fringe can be produced for use with a single channel detector to boost signal strength. Or, a uniform fringe comb can be produced for use with a multi-channel detector. The fringe comb is simpler to analyze than a fringe ring.

The delay is scanned by moving the elements of the relay delay in a coordinated fashion set by a schedule analogous to Figs. 8A, 9A and 9B, where the A.M. is held fixed. The elements, individually or in groups where appropriate, can be mounted on translation stages that are controlled electronically or mechanically to follow the schedule. Fringes from a reference wavelength, such as a HeNe laser, can be used to monitor the A.M. curvature and tilt during the scan and correct for deviations by mounting optics on piezoelectric tilt actuators and using a feedback control loop. The change in τ can also be monitored by counting passing fringes.

Fig. 10A

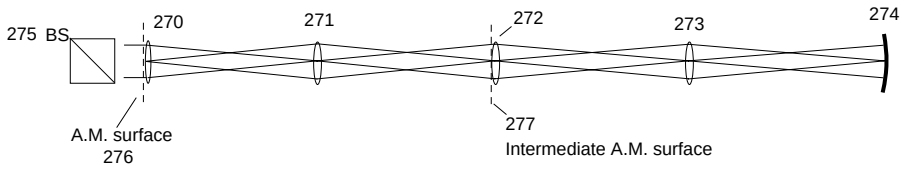

Fig. 10B

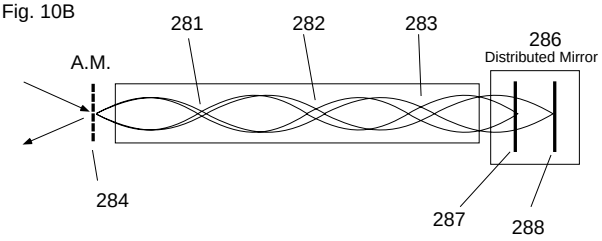

Fig. 10C

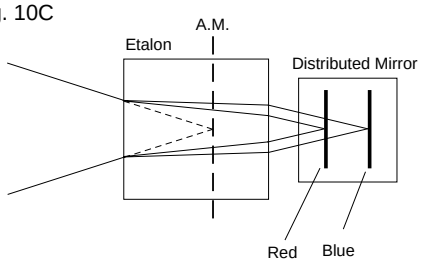

Figure 10A shows a delaying mirror comprising a relay lens delay with added stages to increase its length. Figure 10B shows a delaying mirror implemented by a waveguide and a distributed mirror which compensates for chromatic aberration in the waveguide. Figure 10C Red and blue rays passing through an achromatic etalon formed from the combination of an etalon and a distributed mirror.

D. Multi-stage relay delay and waveguide

Figure 10A shows a method of increasing the length of the relay delay system by adding more stages. That is, besides the A.M. 276, one or more additional intermediate images 277 of the end mirror 274 are created that are intermediate in position between the A.M. 276 and the end mirror 274. The A.M. 276 and intermediate A.M. surfaces 277 do not have to be near any lens, as shown, they could lie in between lenses. The details of the number of lenses, their spacings and focal lengths are not important as long as the last apparent mirror 276 produced has the same curvature as the short arm mirror and significant vignetting does not occur along the chain from 274 to 270.

The logical extrapolation of the multi-stage long relay chain of Fig. 10A is a waveguide (Fig. 10B), since this also forms intermediate A.M. surfaces 281, 282, 283 between the apparent mirror 284 and the distributed end mirror 286. A waveguide is a conduit having a refractive index that varies quadratically cylindrically from the center axis. This could also be formed from an infinite number of infinitely weak positive lenses. A ray traveling through this waveguide makes sinusoidal like paths that periodically come to foci (at 281, 282, 283). These waveguides are commercially available in short lengths. In principle, a very long waveguide could be constructed.

These waveguides require a distributed mirror to counteract the dispersion in the medium. For example, if a simple plane mirror was placed at the end of the waveguide, the apparent mirror would be at different positions for different wavelengths. This chromatic dispersion can be compensated for by using a distributed mirror 286 for the end mirror, where the effective position of the end mirror for red light 288 is different for blue 287 and exactly compensates the dispersion so that the apparent mirror 284 is at the same location for all wavelengths.

The distributed mirror could be constructed using volume holographic or interference filter technology. The distributed mirror would consist essentially of a stack of dielectric mirrors, each reflecting a narrow range of wavelengths and positioned at the appropriate depth to compensate for the dispersion of the waveguide, or other delay optics. Note that the method of using a distributed mirror could be used in any of the optical designs discussed in this document, not restricted to the waveguide kind, to correct for chromatic dispersion of the A.M.. For example, the distributed mirror could be combined with an etalon to make an achromatic etalon as shown in Fig. 10C.

E. Delaying mirrors using virtual imaging

Delaying mirrors can be made using virtual imaging instead of real imaging. Virtual imaging generally occurs when the spacing of optical elements is closer than their focal lengths. One kind of this delay can be called a "2-element" delay to distinguish it from 3-element designs.

An achromatic 2-element delay can be made from the combination of an achromatic lens and a curved mirror. Fig. 11A shows a 2-element delay comprising a positive lens 303 which is close to a convex mirror 302, and Fig. 11C comprising a negative lens 305 which is close to a concave mirror 306. In both kinds, the focal point 301 of the transmissive lens 303 or 305 is arranged to superimpose the center of curvature (CC) of the spherical end mirror 302 or 306. This images the CC to infinity, so that the apparent mirror formed is flat. Other A.M. curvatures can be obtained by appropriately adjusting the

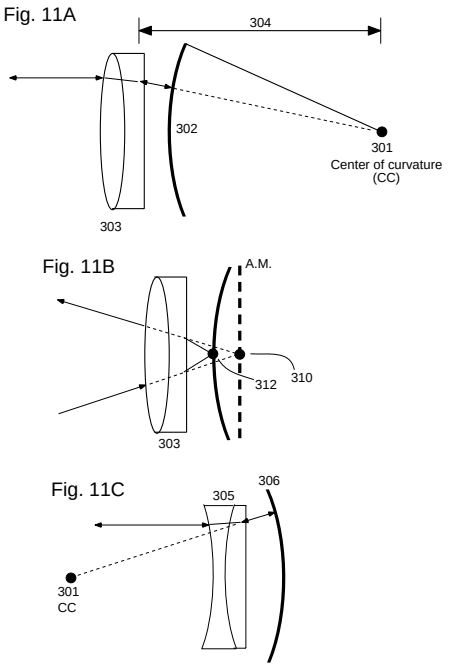

Figure 11A shows a 2-element delaying mirror using a positive lens, a convex mirror and virtual imaging. Figure 11B shows that the apparent mirror position for the delaying mirror of Fig. 11A is a virtual image of the end mirror. Figure 11C shows a 2-element delaying mirror using a negative lens, a concave mirror, and virtual imaging.

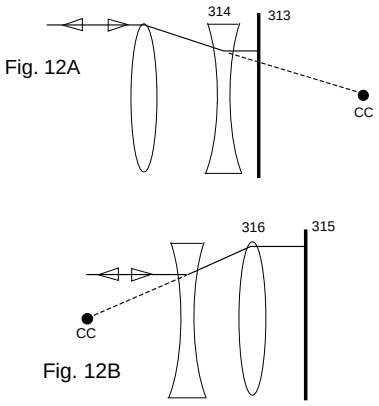

Figure 12A shows a 3-element delaying mirror using virtual imaging. Figure 12B shows another 3-element delaying mirror using virtual imaging.

spacings between elements. Figure 11B shows that the location 310 is found by virtually imaging the end mirror surface 312 by lens 303.

Figures 12A and 12B show 3-element delays described by Pierre Connes ("Deuxieme Journee D' Etudes Sur Les Interferences," Rev. Optique Theorique Instr., vol. 35, p37, 1956). These use a plane mirror and two lenses to create an apparent mirror. The combination of lens 314 and plane mirror 313 acts as a convex spherical mirror

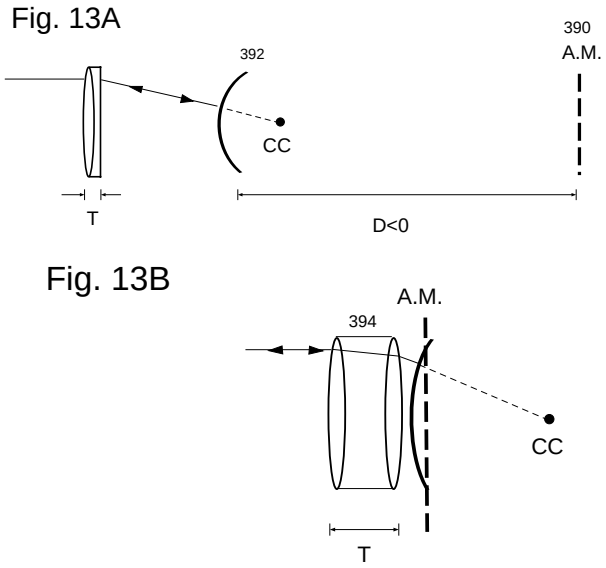

Figure 13A is an example of when the apparent mirror is far behind the end mirror. Figure 13B is an example of when the apparent mirror is very near the end mirror.

analogous to 302, and lens 316 and plane mirror 315 acts as a concave spherical mirror analogous to 306. The advantage of the 2-element configuration over the 3-element is the smaller amount of unwanted reflections at the lens surfaces, the smaller thickness of glass the light has to travel through, which reduces unwanted dispersion in the delay time, and simpler construction and alignment, since one less element is required.

Both positive and negative delay times can be created by the 2-element delay. The net delay time $\tau = 2D/c + 2T(n-1)/c$, which is a sum of a contribution due to the displacement D of the A.M. relative to the end mirror, and a contribution from an insertion delay due to the thickness of the glass lens. The former contribution can be positive or negative. The latter contribution is always positive. The former contribution can be positive when the A.M. is in front of the end mirror, as in Fig. 13C. The former contribution can be negative when the A.M. is behind the end mirror, as in Fig. 13A. Figure 13B shows that a thick lens 394 can produce a positive delay even though the A.M. is slightly beyond the end mirror.

These delays are optimally achromatic by using lenses and mirrors which are individually achromatic, such as standard multi-element achromatic lenses and first surface mirrors. Alternatively, non-achromatic elements having chromatic effects of opposite polarity can be combined so that the net chromatism is reduced. This is shown in Fig. 14 which shows the paths 323, 325 of red and blue rays, respectively, and how the chromatic dispersion of a simple lens 320 can be compensated for by the dispersion of an etalon 322 of a sufficient thickness. The simple lens will refract the blue more than the red toward the optic axis. The etalon will refract the blue so that it has a shallower angle within the etalon. The net

Fig. 13C

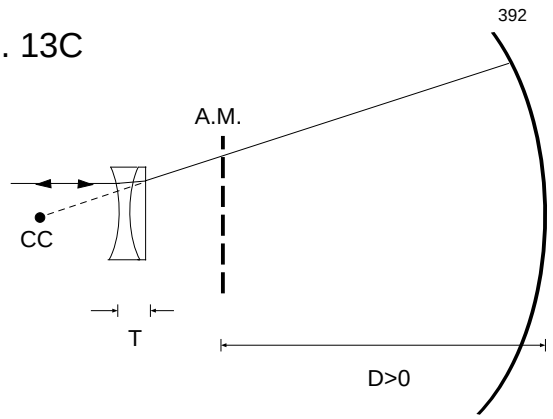

Figure 13C is an example of when the apparent mirror is in front of the end mirror.

Fig. 14

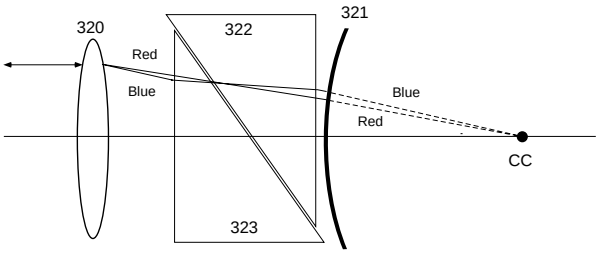

Figure 14 shows how the chromatic dispersion of a simple lens and an adjustable etalon in a delaying mirror can cancel.

Fig. 15A

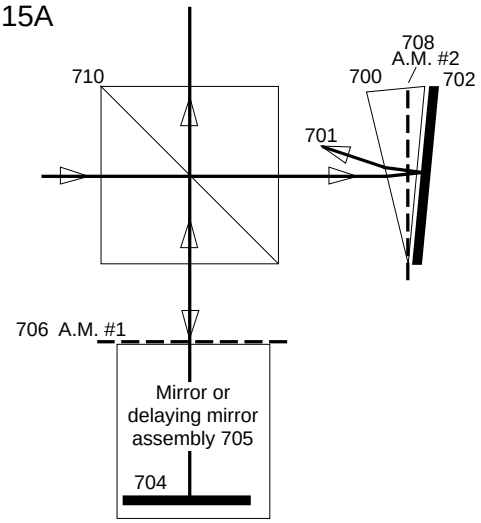

Fig. 15B

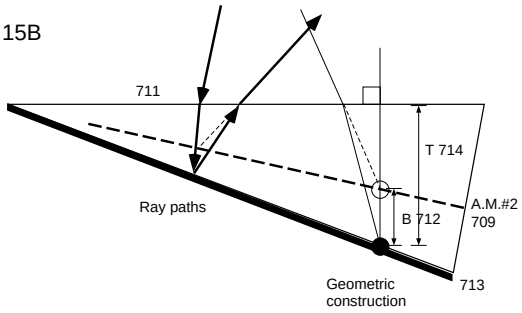

Figure 15A shows the use of a wedge to create a delay which varies transversely across the beam. Figure 15B is a detail of wedge showing ray path entering normal to apparent mirror, and a geometric construction locating apparent mirror surface.

effect is to have both the red and blue share the same focal point, which is arranged to coincide the CC of the end mirror 321. The etalon thickness can be adjusted by using a pair of wedges 322 and 323 having equal angles that slide against each other, or by using one or more etalons in the path and tilting them.

F. Wedge and inclined delay

In many applications it is useful to have a delay value which varies spatially across the apparent mirror, usually linearly, so that an interferometer may produce a fringe comb having parallel fringes. This allows correspondence between a spatial position in the output image and a specific delay value. This might be called an "inclined" delay. A large inclination would be useful for example in Fourier Transform (FT) spectroscopy for taking a snapshot fringe record spanning a large delay range. This allows measuring an accurate fringe record for a pulsating source. (Conventional FT spectrometers mechanically scan the delay, which takes time and therefore isn't suitable for pulsed sources.)

For small degrees of inclination, the incline can be achieved by tilting an interferometer end mirror so that the overlap between the A.M. or the end mirror of each arm varies across the beam. However, for large degrees of tilt this is unsatisfactory because the larger separations degrade the fringe visibility, so visible fringes would only occur in some section of the A.M. where the overlap separation passes through zero.

Figure 15A shows a method of maintaining the A.M. superposition in spite of a large mirror tilt. This is a method of achieving a large delay incline without degrading superposition quality.

A wedge prism 700 is inserted into the optical path. Since this deviates the output beam path of one arm relative to the others, perfect superposition of output paths (as in Fig. 1B) will not be achieved. However, superposition of images can be achieved (as in Fig. 1C and D) if the wedge is located near the input/output plane. The input/output plane is usually best located near the apparent mirror. Thus the wedge could be located near A.M. 706, or the end mirror 702, or near the end mirror 704 of the delaying mirror assembly 705, since this is im-

aged to the A.M.. The detector which records the fringes should be placed at an image of the input/output plane, so that paths from the different interferometer arms converge on the same pixels.

Note that in some applications it is desired to have an interferometer having an inclined delay that passes through zero delay or its vicinity. To achieve this, an ordinary mirror is substituted for the delaying mirror 705.

Figure 15A shows the wedge next to the short arm mirror 702. The angles in Fig. 15A may be exaggerated for clarity. Figure 15B shows a detail of the action of the wedge on rays. The left side of Fig. 15B shows the path of a ray (bold arrows) incident perpendicular to the A.M. #2 (709). The right side is a geometric construction for locating the second apparent mirror A.M. #2 (709), assuming the end mirror 713 is immediately adjacent to the wedge. This is done by pretending that the surface 711 is the first surface of a etalon and that the mirror 713 is embedded inside the etalon. For the same reason that the etalon 76 in Fig. 4A displaces the apparent position of the mirror 72 due to refraction, the refraction at surface 711 makes each point on the surface of mirror 713 appear closer to surface 711 by an amount B that is proportional to the wedge thickness as measured from surface 711. This creates an apparent mirror A.M. #2 (709) which is inclined to both surface 711 and to the mirror 713. The apparent displacement is $B = T(n-1)/n$ at 712, where n is the refractive index, and T at 714 is the thickness of the wedge normal from surface 711. In Fig. 15A, the end mirror 702 and wedge 700 combination is tilted so that A.M. #2 (708) superimposes the first apparent mirror 706 in reflection about the beamsplitting surface 710.

This creates an inclined delay time which varies linearly transversely along the apparent mirror, while satisfying the superimposing condition for monochromatic light. The inclination magnitude $\Delta c\tau$, which is the change in delay across the beam, is given by $\Delta c\tau = 2[T(n-1)/n + T(n-1)]$ is the sum of the component due to apparent mirror displacement, and the component due to the slower speed of light through the wedge thickness. This formula is accurate for small angles of incidence where $\sin\theta \approx \theta$.

Due to wedge glass dispersion, the A.M. overlap is perfect only for a single wavelength. However, the amount of chromatic mis-overlap is only approximately 2% of the delay, so it is much smaller than if the mirror were tilted alone to create the same amount of incline. Since a certain amount of mis-overlap can be tolerated, this method allows a 50 times greater tilt to be created for the same loss of fringe visibility.

An example follows: suppose we desire a round trip delay incline of 1000λ across the A.M. If the wedge refractive index is $n = 1.5$, then $\Delta c\tau = 1000\lambda \approx 2T(0.83)$. Thus we need a thickness T of $600\lambda \approx 300$ microns for green light where $\lambda = 500$ nm. Figure 16 shows that such a shallow wedge can be conveniently made by combination of two component wedges 410, 412 whose wedge angles may be slightly different, or whose refractive indices may be slightly different. The net wedge incline is the sum of component inclines, and can be adjusted by twisting the component wedges relative to each other about the common optic axis 414.

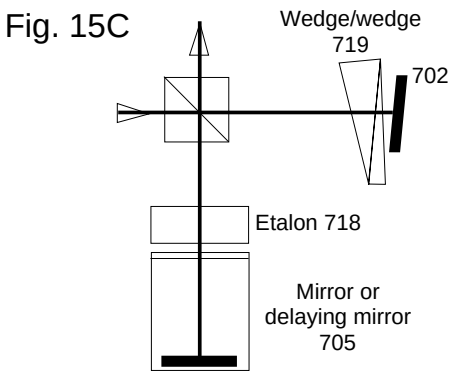

Figure 15C shows an achromatic inclined delay achieved by a wedge combination in one arm and a compensating etalon in another.

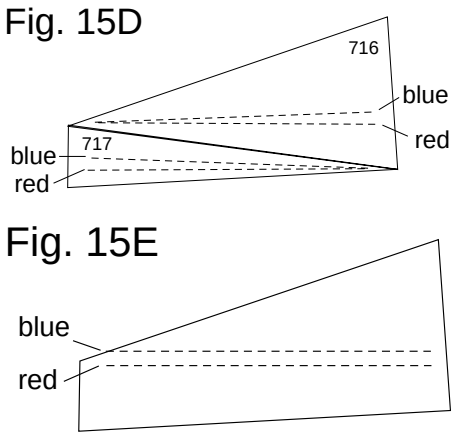

Figure 15D shows the apparent mirror surfaces for red and blue light when the elements of the wedge combination are considered separately. Figure 15E shows the parallelism between red and blue apparent mirrors when the combination of 15D is considered as a whole.

Birefringent wedges can be used to create an incline which has different values for different polarizations. This is useful in a polarization resolving retro-reflecting interferometer, discussed later in Fig. 31, to produce an inclined delay for the detected light, but a uniform delay for the illuminating light, even though the detected and illuminating light pass through the same interferometer apparatus.

G. Achromatic inclined delays

An achromatic inclined delay can be made use of two or more wedges in a combination 719 in one arm together, with an ordinary etalon 718 in the opposite arm

(Fig. 15C). The wedge elements are made of materials having differing dispersive powers, such as crown and flint glass, analogous to the method of making an achromatic lens. (Dispersive power is the ratio $(n_B - n_R)/(n_B + n_R)$, where n_B and n_R are the refractive indices for blue and red light. "Flint" glass has a greater dispersive power than "crown" glass.) The component wedges are oriented thin side to thick side, as shown in Figure 15D.

Figure 15D shows the wedge combination when the A.M. of each component wedge are considered individually, and Fig. 15E show the net effect when they are combined. For any dispersive material, because the refractive index for blue and red differ, the A.M. formed for red light differs from that formed for blue. The red and blue A.M. for each individual wedge 716, 717 are drawn as dashed lines. They make a slight angle to each other. The goal is to match the red/blue angle in wedge 716 to be opposite that in wedge 717. When this is achieved, then the net A.M. for red and blue for the combination of wedges are parallel to each other, as shown in Fig. 15E. The wedge with the more dispersive glass will be the thinner of the wedges.

Since both the red and blue A.M.s are inclined relative to the thickness variation of the net wedge combination, an inclined time delay is created. An etalon 718 is placed in the other arm with an appropriate thickness to cancel the parallel displacement between the blue and red A.M.s.

Specifically, let n_1B, n_1R, n_2B, n_2R be the refractive indices for blue and red light for two wedge materials #1 and #2, and T_1 and T_2 be the thickness of the wedges at their thick sides, and let the thin side of the wedge have zero thickness, then we require

$$T_1\left[\frac{n_{1B}-1}{n_{1B}} - \frac{n_{1R}-1}{n_{1R}}\right] = T_2\left[\frac{n_{2B}-1}{n_{2B}} - \frac{n_{2R}-1}{n_{2R}}\right] \tag{5}$$

in order to make parallel blue and red A.M.s. Then we select the etalon 718 on the other arm having a thickness T_3 and refractive indices n_3B, n_3R by requiring

$$T_3\left[\frac{n_{1B}-1}{n_{1B}} - \frac{n_{1R}-1}{n_{1R}}\right] = T_2\left[\frac{n_{2B}-1}{n_{2B}} - \frac{n_{2R}-1}{n_{2R}}\right] \tag{6}$$

If α is a parameter describing the fractional position across the wedge, then the net delay $c\tau$ varies linearly with α as

$$c\tau = \alpha 2T_1\left[\left(\frac{n_1-1}{n_1}\right) + (n_1-1)\right] + (1-\alpha)2T_2\left[\left(\frac{n_2-1}{n_2}\right) + (n_2-1)\right] - D_E \tag{7}$$

where D_E is the constant delay contributed by the etalon in the opposite arm and is

$$D_E = 2T_3\left[\left(\frac{n_3-1}{n_3}\right) + (n_3-1)\right] \tag{8}$$

and the indices n_1, n_2, n_3 are color dependent refractive indices for materials #1, #2 and #3.

Realistic wedges have non-zero thickness on the thin side. These can be used in the above equations by considering them to comprise a wedge with a zero thickness thin side, plus an etalon. These new etalons add an additional constant displacement between red and blue A.M., so the etalon 781 on the other side must be increased in thickness appropriately to cancel this out.

H. Achromatic Etalon Delays

A conventional etalon delay creates an A.M. that has different locations for red and blue light due to dispersion in the refractive index. This prevents application of thick etalons in broad bandwidth superimposing interferometers. A method of creating an achromatic etalon has already been discussed in Fig. 10C using a distributed mirror. An other method is by using two etalons 680, 682 placed in opposite arms (as shown in Fig. 15F) and having materials of different dispersive powers, such as "crown" and "flint" glass. In analogy with an achromatic wedge discussed above, the thickness of the etalons 680, 682 are chosen so that the red-blue A.M. displacement created by etalon 680 is canceled by the red-blue A.M. displacement by the other etalon 682. Thus if etalons 680 and 682 are identified by subscripts "3" and "2", then we require that the etalon thickness are related by

Fig. 15F

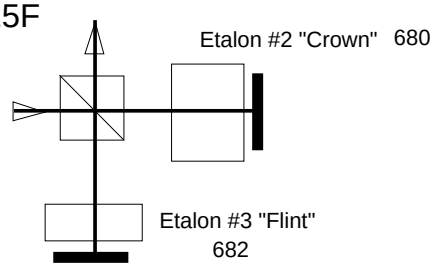

Figure 15F shows etalons having different dispersive powers placed in opposite arms to form an achromatic etalon delay.

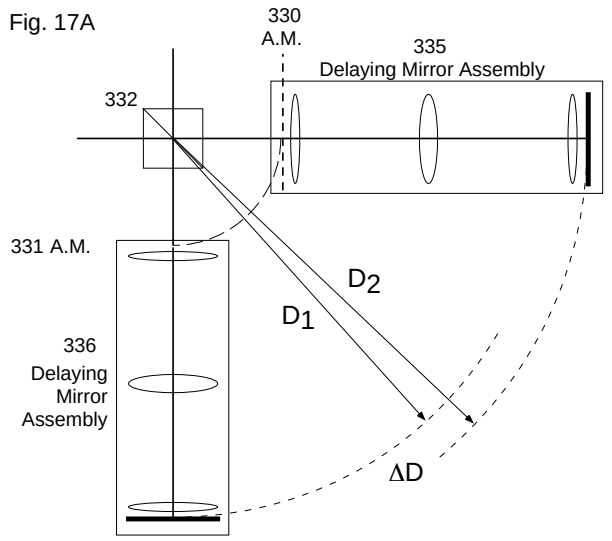

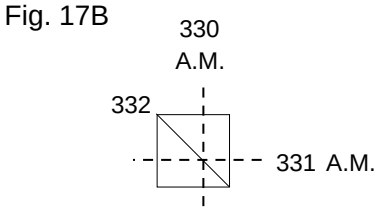

Figure 17A shows a differential superimposing interferometer using real imaging in the delaying mirrors. Figure 17B shows that the apparent mirrors of Fig. 17A can be located in the vicinity of the beamsplitter to reduce effect of beamsplitter surface irregularities.

the same formula Eq. 6, and the net delay created will be described by the formula for $c\tau$ stated in Eq. 7, but with $\alpha = 0$. The etalon of the less dispersive material would be thicker than the etalon of the more dispersive material.

A consequence of creating delays using chromatically dispersive media such as glass is that even though good overlap is achieved for all colors (so that fringe visibility is good), the value of delay τ may be a function of color. This is called dispersion in τ. Thus, the term "achromatic" in this document refers primarily to a wavelength independent A.M. overlap, and only secondarily to a wavelength independent value of τ. Dispersion in τ is not a serious problem, because if the fringe is visible, its phase can be adjusted during data analysis after it is recorded. Secondly, in pairs of matched interferometers, the dispersion in τ can often be matched, so that the fringe phase will not be affected.

Etalon delays are useful because the delay value is independent of transverse position of the etalon, which simplifies alignment compared to delaying mirrors that use lenses.

I. Differential interferometer

A method of creating a superimposing interferometer with a relatively small or zero delay, which can be adjustable, and which has a wide distortionless image field, is to have a delaying mirror in both arms. This is called the differential interferometer. Figure 17A shows a differential embodiment having delaying mirrors 335 and 336 which use real imaging. The apparent mirrors 330 and 331 are overlapped in partial reflection of the beamsplitter 332. The two arms may be only slightly different in length (D_1 and D_2) and the difference in length ΔDforms the net delay, $\tau = 2\Delta D/c$. A key advantage is that since D_1 and D_2 can be much longer than the difference ΔD, the wavefront curvatures inside the delaying mirrors 335, 336 can be very shallow (nearly flat) which reduces aberrations in the A.M. they produce. Secondly, these aberrations tend to be similar in shape and magnitude, and thereby improve the overlap between A.M. 330 and A.M. 331 compared to if one of these A.M. were being overlapped with a flat mirror.

This is an advantage, for example, when using an off-axis reflection in the delaying mirror (such as in Fig. 6B) which introduces astigmatism. Since the astigmatism in each arm will nearly match, then net aberration is reduced. Similarly, chromatic and spherical aberrations can be reduced. The result is that the differential configuration produces a wider diameter region at the A.M. having good overlap than a non-differential configuration, for the same delay time.

For example, suppose the goal is to generate a 1 cm (single-trip) net delay. If this is done by a single ∼1 cm long delaying mirror assembly in one arm overlapped with a flat mirror in the other, then the aberrations at the A.M. grow very rapidly with radius away from the optic axis. (This is because the center lens of a 1 cm real imaging delay would have a small focal length of only 1/4 cm.) The "good overlap region" may only be 1 or 2 millimeters radius. However, if a differential configuration is used with a 400 cm length relay compared against a 401 cm relay, then the wavefront curvature inside each delaying mirror assembly is long. This creates a very large good overlap region of many centimeters radius from the optic axis.

J. Increasing fringe visibility by A.M. placement

In the differential configuration, the apparent mirrors 330 and 331 can be located within the beamsplitter as shown in Fig. 17B. In the non-differential configuration this is not possible, because the A.M. must overlap the short arm mirror, which is necessarily outside the beamsplitter. Having the A.M. overlap the beamsplitter maximizes the fringe visibility in the presence of irregularities in the beamsplitter surface. The explanation is shown by Fig. 18A & B.

In a non-superimposing Michelson interferometer

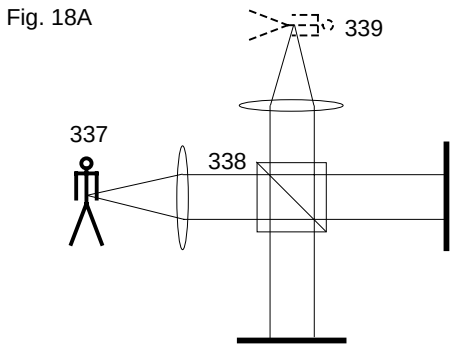

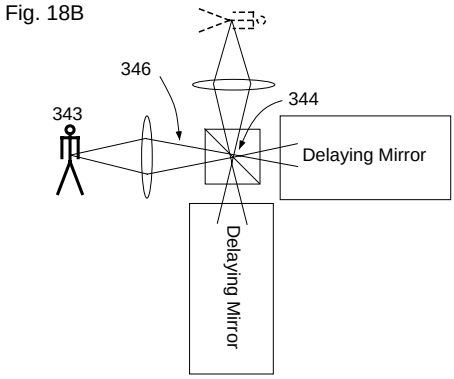

Figure 18A shows how parallel beams in a conventional interferometer are effected by surface irregularities from all of the beamsplitter area. Figure 18B shows that the beams in the superimposing interferometer from a given object pixel may sample only small portions of the beamsplitter.

(Fig. 18A), the beamlet 338 from an object pixel 337 fills the entire beamsplitting surface because the rays must be parallel to produce a coherent delay. This is also the case anytime the A.M. is far from the beamsplitter. The wide beamlet samples the full range of irregularities across the beamsplitting surface. This reduces fringe visibility.

In contrast, by placing the A.M. at the beamsplitter and by making the A.M. the input/output plane, then the beamlet of rays 346 leaving an object pixel 343 passes through a minimal area of the beamsplitting surface, so that over this small region the beamsplitting surface is uniform so the fringe visibility is high. Thus, any irregularities in the beamsplitter cause a irregularities in the *phase* of the fringe and not its *visibility*. This is better, because the phase irregularities are constant and can be corrected numerically at a later time.

K. Recirculating interferometer

The Michelson interferometer is a two-path interferometer which generates one echo in addition to the original pulse, for a given applied pulse. Another kind of interferometer, called the recirculating interferometer, generates an infinite progression of gradually decreasing echos all

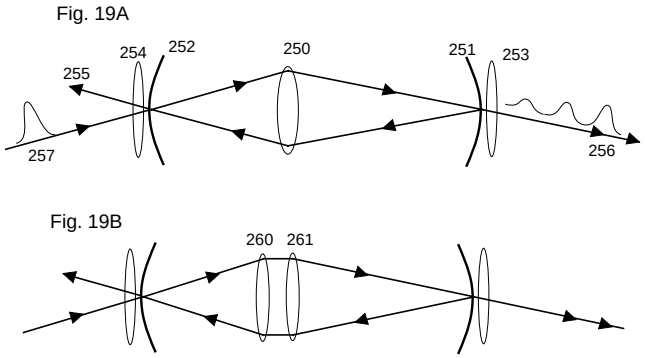

Figure 19A shows a simple superimposing recirculating interferometer. Figure 19B shows use of a center lens combination to increase adjustability.

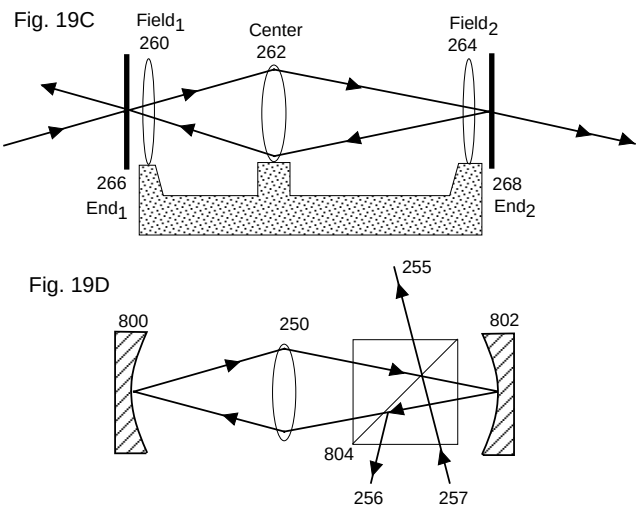

Figure 19C shows a recirculating interferometer with plane end mirrors and lenses substituted for curved mirrors. Figure 19D shows coupling light in and out of a recirculating interferometer using a beamsplitting surface not at the end mirrors.

separated by the same delay τ, which corresponds to the round trip time. A conventional Fabry-Perot is an example of a recirculating interferometer, however it is non-superimposing. The spherical Fabry-Perot of Fig. 3A is a superimposing, but its delay time is not adjustable because the mirror center of curvatures are fixed and must overlap. Secondly, the beam can't pass exactly down the optic axis 31 because it will hit the edge between the fully reflective and partially reflective regions 33, 32. This is unfortunate because the minimum aberrations of the curved mirrors are achieved for rays going down the optic axis.

New superimposing versions of a recirculating interferometer are shown in figures 19A, B C and D. Some of these versions allow adjustability for the mirror spacing, and hence delay, while maintaining the superimposing condition. In Fig. 19A, a positive achromatic lens 250,

called the center lens, lies in between two curved partially reflecting mirrors 251 and 252 and images the surface of mirror 252 to the other mirror 251, and produces positive unity magnification per round trip so that a ray returns to its same place on the mirror surface after one circuit. In contrast, the roundtrip magnification of the spherical Fabry-Perot in Fig.3A is not positive unity, but negative unity, since the ray does not return to the same place on an end mirror after one roundtrip between the two end mirrors. It requires two roundtrips to return to the same place.

The center lens 250 can be replaced by a combination of lens elements to increase the adjustability of configuration. In Fig. 19B, two lens elements 260 and 261 act as the center lens.

The curved mirrors 252 and 251 of Fig. 19A & B can be replaced by combinations of a flat mirror and lens, such as 266 & 260, 268 & 264 in Fig. 19C. In general for Fig. 19A, B & C, the center of curvatures (CC) of the two end mirrors must overlap after accounting for any imaging effect by the internal lenses. Thus, in Fig. 19C, left infinity must be imaged by the 3 lenses 260, 262, 264 to right infinity. It optimal to have the center lens 250 or lens combination 260 and 261 asymmetrically placed between the end mirrors 251 and 252 to create adjustability for imaging the surface of 251 to surface 252.

At least one partially reflecting surface must be provided so that light can be coupled into and out of the cavity. This can be accomplished by making the mirrors 252 and 251 partially transmitting/reflecting. These two mirrors do not have to have the same amount of reflectivity/transmissivity. Alternatively, an explicit beamsplitting surface such as the beamsplitting cube 804 in Fig. 19D can be placed anywhere in the recirculating path. This allows the end mirrors to be totally reflecting, which is very practical. For an input beam 257, two output beams 255 and 256 are created.

The recirculating interferometer has spectral properties that are analogous to the conventional Fabry-Perot used directly on axis. That is, whereas the Fabry-Perot has a circular central fringe which subtends a small cone angle about the optic axis, the superimposing interferometers can have an extremely wide central fringe that fills the entire field of view. This is a practical advantage.

The spectral character of a Fabry-Perot class of interferometer consists of a comb filter with peaks that can be very narrow compared to the spacing between peaks. Smaller loss of intensity per round trip produces narrower peaks (ie., smaller transmittance of the end mirrors or *larger* transmittance of the beamsplitting cube 804). Numerous textbooks describe the spectral behavior of Fabry-Perot class interferometers versus the reflectivity and loss in the cavity. For example, on pages 307-309 in the book by Eugene Hecht and Alfred Zajac, "Optics", Addison-Wesley, Reading, Massachusetts 1976, Library of Congress No. 79-184159. Thus the reflectivities of the elements in a recirculating interferometer are chosen by deciding how narrow of a spectral peak is desired (related to a quantity called the *finesse* in textbooks).

In Fig. 19A, the lenses 254 and 253 outside the recirculating cavity cause the wavefront curvature of light entering and leaving the cavity to match that of light inside the cavity. This allows a collimated incident beam at 257 to pass through the interferometer and be outputted at 256 as collimated. The focal point of lens 254 would be superimposed with the center of curvature of curved mirror 252, for example, to achieve this. Similarly for lens 253 and the CC of mirror 251. This is not necessary for when the end mirrors are flat, as in Fig. 19C.

A convenient method of designing the optics of a recirculating cavity is to consider a group of elements on one side of the cavity to form a delaying mirror which produces some apparent mirror surface, which may be curved or flat. Then the remaining optic or optics must superimpose with this A.M and face it so that the light recirculates. For example, the surface and center of curvature of mirror 252 must match the surface and CC of the A.M. computed for the combination lens 250 and mirror 251 in Fig. 19A. Secondly, the roundtrip magnification of an image must be positive unity, and not negative unity. Otherwise, there will be upside down images combined with the rightside up images in the output. When these conditions are met, superposition of paths is achieved.

Note that the combination of lenses are internal to the cavity in Fig. 19C should form a telescope that passes collimated light as collimated. By making the lens configuration asymmetric, the movement of the telescope allows the end mirror 266 to end mirror 268 spacing to be adjusted while maintaining the superimposing condition. Thus, the chart of Fig. 9B applies to the recirculating interferometer of Fig. 19C by placing a flat end mirror after the field lens 130.

L. Interferometers made without delaying mirrors

Superimposing interferometers can be made without delaying mirrors by explicitly routing the beams using one or more beamsplitters into the topological configuration desired, such as the 2-path topology shown as interferometer 3 of Fig. 5A. The advantage is that this can avoid having the beam come back on itself, so that all of the interferometer output beams are easily accessible. In contrast, for the Michelson configuration (Fig. 4A) where the incident beam 77 enters normal to the mirror 72, there are two complementary outputs at 73 and 75. However, the output 75 comes back in the same direction as the incident beam 77, making it difficult to access. (One solution is to angle the incident beam off-normal. This is more easily done with a superimposing interferometer than non-superimposing because of the lack of strong angle dependence to the delay.)

A large variety of configurations are possible. Figure 20A shows one embodiment for a 2-path interferometer. Beamsplitter 836 splits the incident beam into two paths, and beamsplitter 838 recombines them to form two com-

Fig. 20A

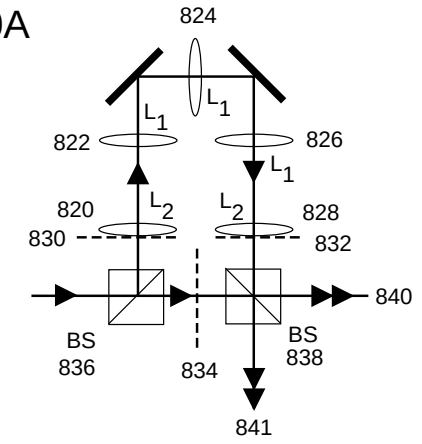

Fig. 20B

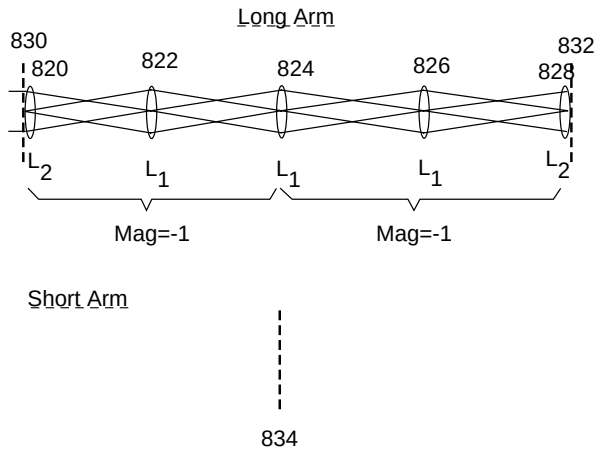

Figure 20A shows a superimposing 2-path interferometer made without a delaying mirror by explicitly routing the beams using relaying optics. Figure 20B shows the relay systems for the long and short arms of Fig. 20A laid out separately in a line.

Fig. 21A

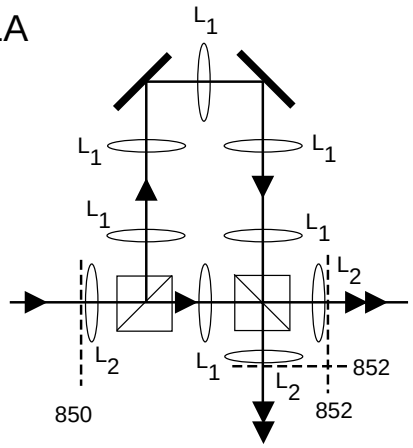

Fig. 21B

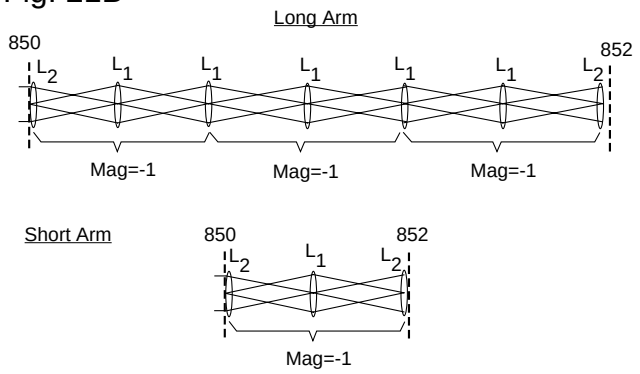

Figure 21A shows another superimposing 2-path interferometer having a different overall polarity of magnification than in Fig 20A. Figure 21B shows the relay systems for the long and short arms of Fig. 21A laid out separately in a line.

plimentary outputs (840, 841). The difference in path lengths yields the delay time. In order to superimpose output paths for a given input ray, a relay lens system is used generally in one or both arms. In the case of Fig. 20A, it is only used in the longer arm. Any relay lens systems that are used must superimpose the input planes for each arm, and superimpose the output planes for each arm, and match magnifications. Optimally, in order to superimpose paths it should further match wavefront curvatures. Otherwise, it will only superimpose images, which is useful but less desirable. In Fig. 20A, the input planes are 834 and 830, superimposed by the beamsplitter 836, and the output planes are 834 and 832, superimposed by beamsplitter 834. Note that 834 is both an input and output plane.

For each arm, the input plane (830 or 834) is imaged by optics to the output plane (832 or 834). This is most easily seen by "unwinding" the two optical paths and displaying them separately in a line, in Fig. 20B. Since the input and output planes are flat, we desire that a point at left infinity be imaged by the relay optics to infinity on the right. (This is a way of matching wavefront curvatures between the two arms.)

The focal lengths and positions of the lenses comprising the relay systems can be anything that satisfies the above conditions. The embodiment shown in Fig. 20A and B was chosen because it is simple to understand. The lenses 820 and 828 at the ends of the system have a focal length L_2 twice the focal length L_1 of the internal lenses 822, 824, 826. Each internal lens images the center of the lens to its left to the center of the lens to its right. Each end lens 820 and 828 focuses collimated light to/from the center of the lens neighboring it. This particular embodiment of the relay chain can be organized into two "stages", each which produces a magnification of negative unity. The total magnification of the system is therefore $(-1)(-1) = 1$ is positive unity. This matches the magnification of the short arm, which is obviously unity because there is no relay system in the short arm.

Figure 21A shows a similar 2-path superimposing interferometer, that differs from that in Fig. 20A by the inclusion of one more "stage" to the relay system of each

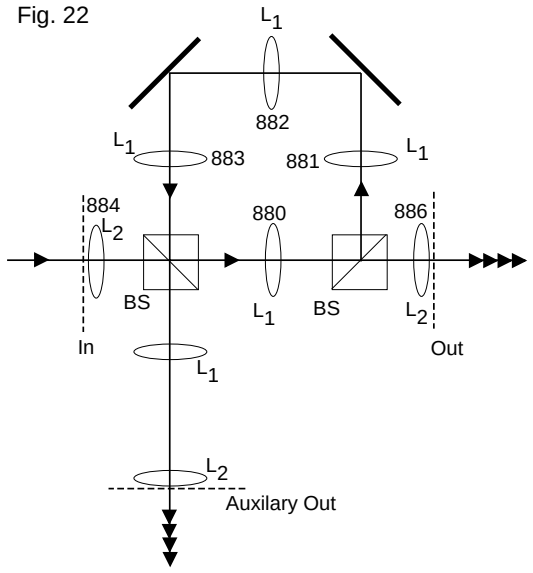

Figure 22 shows a superimposing recirculating interferometer made without a delaying mirror by explicitly routing the beams into a circulating path using relaying optics.

arm. That is, now the short arm has one stage and the long arm three stages. Thus the magnification between the input 850 and output 852 planes is negative unity for both paths. Figure 21B shows the relay systems of each arm of Fig. 21A when they are laid out in a line.

Figure 22 shows a recirculating superimposing interferometer made without a delaying mirror by explicitly routing the beams using relaying optics. Internal to cavity, the four lenses (880, 881, 882, 883) are chosen and positioned so that the magnification per round trip is exactly positive unity and the wavefront curvature is preserved per round trip. This is analogous to taking the relay system of Fig. 20B and making it into a circle by butting up the two end lenses 820 and 828 together. In this embodiment the four internal lenses have the same focal power L_1. The external lenses 884 and 886 help couple collimated external beams into/out of the cavity and have a focal length L_2 twice as long as L_1.

M. Zero delay applications of superimposing interferometers

Although we have been primarily discussing interferometers having non-zero delays, interferometers having zero or near zero delay are also useful for position or thickness measuring applications. A superimposing interferometer is useful in these applications, particularly when a mirror needs to be placed internal or at the surface of an object when this is physically impossible or difficult with a conventional interferometer. Figure 23A shows an application where a mirror surface would ideally be placed internal to an object, in this case a fluid cell 902 which contains a transparent sample 900 whose

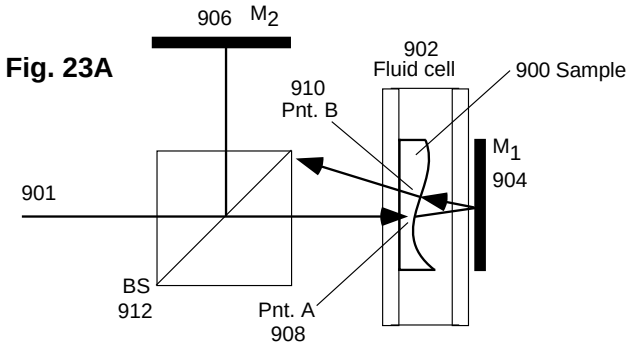

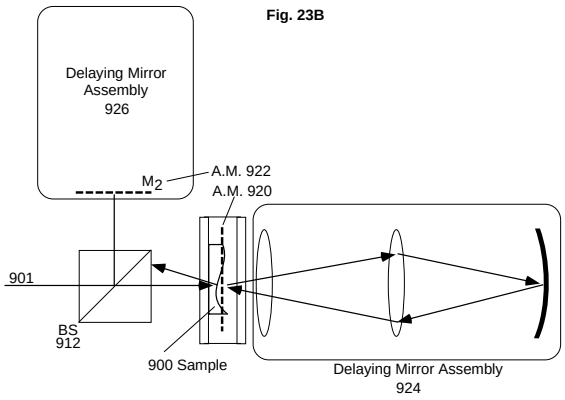

Figure 23A shows how rays do not pass through the same spot in a irregular sample if the mirror of a conventional zero-delay Michelson is not close to the sample surface. Figure 23B shows how a delaying mirror can be used in a zero-delay Michelson to make rays pass through the same spot on an irregular sample.

thickness profile is to be measured interferometrically via transmission through the whole cell. The illuminating light incident along ray 901 may be chosen to have a low coherence length so that the zeroth fringe can be unambiguously determined. In this case, it is necessary to match the lengths of the two arms, between the beamsplitter 912 and mirror 906, and between beamsplitter 912 and mirror 904. If the sample 900 has an irregular surface profile it will deflect the rays through refraction. If the mirror 904 is not close to the surface of the sample, then a ray passing through point A (908) will not pass through the same point A after reflecting from the mirror 904. This can blur the measurement, since the light essentially samples two different places on the sample, points A (908) and point B (910). Ideally, the mirror M_1 (904) should be as close to the sample's surface as possible, but this may not be practical because of the windows of the fluid cell.

A solution to this problem is to use a superimposing interferometer, such as shown in Fig. 23B. The use of at least one delaying mirrors allow the apparent mirror 920 of the delaying mirror assembly 924 to be placed internal to the fluid cell next to the irregular sample surface 900, because it is not a physically real surface. This way, the

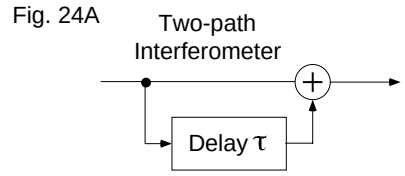

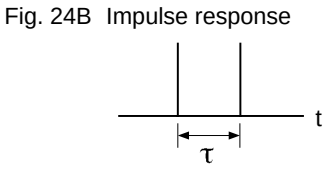

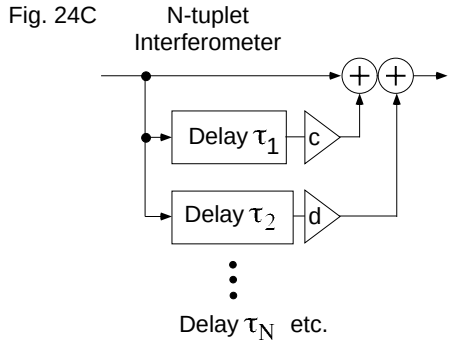

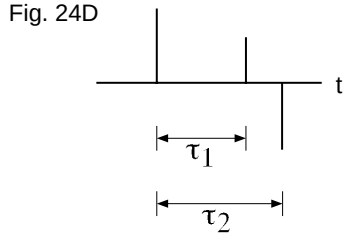

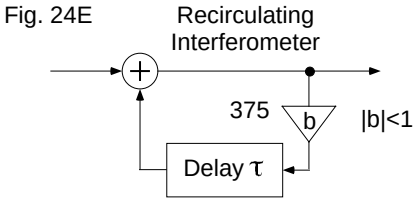

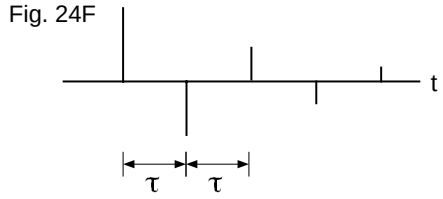

Figure 24A is an electrical equivalent of a generic two-path interferometer. Figure 24B is an impulse response for a two-path interferometer. Figure 24C is an electrical equivalent of a N-path interferometer.

Figure 24D is an example impulse response for a 3-path interferometer. Figure 24E is an electrical equivalent of a recirculating interferometer. Figure 24F is an example impulse response for a recirculating interferometer.

light reflecting from the A.M. 920 passes close to the same place on the sample surface that it passed incident toward the A.M. The A.M. should be in front of the elements that comprise the delaying mirror assembly. This can be done with a real imaging system by choosing the focal lengths and positions of the elements appropriately. For example, in the chart of Fig. 8A at a center lens position of 160 cm, the apparent mirror is in front of the field lens.

The zero or near-zero delay is achieved by using another delaying mirror 926 in the other arm having a matching delay, as in the differential interferometer configuration. If long coherence length illumination is used, then the second delaying mirror 926 is not required. Instead, an actual mirror could be placed at the position M_2 (922). In all cases, it is optimal to superimpose the two mirror surfaces 922 and 920 in partial reflection of the beamsplitter 912.

N. Electrical circuit equivalent

Figure 24A shows the "electrical circuit" representation of a two-path superimposing interferometer, meaning that only the temporal behavior is represented and not the ray paths. Figure 24B shows the impulse response of the optical field. Generally, the spectral behavior of an interferometer is obtained by Fourier transforming its impulse response. Since the superimposing interferometer can generate the same impulse response for all the incident rays, the spectral properties can be uniform for the whole beam. In contrast, the impulse response of a non-superimposing interferometer is the same as a superimposing kind only for the rays traveling exactly down the optic axis of the non-superimposing interferometer. That is, the superimposing interferometer has a fringe which could be infinitely wide and corresponds to the finite diameter center fringe (in a system of fringe rings) of a non-superimposing interferometer. The advantage of the superimposing interferometer is the ability to make the fringe infinitely wide if desired, or into a uniformly parallel comb of fringes, and not be limited to a system of fringe rings with a periodicity set by the delay value.

For Fig. 24A, a single applied pulse generates two output pulses separated by a delay τ. Figure 24C illustrates an interferometer with more than 2 paths, which could be called a N-tuplet interferometer with N representing the number of paths. For each path beyond the first, a delay is added in parallel to the circuit. The impulse response for Fig. 24C has one spike for each of N paths. Figure 24D shows the case when N is three. In some applications the output spikes could be separated by different

delay intervals.

A Michelson interferometer usually has just two arms and so is described by Fig. 24A. If an additional beamsplitter is now added to one of the arms (such as Fig. 26A), splitting it, then we essentially have 3 arms. This can be a 3-path interferometer described by Fig. 24C. Additional beamsplitters can be further added to any of these arms, creating more arms, and so on. The apparent mirrors or end mirrors associated with each arm could be made to superimpose. This is one method of creating an N-path superimposing interferometer with an arbitrary N. Another method is to use beamsplitters to explicitly route the beams along an N-path topology given by Fig. 24C. Relay lens systems can be used to superimpose the input/output planes of each path, as in Fig. 19A, so that the interferometer is superimposing. Any arbitrary number of paths N can be made. Combinations of the two methods are possible.

Figure 24E shows the electrical equivalent to a recirculating interferometer. The factor b is a gain of an amplifier 375 which represents the loss per round trip incurred at the partial reflection of the mirrors or beamsplitters. The factor b has a magnitude less than unity, to represent loss. The impulse response (Fig. 24F) is an infinite geometric series of decreasing amplitude spikes, having an interval given by a round trip time τ.

O. Two-delay interferometer

A superimposing interferometer can be created having more than 2 arms by inserting additional beamsplitters into a Michelson, by using actual mirrors or delaying mirrors in each arm, and by superimposing all the apparent mirrors and end mirrors using the beamsplitters. Figure 26A shows an embodiment which has a secondary beamsplitter in one arm, which splits the arm into two subparts, each which has a delaying mirror (432, 434). Figure 25 is a legend of some symbols used. The apparent mirrors 433, 435 of each delaying mirror assembly superimpose the short arm end mirror 436 in partial reflection of the main beamsplitter 438. This creates a superimposing interferometer having two delay values, τ_1 and τ_2, which can be different.

The fringe pattern produced from a two delay interferometer is a combination of the separate fringe patterns from single delay interferometers having delay τ_1, τ_2 and $|\tau_1 - \tau_2|$. This can be useful in velocity interferometry to reduce the ambiguity of a velocity determination, even when using one color. In other words, the velocity per fringe proportionality $(\lambda/2\tau)$ is set by both the color and the interferometer delay. Having simultaneous measurements using different proportionalities can reduce the ambiguity of the velocity determination, and this can be achieved either by using simultaneously different colors or delays. It is possible, particularly when an inclined delay and short coherence light is used in an interferometer pair, to arrange for the place where fringes are visible for one delay to be where fringes are washed out for the other delays, so there is no confusion between overlapping fringe patterns.

Figure 26B is the configuration of Fig. 26A where the secondary beamsplitter 430 has been replaced by a polarizing beamsplitter 440. When the input beam has intensity in both horizontal and vertical polarizations, such as if it is polarized at 45°, then two echos 442 and 444 are outputted having orthogonal polarizations. The undelayed output pulse 446 has its original polarization. This is a method of distinguishing the two different delays of a two-delay interferometer so that the associated fringe patterns don't confuse each other. The fringe patterns share the same output path but are distinguishable by polarizers placed before the detectors. This could be useful in a Fourier Transform spectroscopic application, by measuring two delays at once to help distinguish output fluctuations due to common mode intensity fluctuations from the desired fluctuations due to spectral character. The end mirrors 441, 443 can be tilted independently to produce a fringe comb with a different spacing for different polarization.

Figure 26C shows another method of producing a polarization dependent delay value, where τ_1, τ_2 differ only slightly. The secondary polarizing beamsplitter 450 is placed in the arm without the delaying mirror. This splits the short arm into two paths ending in two end mirrors 452, 454. These are nearly superimposed with the apparent mirror 456 of the delaying mirror assembly. Only small differences in the overlap between mirrors 452 and 454 can be tolerated, so only small differences between τ_1 and τ_2 are possible. Larger differences or inclinations can be achieved using etalons or wedges near the end mirrors 452, 454.

P. Delaying a beam using a delaying mirror

Delaying mirrors have been discussed integral with their use in interferometers. However, they can be discussed as an independent element used to delay a beam. Other users may then use this element inside interferometers of their own design. For example, in stellar interferometers, the path lengths of the beams from satellite telescopes to a central station must be equalized coherently, before they can interfere. This is presently done without a delaying mirror by the design shown in Fig. 27A. These delays require parallel light to produce a coherent delay between input and output planes 500 and 501. Light from a telescope viewing an extended source may not be sufficiently parallel for the delay to be coherent. Delaying mirrors are useful because they can coherently delay any beam including an uncollimated beam, and this delay value may be adjustable.

An important practical concern is how to separate the input beam from the output beam reflected off the delaying mirror. Figures 26B, C and D show different methods. In general, the input and output planes are opti-

Fig. 25

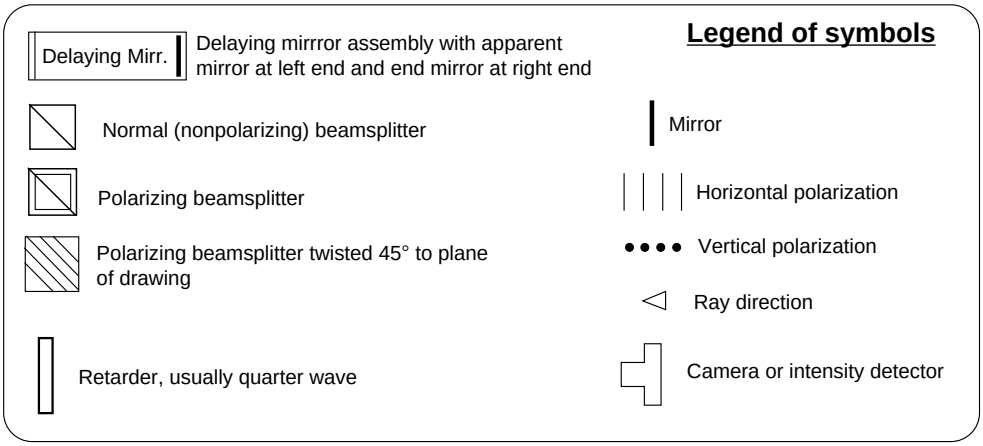

Fig. 26A

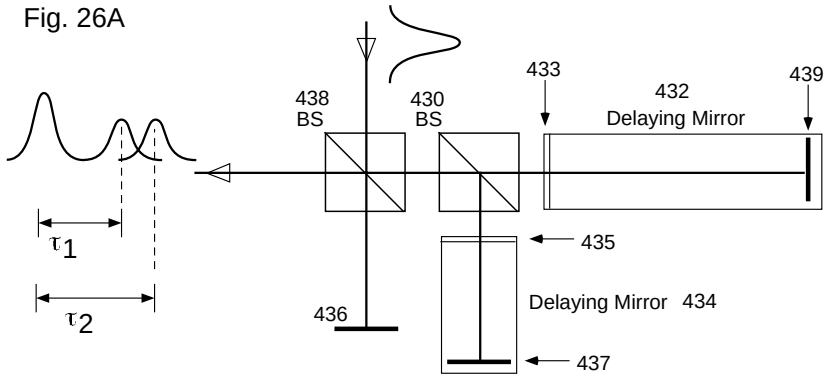

Figure 25 is legend of symbols. Figure 26A shows a superimposing interferometer that imprints two echos having a different delay times.

mally placed at the A.M. of the delaying mirror. Figure 27B shows the input 514 and output beams 515 distinguished by angle of incidence into the apparent mirror 516 at the beginning of the delaying mirror 513. The maximum practical angle of separation is determined by the details of the optics internal to the delaying mirror 513, such as the numerical aperture of the center lens, if real imaging is used. Figure 27C uses non-polarizing beamsplitter 503 to separate a portion of the output beam 510 from the input path 504. The arrangement of Fig. 27D avoids the backwards output 504 by using a polarizing beamsplitter 506 (PBS) and a quarter wave retarder 507 with its axis rotated 45° to the vertical axis defined by the PBS. The light makes two passes through the retarder. This rotates the polarization by 90°, so that the path of the outgoing light is separated from incoming path by the PBS. The retarder 507 can be replaced by any optical element that rotates by 90° the polarization of light making a double pass, such as a prism assembly.

For delaying mirrors using real imaging, the delay time can be changed while holding the apparent mirror it creates fixed by moving the optics internal to the delaying mirror in a coordinated fashion analogous to the charts in Fig. 8 and 9. By keeping the apparent mirror fixed, the alignment of the external system using the delay is not disturbed while the delay value changes.

Q. Superimposing interferometer in series with spectrometer

It is useful to combine a superimposing interferometer in series with a chromatically dispersive spectrometer (such as prism or grating). This can enhance fringe visibility in spectroscopic and velocimetry applications because it prevents crosstalk between fringes of different wavelengths having different phases. The interferometer 726 can precede (Fig. 28A) or follow (Fig. 28C) the spectrometer 727. The advantage of using a superimposing interferometer instead of a non-superimposing interferometer, when combined with the spectrometer, is the ability to imprint a constant delay or a uniformly inclined delay with adjustable inclination across the spectrum.

Figure 28A shows the interferometer 726 preceding the spectrometer 727. Since the spectrometer has a slit-like entrance pupil 723, the light passing through the interferometer should be line-like in cross-section. If the source is an optical fiber 720, the light is formed into a line 721 by cylindrical optics 722, or by use of a fiber bundle

Fig. 26B

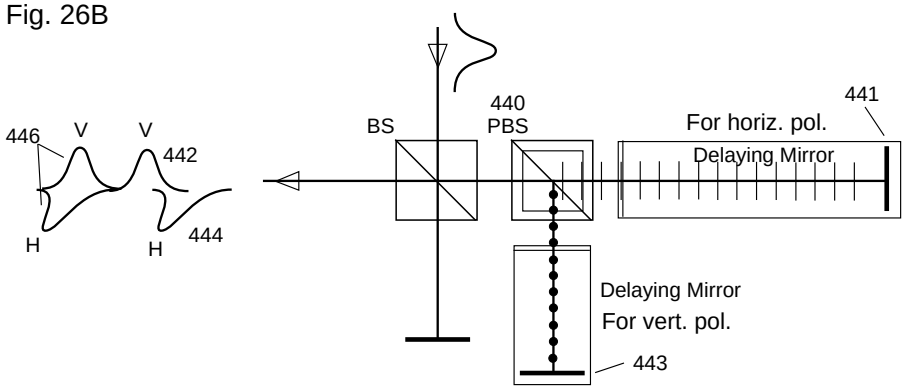

Fig. 26C

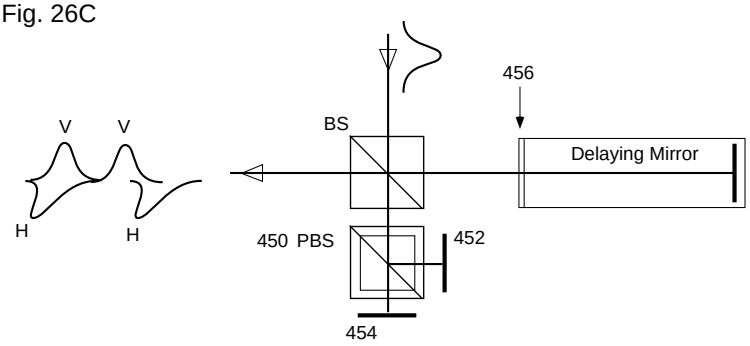

Figure 26B shows use of polarizing beamsplitter to make a polarization dependent delay. Figure 26C shows a configuration producing polarization dependent delays that are only slightly different.

Fig. 27A

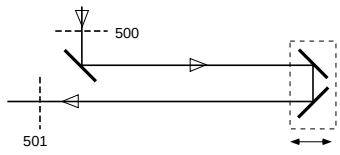

Fig. 27B

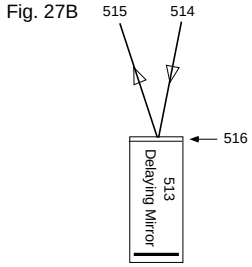

Fig. 27C

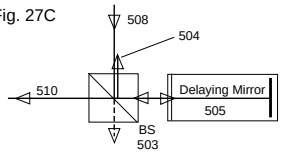

Fig. 27D

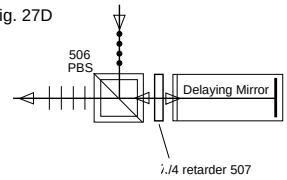

Figure 27A shows a conventional adjustable length delay line. Figure 27B shows an adjustable length delay using reflection from the apparent mirror of a delaying mirror. Figure 27C shows an adjustable delay line implemented by a delaying mirror and a normal beamsplitter. Figure 27D shows a delay line with a polarizing beamsplitter and quarter wave retarder to avoid backward going beam.

where individual fibers are rearranged into a line. This line-like beam 721 is sent into the input plane 724 of the interferometer, leaves the interferometer at the output plane 728 and enters the spectrometer system slit 721 as a line-like beam having fringes. The spectrometer is represented by the prism symbol 732. The actual details internal to the interferometer and spectrometer are omitted. The spectrometer disperses the incident light perpendicular to the direction of the slit to form a rectangular spectrum 726. This spectrum could have fringes, as suggested by Fig. 28B.

The interferometer can imprint either a constant delay or a delay that varies rapidly across the slit-like length, so that periodicity of the fringes can be arbitrarily adjusted, and could be infinitely wide. In spectroscopy of sources that have a non-smooth spectrum, such as the absorption lines in sunlight or starlight, the fringes may vary in phase and amplitude from wavelength channel to channel. In velocimeter applications, where light from the detecting interferometer is dispersed by a spectrometer, then the fringes could form a systematically varying pattern versus wavelength and delay (position along the slit).

Figure 28C shows the spectrometer 725 preceding the interferometer 729. In this case the spectrometer presents a rectangular spectrum as an input 731 to the interferometer. The interferometer passes this spectrum to its output image plane 733 while imprinting a fringe pattern on the spectrum. The orientation of the fringes could be in any direction relative to the wavelength axis, depending on which direction the inclined delay is made.

Fig. 28A

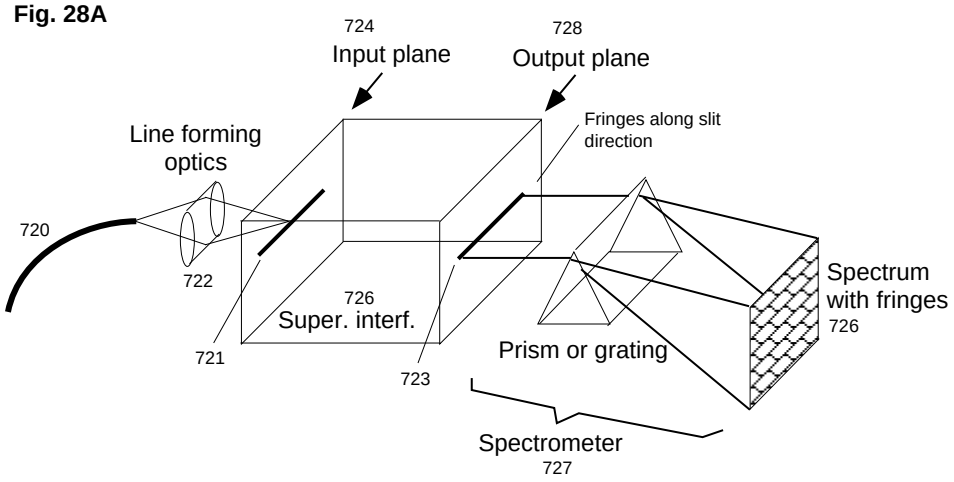

Fig. 28C

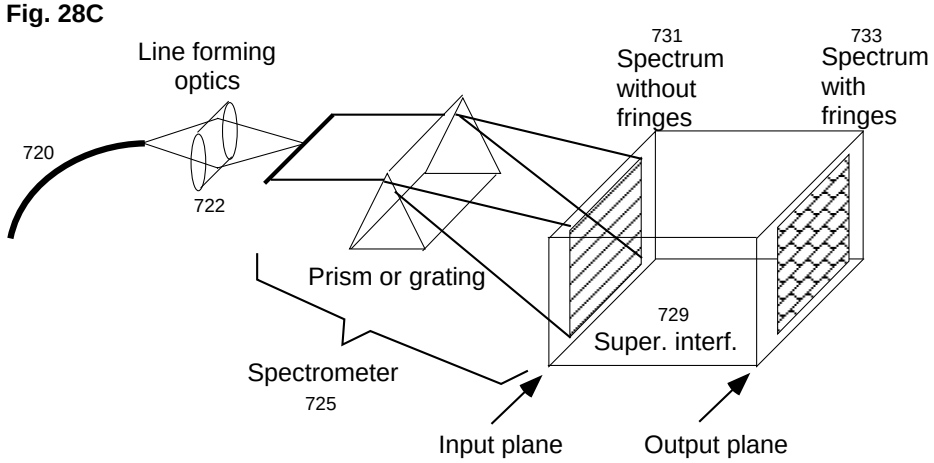

Figure 28A shows a spectrometer following a superimposing interferometer chromatically dispersing the fringes. Figure 28C shows a superimposing interferometer following a spectrometer imprinting fringes in any direction relative to the wavelength axis.

Fig. 28B

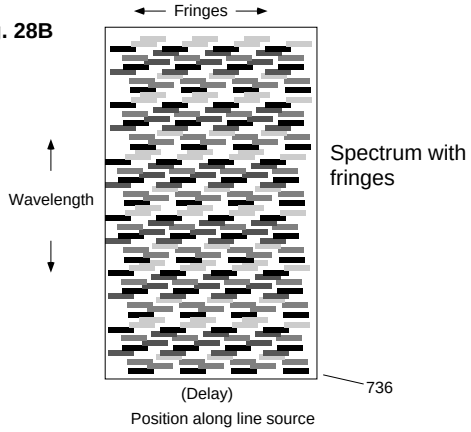

Figure 28B is suggested appearance of a spectrum having fringes perpendicular to the wavelength axis.

R. Double superimposing interferometer

A system of two superimposing interferometers in series having matched delays and dispersion characteristics is useful for Doppler velocity measurement and optical communications. Figure 5A is a topological schematic of a double interferometer for a velocimeter application consisting of an illuminating interferometer 3 having delay τ_1 and detecting interferometer 7 having delay τ_2, with a target 5 interposed between the interferometers. When the delays match $\tau_1 \approx \tau_2$ within the coherence length of the source 1, partial fringes are produced in the detecting interferometer outputs 8, 9. The target displacement during the interval τ_1, which is an average velocity, is proportional to the fringe phase shift by multiplying by $\lambda/2\tau$, for the typical case when the target-reflected light and illuminating light are anti-parallel. A change in refractive index along the optical path between the apparatus and the target will also produce a fringe shift analogous to target motion.

1. Optical communication with a double superimposing interferometer

When the target 5 is replaced by any arbitrary optical path which could be an optical fiber, an open beam, or a beam reflected off obstacles, communication can be achieved between the illuminating and detecting sides. The fringe phase in outputs 8, 9 can be modulated by varying τ_1 slightly about its nominal value $\tau_1 \approx \tau_2$. Thus a message can be communicated, if the illuminating 3 and detecting 7 interferometers are matched in delay within a coherence length of the illumination, and matched in dispersion. (Delay dispersion is the variation of τ with wavelength.) If delay and dispersion are not matched, then significantly visible fringes are not produced. This has been discussed in the prior art using non-superimposing interferometers and called "coherence multiplexing".

Figure 5B shows an embodiment for optical communication. The use of superimposing interferometers gives the apparatus the useful ability to use any commonly available light source 930, such as a candle, an incandescent lamp or sunlight, and the ability to use a wide diameter optical fiber 944 or any imaging or non-imaging path, which can include reflection off buildings or other obstacles. The delay and dispersion of the illuminating 932 and detecting interferometer 934 are arranged to be matched. Optimally, when a non-imaging path 944 is used, there should be no inclination in the illuminating interferometer delay, so that all transmitted rays have the same imprinted delay. This way they can scramble together without blurring the imprinted delay.

The signal is sent by modulating the delay of the illuminating interferometer by a slight amount such as $\lambda/2$ so that a fringe shift is seen in the detected light of the detecting interferometer. Analog or digital signals could be sent depending on whether the fringe is smaller than or similar to $\lambda/2$; analog modulation would be easier with small phase changes. The delay could be modulated by a piezoelectric transducer 938. Alternatively, a mechanical means could be provided so that the pressure of a finger of the operator moves the mirror by a small amount comparable to $\lambda/4$.

By using sunlight, this is a means of communicating in the outdoors in an encrypted form using little or no electrical power, which could be useful for military or surreptitious applications. Only the intended recipient of the message will see fringes in the transmitted beam 946. Other viewers lacking the interferometer or lacking knowledge of the proper delay and dispersion will not detect a significantly visible fringe. Since the phase of the optical field is not possible to be recorded by conventional detectors (which only measure intensity) without the proper interferometer, it is not possible to record the coherence properties of the signal and then later analyze it for an encoded message. The signal must be detected in real time using an interferometer of the matching delay and dispersion.

Analogous to channels on a radio, if the receiving party does not use an interferometer with the matching delay and dispersive qualities, no fringes are seen and the light from the transmitter 932 appears innocuous. A variety of superimposing designs could be used for the interferometers 932 and 934. Figure 5B shows use of achromatic etalons, as discussed in Fig. 15F, along with adjustable thickness etalons 940 and 942 to help match dispersion. Because the method of detecting the communication involves the coherence properties of the light, and not the intensity, it is possible to detect the communication even in the presence of extraneous light such as daylight. This could make the technique useful for surreptitious communication by shining the encoded beam on the side of a building where it would be hidden by virtue of combining inconspicuously with other natural light. The interferometers could be fashioned into a small portable case similar in size to an ordinary pair of binoculars. The interferometer pair would be matched initially before being separated and used "in the field". Since there is a large number of possible delays and dispersive qualities available to choose from, it would be unlikely that an unintended recipient could search for the delay and dispersion values during the short time that a message would be sent, thus providing the security.

2. Matching delay and dispersion in a double superimposing interferometer

The advantage of using superimposing interferometers for a double interferometer systems is that this allows the source 1 to be broadband and extended, such as an incandescent or flash lamp. It allows the use of wide diameter optical fibers, other non-imaging conduits, or poorly imaging (out of focus or blurry) systems to conduct light between the target 5 to/from the detecting/illuminating interferometers. This can be a great practical advantage because the sources can then be inexpensive, lightweight, rugged, compact and consume much less electrical power than many lasers. Secondly, it allows a large depth of field (range of target motion) because strictly parallel light does not have to be maintained through the detecting interferometer.

Since the coherence length of white light is about 1.5 micron (a micron is $1/1000^{th}$ of a millimeter), it can be tedious to achieve the matching condition $\tau_1 \approx \tau_2$ and the dispersion matching condition while simultaneously optimizing the superimposing overlap in both interferometers.

Figure 29A shows a double superimposing interferometer embodiment which can achieve this matching, using two superimposing interferometers of the type shown in Fig. 6B. The embodiment includes a target 228. Other targets more remote from the apparatus could be measured by relaying their image through a telescope to the plane 228. The apparatus of Fig. 29A can be used for other double interferometer applications such as communication by introducing a means for modulating the illu-

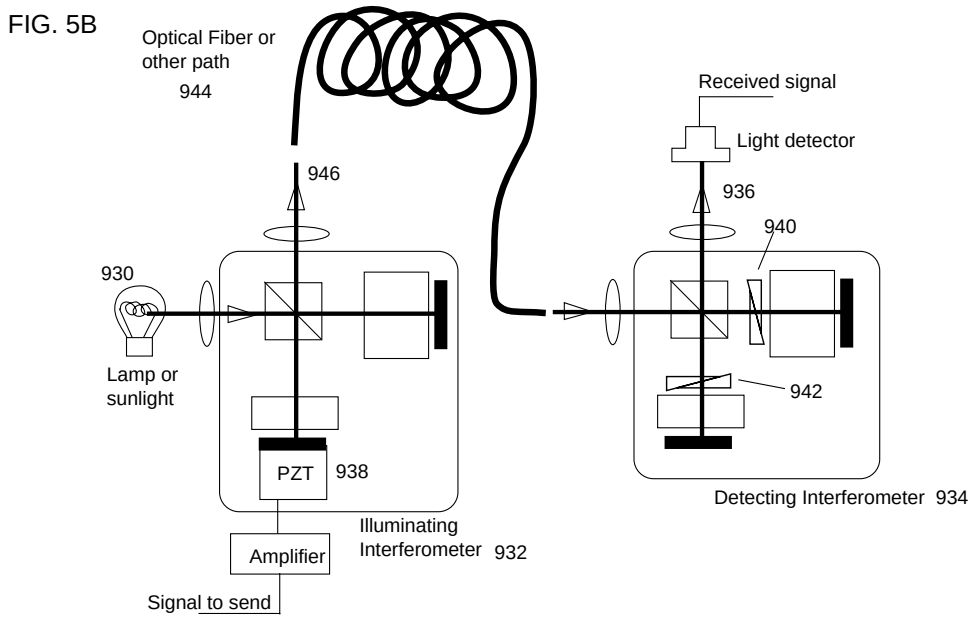

Figure 5B is a double superimposing interferometer system capable of communication.

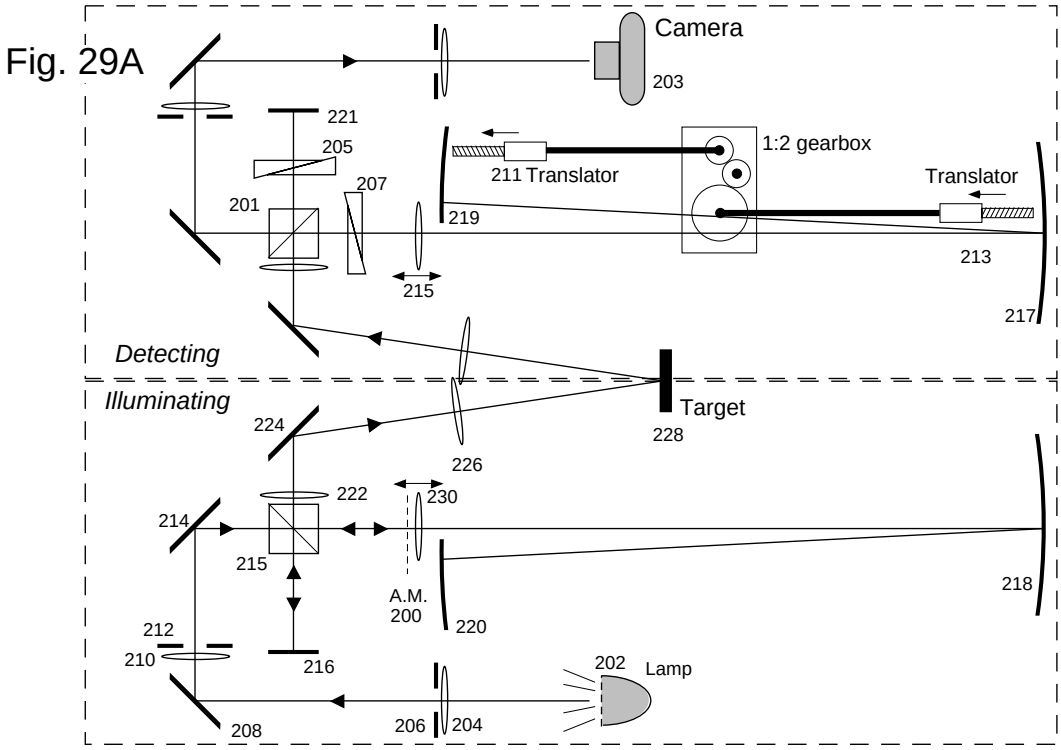

Figure 29A shows a double superimposing interferometer with means for matching delay, dispersion while optimizing apparent mirror overlap.

minating interferometer delay and substituting an optical conduit such as a fiber for the target 5.

The apparatus of Fig. 29A consists of two nearly identical halves; each is a superimposing interferometer system enclosed in dashed boxes and labeled "illuminating" and "detecting." The optics in the two halves are not required to be identical, but this makes it easier to match dispersive characteristics. Some parts that are not identical between the two halves include the lamp 202, which is replaced by a camera 203, and the adjustable thickness

Fig. 29B

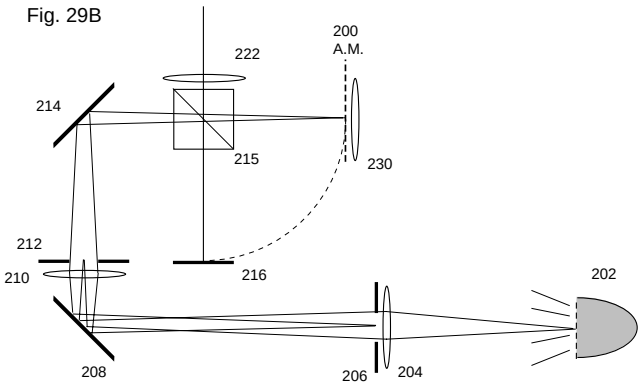

Fig. 29C

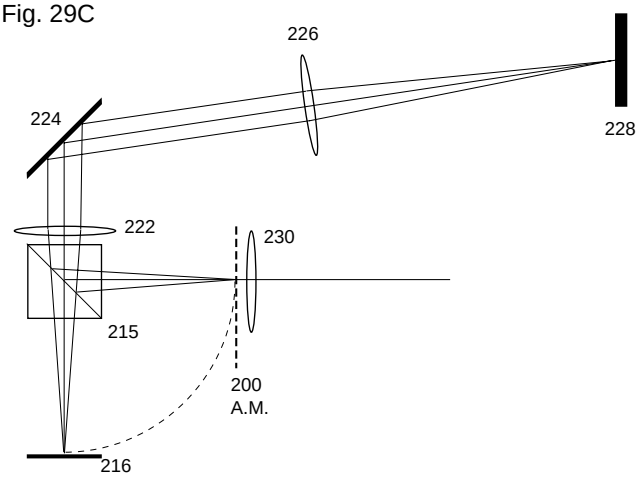

Figure 29B details the subsystem in Figure 29A conveying light from the lamp to the apparent mirror of the interferometer. Figure 29C details the subsystem in Figure 29A conveying light between the apparent mirror of the interferometer and target.

etalons 205 and 207, which are necessary in only one of the two interferometers. The gearbox or other means for translating the mirrors 217 and 219 in a 2:1 ratio is shown only in one half. The gearbox may also exist on the illuminating side instead of or in addition to being on the detecting side. Either gearbox is a convenience and are not required. Some duplicated optics are not labeled for clarity.

Each half enclosed in the respective dashed box consists of three subsystems: a subsystem conveying light between the lamp/camera and the interferometer; the interferometer; and a subsystem conveying light between the interferometer and the target. Figure 29B shows the first subsystem in detail. An important purpose of this subsystem is to limit the range of ray angles (numerical aperture) and transverse extent of the beam passing through the interferometer by means of irises 206 and 212, so that none of the light is vignetted by mirrors 218, 216 or 220. That is, so that every ray of the beam passes through each of the arms, so that there is no unequal vignetting of the different paths that would let rays travel through some paths but not others. This limiting can be accomplished either before or after the rays travel through the interferometer. Lens 204 images the lamp/camera 202 to iris 212. Lens 210 images iris 206 to the A.M. surface 200. Mirrors 208, 214 steer the beam to make the configuration more compact. Iris 212 controls the ray angle range, and iris 206 controls the width of the beam at the A.M. 200.

Some kind of numerical aperture limiting system should be included with every superimposing interferometer described in this document, unless the light source is known to have a limited numerical aperture less than the smallest numerical aperture of any interferometer arm.

Figure 29C shows the subsystem conveying light between the interferometer and the target. Lens 222 and lens 226 together image the A.M. 200 to the target surface 228. Lens 222 is a field lens to reduce vignetting and should be as close to the A.M. surface as possible and yet be outside the interferometer cavity (so that it doesn't introduce wavefront distortion inside the cavity where it is critical). Thus, it lies close to the beamsplitter 215. Mirror 224 folds the beam to make the configuration more compact.

3. Matching dispersion

Adjustable thickness etalons 205 and 207 are used to balance dispersion between the illuminating and detecting interferometers. Only one of the two interferometers needs to have its dispersion adjusted. One embodiment of a variable thickness etalon is the combination of two identical wedge prisms that slide against each other. A fluid filled parallel cavity is another method of creating a variable thickness etalon. One or more tiltable parallel glass plates at an angle to the beam, is a third method.

The source of the unbalanced dispersion is the variance in thickness of transmissive optics (lenses and beamsplitters) that are purchased off-the-shelf. This amount of unbalanced dispersion is usually equivalent to less than 1 millimeter of glass. Since a single thin glass etalon is not rigid and hard to polish flat, it is better to use two separate thick etalons 205 and 207 placed in opposite interferometer arms, so that their effects subtract from each other. For example, a 5 millimeter etalon and 4.8 millimeter etalon placed in opposite arms would have the same dispersion as a 0.2 millimeter etalon. This allows adjustable dispersion in the neighborhood of zero to be made.

It is optimal that the adjustment of the effective etalon length does not change the angle or position of the beam from one arm compared to the other, because that could degrade alignment of the interferometer. Thus the etalons should be normal to the beam, and if tiltable etalons are used, their effect on the beam position needs to be considered.

4. Constant-delay mirror motion

To adjust the position of the apparent mirror without changing the interferometer delay, the center mirror 217 should be moved without changing the total path length from mirror 219 to mirror 217 to the beamsplitter 201. This requires moving mirror 217 half the displacement of the displacement of mirror 219. This can be done manually by incrementing the micrometer screws of the translators 211 and 213 in a 2:1 ratio, or done automatically by an electrical or mechanical means, such as a gearbox or a coordinated pair of stepper motors. After movement of mirrors 217, 219, the field lens 215 is adjusted to keep the A.M. flat. Since it is a transmissive lens, its adjustment does not change the time delay.

5. Matching procedure

Due to the small (∼1 micron) positional tolerance of the delay matching condition $\tau_1 = \tau_2$, the interrelation between the mirror positions, time delay, and A.M. position, the interrelation between the etalon thickness and time delay, and the weakness of the fringes when not under a perfectly matched and aligned state, the process of matching the two interferometers can be tedious if the correct procedure is not followed. The following procedure is recommended:

1. Using string and a ruler, to the nearest millimeter, position the optics of both interferometers to have the same delay lengths and be at the same calculated positions which will overlap the A.M. with the short arm mirror. (This adjustment will be called adjustment of longitudinal overlap.) Set the variable thickness etalons to have equal thickness in each arm of the detecting interferometer.

2. Use broad diameter HeNe laser illumination to focus the relay lens systems 230, 218, 220 and 215, 217, 219 to each produce a flat A.M. by producing parallel comb of fringes instead of rings.

3. Add neutral density filters if necessary to balance the intensities between the two arms of each interferometer.

4. By moving the short arm mirrors 216 and 221, optimize the longitudinal overlap of each interferometer by the retro-reflection method described below. Confirm this with the stationary fringe method described below.

5. The delay τ_1 of the illuminating interferometer is now set. For the remainder of the procedure, the illuminating interferometer optics will not be disturbed, only the detecting interferometer will be touched. Search for the matched delay condition $\tau_1 = \tau_2$, by changing the detecting interferometer delay until "white light" fringes are seen using a short coherence length source. The delay can be changed by movement of the short arm mirror 221. The temporary use of a sodium vapor lamp can help localize fringes to a few tenths of a mm. Initially, the fringes may be very weak due to uncompensated dispersion. The fringes are most visible when a fringe comb is presented instead of a single infinitely wide fringe. A fringe comb is obtained by slightly tilting one of the mirrors, such as the short arm mirror 221. This can be done while temporarily observing fringes under HeNe illumination, since the HeNe fringes and the eventual white light fringes will have the same approximate appearance.

6. Null the dispersion. By viewing the white light fringes through a red color filter, and then through a green color filter, the delay location of the maximum visibility of the red and green fringe components is noted and compared. That is, scan the micrometer screw which changes the detecting interferometer delay τ_2 until the red/green fringes are at maximum contrast and note the associated micrometer value. When uncompensated dispersion is present, the red and green maxima while lie at different locations. Change one of the etalon thicknesses slightly and remeasure the red/green maxima. Keep changing the etalon thickness until the red and green maxima overlap. This will also produce white light fringes with a minimum width and maximal visibility.

7. Re-optimize the longitudinal overlap in the detecting interferometer while keeping the delay constant. The short arm mirror is left fixed and mirrors 217 and 219 are moved in a 1:2 ratio to maintain constant path length between end mirror and beamsplitter, while changing the inter-mirror (217 to 219) separation. A chart analogous to Fig. 8B should be calculated to confirm that the configuration is not at a stagnant point. Confirm optimal overlap by the stationary fringe method.

6. Retro-reflecting overlap adjustment subprocedure

The retro-reflecting method of optimizing the longitudinal overlap between the A.M. and the short mirror is as follows: A target is temporarily used which strongly retro-reflects light, such as a bead-painted surface. A 50% beamsplitter is inserted into the illuminating beam so that the temporary target can be observed in partial reflection off this beamsplitter. Iris 206 is reduced to a small pinhole to ease the light load on the eye, since a specular back-reflection of the lamp of the beamsplitter and mirror 216 will be in the same field of view as the white light fringes to be observed. The short arm mirror 216 is translated longitudinally several millimeters until white light fringe rings are seen which vary in size as

a function of mirror position. The mirror is translated until the rings become infinite in diameter. This has empirically been determined to approximately produce optimal longitudinal overlap between the A.M. with the short arm mirror. Leave the mirror in this position. The beamsplitter and temporary target are then removed and the iris restored to its original size.

7. Stationary fringe overlap adjustment subprocedure

The stationary fringe method of confirming longitudinal overlap is as follows: an approximately collimated and wide diameter HeNe laser beam is used as a temporary source of illumination in place of the white light beam from lens 210. A temporary mirror may be inserted into the path after the iris 212 to introduce this HeNe beam. This temporary mirror is swiveled by hand while inspecting the fringe pattern produced on the target. In an aberrationless superimposing interferometer, when the longitudinal overlap is optimum, the fringe pattern is stationary despite tilting the angle of incidence of the input rays. In the presence of aberrations such as spherical or astigmatic, only the portion of the fringe at the center of the image area may appear stationary with respect to tilting of the temporary mirror, while the periphery changes somewhat. It is optimal that this stationary portion be as large as possible.

S. Retro-reflecting interferometer as double interferometer

Instead of using two separate interferometer apparati, a single interferometer apparatus can function as a pair by sending light reflected from the target back through the same or nearly the same optics. This is called a retro-reflecting configuration, even though the light may actually travel a slightly different path than true retro-reflection (differing in angle, polarization or position in the image plane).

The retro-reflecting configuration provides a great practical advantage because the delays τ_1, τ_2 and the dispersion are then automatically nearly matched, even in the presence of large mechanical vibration that changes the delay. Thus this configuration is attractive for use in industrial settings where vibration is present. Secondly, a rigid optical platform and mounting hardware is not as important. This reduces cost and weight. Alignment is greatly simplified.

There are two kinds of light which must be distinguished from each other: first passed light and second passed light. The first passed light is light going through the interferometer for the first time and is used to illuminate the target. It does not carry any useful velocity information about the target. The second passed light is first passed light after it has reflected from the target and is going through the interferometer for the second time. It is the light which should be detected to produce fringes carrying target velocity information. There should be methods in place which prevent the first passed light from reaching the detector and being confused with the second passed light. Because the first and second passed light may be sharing portions of the same optical path, unwanted reflection from air/glass interfaces or dust on the optics may cause the first passed light to reach the detector. This is a concern, especially since the first passed light could be much brighter than the second passed light, especially for dark targets. Thus, methods for discriminating the two kinds of light are important to practical use of the retro-reflecting configuration.

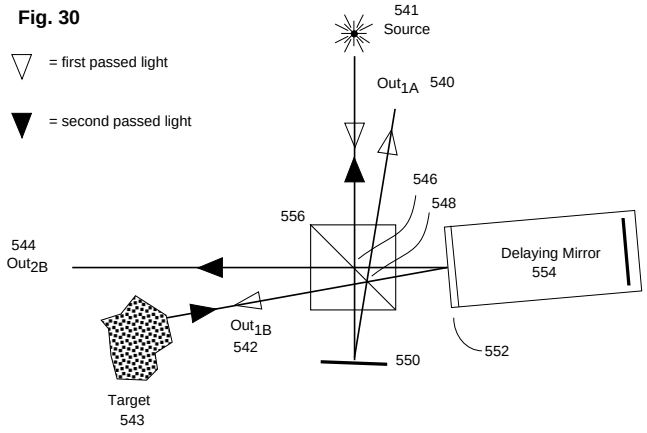

Figure 30 shows the use of beam angle to separate double passed light from first passed light in a retro-reflecting application of an interferometer.

Since any diffusely reflecting target will produce some light scattering back toward the source, any single interferometer, including single interferometers of a double interferometer system, can be used in a retro-reflecting mode if a means is provided to separate second passed light from first passed light. This is useful as a diagnostic tool in aligning each individual interferometer to achieve good superposition, prior to being used as a pair. This method was previously described in the section on pair-matching procedures.

There are several methods of distinguishing the second passed light from first passed in a retro-reflecting configuration: by angle of incidence, by position in the image plane, and by polarization. These are discussed below.

T. Methods of Discriminating Beams in a Retroreflecting Interferometer

1. Discrimination by beam angle

Figure 30 shows use of beam angle to provide discrimination between first and second passed rays. The first passed rays are indicated by the open arrowheads and the second passed light by the dark arrowheads. Consider

that for each pass, the interferometer offers two output paths. For the first passed light, the outputs are Out_{1A} 540, which heads back approximately toward the source 541, and Out_{1B} 542, which heading in the target 543 direction. For the second passed light originating at the target 543, the two outputs are Out_{2A} heading exactly toward the source, and Out_{2B} 544 heading only generally toward the target. The mirrors of each arm (short arm mirror 550 and the apparent mirror 552 of the delaying mirror assembly 554) are tilted so that light does not reflect normally off these mirrors. That is to say, the light reflecting off the mirrors 550, 552 makes two different spots 546, 548 where they intersect the beamsplitting surface 556. This puts the output 544 at a sufficiently different angle from the target beam to allow separation from it.

2. Discrimination by polarization and image offset

Figure 31 shows a retro-reflecting superimposing interferometer embodiment using two methods of discrimination: polarization and image position, which could be used independently. Thirdly, a birefringent wedge is used to produce a inclined delay for the second passed light while the first passed light sees a uniform delay. Light from source 600 is horizontally polarized by polarizer 602 and passes through aperture 604 which defines the extent of the first passed light at the image planes 606, 608, 612 and the A.M. 610. These planes are all imaged to each other by lenses, such as 614, 616. Field lenses analogous to lenses 222 or 204 of Fig. 29A may optimally also be used, but are not shown in Fig. 31 for clarity. The field lenses could be placed near the image planes or near the beamsplitter to reduce vignetting.

A polarizing beamsplitter 601 transmits the first passed light, but reflects the second passed light, which will be arrange to be polarized in the orthogonal direction. The first passed light leaves the interferometer through input/output plane 608 to be conducted to the target either by an imaging, non-imaging or combination of imaging and non-imaging systems (618, 622).

Figure 31 shows a combination of imaging and non-imaging systems. Fiber 618 conducts light to the target image 628 created by lens 622. Both fibers 618, 620 conduct light from the target due to intentional slight defocusing of the lens 622 between target surface and plane 628. However, in this embodiment the exactly retro-reflected light coming back through fiber 618 is not used, since spurious glare from the end of this fiber at plane 608 would compete with light from the target. (However, an anti-reflection coating could be used to reduce this.)

Instead, a second fiber 620 is used to conduct light back toward the interferometer. This way it can be positioned in a separate location in the input/output plane 608 from the first passed light beam, so that it can be distinguished by position. This is done by the use of an aperture 624 that is offset in location in reflection of the beamsplitter 601 so that it does not overlap with the aperture 604, so that aperture 624 blocks first passed light reaching the detector.

In addition to discrimination by position in the image plane, the light can be discriminated by polarization. The fiber 620 is twisted 90° so that there is significant intensity in the vertical polarization. (For long fibers, twisting may be unnecessary because of the polarization scrambling that occurs). The light then passes through a vertical polarizer to eliminate polarization parallel to the first passed light. If a purely imaging system is used which is unlikely to scramble or twist the polarization, then a retarder (not shown) can be inserted into the reflected light beam prior to the polarizer 622 to create significant intensity in the orthogonal (vertical) polarization. The polarizing beamsplitter 616 diverts the second passed light and not the first passed light toward the detector 618. A vertical polarizer offers additional polarization discrimination, in case the polarizing beamsplitter is not ideal.

U. Birefringent wedge

A birefringent wedge 626 can be used to create an inclined delay for second passed light but not for first passed light, because it acts like a wedge for one polarization and a different wedge (or a wedge with zero angle) for the other polarization. When light travels to the target through a non-imaging system (the fiber), there must be a uniform delay imprinted to the light. Otherwise rays having different imprinted delay values differing more than $\lambda/4$ will scramble together, and no fringes may be produced when the target is subsequently observed through an interferometer. However, for the second passed light an inclined delay is possible, since the interferometer uses imaging systems so that pixels between the input/output planes are not scrambled.

An inclined delay is useful for determining fringe phase by recording the fringe comb with a multi-channel detector, such as the CCD camera 618. When using an inclined delay, the source of the second passed light at the plane 608 should optimally be a line source so there is light at every delay value in a range. This could be created by use of cylindrical optics (not shown) or a fiber bundle whose component fibers rearrange from a circle to a line. The line direction would be into the Figure, perpendicular to the offset direction.

The birefringent wedge 626 appears as a parallel slab for first passed light (horizontal polarization) and a wedge for second passed light (vertical polarization). The net wedge can be constructed of component wedges 401, 412, as in Fig. 16, and the net wedge angle and birefringent properties adjusted by rotating the component wedges about the common optic axis.

Fig. 31

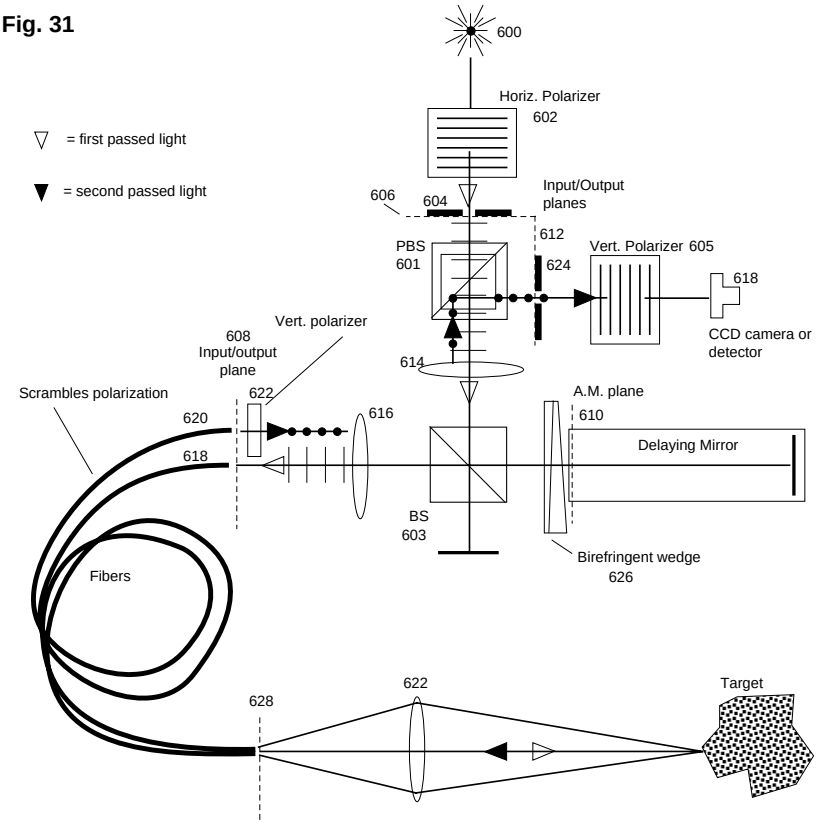

Figure 31 shows use of offset images to separate double passed light from first passed light in a retro-reflecting application of an interferometer.

Fig. 16

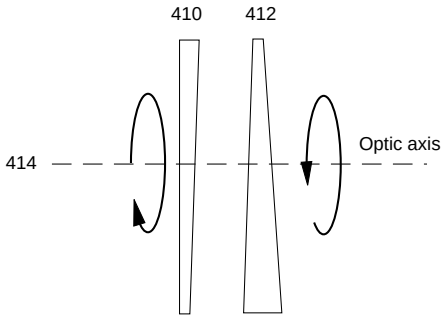

Figure 16 shows the net wedge angle being adjusted by twisting component wedges about a common axis.

V. Other offset target image methods

In Fig. 31, distinctly different fibers were used to position input and output light in the image plane 608, so that first passed and second passed light could be distinguished by position. Figure 32A, B, C shows other methods of offsetting the incoming from outgoing light, by creating twin images of the target.

Figure 32A shows a prism 650 overlapping a portion of the lens 652 which images the target 651 to the input/output plane 658. This plane could be the input/output of the interferometer 608 or the plane 628 where the fibers are placed. The latter case is a more light efficient method of sending light to fiber 620 without blurring the lens 622. The prism deviates the angles so the target appears in two places 656 and 654. One place is used for aiming the illumination, the other for aiming the collection of reflected light. Places 656 and 654 are analogous to where fibers 618 and 620 meet the plane 608 in Fig. 31.

Figure 32B shows image offsetting accomplished by a segmented mirror with a nonzero angle θ between the segments 662, 664. This has the advantage over the method of Fig. 32A in that it is achromatic. (However, the chromatic blurring of prism 650 may be unimportant if a non-imaging system is used or if the target has a uniform velocity across its surface.)

Figure 32C shows image offsetting accomplished by a segmented imaging lens 665, where the optical center of each lens segment are not co-axial with the others. This could be created conceptually by removing a rectangular section 666 from a lens and moving the separate segments 668, 670 together.

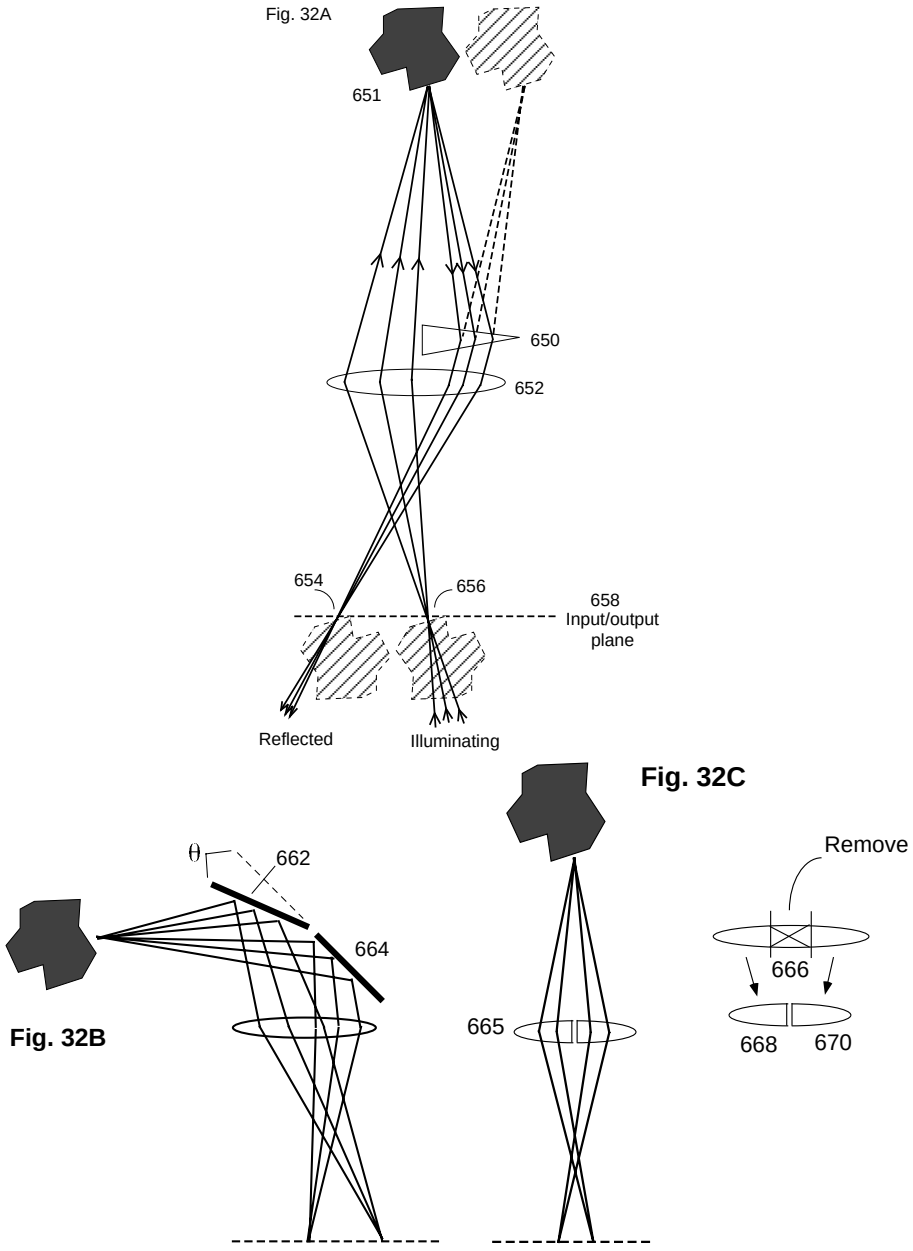

Figure 32A shows use of a prism to create a double image of target to distinguish illuminating from reflected light. Figure 32B shows use of a segmented mirror instead of prism in Fig. 32A. Figure 32C shows use of a split lens instead of the prism in Fig. 32A.

W. Kinds of waves

For concreteness, light was discussed as the illumination wave kind. However, the interferometer and delaying mirror designs can be used with any wave kind which travels as rays in 2 or 3 dimensions, such as sound, electromagnetic waves (infrared, ultraviolet, x-rays etc.) or matter waves (de Broglie waves) provided elements that function analogous to the necessary beamsplitters, lenses and mirrors etc. are used.

Acknowledgments

This work was performed under the auspices of the U.S. Department of Energy by the University of California, Lawrence Livermore National Laboratory under contract No. W-7405-Eng-48.

IV. CLAIMS

(Not official version. There is a high probability that this version is incomplete or differs from the official version due to many post-submission amendments. Due to the length and tediousness of the task, I have not retyped the official version beyond claims 1-7.)

1. An interferometer, comprising:

means for splitting an input beam of light into a first beam of light and a second beam of light;

means for producing a difference between the apparent and actual path lengths of said first beam using real imaging, wherein said difference is called beam shortening;

means for coupling said first beam of light out of said interferometer to produce a first output beam of light; and

means for coupling said second beam of light out of said interferometer to produce a second output beam of light,

wherein said first output beam of light and said second output beam of light superimpose to produce a superimposed beam, wherein an object in said input beam seen through the interferometer appears in both images which superimpose longitudinally, transversely and in magnification.

wherein said means for producing a difference between the apparent and actual path lengths of said first beam comprise an apparent mirror,

wherein said means for producing a difference between the apparent and actual path lengths of said first beam comprise an apparent mirror, wherein said interferometer further comprises means for producing a difference between the apparent and actual path lengths of said second beam, wherein said means for producing a difference between the apparent and actual path lengths of said second beam comprises a second apparent mirror.

2. The interferometer of claim 1, wherein said first apparent or said second apparent mirror is formed by real imaging of an actual mirror.

3. The interferometer of claim 1, wherein the difference between the beam shortening of said first beam and the beam shortening of said second beam is small compared to the absolute value of either beam shortening.

4. The interferometer of claim 1, wherein said apparent mirror is formed by real imaging of a firs actual mirror and said second apparent mirror is formed by real imaging of a second actual mirror.

5. An interferometer, comprising:

means for splitting an input beam of light into a first beam of light and a second beam of light;

means for producing a difference between the apparent and actual path lengths of said first beam using virtual imaging, wherein said difference is called beam shortening; wherein said virtual imaging is accomplished by a lens and a curved mirror;

means for coupling said first beam of light out of said interferometer to produce a first output beam of light; and

means for coupling said second beam of light out of said interferometer to produce a second output beam of light,

wherein said first output beam of light and said second output beam of light superimpose to produce a superimposed beam, wherein an object in said input beam seen through the interferometer appears in both images which superimpose longitudinally, transversely and in magnification.

6. An interferometer, comprising:

means for splitting an input beam of light into a first beam of light and a second beam of light;

means for producing a difference between the apparent and actual path lengths of said first beam using real imaging, wherein said difference is called beam shortening;

means for coupling said first beam of light out of said interferometer to produce a first output beam of light; and

means for coupling said second beam of light out of said interferometer to produce a second output beam of light,

wherein said first output beam of light and said second output beam of light superimpose to produce a superimposed beam, wherein an object in said input beam seen through the interferometer appears in both images which superimpose longitudinally, transversely and in magnification.

wherein said means for producing a difference between the apparent and actual path lengths of said first beam comprise an apparent mirror,

wherein said means for producing a difference between the apparent and actual path lengths of said first beam comprise an apparent mirror, wherein said beam shortening is produced by imaging using a waveguide.

7. An interferometer, comprising:

means for splitting an input beam of light into a first beam of light and a second beam of light;

means for producing a difference between the apparent and actual path lengths of said first beam using at least one transparent wedge; wherein said difference is called beam shortening; wherein said at least one transparent wedge creates a beam shortening that varies across said first beam;

means for coupling said first beam of light out of said interferometer to produce a first output beam of light; and

means for coupling said second beam of light out of said interferometer to produce a second output beam of light,

wherein said first output beam of light and said second output beam of light superimpose to produce a superimposed beam, wherein an object in said input beam seen through the interferometer appears in both images which superimpose longitudinally, transversely and in magnification.

9. The interferometer of claim 7, wherein said at least one transparent wedge comprises a plurality of wedges, wherein each wedge of said plurality of wedges has a unique dispersive power with respect to the other wedges of said plurality of wedges, wherein the thickness of each wedge of said plurality of wedges is chosen so that the slope of said beam shortening versus location across said first beam is achromatic.

11. The interferometer of claim 7, wherein an etalon is placed in said second beam, wherein the thickness and dispersion of said etalon are chosen to compensate the wavelength dependence of the beam shortening created by said wedge.

13. The interferometer of claim 7, wherein said at least one transparent wedge comprises birefringent properties; wherein the slope of the beam shortening for one polarization of light may be different than for the orthogonal polarization; wherein a slope of beam shortening is a rate of change of beam shortening versus position across a beam;

16. The interferometer of claim 3, wherein the difference between the beam shortening of said first beam and the beam shortening of said second beam is small compared to the absolute value of either beam shortening.

17. The interferometer of claim 3, wherein said apparent mirror is formed by real imaging of a first actual mirror and said second apparent mirror is formed by real imaging of a second actual mirror.

18. An interferometer, comprising:

means for splitting an input beam of light into a first beam of light and a second beam of light;

means for producing a difference between the apparent and actual path lengths of said first beam using a first etalon, wherein said difference is called first beam shortening;

means for producing a difference between the apparent and actual path lengths of said second beam using a second etalon, wherein said difference is called second beam shortening; wherein the refractive properties of said second etalon over the operational wavelength range of said interferometer differ from refractive properties of said first etalon;

means for coupling said first beam of light out of said interferometer to produce a first output beam of light; and

means for coupling said second beam of light out of said interferometer to produce a second output beam of light,

wherein said first output beam of light and said second output beam of light superimpose to produce a superimposed beam, wherein an object in said input beam seen through the interferometer appears in both images which superimpose longitudinally, transversely and in magnification.

20. An interferometer, comprising:

means for splitting an input beam of light into a first beam of light and a second beam of light;

means for producing a difference between the apparent and actual path lengths of said first beam wherein said difference is called beam shortening;

means for beamsplitting inserted into either said first beam or said second beam to create a finite number of additional split beams; wherein said split beams are coupled out of said interferometer to produce additional output beams;

means for coupling said first beam of light out of said interferometer to produce a first output beam of light; and

means for coupling said second beam of light out of said interferometer to produce a second output beam of light,

wherein said first output beam of light and said second output beam of light and said additional output beams superimpose to produce a superimposed beam, wherein an object in said input beam seen through the interferometer appears in multiple images which superimpose longitudinally, transversely and in magnification.

21. The interferometer of claim 20, wherein said at least one means for beamsplitting are polarization dependent, wherein the polarization state among said said first output beam of light and said second output beam of light and said additional output beams may differ.

22. The interferometer of claim 1, wherein at least one transparent lens of positive focal length is used to produce said means for producing a difference between the apparent and actual path lengths of said first beam using real imaging, wherein said first beam makes a circulating path so that it periodically reaches said means for coupling said first beam of light out of said interferometer, wherein for a given input pulse entering said interferometer along said input beam, said second output beam and said first output beam comprise an infinite number of geometrically decreasing intensity output pulses that leave said interferometer.

23. The interferometer of claim 22, wherein said circulating path is created between a first end mirror and a second end mirror, wherein an imaging system lies between said first end mirror and said second end mirror; wherein the surface of said first end mirror forms a real image on the surface of said second end mirror. Wherein the center of curvature of said first end mirror is imaged to the center of curvature of said second mirror.

24. An interferometer, comprising:

means for splitting an input beam of light into a first beam of light and a second beam of light;

means for producing a difference between the apparent and actual path lengths of said first beam, wherein said difference is called beam shortening;

means for coupling said first beam of light out of said interferometer to produce a first output beam of light; and

means for coupling said second beam of light out of said interferometer to produce a second output beam of light,

wherein said first output beam of light and said second output beam of light superimpose to produce a superimposed beam, wherein an object in said input beam seen through the interferometer appears in both images which superimpose longitudinally, transversely and in magnification; and

means for separating into distinct paths light incident upon a target from light returning from said target when said target is placed in the superimposed path of said first output beam and said second output beam; wherein said means for separating includes an optical system that creates a double image of a target, wherein each image of said double image of said target are transversely shifted as they appear to said interferometer output beam.

29. An interferometer, comprising:

means for splitting an input beam of light into a first beam of light and a second beam of light;

means for producing a difference between the apparent and actual path lengths of said first beam, wherein said difference is called beam shortening;

means for adjusting the amount of dispersion in said first beam by varying the pathlength of said first beam through a transparent medium having a dispersive refractive index;

means for coupling said first beam of light out of said interferometer to produce a first output beam of light; and

means for coupling said second beam of light out of said interferometer to produce a second output beam of light,

wherein said first output beam of light and said second output beam of light superimpose to produce a superimposed beam, wherein an object in said input beam seen through the interferometer appears in both images which superimpose longitudinally, transversely and in magnification.

30. The interferometer of claim 1, further comprising means for moving said imaging elements that affect said beam shortening in a coordinated fashion, wherein said coordination is intended to change primarily one parameter while minimizing change of other parameters, wherein said one parameter includes said actual path length, said apparent path length, beam wavefront curvature, image magnification, and tranverse superposition, wherein said beam wavefront curvature is the center of curvature of the wavefront of said beam when plane wavefronts are incident on said interferometer; wherein said means for producing a difference between the apparent and actual path lengths of said first beam are called imaging elements;

31. An interferometer, comprising:

means for splitting an input beam of light into a first beam of light and a second beam of light;

means for producing a difference between the apparent and actual path lengths of said first beam, wherein said difference is called beam shortening;

means for coupling said first beam of light out of said interferometer to produce a first output beam of light; and

means for coupling said second beam of light out of said interferometer to produce a second output beam of light,

wherein said first output beam of light and said second output beam of light superimpose to produce a superimposed beam, wherein an object in said input beam seen through the interferometer appears in both images which superimpose longitudinally, transversely and in magnification; and

means for chromatically dispersing said superimposed beam, wherein said means for chromatically dispersing include means for directing said superimposed beam into multiple channels organized by wavelength.

32. An interferometer, comprising:

means for chromatically dispersing an input beam into an input spectrum;

means for splitting said input spectrum into a first beam of light and a second beam of light;

means for producing a difference between the apparent and actual path lengths of said first beam, wherein said difference is called beam shortening;

means for coupling said first beam of light out of said interferometer to produce a first output beam of light; and

means for coupling said second beam of light out of said interferometer to produce a second output beam of light,

wherein said first output beam of light and said second output beam of light superimpose to produce a superimposed beam, wherein an object in said input spectrum seen through the interferometer appears in both images which superimpose longitudinally, transversely and in magnification.

35. A double interferometer, comprising:

a source of illumination;

a first interferometer comprising:

means for splitting an input beam of light into a first beam of light and a second beam of light;

means for producing a difference between the apparent and actual path lengths of said first beam, wherein said difference is called beam shortening;

means for coupling said first beam of light out of said interferometer to produce a first output beam of light; and

means for coupling said second beam of light out of said interferometer to produce a second output beam of light,

wherein said first output beam of light and said second output beam of light superimpose to produce a superimposed beam, wherein an object in said input beam seen through the interferometer appears in both images which superimpose longitudinally, transversely and in magnification, wherein delay between said first output beam and said second output beam is called delay 1;

a second interferometer comprising:

second means for splitting a second input beam of light into a third beam of light and a fourth beam of light, wherein said second input beam of light comprises said superimposed beam, wherein the distance between said means for coupling said second beam of light out of said interferometer to said second means for splitting said second input beam is defined as optical path;

second means for producing a difference between the apparent and actual path lengths of said third beam, wherein said difference is called beam shortening;

second means for coupling said third beam of light out of said second interferometer to produce a third output beam of light; and

second means for coupling said fourth beam of light out of said second interferometer to produce a fourth output beam of light,

wherein said third output beam of light and said fourth output beam of light superimpose to produce a second superimposed beam, wherein a second object in said second input beam seen through said second interferometer appears in both images which superimpose longitudinally, transversely and in magnification wherein delay between said third output beam and said fourth output beam is called delay 2; wherein said delay 2 approximately matches said delay 1 so that fringes are observed in second superimposed beam,

wherein said said superimposed beam is directed to and reflected from a target before said superimposed beam enters said second interferometer, wherein time rate changes in length of said optical path cause a shift in the phase of said fringes, wherein the length of said optical path is the integration of the refractive index along physical path of said optical path, wherein said time rate changes of optical path include motion of said target and changes in dielectric properties of said target,

wherein communication is transmitted from said first interferometer to said second interferometer by modulating said delay 1, which changes appearance of said fringes in said second interferometer.

36. A method of matching delay and dispersion of two interferometers of a double interferometer, comprising:

setting a first delay of a first interferometer and second delay of a second interferometer to be the same within a few milllimeters by initial positioning of optical elements of said first interferometer and said second interferometer, wherein said first delay is called delay 1 and said second delay is called delay 2;

maximizing the longitudinal overlap of said first interferometer,

maximizing the longitudinal overlap of said second interferometer, adjusting said delay 2 to match said delay 1, wherein a short coherence length illumination source is used to send a beam through said first interferometer which then passes through said second interferometer, wherein the visibility of fringes seen in said second interferometer are maximized while said delay 2 is adjusted by movement of optical elements of said second interferometer;

matching dispersion between said first interferometer and said second interferometer; wherein at least one variable thickness etalon is adjusted in thickness to minimize difference in location of the center of fringes for two different wavelengths of illumination, wherein said delay 2 is held constant; and

maximizing longitudinal overlap of said second interferometer using a retro-reflective configuration, further comprising holding said delay 2 constant, wherein positions of optical elements of said second interferometer are moved in a coordinated schedule calculated to hold said delay 2 constant while adjusting said longitudinal overlap of said second interferometer.

41. A delay line comprising:

an input beam;

a beamsplitter which redirects some or all of said input beam of light into a new direction to produce a first beam of light;

means for producing a difference between the apparent and actual path lengths of said first beam of light using real imaging of a mirror, wherein said first beam of light is reflected from said apparent mirror to form a reflected beam; wherein said reflected beam has a path distinct from said input beam.

42. The delay line of claim 41, wherein said beamsplitter is polarization dependent; wherein said beamsplitter has enhanced reflectance for a specific state of polarization of said input beam and enhanced transmission for the complementary polarization state; further comprising a means for changing polarization of said reflected beam to enhance in said reflected beam the amount of intensity in said complementary polarization state.

43. The interferometer of claim 7, further comprising a means for producing a difference between the apparent and actual path lengths of said second beam.

44. The interferometer of claim 43, wherein said means for producing a difference between the apparent and actual path lengths of said second beam uses real imaging.

45. The interferometer of claim 43, wherein said means for producing a difference between the apparent and actual path lengths of said second beam uses virtual imaging.

46. The interferometer of claim 7, further comprising a second means for producing a difference between the apparent and actual path lengths of said first beam.

47. The interferometer of claim 29, wherein said means for adjusting the amount of dispersion comprises at least one variable thickness etalon.

48. The interferometer of claim 29, wherein said means for adjusting the amount of dispersion comprises at least one element selected from a group of wedge and etalon; wherein orientation of said at least one element relative to said first beam is changed thereby producing a changing pathlength through said at least one element.

49. The interferometer of claim 29, wherein said means for adjusting the amount of dispersion comprises a plurality of wedges; wherein orientation of component wedges of said plurality of wedges relative to each other is changed thereby producing a changing pathlength through said plurality.

Part 6

Combined Dispersive/Interference Spectroscopy for Producing a Vector Spectrum

US Patent 6,351,307
Issued Feb. 26, 2002

David J. Erskine*
Lawrence Livermore Nat. Lab.

A method of measuring the spectral properties of broadband waves that combines interferometry with a wavelength disperser having many spectral channels to produce a fringing spectrum. Spectral mapping, Doppler shifts, metrology of angles, distances and secondary effects such as temperature, pressure, and acceleration which change an interferometer cavity length can be measured accurately by a compact instrument using broadband illumination. Broadband illumination avoids the fringe skip ambiguities of monochromatic waves. The interferometer provides arbitrarily high spectral resolution, simple instrument response, compactness, low cost, high field of view and high efficiency. The inclusion of a disperser increases fringe visibility and signal to noise ratio over an interferometer used alone for broadband waves. The fringing spectrum is represented as a wavelength dependent 2-d vector, which describes the fringe amplitude and phase. Vector mathematics such as generalized dot products rapidly computes average broadband phase shifts to high accuracy. A Moire effect between the interferometer's sinusoidal transmission and the illumination heterodynes high resolution spectral detail to low spectral detail, allowing the use of a low resolution disperser. Multiple parallel interferometer cavities of fixed delay allow the instantaneous mapping of a spectrum, with an instrument more compact for the same spectral resolution than a conventional dispersive spectrometer, and not requiring a scanning delay.

I. INTRODUCTION

A. Field of the Technology

The present invention relates to interferometric and dispersive spectroscopy of broadband waves such as light, and more specifically the interferometric measurement of effects which can be made to produce phase shifts such as Doppler velocities, distances and angles, and furthermore the mapping of spectra.

B. Description of Related Art: Spectroscopy

Spectroscopy is the art of measuring the wavelength or frequency characteristics. There are two complementary forms of spectroscopy method currently used today.

*erskine1@llnl.gov

Dispersive Spectrographs In the oldest form, a prism or grating disperses input illumination (let us call it light) into independent channels organized by wavelength or frequency. A spectrum is created which is the intensity versus wavelength channel. This is a scalar versus wavelength channel.

Interferometric Spectrographs In the other method, called Fourier transform spectroscopy, an interferometer having a variable path length difference (called the delay) interferes the illumination with a delayed copy of itself, creating an interferogram. The Fourier transform of this yields the spectrum. Previously, the two methods have not been used together where the interferometry and dispersiveness have had equal emphasis.

1. Doppler Velocimetry

An important practical use of spectroscopy is the measurement of Doppler shifts. In addition to many industrial applications of Doppler velocimetry, astronomers

Figure 1

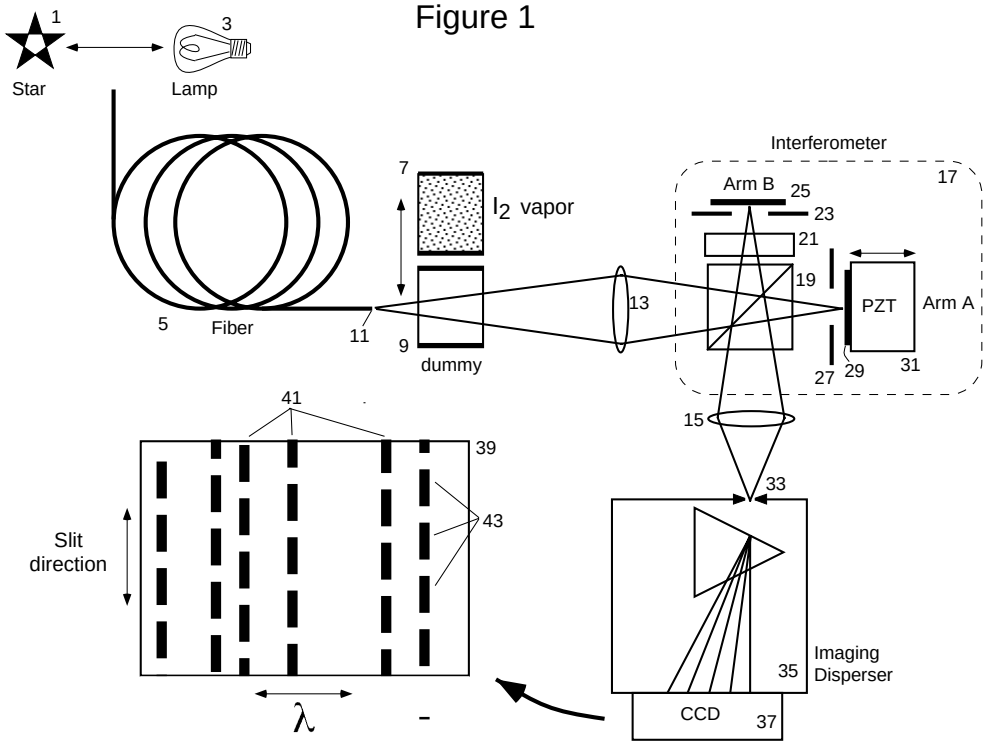

Figure 1A shows an embodiment that measures Doppler shifts of starlight. Figure 1B shows a fringing spectrum or 2-dimensional intensity image produced by the embodiment of Figure 1A.

measure the Doppler velocity of stars in order to deduce the presence of planets orbiting around the star. The stellar spectrum contains numerous dark absorption lines against a bright continuum background. These spectral lines are randomly distributed about 1 Å apart from each other. A slight change in the average position of these lines is the Doppler effect to be measured. The average width of these stellar lines is about 0.12 Å in the visible, which corresponds to an equivalent Doppler velocity width of about 6000 m/s. Hence, measuring Doppler velocities below 6000 m/s is extremely challenging and requires carefully dividing out the intrinsic behavior of the instrument from the raw data.

A 1 m/s velocity resolution is desired in order to reliably detect the presence of Jupiter and Saturn-like planets, which produce 12 m/s and 3 m/s changes respectively in the stars intrinsic velocity. Current astronomical spectrometers are based on the diffraction grating. These have a best velocity resolution of 3 m/s, but is often 10 m/s in practice. This resolution is insufficient to reliably detect Saturn-like extrasolar planets. This limit is related to the difficulty in controlling or calibrating the point spread function (PSF).

2. Drawbacks of Purely Dispersive Spectrosgraphs

The PSF is the shape of the spectrum for a perfectly monochromatic input. Ideally this is a narrow peak of well-determined shape. Unfortunately, the PSF of actual gratings varies significantly and in a complicated way against many parameters such as temperature, time, and average position in the spectrum. It is a complicated function that requires many mathematical terms to adequately approximate it. This is fundamentally due to the hundreds or thousands of degrees of freedom of the diffraction grating– at least one degree of freedom per groove of the grating. These degrees of freedom must be carefully calibrated, otherwise drifts can cause apparent Doppler velocities much larger than the effect being sought. The calibration process is time consuming.

Another disadvantage of conventional astronomical spectrometers is their large size, which can be several meters in length. Large distances between optical components, which need to be held to optical tolerances, require very heavy and expensive mounts and platforms to prevent flexure. This dramatically increases expense and prevents portability. Practical use aboard spacecraft or aircraft is prevented. The high expense limits the number of spectrometers which can be built to a few, only by well-endowed institutions.

Other disadvantages include a very limited field of view, which is called etendue and is the area of the input beam times its solid angle. This is due to the narrowness of the slit at the instrument entrance that defines the range of entry angles. In a grating or prism based instrument the entry angle and the wavelength, and hence deduced Doppler velocity, are directly linked. The slit

needs to be narrow to provide better than 0.05 Å resolution to resolve the stellar spectral lines. Atmospheric turbulence causes the star image to dance around, sometimes off the slit opening. This reduces the effective instrument throughput. Furthermore, changes in intensity profile across the slit have to be carefully deconvolved from the data, since the Doppler velocity gradient across the slit is approximately 3000 m/s. Thus achieving 3 m/s velocity accuracy is extremely difficult with a dispersive spectrometer, and 1 m/s has never been achieved.

3. Drawbacks of Purely Interferometric Spectrosgraphs

An interferometer is attractive for spectroscopy because its angular dependence can be made very small or zero. This allows wider slits, and hence accommodating blurrier star images at high throughput, for the same equivalent spectral resolution. Secondly, its PSF is a sinusoid, which is a simple mathematical function having only 3 degrees of freedom (phase, amplitude and intensity offset). This makes calibration of instrument and processing of data fast, since standard vector mathematics can be used. Secondly, this makes it easy to reject noise not having the expected sinusoidal shape. Furthermore, the spectral resolution can be made almost arbitrarily large simply by increasing the delay (difference in path length between the two interferometer arms). The interferometer is compact and inexpensive, because the optical components need only be a few millimeters or centimeters from each other.

The important difficulty of an interferometer measuring broadband illumination is poor fringe visibility. Fringe phases naturally changes with wavelength. When component fringes of many wavelengths combine on the same detector, they reduce the visibility of the net fringe. For this reason conventional interferometer based instruments such as Fourier transform spectrometers without any wavelength restricting filters are rarely used in low light applications.

4. Prior Dispersive Interferometers

A solution to this problem is to combine a wavelength disperser with the interferometer so that fringes of different wavelengths do not fall on the same place on the detector. The combination of disperser and Fabry-Perot interferometer is described in the book "Principles of Optics" by Max Born and Emil Wolf, Pergamon Press, 6th edition, on page 336, section 7.6.4 and their Figure 7.63, 7.66 and references therein. Distinctions exist between apparatus described in "Principles of Optics" and the present invention. The Born & Wolf device produces fringes that are narrow and peak-like, not sinusoidal. Consequently, the fringe shape is not described by a 2-element vector. This reduces accuracy when trying to measure small phase shifts. Furthermore, phase stepping is not involved. Thirdly, a heterodyning action is not employed to shift high-resolution spectral details to low spectral resolution.

5. Prior Non-dispersed Interferometer for Metrology

In some kinds of metrology a secondary effect, such as temperature, pressure or acceleration, is measured by the change it induces in the delay of an interferometer, such as through changing the position of a reflective surface or altering a refractive index. The delay is then sensed by the phase of a fringe. In current devices monochromatic illumination, such as laser illumination, is needed to produce visible fringes from non-zero delays. (The delays are often non-zero for practical reasons, or to have a significant range of travel.) However, the use of monochromatic illumination creates fringe skip ambiguities which make the absolute size of the effect being measured ambiguous. Only small changes can be reliably measured. Broadband light solves the fringe skip problem, but produces insufficient fringe visibility because its coherence length (about 1 micron) is usually very much shorter than the delay.

6. Prior use of Interferometry for Angle Measurement

In a related metrology, fringe shifts can be used to measure angles of distant objects such as stars. Light from the star is collected at two separate places a baseline distance apart, and interfered against each other at a beamsplitter. This is called long baseline interferometry. Effectively, an interferometer is created in the triangle consisting of the target and the two collecting ports. In the case of broadband targets such as starlight, the short coherence length of the illumination (about 1 micron) restricts the interferometer delay to be very near zero in order to produce visible fringes. This restricts the angular range. Secondly, an interferometer's phase is sensitive to the illumination's spectral character on bandwidth scales given by 1/(delay). Having a small or zero delay means the interferometer phase is sensitive to the overall shape of the illumination spectrum, and this can vary erratically due to atmospheric turbulence. More accuracy could result if the interferometer were only sensitive to behavior on short bandwidth scales, such as 1 Å, because this is less affected by the atmosphere. This would require using large delays (several millimeters at least), which can't be done with the present long baseline interferometers.

A related spectroscopic long-baseline interferometer technique is described by Kandpal et. al., in Journal of Modern Optics, vol. 42, p447-454 (1995). Intensity modulations are observed in a spectrometer which are due to the angular separation of two stars. However, this technique does not use heterodyning, nor phase stepping nor slit fringes, nor an iodine cell, nor use vectors to describe the data at each wavelength channel. Because of

this, the typical maximum angle it can measure is 8000 times smaller than what my invention can measure.

II. SUMMARY OF THE INVENTION

A. Combine Dispersion with Interference

It is an object of the invention to measure the spectral characteristics of waves, especially broadband waves. These waves include electromagnetic waves, and any other waves that can be passed through an interferometer where they interfere with a delayed copy of themselves, and can be dispersed into intensity-detecting channels organized by frequency or wavelength. The dispersion can be either before or after the interference. Broadbandedness could be defined as when, with the interferometer were used by itself without the disperser, the phases of the fringes of different spectral regions within the input illumination are more than 90°different from each other, and thereby start to diminish the net fringe visibility.

The invention comprises the series combination of a disperser which organizes the waves by frequency or wavelength, and the interference of the waves with a delayed copy of themselves. It is an object of the invention to create a spectrum which has fringes whose phase and amplitude can be determined for a given wavelength channel independent of information from other wavelength channels. Such a spectrum is called a fringing spectrum.

B. Spatial or Temporal Phase Stepping

To determine fringe phase and amplitude of a given wavelength channel independent of other channels, the interferometer delay is arranged to vary, either spatially along the slit of the disperser (which is perpendicular to the dispersion axis), or temporally by "phase stepping", which is to take repeated exposures while changing the overall interferometer delay for all channels. When the delay changes along the slit, such as by tilting an interferometer mirror or beamsplitter, fringes are created which cause the intensity profile along the slit to vary sinusoidally with a finite period.

Regardless of any fringing behavior along the slit direction, an interferometer always has sinusoidal behavior versus frequency. This is called the "spectral comb". This comb may not be resolved by the disperser, but its presence is still key in producing Moire fringes.

C. A Heterodyning Effect

The effect of passing light through both the interferometer and disperser is to multiply the spectral comb with the illumination spectrum. Together with the presence of blurring along the dispersion axis, a heterodyning effect occurs which creates Moire fringes. These shift high spectral resolution details to low spectral resolution. Hence, a low spectral resolution disperser can be used, even though high spectral resolution information is being sensed. This lower costs, increases throughput and increases field of view compared to a high-resolution disperser used alone.

D. Vector Spectra

It is an object of the invention to express the fringing spectrum as a 2-dimensional vector versus wavelength or frequency channel, which is called a vector spectrum. This data format is also called a "whirl". The length and angle of the vector when expressed in polar coordinates represent the fringe amplitude and phase, respectively. The vectors can be computed by evaluating the Fourier sine and cosine amplitudes, for a periodicity near the natural fringe periodicity along the slit axis, and assigning these to the X and Y rectangular coordinates of the vector. In the case of infinite fringe periodicity along the slit, the Fourier components cannot be determined from a single exposure, but can be determined if the several exposures are made while incrementing the interferometer by a small amount, such as equivalent to a quarter wave, and knowing that the fringes will shift in phase proportional to the delay change. This technique is called phase stepping. Phase stepping is recommended even for finite fringe periodicity along the slit, because it assists in distinguishing true fringes from common-mode noise.

E. Use for Doppler Velocimetry

The embodiment of the invention having a single approximately fixed interferometer delay can measure broadband phase shifts due to the Doppler effect of a moving source. Due to the action of the disperser, the optimum delay value is approximately half the coherence length ($\lambda^2/\Delta\lambda$) of the illumination that is due to the spectral lines or other narrow features, not the short coherence length due to the continuum background. That is, $\Delta\lambda$ is given by the 0.12 Å width of the spectral line instead of hundreds of Å of the continuum. In the absence of a disperser the relevant coherence length would be due to the broad continuum background, and therefore thousands of times shorter.

This delay choice provides a good tradeoff between fringe visibility and phase shift per velocity ratio. For starlight this is a delay of about 11 mm. The Doppler velocity is proportional to the whirl rotation. This can be found by taking the dot product of the input whirl against an earlier measured whirl, and against the earlier measured whirl rotated by 90°. The whirl dot products are generalized dot products evaluated by summing or averaging the channel dot product over all wavelength channels. The dot product is called "generalized" be-

cause it sums products over both the spatial and wavelength indices. The subsequent arctangent of the two aforementioned dot products yields the whirl angle. Note that a key advantage implicit in the generalized dot product is that the summation over wavelength channels happens prior to applying the arctangent function. This prevents large discontinuities in the arctangent function that would occur for spectral channels that have zero or small fringe visibility.

Since the whirl rotation is dependent on both the interferometer delay and the illumination spectrum, measuring a Doppler effect requires independently determining the interferometer delay, which could be wandering due to vibration and thermal drift. This can be accomplished by including a reference spectrum with the target illumination, such as by passing the light through an iodine vapor cell which imprints its own absorption lines, which have stable positions unrelated to the Doppler effect. This creates a net whirl which contains two components, corresponding to the target illumination and the reference spectrum. The difference in rotation between the target whirl and the reference whirl components yields the target Doppler velocity. The rotational positions of the target and reference whirl components can be found by expressing the total whirl as a linear combination of component whirls with unknown coefficients, and applying generalized dot products.

The advantage of this invention is an instrument which is much more compact, lower cost, and having a greater field of view than a conventional dispersive spectrometer of 0.05 Å, and has much greater signal to noise ratio than an interferometer used alone.

F. Use for Metrology of Secondary Effects

Another embodiment of the invention uses the interferometer delay as a means of measuring secondary effects such as temperature, pressure and acceleration. These effects are arranged to change the delay in a known manner, such as by moving a reflective part of the interferometer cavity or altering the refractive index of the cavity medium. A steady reference spectrum is used for the illumination. Then changes in the whirl rotation can be ascribed to changes in the interferometer delay and hence the secondary effect. Since the interferometer delay may already be changing due to deliberate phase stepping, it is advantageous to include a second interferometer in series with the probe interferometer cavity to act as a reference cavity. Then the change of one interferometer delay compared to the other provides the measurement of the secondary effect being probed. This method differs from conventional interferometric measurements of cavity lengths by the use of broadband instead of monochromatic illumination. This allows a unique determination of the absolute cavity length without the fringe-skip ambiguity of monochromatic waves.

G. Use for Measuring Angles

A variation of this method can measure the angular position of distant objects such as stars if the interferometer cavity is replaced by a long baseline interferometer, which collects starlight at two separate places a baseline apart from each other and interferes them. Effectively, the triangle consisting of the star and the two collection ports forms the interferometer cavity. Changes in star angle cause an arrival time difference in the starlight interfering with itself. This creates a rotation of the whirl which is measured. The target light can be passed through an iodine vapor absorption cell to imprint a known spectrum. This way, the star's velocity will not affect the measurement because the stellar spectrum can be ignored, and targets having no intrinsic spectral lines or narrow features can be used. Furthermore, greater angular separations can be measured because the iodine linewidths are much narrower (by a factor 8) than stellar linewidths, so proportionately greater arrival time differences at the beamsplitter can be measured. By observing two or three stars simultaneously through the use of beamsplitters at the collection ports, poorly known instrumental parameters such as the baseline length and the phase stepping amount can be determined from the data. The advantage of using this technique is that more precise phase shifts can be measured than in conventional long baseline interferometry, over larger angular range, because the imprinted iodine spectrum is much more information rich than the star's intrinsic spectrum.

Furthermore, the 2-d vector format of the whirl preserves the polarity of the Moire fringes, which preserves polarity of arrival time difference and hence the target angle relative to the baseline. This is not possible with devices that only record the intensity (scalar) spectrum.

H. Use for Mapping a Spectrum

Measuring a Doppler shift of a spectrum is a different task than mapping a spectrum, which is the purpose of many conventional spectrometers. The former task requires only a subset of the full spectral information. An embodiment of the invention which modifies the interferometer to have several parallel channels of different delay striking separate positions of the detector can indeed map a spectrum. Each interferometer delay produces a whirl which is responsible for measuring a particular subset of the full spectral information. The interferometer delays are chosen to be different from each other so that the set of them samples all the desired spectral information. The separate spectral information is combined together mathematically, using the knowledge that the Moire fringes of the fringing spectrum manifest a heterodyning process that beats high spectral detail to low spectral detail. The reverse process is employed to mathematically reconstruct the full spectrum of the input illumination. This process involves Fourier transforming

each whirl from frequency-space to delay-space, translating each in delay-space by the specific interferometer delay used, concatenating all these together, then inverse Fourier transforming to yield a net spectrum. The advantage of this invention for mapping a spectrum is that it forms a more compact, lower cost device than dispersive spectrometers for the same equivalent spectral resolution. And compared to conventional Fourier transform spectrometers it can measure single shot events (instantaneous measurement) because it does not require waiting for an interferometer delay to be scanned. The delays are fixed. The lack of significant moving parts is also an advantage for space-based operation.

III. DETAILED DESCRIPTION OF THE INVENTION

A. An Embodiment For Doppler Velocimetry

Figure 1A shows an embodiment of the invention optimized to detect small Doppler shifts from starlight. The series combination of an interferometer 17 and a disperser 35 creates a fringing spectrum 39, shown in Figure 1B, which is a 2-dimensional intensity image. The dimensions are direction along a slit 33 versus dispersion axis (frequency or wavelength). This image is recorded at the CCD detector 37 or similar 2-dimensional intensity detector. In general the interferometer can either precede or follow the disperser, since the transmission behavior of the net instrument is the product of multiplying the two transmission behaviors of its components. The slit 33 which defines the entrance to the disperser 35 is perpendicular to the dispersion direction, which is in the plane of the paper. When the interferometer precedes the disperser, the disperser should be an imaging disperser, whereby the intensity variations along the slit direction are faithfully imaged to the detector. Otherwise, the apparatus must be operated in mode of infinitely tall fringe period, which relies on phase-stepping to determine fringe phase and amplitude. If the disperser precedes the interferometer, then it is not necessary for the disperser to preserve the image along the slit.

The choices of the source of light may include a target 1, or a lamp 3 having a broad featureless spectrum (such as an incandescent lamp). The light can conveniently be conducted to the apparatus via a fiber 5. The lamp is needed during calibration procedures that measure the iodine cell 7 spectrum by itself, or the interferometer by itself.

1. Spectral Reference

The iodine vapor cell 7 is used to imprint a reference spectrum on the input illumination so that unavoidable changes in interferometer delay such as due to thermal drift, air pressure changes, mechanical vibrations and uncertainties in the PZT transducer can be distinguished from legitimate changes in fringe phase due to the Doppler effect. These delay drifts can easily exceed the desired instrument phase accuracy by many orders of magnitude. For example, measuring a 1 m/s Doppler shift with an 11 mm delay corresponds to a phase change of $1/14000^{th}$ of a wave of green light.

The spectral reference should have many narrow and stable spectral lines distributed evenly over the spectrum. The spectral reference can be absorptive, such as iodine or bromine molecular vapors, or emissive such as a thorium lamp. An iodine vapor cell heated to 40 to 50 C temperature is a common spectral reference used for green light. Since absorption is a multiplicative effect, the cell can be placed anywhere upstream of the detector. An identical but empty dummy cell 9 can be swapped with the iodine cell 7 to reduce the change in beam profile due to the glass windows. If a reference emission lamp is used, its light should join the target light prior to the interferometer and disperser, and be superimposed in path such as by use of a beamsplitting surface.

Fig. 2

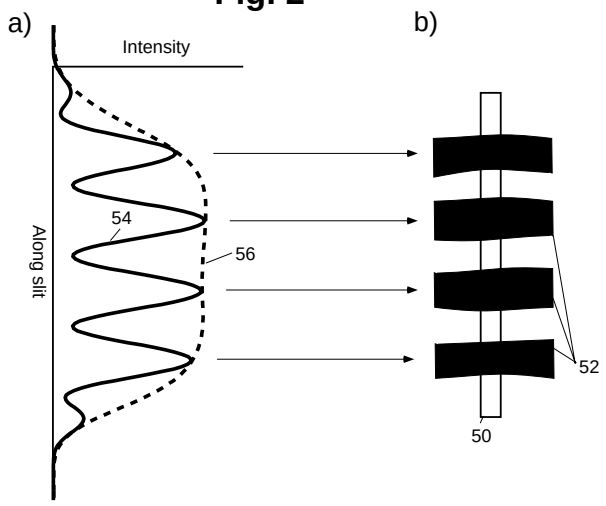

Figure 2a and 2b show a ladder of fringes overlaying the slit.

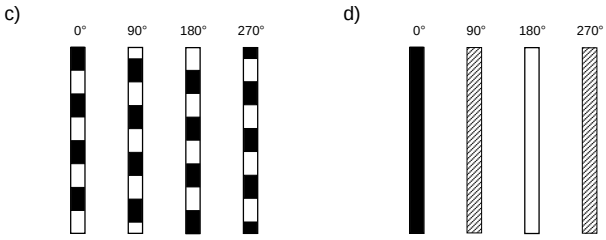

Figure 2c and 2d show how the ladder cycles versus fringe phase.

2. Optics Preparing Beam

An optical system represented by lenses 13 and 15 images the light from the fiber end 11 through the interferometer and to the disperser slit 33. Other lenses such as field lenses are not shown but can be included to help relay the beam and control the pupil from expanding too large. These field lenses could image the pupil at lens 13 to the pupil at lens 15, for example. For maximum throughput the lens magnifications are chosen so that the size and numerical aperture of the light leaving the fiber is matched to the slit width and accepting numerical aperture of the disperser. It is useful to first image the fiber end 11 to a real image near the interferometer mirror 29 and 25, then to relay this to another real image at the slit. This minimizes the area of the beamsplitter which needs to be optically flat.

It is optimal to make several fringe periods span along the slit length, so that fringe phase and amplitude can be determined for each wavelength channel independent of others in a single exposure. This requires illuminating a length of the slit. To avoid wasting light, the beam cross-section at the slit should be rectangular with a high aspect ratio so that it is not unnecessarily wider than the slit. The beam should also be rectangular at the interferometer mirrors 25, 29 so that a fringe ladder 52 and 54 (Fig. 2a and 2b) can be imprinted on it. In applications where efficiency is not important, it is sufficient to use round beam cross-sections.

There are several methods of creating a rectangular beam cross-section. One method is to use cylindrical optics. The optical system represented by lens 13 between the fiber 5 and interferometer 17 could be astigmatic so that for the plane out of the paper the light would not focus at the mirrors 25, 29 but instead have a large extent. In the plane of the paper it would form a narrow focus at the mirrors 25, 29. Another method is to use a fiber bundle to change a round cross-section to a rectangular cross-section at position 11. Then the optical system represented by lens 13 could be ordinary (not astigmatic). A third method is to use various "image slicing" techniques developed by astronomers using mirrors etc. to dissect a round beam cross-section and reassemble it in a different order to form a rectangle at position 11. If the disperser precedes the interferometer, then the beam entering the disperser could be small and round. The disperser could make a spectrum which could have finite vertical height (the dispersion direction assumed horizontal), possibly using either non-imaging paths inside the disperser or using cylindrical optics after the disperser and before the interferometer.

B. The Interferometer

The interferometer 17 is responsible for creating a sinusoidal-like frequency dependence to the transmitted intensity. These fringes in frequency space are called "spectral comb" fringes, shown as 67, 69 in Fig. 3a and 3b. In addition, it is optimal to have spatial fringes 65 along the slit direction, so that without phase stepping the fringe phase and amplitude can be determined for a given wavelength channel. That way the inclusion of phase stepping results in even better accuracy because then there are redundant methods of determining fringe phase and amplitude.

Fig. 3

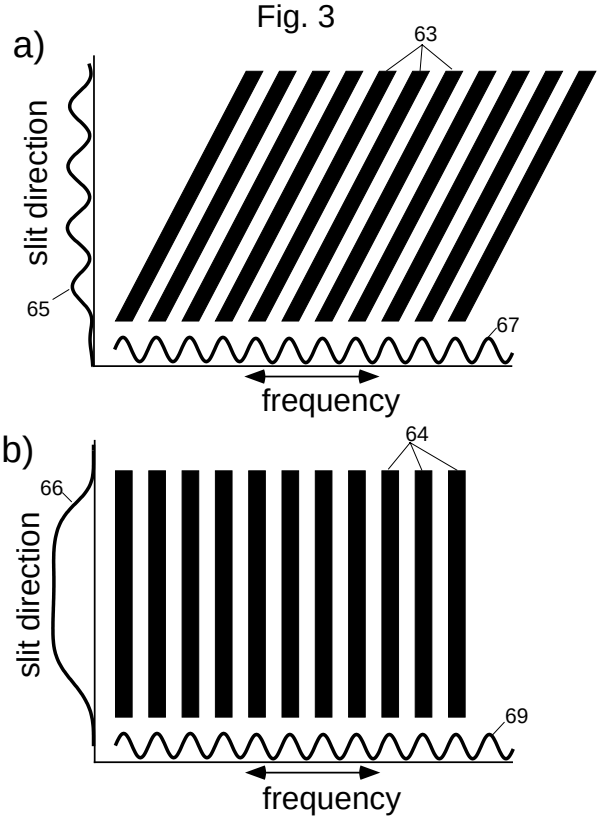

Figure 3a shows a slanted spectral fringe comb created by interferometer when a ladder of fringes exists along the slit. Figure 3b shows a nonslanted spectral fringe comb created by interferometer when a single tall fringe overlays the slit.

A variety of interferometer types can be used, with the desirable properties being high throughput, and the creation of fringes with a large sinusoidal component. A Michelson type interferometer, as opposed to a high-finesse Fabry-Perot type, creates the most sinusoidal fringes. The optical path length difference between the interferometer arms is called the "delay", which is usually in length units. The symbol τ represents the delay in time units,

$$\tau = (delay)/c, \tag{1}$$

where c is the speed of light.

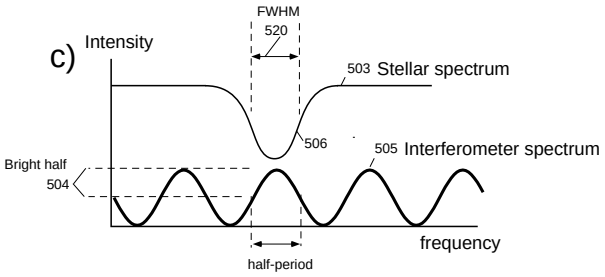

Figure 3c shows that this delay choice is equivalent to making the half-period 500 of the comb fringes 505 about equal to the typical FWHM linewidth 502 of features in the stellar spectrum 503.

1. *Fringes in Frequency and/or Space*

A Michelson with a non-zero delay will produce a sinusoidal transmitted intensity component of the form $\sin(2\pi f\tau)$ or $\sin(2\pi\tau c/\lambda)$. Hence there are three ways that fringes can be made: 1) Versus wavelength or frequency; these produce spectral comb fringes which create the heterodyning effect through the Moire fringes. These may or may not be resolved at the detector depending on the disperser resolution, which is affected by its slit width. The invention does not need them to be resolved, but resolving them can improve signal to noise. 2) Versus position along the slit. These are called "slit fringes" and exist when τ varies linearly along the slit, such as when an internal interferometer mirror 25, or 29 or beamsplitter 19 is tilted. These fringes are not required but are helpful. 3) Versus phase stepping. This is where τ is increment the same amount everywhere along the slit, such as by moving mirror 29 by a PZT transducer 31. These are required to determine fringe phase and amplitude if there are no slit fringes. However, even when slit fringes exist phase stepping is useful for improving accuracy, especially to distinguish common-mode errors.

2. *Fixed Delay Size*

For the embodiment of Fig. 1 that measures Doppler shift, the interferometer delay is approximately fixed (within a few waves), because that is simple, and sufficient to determine a Doppler effect by observing a phase shift. This is in contrast with a conventional Fourier Transform spectrometers which scan the delay over a large range (tens of thousands of waves). The optimum fixed delay to use is approximately half the coherence length ($\lambda^2/\Delta\lambda$) of the spectral lines, where $\Delta\lambda$ is the typical spectral linewidth of about 0.12 Å. Linewidth is the full width at half maximum (FWHM). This coherence length is about 23 mm for starlight at λ=540 nm. This choice yields a good compromise between Moire fringe visibility and sensitivity of the Moire fringe phase to a given Doppler velocity of target. (Larger delay will give greater phase shift per velocity, but the fringe visibility will drop significantly when it is larger than this coherence length.) For use on sunlight and starlight, in one embodiment, a delay of approximately 11.5 mm was used.

Note that this 23 mm coherence length due to the spectral lines is much larger than the approximately 1 micron coherence length of the continuum portion of the spectrum. The inclusion of a disperser to an interferometer allows this larger coherence length component to be sensed with reasonable fringe visibility.

Figure 3c shows that this delay choice is equivalent to making the half-period 500 of the comb fringes 505 about equal to the typical FWHM linewidth 502 of features in the stellar spectrum 503. This way the "bright" half 504 of the sine wave nicely overlaps the peak or dip 506 of the spectral line. The spectral comb period is given by

$$\Delta\lambda = (\lambda^2/c\tau). \tag{2}$$

For a wavelength of 540 nm, a delay of 11.5 mm produces a comb periodicity of 0.25 Å, which is indeed about twice the typical stellar linewidth.

3. *Wide-angle Ability from Superimposing Condition*

In Fig. 1 the interferometer is a superimposing Michelson design similar to that described by R.L.Hilliard and G.G. Shepherd, J. Opt. Soc. Amer., vol. 56, p362-369, (1966). The superimposing character improves the fringe visibility from extended sources such as wide fibers that can't be perfectly collimated. Wide fibers are desired to collect star images blurred by atmospheric turbulence. The superimposing type is where the mirror of one arm and the image of the mirror of the other arm are superimposed longitudinally. This can be accomplished by inserting a transparent slab 21 (called the etalon) in one of the arms. This creates a virtual image of the mirror 25 which lies closer to the beamsplitter than the actual distance. The mirror 29 of the other arm is arranged to superimpose via the beamsplitter the virtual image of mirror 25. This creates a non-zero temporal delay, while superimposing the output paths of the rays from both arms. If n and d describe the refractive index and thickness respectively of the etalon, then the resulting delay at the superimposing condition is approximately

$$\tau c = 2d[(n-1)/n + (n-1)]. \tag{3}$$

(The delay is a roundtrip length). For longer delays than several centimeters, the etalon 21 can be replaced by a real imaging system.

4. *Finding the Delay from the Data*

The exact delay can be measured from the fringing spectra of a known spectral reference source, which could be an iodine vapor cell or a neon emission lamp. The

wavelengths of the neon spectral lines are well known, and each delay value produces a particular combination of phase shifts for the set of spectral lines. Alternatively, the broadband featureless lamp 3 is used for illumination and the disperser's slit is temporarily made very narrow so that the spectral comb can be resolved. Then the number of comb fringes is counted from one end of the spectrum to the other. The spacing of the fringes is related to the delay. For any wavelength the absolute number of fringes that fit "inside" the delay is $N = c\tau/\lambda$, so that counting the change in N across the spectrum is equated to $c\tau(1/\lambda_1 - 1/\lambda_2)$. This yields $c\tau$.

5. Two Complementary Outputs Available

In general a Michelson interferometer produces two complementary outputs. In Fig. 1 only one is used, for simplicity. The output traveling back towards the source (toward lens 13) is ignored. To improve efficiency however, both outputs should be used. This can be done with schemes that distinguish the outputs by angles or polarization. If the ingoing beam enters at an angle to the optic axis, then the outgoing beam will travel a different path than the ingoing and it is possible to introduce a mirror to pick it off. An example scheme using polarization is as follows: if the beamsplitter 19 is a polarizing beamsplitter and the incident light is non-polarized or polarized at 45° to the beamsplitter (so that there is significant intensity in both polarizations), and if means to flip the polarization such as quarter-wave retarders are placed in each arm, then both complementary outputs will travel along the same path toward lens 15. They won't create fringes until they are separated by polarization, which can be accomplished for example by a birefringent element downstream from the interferometer but prior to the CCD detector that causes one polarization to strike a different place on the CCD than the other polarization.

6. Means for Phase-stepping the Delay

In general, a means for slightly varying the interferometer delay for all wavelength channels as a group should be provided, so that the delay can be changed between exposures in evenly sized steps around the circle (360° or 1 average wavelength). This is called phase-stepping. At least three exposures evenly spaced around the circle are needed to uniquely determine fringe phase and amplitude for a given channel if the slit fringe period is infinite. Steps of 90° however are sometimes more convenient than 120° steps. In this case, usually 4 or 5 exposures every 90° are made. Since the wavelength changes across the spectrum, the actual detailed value of phase step for a given delay increment $\Delta\tau$ will vary with wavelength or frequency channel ($\Delta\phi = 2\pi c\Delta\tau/\lambda = 2\pi f\Delta\tau$). The second reason for phase stepping is that it allows common-mode errors that appear to be fringes (such as CCD pixel to pixel gain variations) to be distinguished from true fringes, for only the true fringes will respond the delay in a sinusoidal fashion versus stepped phase.

The means of stepping could be a piezoelectric transducer (PZT) 31 which moves one of the interferometer mirrors 29 or 25. For steps of 90° or less, the PZT could be linearly ramped during the exposure. This is simpler to implement than discrete stepping but washes out the fringe amplitude slightly. For long exposures a stabilization scheme to step and then hold the phase stable against drifts is useful. The approximate phase of the interferometer can be monitored by passing a laser such as a HeNe laser through the same or similar portion of the interferometer cavity and recording the HeNe fringe phase, (taking into account the wavelength ratio of the HeNe to the starlight.)

7. Temporarily Preventing Interference

A means for temporarily preventing interference or fringing behavior should be provided so that an ordinary (non-fringing) intensity spectrum can be recorded on the instrument, while the keeping the rest of the instrument as much as possible in the original configuration. This allows some common-mode behavior to be measured without the confusing effect of fringes, such as measuring the beam profile at the slit and the CCD pixel to pixel gain variation. These common-mode behaviors can then be used during data analysis to divide the fringing spectrum and thereby reduce the common mode errors. Otherwise bumps in the slit beam intensity profile due to vagaries in the optics that have similar periodicity to the fringes could be confused with the true fringes.

Interference can be prevented by blocking either of the interferometer arms, arm A or arm B, such as by shutters 23 and 27 or opaque cards placed manually into the arms. Since the beam profile passing through arm A may be slightly but significantly different than that passing through arm B, both nonfringing spectra (blocking A, blocking B) should be taken and then added later numerically.

8. Finite vs Infinitely Tall Spatial Fringes

When the two interferometer mirrors 25 and 29 are aligned so that the output rays from both arms superimpose, then an "infinitely tall" fringe is created on the output beam that entirely fills the height of the output beam measured along the slit length (Fig. 2a, item 56). When one of the mirrors is tilted from this condition, a parallel ladder 54 of fringes can be created. To observe the fringes by eye (without the disperser) a temporary monochromatic source such as a laser or mercury lamp can be used. In Fig. 1, a lens system 15 images any ladder of fringes effectively created at mirror planes 29 and

Fig. 4

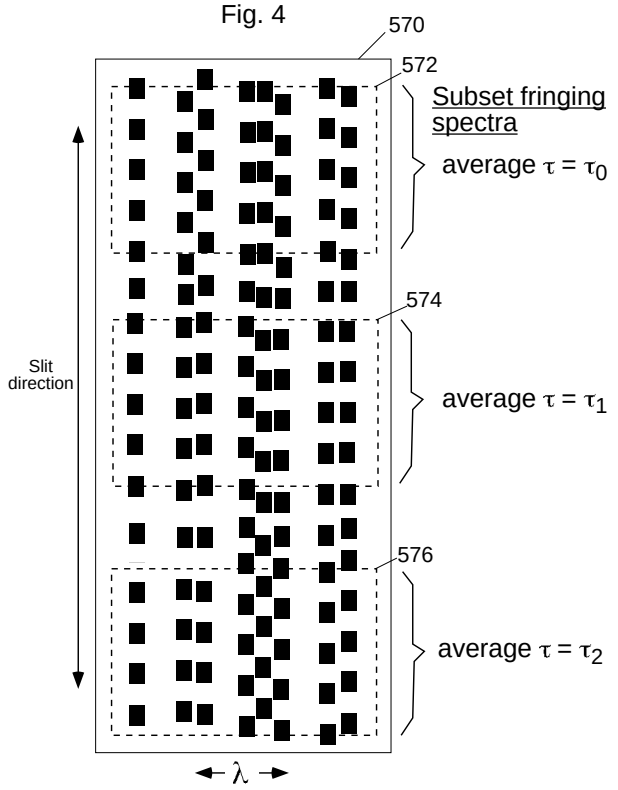

Figure 4 shows a fringing spectrum having many fringe periods along the slit because the delay varies significantly.

25 to a plane near the slit 33. Figure 2b shows the appearance to the eye of the fringe ladder 52 overlaying the slit 50. Figure 2a shows the intensity profile of the beam passing through the slit. The profile 54 has fringes and the profile 56 is for the infinite fringe period case. Figure 2c shows the action of the phase stepping is to cycle the fringe ladder along the slit. Figure 2d shows that in the case of infinitely tall fringes, the action of phase stepping is to vary the average intensity sinusoidally versus stepped phase.

9. Best Size of Spatial Fringe

The optimum number of fringes in the ladder to span the beam is that which creates the most contrast relative to noise effects. It depends on the imaging capability (and astigmatism) of the disperser along the slit direction. A poorly imaging disperser requires tall or infinitely tall fringes. One should also avoid the spatial scales where the nonfringing intensity variations along the slit or across the CCD in the slit direction are large. In my apparatus measuring starlight I found having 4 to 10 periods spanning the beam produces good contrast against noise. Since my beam occupies about 80 pixels in the slit direction on the CCD, I have about 10 to 20 pixels per slit fringe period.

10. Case of Very Many Spatial Fringes

In principle, if hundreds or thousands pixels of the CCD along the slit axis were used to record the slit intensity, then hundreds or thousands of fringes could be recorded along the slit. There is a logical distinction to be made regarding the number of fringes in the slit direction compared to the spectral resolution of the disperser. If I have M fringes along the slit, the wavelength for that channel can be determined independent from knowing the dispersion of the disperser by measuring the period of slit fringes. This can be done to a fractional precision of $1/M$. That is, if 1000 fringes exist along the slit, then just from the fringes the relative wavelength of that channel can be determined to 1 part in 1000.

If this spectral resolution is finer than the spectral resolution of the disperser (such as controlled by the slit width), and if the illumination spectrum contains fine details of interest on this scale, then it is advantageous to subdivide the fringing spectrum (570 in Fig. 4) vertically (the slit being defined vertical) into subset fringing spectra 572, 574 and 576 etc., each having a slightly different average interferometer delay τ_0, τ_1, τ_2 etc. Then this is a method of creating a set of fringing spectrum taken with a parallel set of different interferometer delays. This method is similar to the method described later where a staircase-like etalon having different thickness segments is substituted for the single thickness etalon 21 in the interferometer cavity. Here, the parallel interferometers are effectively created by the tilt of an interferometer mirror, because different portions of the CCD perpendicular to the dispersion direction are sensing significantly different interferometer delays.

The motivation of using parallel delays is that by using a wide range of delays the full information content of the illumination spectrum can be determined so that the spectrum can be mapped. A single delay having only a few fringes together with a low resolution disperser only measures a subset of the full information. This subset is sufficient to determine a Doppler dilation, but is not in general sufficient to map the spectrum at all levels of detail.

C. The Disperser

1. Combating Astigmatism

Some dispersers have intrinsic astigmatism which reduces contrast of the fringes at the CCD detector in the slit direction. This astigmatism can be compensated for by focusing the fringes to a position slightly ahead or slightly behind the slit plane.

2. Discussion

The disperser can be of any type, such as grating or prism. The necessary disperser spectral resolution is approximately the typical feature to feature separation, to reduce crosstalk which mixes fringe phases and tends to reduce average fringe visibility. For stellar spectra this is approximately 1 Å. However, having a higher spectral resolution produces a better signal to noise if it can be obtained without sacrificing throughput, particularly if it is fine enough to resolve the spectral comb due to the interferometer by itself, about 0.25 Å for a 11.5 mm delay. The optimum slit width thus also depends on the size of the source (fiber 5 diameter), since narrow sources allow narrower slit widths without reducing throughput.

3. Use of a 2nd Interferometer for Fiducials

It was mentioned that using a narrow slit to resolve the spectral comb improves the signal to noise of determining the whirl. This is because it creates a significant fringe amplitude in every wavelength channel, which helps determine overall common mode errors. However, in order to efficiently collect light the slit should be wide. This may prevent resolving the spectral comb and hence there may be channels with zero or little fringe amplitude. This problem can be alleviated by artificially creating a new set of Moire fringes that are superimposed on the existing ones.

This can be accomplished by including an additional interferometer into the beam path anywhere ahead of the detector in Fig. 1, to act as an auxiliary spectral reference. For example, it can be inserted ahead of the iodine cell 7 by using new appropriate imaging optics to reimage the beam at point 11 to create a new small spot similar to point 11. The delay of the additional interferometer can be chosen to be slightly different than the delay of the original interferometer. The sinusoidal spectrum of the new interferometer multiplies the existing spectrum of the beam and creates new Moire fringes and a new component to the net whirl. These new Moire fringes are easily distinguished from the random-like Moire fringes due to the target spectrum by their regular sinusoidal nature. Thus, the detailed value of the new delay does not have to be known. A secondary benefit is that it allows some instrumental error to be determined. Since the new Moire fringes should theoretically be perfectly regular, any deviation of the measured fringe can be assumed to be due to instrumental artifacts.

As an example, if the instrument bandwidth is 6.5% (350 Å out of 5400 Å), then 16 waves of delay change creates $16 \times 6.5\% = 1$ wave of Moire fringe across the 350 Å spectrum. Thus a delay difference between the new and original interferometers of 1600 waves will create a Moire pattern with 100 waves spanning the spectrum

IV. THEORY OF OPERATION

A. Moire or Heterodyning Effect

The invention takes advantage of the Moire effect between the sinusoidal frequency behavior of the interferometer and any similar-period sinusoidal-like components of the illumination spectrum. This occurs because the sinusoidal transmission function of the interferometer multiplies the illumination intensity spectrum creating sum and difference "frequency" components, and the sum-frequency components are eliminated by either the blurring of the disperser or equivalent blurring done numerically during data analysis. (Warning, the use of the term "frequency" in this paragraph is different than elsewhere in the document because it's a frequency of a function that is already in frequency-space.) The Moire effect heterodynes high spectral detail to low spectral detail, allowing the use of a low resolution disperser to effectively detect high resolution phenomena. The Moire fringe phase and amplitude versus wavelength channel is represented by a set of vectors called a "whirl". Another way to describe the heterodyning is to take the Fourier transform of the illumination intensity spectrum to produce an interferogram. The Moire effect translates the interferogram horizontally by a constant offset τ_k which is the fixed interferometer delay used.

If the goal is to map a spectrum, then during data analysis the heterodyning process can be reversed mathematically, beating the whirl up to higher "frequencies" to restore the original high detail information. If the goal is to measure a Doppler dilation of the spectrum for a fixed delay, or equivalently a change in delay for a fixed spectrum, then the up-heterodyning is unnecessary. The dilation or delay change is determined from the rotation of the Moire whirl.

B. Interferometer Spectral Comb

Figure 3a and 3b show the 2-dimensional spectrum of white light after passing through an interferometer of non-zero delay, frequency versus position along the slit. Pretend for the moment that the disperser has perfect spectral resolution– no blurring. A spectral fringe comb 67 exist along the dispersion direction having period $\Delta f = 1/\tau$, which for an 11.5 mm delay corresponds to a period of 0.25 Å of green light (5400 Å). In the case of Fig. 3b the interferometer mirrors are in alignment so that there is a tall fringe 66 completely covering the slit. This makes a comb 64 which has vertical fringes parallel to the slit. Figure 3a shows the case when an interferometer mirror is tilted so that several fringes 65 are created along the slit. This creates a slanted comb 63.

Figure 5a shows how overlapping the slanted fringe comb 70 with the vertical features 72 of a stellar spectrum creates Moire fringes. These appear as beads along the slit direction if one squints ones eyes at the Figure. A

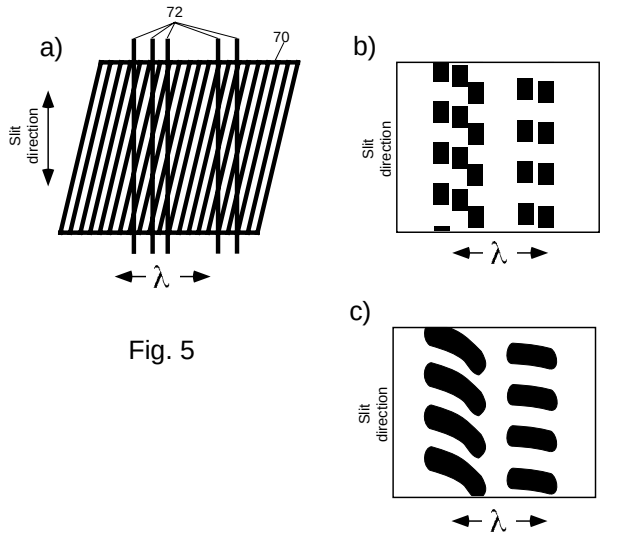

Fig. 5

Figure 5a shows through 5c show the generation of Moire fringes from a slanted fringe comb overlaying spectral lines.

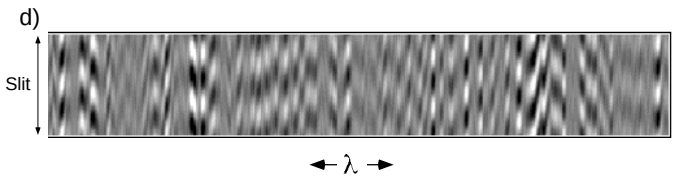

Figure 5d shows a whirl of Arturus starlight data displayed as pseudofringes.

Doppler effect will shift the features slightly in the wavelength direction. This causes the phase of all the Moire fringes to shift vertically, almost uniformly as a block. Not exactly as a block because the phase shift is proportional to frequency, so it grows linearly from the red to blue ends of the spectrum. In my apparatus for example, the spectrum spans 350 Å centered about 5400 Å, so the Doppler phase shift on one end of the spectrum is 7% different than the other end. When the Moire fringe data are expressed as a whirl, a Doppler shift causes the whirl to rotate with a little bit of twist.

Figure 5b would be the appearance when the disperser resolution is made coarser to blur away the spectral comb. Figure 5c would be under further blurring, which could be done numerically when the data is processed.

C. Benefit of Randomness of Systematic Errors

Figure 6a shows the benefit of illumination such as starlight or the back-lit iodine spectrum which have spectral features whose detailed wavelengths are randomly related, and the interferometer delay is sufficiently large to cause the phase of these fringes to be randomly and evenly distributed around a cycle. The advantage is

Fig. 6

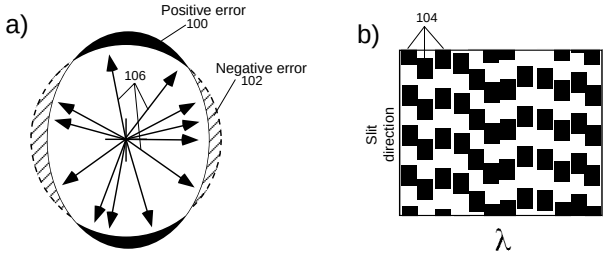

Figure 6a and 6b show the vector angles and fringing spectrum when the fringe phases are randomly distributed over a large range.

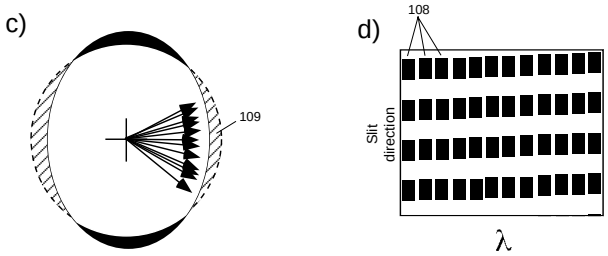

Figure 6c and 6d show the vector angles and fringing spectrum when the fringe phases are too similar.

that some systematic errors are reduced because they are evenly sampled over all phase-space. Figure 6b shows a hypothetical fringing spectrum with randomly related phases. Figure 6a shows that the phases 106 of those fringes are randomly distributed about a circle. Often in interferometry, a systematic error will exist which is dependent on phase. For example, if two signals which are supposed to be in quadrature (so that the arctangent function can be applied to measure their phase angle) are not perfectly in quadrature, then an ellipticity error will result, which has polarity which is positive 100 for some phase angles, and negative 102 for others. Having many fringes sampling all kinds of angles will reduce the net systematic error by a factor of square root of the number of independent fringes, statistically. This can be a significant reduction when many hundreds of stellar or iodine lines are used.

In contrast, Fig. 6d and 6c show fringe phases 108 which are too similar to each other, such as when a small delay is used, or if the illumination is too monochromatic, or if the continuum portion of a stellar spectrum is used instead of the narrow spectral lines (which is the case for conventional long-baseline interferometers). The similarity of the phases causes the systematic error to be sampled too coarsely, predominantly on one segment 109 of a cycle, increasing the net systematic error.

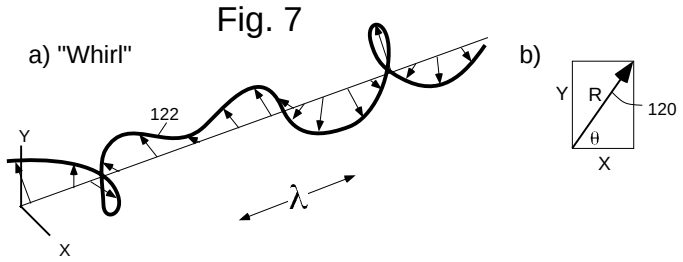

Figure 7a shows the whirl as a meandering path traced by a wavelength dependent vector. Figure 7b shows the relation between polar and rectangular coordinates.

D. Relation Between Velocity and Moire Rotation

The relation between the target velocity and whirl rotation is as follows. For a target moving with velocity v toward the apparatus, the wavelength spectrum appears contracted (more energy in the blue) by a factor $(1 + v/c)$. This is equivalent to having the delay appear larger by that same factor. This an increase in delay by $\Delta\tau = \tau(v/c)$. This is a phase shift (which is equivalent to rotation of a vector in radians) by

$$\Delta\phi = 2\pi c\Delta\tau/\lambda = 2\pi\tau v/\lambda. \tag{4}$$

The velocity per fringe proportionality is $(\lambda/\tau) = 14090$ m/s for a 11.5 mm delay and 540 nm light.

V. DATA TAKING PROCEDURE

To measure the Doppler velocity of the sun or star one must measure three kinds of sources 1) the sun/star by itself without the iodine cell, to produce a "sol" whirl; 2) the iodine by itself without the sun/star, illuminated by a featureless lamp, to produce an "io" whirl; and 3) the sun/star with the iodine cell to produce a "solio" whirl. The order of these three steps is unimportant. The terminology comes from the use of sunlight as a test source that has a similar spectrum as starlight. The sol and io whirls need only be measured once, and they are treated as reference whirls. For each solio whirl produced, a Doppler velocity can be determined, using the same sol and io reference whirls.

For each source, ideally four or five fringing spectra exposures are recorded with phase steps of approximately 90°. Also, for each source a nonfringing spectrum is recorded by blocking arm A, and another by blocking arm B.

VI. MAKING THE WHIRL FROM THE FRINGING SPECTRUM

A. Finite Fringe Period Case

For the case of finite slit fringe periodicity, the whirl is obtained from the fringing spectrum by evaluating for each wavelength channel the Fourier sine and cosine amplitudes of the intensity profile along the slit direction at the expected fringe periodicity. This is easily done by multiplying each vertical column of CCD data by a sine wave or cosine wave having the expected periodicity and then summing along the column. To compute Fourier amplitudes properly, the boundary conditions should be periodic. Hence, one should limit the number of pixels in the column to be a integer number of periods. Prior to computing the Fourier amplitude, it is beneficial to normalize the data by dividing out the average intensity profile along the slit. The resulting fluctuations around their average are multiplied by a smooth enveloping function. This envelope smoothly goes to zero at each boundary point, to minimize sharp discontinuities.

The Fourier sine and cosine amplitudes are assigned to be the rectangular coordinates X, Y of a vector (120 in Fig. 7), for each wavelength channel. In polar coordinates, the vector length (R) and angle (θ) represent the fringe amplitude and phase, respectively. The set of vectors over all channels is called the whirl. Figure 7a shows the whirl as a meandering path 122 traced out by a wavelength dependent vector, and Fig. 7b the relation between polar and rectangular coordinates. Figure 5d shows a measured whirl of Arcturus starlight over approximately 140 Å near 5400 Å. This shows only 1000 channels of the 2500 channel CCD. In this method of display, the phase and amplitude are represented by artificial fringes in a calculated intensity map.

B. Infinite Fringe Period Case

For the case of infinite period slit fringes, standard phase stepping algorithms may be used to determine fringe phase and angle for each wavelength channel, using several exposures with incremented delays distributed around the circle. For example, suppose I_1, I_2, I_3, and I_4 are the intensities for a given λ channel taken every 90° in phase, sequentially, where the intensity is summed or averaged over all the pixels of a channel. Then the tangent of the average phase angle is given by

$$\tan\phi = (I_2 - I_4)/(I_1 - I_3), \tag{5}$$

and the average amplitude R given by

$$R^2 = (I_1 - I_3)^2 + (I_2 - I_4)^2. \tag{6}$$

If five exposures are taken, then I_1 can be replaced by the average of I_1 and I_5. This has the advantage of making ϕ less sensitive to changes in the phase step amount due

Fig. 8

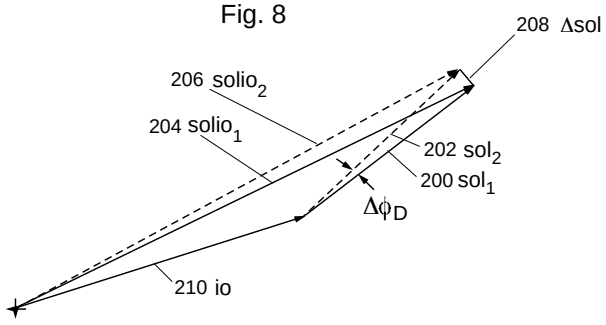

Figure 8 shows the vector relationships of the sol and is whirl components under effect of a Doppler rotation.

to twisting versus wavelength. Note, the ideal 90° step is an average value– the actual step value is proportional to the frequency (c/λ) at the channel, which changes across the spectrum.

C. Phase Stepping to Reduce Fixed-pattern Errors

Now back to the case of finite fringe period. Even though phase stepping is not required to determined fringe phase and amplitude, phase stepping is recommended as an additional step because it can be used to compute an average whirl which has reduced common-mode errors. These are errors that do not move synchronously with the phase stepping, such as effects of bumps in the slit intensity profile due to beam aberrations, and that escaped complete removal during the normalization step. Let W_1 through W_4 be the individual whirls computed as described above via Fourier amplitudes, one whirl for each phase step. First one rotates whirls W_2 through W_4 backwards by the same phase stepped angle each was exposed at, so that all the whirls have the same approximate rotation as W_1. Implementing this rotation is easiest if the whirl vectors are in polar coordinates, by offsetting the angle parameter. Then one converts each vector from polar to rectangular coordinates. Then one simply computes the average whirl by vector-adding all the whirls together while in rectangular coordinates and dividing by the number of whirls. If the exposures are taken at even positions around the circle, such as 3 exposures every 120° or 4 exposures every 90°, then the common-mode error component will be zeroed or greatly reduced by this rotate-then-sum process.

Also, as above, a fifth exposure can be taken at the 360° phase step position, and averaged together with the 0° exposure before substituting for the original 0° exposure in the whirl averaging process. This helps reduce the affect of a wavelength dependent phase step by increasing the symmetry of the problem.

D. Finding Whirl Rotation for Determining Doppler Shift

The data analysis procedure for determine the Doppler shift will be described. The first step is to prepare the whirls so that they are approximately aligned, to remove any coarse effects of various drifts. The alignment occurs in rotation, twisting, radial magnitude and horizontal (wavelength) translation. These drifts have nothing to do with Doppler shifts and therefore can legitimately be removed. Because the target is measured simultaneous with the iodine spectrum, ideally the drifts should effect both whirl components, sol and io. However, in reality because the iodine lines and stellar lines don't occur at exactly the same place, the drifts can slightly affect the Doppler result, and therefore it is best to remove the drifts when possible.

During this alignment procedure, a solio whirl, usually the first, is designated to be the "standard" to which all other whirls are aligned. Then the input whirl to be aligned is rotated, twisted, expanded in magnitude and translated horizontally to essentially minimize the root means square difference between it and the standard whirl. This is only an approximate process meant to remove gross drifts. all the solio whirls and the sol and io reference whirls are aligned this way to the standard solio.

Figure 8 illustrates that a Doppler effect rotates the sol whirl component relative to the io whirl component by an angle $\Delta\phi$. The vectors of Fig. 8 represent whirls, which are themselves aggregates of vectors. It is presumed that the solio whirl is a linear combination of sol and io whirls, added vectorally channel by channel. Suppose solio_1 and solio_2 are the solio whirls measured on two different occasions. Figure 8 supposes that these whirls have already been aligned so that their io components 210 are superimposed. Then a Doppler effect rotates the sol_2 component (202) relative to the sol_1 component 200. Therefore, the difference between solio_1 and solio_2 is a small vector Δsol (208) which is approximately perpendicular to sol_1 or sol_2. The phase angle due to the Doppler effect, $\Delta\phi$, can be found by taking the arctangent of length of Δsol relative to the length of sol_1. The length of Δsol can be found by applying dot products, since it is known that Δsol is perpendicular to sol_1.

1. Dot Product Between Two Whirls

The dot product between two whirls is defined to be the individual dot product of the two vectors for a channel, summed or averaged over all channels. Let a whirl in rectangular coordinates be the set of vectors $W = [X(\lambda), Y(\lambda)]$, where X, Y are the cosine and sine fringe amplitudes respectively. Then the dot product between two whirls W_1 and W_2 is

$$W_1 \cdot W_2 = \sum X_1(\lambda)X_2(\lambda) + Y_1(\lambda)Y_2(\lambda) \qquad (7)$$

summed over all λ channels. This could be called a "generalized" dot product because it sums products over both the spatial and wavelength indices.

2. A More Exact Dot-product Analysis

The procedure of Fig. 8 was a simple approximation that made assumptions about the constancy of the magnitude of sol and io components. A more exact analysis is now described. This solves for the rotational position of the sol whirl component relative to the io whirl by application of (generalized) dot products and solving the resulting 4 equations in 4 unknowns. The input to the process is a solio whirl and the output is an angular difference which can be converted to a velocity. It is assumed that the sol and io whirls have previously been measured and are used as reference whirls, the same each input solio.

The solio whirl is assumed to be a linear combination of 4 components: sol, sol$_\perp$, io and io$_\perp$, where sol$_\perp$ and io$_\perp$ are perpendicular whirls made by rotating sol and io by 90°. (This can be conveniently done by switching the $X(\lambda)$ and $Y(\lambda)$ components and flipping the polarity of one of them.) If low pass filtering is not performed and a significant spectral comb component due to the interferometer on the continuum is present, then two additional terms of comb and comb$_\perp$ can be added. The analysis below assumes these terms are not needed because these spectral comb components have been filtered away.

Let a solio be expressed as the linear combination:

$$\mathbf{solio} = A_s\mathbf{io} + A_t\mathbf{io}_\perp + B_s\mathbf{sol} + B_t\mathbf{sol}_\perp, \tag{8}$$

where the coefficients A_s, A_t, B_s, and B_t hold the magnitude and rotational information. For each **solio** whirl measured the following set of dot products are computed using the same **io** and **sol** whirls, measured separately:

$$T_{ik} = \mathbf{io}\cdot\mathbf{solio} \tag{9}$$
$$T_{ipk} = \mathbf{io}_\perp\cdot\mathbf{solio} \tag{10}$$
$$T_{sk} = \mathbf{sol}\cdot\mathbf{solio} \tag{11}$$
$$T_{spk} = \mathbf{sol}_\perp\cdot\mathbf{solio} \tag{12}$$

Hence a set of T_{ik} etc. coefficients are computed for each solio to be processed.

Previously, the dot products involving the reference whirls have been computed:

$$T_1 = \mathbf{io}\cdot\mathbf{sol} \tag{13}$$
$$T_2 = \mathbf{io}\cdot\mathbf{sol}_\perp \tag{14}$$
$$T_3 = \mathbf{sol}\cdot\mathbf{sol} \tag{15}$$
$$T_4 = \mathbf{io}\cdot\mathbf{io} \tag{16}$$

Now we have 4 equations in 4 unknowns (A_s, A_t, B_s, B_t) which can be exactly solved by standard linear algebra procedures, such as by "Kramers rule" which uses determinants. The 4 equations are:

$$T_{ik} = T_4A_s + 0 + T_1B_s + T_2B_t \tag{17}$$
$$T_{ipk} = 0 + T_4A_t - T_2B_s + T_1B_t \tag{18}$$
$$T_{sk} = T_1A_s - T_2A_t + T_3B_s + 0 \tag{19}$$
$$T_{spk} = T_2A_s + T_1A_t + 0 + T_3B_t \tag{20}$$

Once (A_s, A_t, B_s, B_t) have been determined for a given **solio**$_n$, then the values for the angles ϕ_{io} and ϕ_{sol} are found corresponding to that solio, which describe the rotational orientation of the component **io** and **sol** within **solio**. The values are found through

$$\phi_{io} = \arctan(A_t/A_s) \tag{21}$$
$$\phi_{sol} = \arctan(B_t/B_s) \tag{22}$$

The Doppler shift $\Delta\phi_D$ involves the rotation of **sol** *relative* to **io**. Hence,

$$\phi_D = \phi_{sol} - \phi_{io} \tag{23}$$

is the net angle between **sol** and **io**; and the change in the net angle between two occasions 1 and 2 is

$$\Delta\phi_D = \phi_{D2} - \phi_{D1} \tag{24}$$

The Doppler velocity Δv is found from the angle $\Delta\phi_D$ by

$$\Delta v = (\Delta\phi_D/2\pi)c(\lambda/c\tau), \tag{25}$$

where λ is the average wavelength.

3. High Precision Verified by Experiment

The capabilities of this apparatus have been tested by measuring Doppler velocities of a stationary source consisting of a bromine lamp back-illuminated by white light. Over 20 minutes and seventeen independent measurements the repeatability of the measurements was 0.76 m/s, of which a significant portion may have been photon noise. This corresponds to a broadband phase shift repeatability of $1/20{,}000^{th}$ of a wave, which is much better than conventional phase shift measurements using monochromatic illumination.

E. Metrology Based on Dilation of an Interferometer Cavity

Figure 9 shows an embodiment of the invention for measuring secondary effects such as temperature, air pressure and acceleration which can be made to change an interferometer delay, such as through motion of a cavity mirror or the refractive index of a medium internal to the interferometer. This operates on the principle that if the illumination spectrum is constant, then a rotation of the whirl must be due to the delay change

$$c\Delta\tau = (\Delta\phi/2\pi). \tag{26}$$

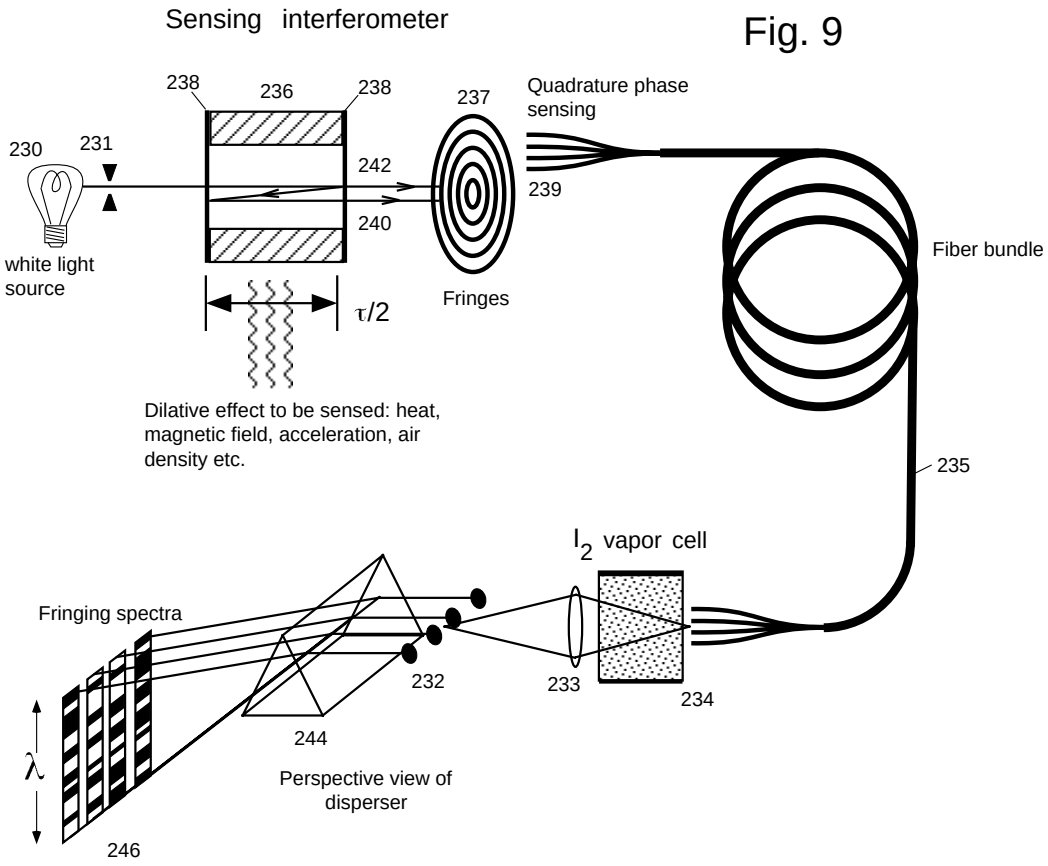

Figure 9 shows an embodiment that measures a secondary effect through changes in interferometer delay using broadband illumination.

A convenient spectrum to use is the iodine absorption spectrum illuminated by featureless light. This is provided by the iodine cell 234 back-illuminated by a white lamp 230. The iodine cell can be anywhere along the optical path. It may be convenient to have it just ahead of the disperser, rather than near the interferometer, because presumably it is desirable to make optics near the interferometer compact so that it can be used as a remote probe at the end of an optical fiber 235. Figure 9 uses a low-finesse Fabry-Perot interferometer as the interferometer to illustrate that it is possible to use non-Michelson interferometers to produce sinusoidal-like fringes provided means are employed to discriminate against the higher harmonics of the fringe shape. Such means include phase stepping at 90° steps or sampling the slit fringe at quarter wave intervals. Fabry-Perot interferometers are advantageous because they are compact. The finesse must be low, which is accomplished by using poorly reflective mirrors in the Fabry-Perot cavity, for example, a reflectivity of 27%.

In Fig. 9 the light from lamp 230 passing through a pinhole 231 creates ring-like fringes 237 due to the interference of multiple reflections 240, 242 between the two partially reflecting mirrors 238 that define the interferometer cavity. The delay is equal to the roundtrip length of a ray between the mirrors. The effect to be measured is presumed to alter the optical path length between the two mirrors. For example, temperature could dilate the length of the spacer 236 that controls the mirror spacing. A means for sampling the ring fringes every quarter wave at 239 (quadrature sensing) is provided by the 4-fiber bundle 235. A lens 233 images the four fiber outputs to separate spots 232 on the disperser slit. A detector with an imaging disperser symbolically represented by the prism 244 records a fringing spectrum for each of the four quadrature sensing spots 238.

Figure 10a through 10c show how the non-sinusoidal component of the Fabry-Perot fringes can be discriminated against using quadrature sampling along the "slit". Figure 10a shows the fringe intensity across the diameter of the ring pattern for a Fabry-Perot with mirror reflectivity approximately 27%. It has a large fundamental sinusoidal component (Fig. 10b), but with significant components at higher harmonics, such as the 2nd harmonic shown in Fig. 10c. The principle is to sample the fringe with few enough samples so that only the fundamental period is resolved, and the shorter spatial period harmonics are not resolved because they do not satisfy the Nyquist criteria. When the intensity is measured every 90°, then the fundamental is resolved, but the 2nd and

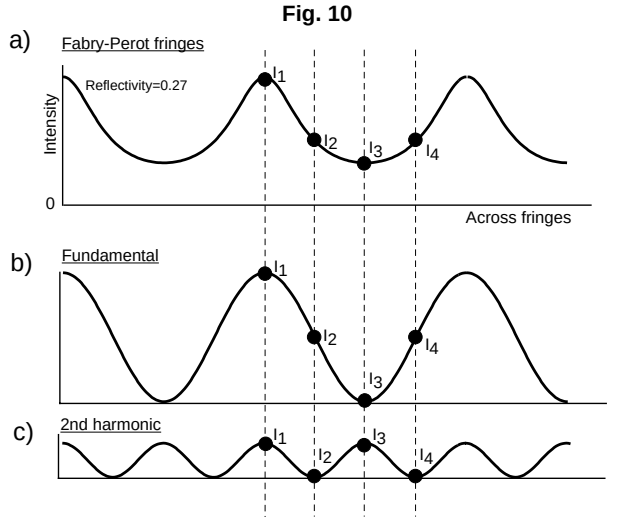

Figure 10a through 10c shows how to use the sinusoidal component of a low-finesse Fabry-Perot interferometer.

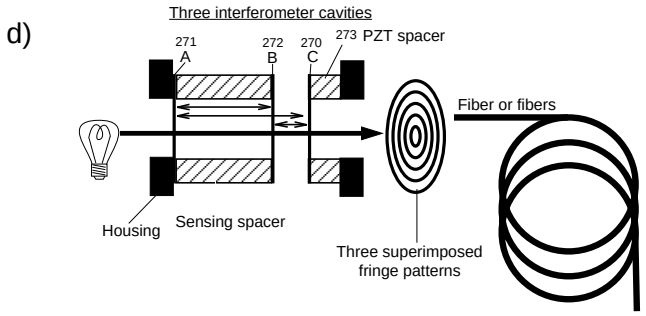

Figure 10d shows the inclusion of an additional cavity as a means for phase stepping.

higher harmonics have only 2 samples per period, and so are unresolved. For example for the second harmonic, if we apply the $R^2 = (I_1 - I_3)^2 + (I_2 - I_4)^2$ relation to find the fringe amplitude, Fig. 10c shows that the differences $(I_1 - I_3)$ and $(I_2 - I_4)$ are zero.

Another method of quadrature sampling is to phase step every quarter wave. This can be done with a single fiber instead of a 4-fiber bundle. However, because the delay is now being changed, an independent method of determining the delay accurately is needed. This can be provided by inserting an additional partially reflective surface C in series with the first interferometer, and have the secondary effect affect only one of the interferometer cavities AB. In Fig. 10d, a partially reflective surface 270 (labeled "C") is included in addition to the existing surfaces A (271) and B (272). A PZT transducer 273 moves this surface to create phase stepping. Three Fabry-Perot cavities exist instead of one: A to B, B to C, and A to C. Three sets of ring fringes will be produced. Thus the net whirl derived from this apparatus will have three component whirls corresponding to the three interferometer delays, τ_{AB}, τ_{BC} and τ_{AC}. The delays are chosen to be different enough so that the whirls are approximately orthogonal. Orthogonal means that their dot product is several times smaller than either self-dot product. This occurs when the delay is many waves different from each other so that there is at least one cycle of twist. For example, if the spectrum spans a 5% change in wavelength, then 20 waves (average wavelength) of delay difference will create 1 cycle of twist, which makes the two whirls orthogonal. Greater number of twists are preferred to improve orthogonality.

A dot-product analysis analogous to that described above for the Doppler effect can be used to determine the rotations of the three whirl components corresponding to the three delays. The twists can be anticipated by twisting the reference whirls by an appropriate amount. Then the delay change corresponding to cavity AB yields the secondary effect to be measured.

VII. MEASUREMENT OF ANGLES USING A LONG-BASELINE INTERFEROMETER

Long baseline interferometers use phase shifts to measure angular positions of a distant targets. Hence, an embodiment of this invention substituting a long baseline interferometer for the interferometer can measure angular positions very accurately, by associating whirl rotation and twist with target angle. Figure 11 shows an embodiment that incorporates a long baseline interferometer. The interferometer consists of the triangle formed by the target 300, and the left 302 and right 304 collection ports. (In order to draw the nearly parallel rays of light from the distant target, the target 300 is drawn twice.) The collection ports are spaced a distance D apart, called the baseline distance. The light entering the collection ports are conducted via paths 314 and 316 to a beamsplitter 306 where the light interferes with light from the other collection port.

Since the two streams of light originated from the same star at small angle, they are nearly identical but arrive at different times depending on the angular position θ of the target relative to the baseline. Suppose for the moment that the two optical paths 314 and 316 have the same length, so we can ignore their contribution to the arrival time difference. The arrival time difference forms the delay τ of the invention, and the inclusion of a disperser 308 creates a fringing spectrum recorded at a CCD detector 310. Tilting the beams slightly with respect to each other at the beamsplitter creates fringes across the slit of the disperser. A mirror moved by a PZT transducer that changes the path of one of the beams prior to interfering could provide the phase stepping.

1. Iodine Cell Imprints a Reference Spectrum

Narrow spectral features are desired to measure large angles. Although it is possible to use the intrinsic spec-

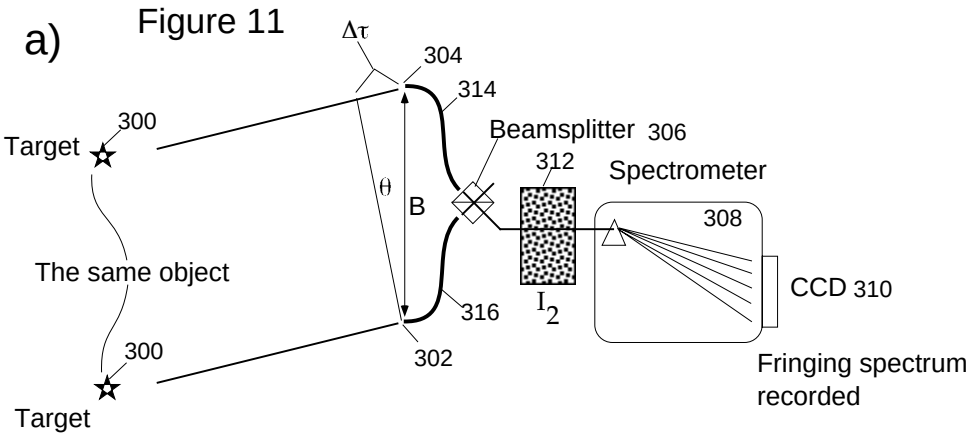

Figure 11a shows an embodiment that measures angles through phase shifts of a long baseline interferometer.

tral lines of the star (target), if the star is moving the Doppler effect may confuse the angular determination. Hence it is much better to insert an iodine vapor cell 312 into the beam to imprint a known and stable spectrum. This allows measuring angles of targets lacking spectral features, not limited to stars. Furthermore, the linewidths of iodine are about 8 times narrower than stellar lines, so that the maximum delays can be 8 times longer (about 80 mm). This allows measuring angles 8 time larger than without the iodine cell. (The stellar component of the whirl can be ignored because it is sufficiently orthogonal to the iodine whirl for large bandwidth spectra. Hence, lets omit further discussion of the stellar component.)

2. Relation Between Target Angle and Whirl Rotation

Let an earlier measurement of the target be defined as a reference whirl. Then the rotational position of the current target whirl relative to the reference can be determined by taking dot products against the reference whirl an its perpendicular whirl, analogous to the Doppler analysis described earlier. The reference whirl may have to be artificially twisted in order improve the alignment with the target whirl if the angle is large. The resulting whirl angle change $\Delta\phi$ is related to the target angle change by

$$\Delta\theta = (\lambda/D)(\Delta\phi/2\pi) \tag{27}$$

Alternatively, a reference whirl is constructed mathematically from the known iodine spectrum. This can be done by Fourier transforming the iodine spectrum to form an interferogram, translating it by a delay τ_0, mimicing the enveloping action of the disperser blur, and then inverse Fourier transforming to form the theoretical whirl. The τ_0 that produces the best agreement with the measured whirl yields the angle through

$$\theta = c\tau_0/D, \tag{28}$$

if the paths 314, 316 are of equal length. The rotational polarity of the whirl (which is controlled in an actual instrument by the polarity of mirror tilt) will determine the polarity of the angle θ.

3. Works with Non-zero Angles

Note that the technique works with arrival times that are significantly non-zero, and cannot work with exactly zero arrival times because then the spectral comb is too broad compared to the spectrum's total width (the continuum portion). This is distinct from conventional long baseline interferometers which work best for near zero arrival times.

4. Use of Reference Stars to Take Angular Difference Independent of Pathlength Drifts

The paths 314 and 316 may be different by some amount Δs, which directly adds to the apparent delay τ. In practice it may be difficult to measure or stabilize Δs to sufficient accuracy. Furthermore, when slit fringes or phase stepping is used this creates an uncertainty in the delay. Figure 11b shows that a solution is to use a second star (reference$_A$ star, 318) and have light of both stars travel through the same paths 314 and 316. This can be accomplished by using beamsplitting systems to combine light at the collection ports 302 and 304. The net whirl will then contain two component whirls, which can be distinguished during the dot product procedure when the angles are sufficiently different, so that there are at least one twist in the whirl relative to each other. In other words, so that whirls are sufficiently orthogonal that they can be distinguished from each other. This method yields a difference in angles between the target star 320 and reference$_A$ star 318. The slit fringes can be implemented by tilting the angle at which the light

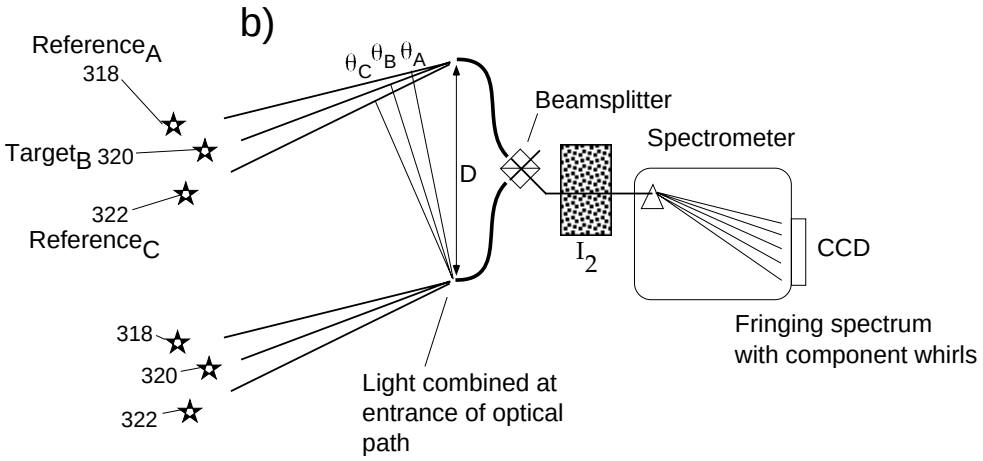

Figure 11b shows another embodiment that measures angles through phase shifts of a long baseline interferometer.

from the two paths 314 and 316 join each other at the beamsplitter.

In a similar way, the baseline distance D may be uncertain. This uncertainty can be removed from the problem by observing a third star, and having its light pass through the same paths as the other two stars, by means of beamsplitting at the collection ports 304 and 306. This can measure the angular distance of the target star 320 relative to the angular separation between the two reference stars 318 and 322.

5. Distinction from Prior Art

The technique is distinct from the spectroscopic method of Kandpal in several important ways:

1. The Kandpal technique does heterodyne or produce Moire fringes between the interferometer and any narrow spectral features of the target spectrum. The modulations created by the interference are resolved directly by the disperser.

2. An iodine cell or other imprinted reference spectrum having narrow lines is not used in the Kandpal method.

3. There is no phase stepping or slit fringes. Consequently, fringe phase and amplitude (2-d vector information) is not obtained from a given λ-channel independent of others. Only a scalar (intensity) spectrum is measured. The modulations they observed are versus wavelength channel rather than versus delay. Hence, the phase and amplitude of a fringe for a given wavelength channel in isolation from other, cannot be determined without prior knowledge of the intensity spectrum. This is especially critical when the intrinsic (nonfringing) stellar spectrum has narrow dips and peaks of similar width as the sinusoidal modulations, such as is the case when larger delays are used. Because only scalar and not vector information is measured for each wavelength channel, the polarity of the modulations cannot be determined, so whether light from a star comes from the left or right of the perpendicular to the baseline cannot be distinguished.

4. The interferometer delay for Kandpal is limited to very small values of about 10 microns, set by the reciprocal of the spectral resolution of the disperser. In contrast, in my invention the delay can be 8000 times larger (80 mm versus 10 microns) because the iodine spectrum is heterodyning against the interferometer spectral comb. This means 8000 times larger angles can be measured for the same baseline. This is a significant practical advantage because it makes it much more likely to find neighboring stars to use as positional references.

VIII. SPECTRAL MAPPING

A. Stepped Mirror and Etalon

An embodiment of the invention which is useful for mapping a spectrum is shown in Fig. 12a. The single delay is replaced by a parallel set of delays having a range of values that cover the coherence length of the illumination. An internal interferometer mirror 25 is replaced by a stepped or staircase-like mirror 362 which is segmented into steps of different thickness labeled A through E. Furthermore, in order to preserve the superimposing condition which improves fringe visibility, the etalon 21 of the instrument in Fig. 1 is optimally replaced by a staircase etalon 360 which is segmented into steps also labeled A through E that correspond to the steps of the staircase mirror. Each segment A of the mirror 362 and etalon 360 is imaged to an independent location of the disperser slit 370 by a lens system 364. Similarly, a lens system 366

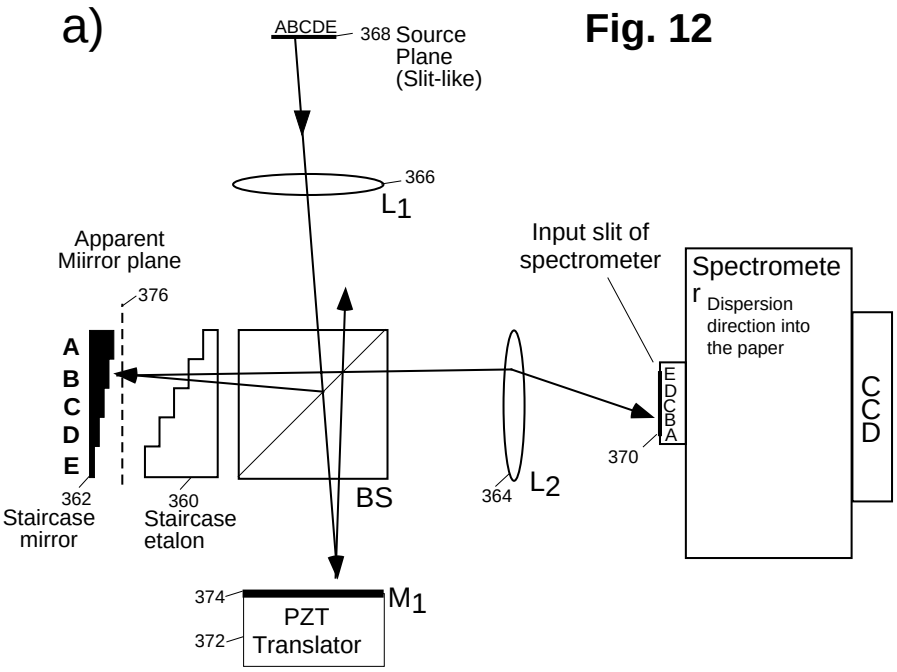

Figure 12a shows an embodiment that creates multiple simultaneous fringing spectra having different delays.

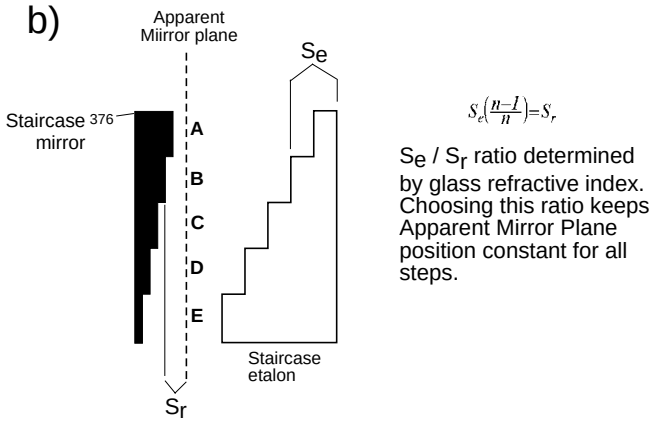

Figure 12b shows another embodiment that creates multiple simultaneous fringing spectra having different delays.

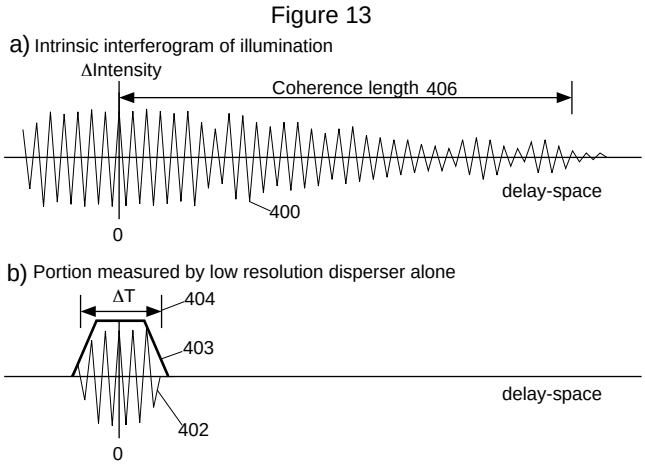

Figure 13a through 13d shows how to reconstruct an interferogram from interferogram segments made from whirls.

images a slit-like source 368 to the segments, presenting the same spectrum to all segments.

The stepped nature of the etalon and mirror are not to be confused with a grating, because the beamlets from the etalon segments do not interfere with each other, as they would in a grating. Instead, they are imaged to separate locations on the CCD to form separate fringing spectra. All these fringing spectra can be phase stepped simultaneously by the PZT 372, and have the same slit fringe periodicity by tilting mirror M_1 (374).

Figure 12b shows that the individual etalon segment thickness S_e and mirror segment location S_r are chosen so that for each segment the apparent mirror segment so-created lies in the same plane 376. This is done by setting

$$S_e(n-1)/n = S_r \tag{29}$$

(The apparent mirror is the actual mirror shifted forward by the virtual imaging of the etalon slab.) This apparent mirror 376 is optimally superimposed with the mirror M_1 (374) of the other interferometer arm by action of the beamsplitter.

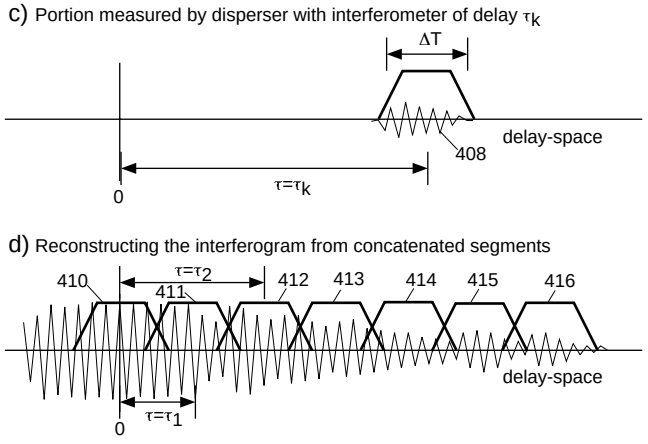

Figure 13d shows the concatenating step in reconstructing an interferogram from interferogram segments made from whirls.

B. Explanation of Behavior through the Interferogram

Figure 13a represents an interferogram 400 of the instrinsic illumination spectrum at the slit 368, with perfect spectral resolution. An interferogram is the Fourier transform of the intensity spectrum. It's shape contains all the information needed to reconstruct a spectrum. (It will be symmetrical about zero delay, so only one side needs to be shown or measured. This is consequence of the intensity spectrum being a real function.) An interferogram is useful to explain the action of the heterodyning process that creates a whirl, and the spectral resolution of a system.

Figure 13b shows that a disperser that has low spectral resolution only preserves the portion 402 of the original interferogram 400 in a small range 404 near zero, having width ΔT. The goal of a high resolution spectrometer system is to preserve all the interferogram information by having a large range, which is at least as large as the illumination coherence length 406. Figure 13c shows that due to the heterodyning process that creates Moire fringes, the Fourier transform of a whirl created with delay τ_k will be the portion 408 of interferogram 400, centered at $\tau = \tau_k$ with width ΔT. Hence, Fig. 13d shows that with a set of parallel delays of different values τ_a, τ_b, τ_c, τ_d etc., the apparatus of Fig. 12a can measure the whole range of the interferogram using a contiguous set of segments (410 through 416), the delay values chosen so that each range is shoulder to shoulder with its neighbor.

C. Data Analysis for Reconstructing the Spectrum

Hence the data analysis procedure for mapping a spectrum is as follows: For each whirl W_k measured with delay τ_k, the Fourier transform is performed to create an interferogram segment Q_k. This segment is shifted toward increasing τ by the amount τ_k to form an adjusted interferogram segment. After this is done for all the whirls, all the adjusted segments are concatenated together to form a 1-sided concatenated interferogram. The 2-sided interferogram must be symmetric about zero delay, since the intensity spectrum is known to be a real function. Therefore the next step is to copy the 1-side to the other side by reflecting about zero delay to form the full spectrum. This is then inverse Fourier transformed to form the net output whirl. The magnitude (vector length) of this whirl versus wavelength channel forms the output intensity spectrum.

The Fourier transforms of whirls should be a complex Fourier transform. Since frequency and delay τ are Fourier transform pairs, I should use here the terminology of "frequency" instead of "wavelength" to be mathematically correct. Let each frequency (wavelength) channel be designated by an index f. The vector of each f-channel needs to be expressed in rectangular coordinates, so that the whirl consists of real and imaginary functions of f having N points, where N should be even and ideally padded by zeros so that it is a power of two to speed computation. The discrete fast Fourier transform (FFT) of a complex function $W(f)$ having N points produces another complex function $Q(\tau)$ of N points. FFT algorithms are well known. For example,

$$Q(\tau) = \sum W(f) e^{i2\pi f\tau/N}, \tag{30}$$

where the sum is over $f = 0$ to $f = N - 1$.

The concatenation process needs to use appropriate enveloping to undo the non-constant enveloping effect of the disperser, so that the transition from one adjusted interferogram segment to the neighboring one, which may overlap, is smooth and does not artificially emphasize or de-emphasize portions of the true interferogram. In other words, realistic dispersers will envelope or multiply the true interferogram amplitude by a function which is bumpy and non-uniform. This is undesirable. This instrument enveloping behavior can be determined through calibration procedures where a known spectrum is measured. The instrumental enveloping behavior is divided out the of the interferogram segment Q. Then to facilitate gradual transition in the concatenation between neighboring segments, an artificially created envelope 403 having the shape of a trapezoid with sloping sides is multiplied against segment Q. That way, in the transition regions where the segments overlap and sum, the concatenated interferogram will have the proper total amplitude while gradually changing from one segment to another.

Acknowledgments

This work was performed under the auspices of the U.S. Department of Energy by the University of California, Lawrence Livermore National Laboratory under contract No. W-7405-Eng-48.

IX. CLAIMS

(Submitted, not official version)

1. An apparatus for measuring the spectral characteristics of a multifrequency source of electromagnetic radiation, comprising:

means for receiving a beam of electromagnetic radiation from said source; and

means for producing a vector spectrum from said electromagnetic radiation.

2. The apparatus of claim 1, wherein said means for producing a vector spectrum from said electromagnetic radiation comprises;

means for dispersing said electromagnetic radiation into individual channels organized by wavelength;

means for interfering said electromagnetic radiation with a delayed copy of itself to produce fringes; and

for at least one individual channel, means for determining fringe phase and amplitude of the sinusoidal component of said fringes.

3. The apparatus of claim 2, further comprising means for dithering the amount of delay between said electromagnetic radiation and said delayed copy by at least 1/2 of a wavelength to separate the sinusoidal variation due to fringes from the sinusoidal variation due to noise.

4. The apparatus of claim 1, wherein said means for producing a vector spectrum comprises:

means for interfering said electromagnetic radiation with a delayed copy of itself to produce an interfered beam, wherein said interfered beam comprises fringes;

means for dispersing said interfered beam into independent channels organized by wavelength to create a fringing spectrum; and

for at least one individual channel, means for determining the fringe phase and amplitude of the sinusoidal component of said fringing spectrum to produce a vector spectrum.

5. The apparatus of claim 1, wherein the step of producing a vector spectrum comprises:

means for dispersing said electromagnetic radiation into independent channels organized by wavelength to create a fringing spectrum;

means for interfering said electromagnetic radiation with a delayed copy of itself to produce an interfered beam, wherein said interfered beam comprises fringes; and

for at least one individual channel, determining the fringe phase and amplitude of the sinusoidal component of said fringing spectrum to produce a vector spectrum.

6. The apparatus of claim 4, wherein said fringes comprise at least one half wave of spatial delay change that is spatially splayed across said interfered beam in a direction that is perpendicular to the dispersion direction of said means for dispersing said interfered beam.

7. The apparatus of claim 6, wherein said spatial delay change across said beam measured in waves is less than the relative spectral resolution of said means for dispersing said interfered beam, which is the ratio of the wavelength divided by the blurring of the slit in the dispersion direction ($\lambda/\Delta\lambda$).

8. The apparatus of claim 4, wherein said means for dispersing said interfered beam comprises a slit, wherein said spatial delay change across said beam measured in waves is at least the relative spectral resolution of said means for dispersing said interfered beam, which is the ratio of the wavelength divided by the blurring of said slit in the dispersion direction.

9. The apparatus of claim 6, wherein said spatial delay change across said beam occurs in discrete steps.

10. The apparatus of claim 4, wherein said means for interfering said electromagnetic radiation with a delayed copy of itself to produce an interfered beam comprises an interferometer, wherein said interferometer further comprises a stepped mirror, wherein said discrete steps are accomplished by said stepped mirror which defines a path length of said beam in said interferometer, wherein said interferometer further comprises a stepped etalon, wherein a stepped etalon may be used in conjuction with said stepped mirror.

11. The apparatus of claim 6, wherein said spatial delay change for all positions across said beam can be incremented versus time to produce an incremented delay change, wherein the average delay for a given exposure of said detector can be made different than said average delay for a later exposure, wherein an incremented delay change is optimally an even fraction of a wave such as one quarter wave or one third wave, wherein this is called phase stepping, wherein the total travel of a sequence of incremented phase changes is optimally an integer number of waves.

12. The apparatus of claim 6, wherein said spatial delay change, for all positions across said beam, can be incremented versus time, wherein an average delay for a given exposure of a detector can be made different than said average delay for a later exposure, wherein said increment is optimally an even fraction of a wave such as one quarter wave or one third wave, wherein this is called phase stepping, wherein the total travel of a sequence of said increments is optimally an integer number of waves.

13. The apparatus of claim 6, wherein said spatial delay change varies spatially less than half a wave across said beam, wherein said fringe is said to be taller than the beam and spatially unresolved, wherein said phase and said amplitude of said fringe for a given wavelength channel of said independent channels is determined using two or more phase stepping exposures and an assumed sinusoidal dependence of said fringe intensity with phase stepping phase.

14. The apparatus of claim 6, wherein said spatial delay change varies spatially by at least one half a wave across said beam, wherein said phase and said amplitude of said fringe for a given wavelength channel of said independent channels can be determined from its spatial variation across said beam for a single exposure.

15. The apparatus of claim 14, wherein additional phase stepping exposures improve the determination of fringe phase and amplitude for a given wavelength channel apart from common mode errors, by assuming said fringe phase varies sinusoidally with phase stepping phase and assuming common mode errors are stationary with respect to phase stepping phase.

16. The apparatus of claim 4, wherein said means for dispersing comprises a disperser having a spectral resolution, wherein said means for interfering comprises an interferometer having a spectral comb, wherein said spectral resolution of said disperser is sufficient to resolve said spectral comb of said interferometer, wherein said interferometer has a periodicity along the dispersion axis of $\lambda^2/(\text{delay})$.

17. The apparatus of claim 4, wherein said means for dispersing comprises a disperser having a spectral resolution, wherein the spectral resolution of said disperser is insufficient to resolve the spectral comb of said interferometer, which has a periodicity along the dispersion axis of $\lambda^2/(\text{delay})$.

18. The apparatus of claim 4, further including a spectral reference which is recorded together with a target beam so that said vector spectrum contains components of both target and reference.

19. The apparatus of claim 18, wherein said spectral reference is an absorption spectrum, such as provided by an iodine vapor cell.

20. The apparatus of claim 18, wherein said spectral reference has an emission spectrum.

21. The apparatus of claim 20, wherein said emission spectrum comprises a thorium lamp.

22. The apparatus of claim 4, further comprising at least one additional interferometers in series with said beam, wherein each interferometer of said at least one additional interferometers imprints additional components in said vector spectrum.

23. The apparatus of claim 4, wherein said means for interfering comprises an interferometer, wherein said interferometer is a Michelson interferometer, wherein an input beam is split into two paths which are interfered to produce an output.

24. The apparatus of claim 23, wherein said Michelson is a superimposing interferometer, wherein rays of said two paths superimpose in said output.

25. The apparatus of claim 4, wherein said means for interfering comprises an interferometer, wherein said interferometer is a

Fabry-Perot interferometer, wherein an input beam enters into a recirculating path, which effectively interferes an infinite series of copies of said input beam having geometrically decreasing amplitudes.

26. The apparatus of claim 25, wherein Fabry-Perot comprises partially reflective mirrors having a reflectance that produces fringes that are approximately sinusoidal.

27. The apparatus of claim 26, wherein said fringes comprise a nonsinusoidal component, wherein said nonsinusoidal components of said fringes are discriminated against by sampling said fringes at four or less discrete places per period.

28. The apparatus of claim 4, wherein a dot product operation between said vector spectrum and an assumed component of said vector spectrum yields a rotational position and magnitude of an actual vector spectrum.

29. The apparatus of claim 28, wherein said dot product operation includes for each wavelength channel a dot product between spatial components of said vector spectrum and said vector component, to form a channelized dot product.

30. The apparatus of claim 29, wherein said dot product operation includes summing or averaging said channelized dot product over groups of wavelength channels to produce a generalized dot product.

31. The apparatus of claim 28, wherein said vector spectrum is expressed as a linear combination of assumed vector spectrum components, wherein rotation and magnitude of said vector spectrum components are solved for by applying dot products between linear combination and individual assumed vector spectrum components.

32. The apparatus of claim 4, wherein a Fourier transform operation applied to said vector spectrum produces an interferogram segment, wherein said interferogram segment can be shifted in delay-space by an amount equal to said interferometer delay to produce an adjusted interferogram segment, wherein said adjusted interferogram segment represents a measurement of a portion of a theoretical interferogram of the vector spectrum to invert the instrument behavior that generates Moire fringes in said vector spectrum from said input spectrum.

33. The apparatus of claim 32, wherein said adjusted interferogram segment can be concatenated with other interferogram segments which have different delay values to produce a concatenated interferogram, wherein said concatenated interferogram represents a measurement of a theoretical interferogram of said vector spectrum, wherein said concatenation process produces a more accurate representation of said theoretical interferogram.

34. The apparatus of claim 4, wherein said means for interfering comprises an interferometer, wherein said interferometer is formed by a long baseline interferometer, wherein light from a target is collected at two places separated by a baseline distance, wherein changes in angular position of said target relative to said baseline produce changes in arrival times between two said beams at a beamsplitter of said interferometer, wherein said changes in arrival time are equivalent to changes in the delay of said interferometer, wherein changes in angular position of a target can be inferred from corresponding changes in phase of said vector spectrum.

35. The apparatus of claim 34, wherein a multiplicative spectral reference is inserted into the optical path of said beam at a place where it imprints a spectrum of both said beams by the same said spectral reference, after said beamsplitter and at said separate collection places if two identical references are used.

36. The apparatus of claim 35, wherein said multiplicative spectral reference is an absorptive spectral reference, wherein said reference spectrum has many narrow spectral features having stable center wavelengths.

37. The apparatus of claim 36, wherein said absorptive spectral reference comprises an iodine vapor cell.

38. The apparatus of claim 4, wherein the illumination from additional targets collected passed through said interferometer along a common path with said beam produce a plurality of vector spectrums each containing several components corresponding to each said additional targets, wherein relative changes in phase of said components represent relative changes in angular position of targets, wherein this can be inferred independent of detailed knowledge of said optical path lengths between said collection ports which effect all said target light in common.

39. A method for measuring the spectral characteristics of a multifrequency source of electromagnetic radiation, comprising:

receiving a beam of electromagnetic radiation from said source; and

producing a vector spectrum from said electromagnetic radiation.

40. The method of claim 39, wherein said step for producing a vector spectrum from said electromagnetic radiation comprises;

dispersing said electromagnetic radiation into individual channels organized by wavelength;

interfering said electromagnetic radiation with a delayed copy of itself to produce fringes; and

for at least one individual channel, determining fringe phase and amplitude of the sinusoidal component of said fringes.

41. The method of claim 40, further comprising dithering the amount of delay between said electromagnetic radiation and said delayed copy by at least 1/2 of a wavelength to separate the sinusoidal variation due to fringes from the sinusoidal variation due to noise.

42. The method of claim 39, wherein the step for producing a vector spectrum comprises:

interfering said electromagnetic radiation with a delayed copy of itself to produce an interfered beam, wherein said interfered beam comprises fringes;

dispersing said interfered beam into independent channels organized by wavelength to create a fringing spectrum; and

for at least one individual channel, determining the fringe phase and amplitude of the sinusoidal component of said fringing spectrum to produce a vector spectrum.

43. The method of claim 39, wherein the step of producing a vector spectrum comprises:

dispersing said electromagnetic radiation into independent channels organized by wavelength to create a fringing spectrum;

interfering said electromagnetic radiation with a delayed copy of itself to produce an interfered beam, wherein said interfered beam comprises fringes; and

for at least one individual channel, determining the fringe phase and amplitude of the sinusoidal component of said fringing spectrum to produce a vector spectrum.

44. The method of claim 42, wherein said fringes comprise at least one half wave of spatial delay change that is spatially splayed across said interfered beam in a direction that is perpendicular to the dispersion direction of said means for dispersing said interfered beam.

45. The method of claim 44, wherein said spatial delay change across said beam measured in waves is less than the relative spectral resolution of said means for dispersing said interfered beam, which is the ratio of the wavelength divided by the blurring of the slit in the dispersion direction ($l/\Delta l$).

46. The method of claim 44, wherein said means for dispersing said interfered beam comprises a slit, wherein said spatial delay change across said beam measured in waves is at least the relative spectral resolution of said means for dispersing said interfered beam, which is the ratio of the wavelength divided by the blurring of said slit in the dispersion direction.

47. The method of claim 44, wherein said spatial delay change across said beam occurs in discrete steps.

48. The method of claim 47, wherein the step of interfering said electromagnetic radiation with a delayed copy of itself to produce an interfered beam comprises an interferometer, wherein said interferometer further comprises a stepped mirror, wherein said discrete steps are accomplished by said stepped mirror which defines a path length of said beam in said interferometer, wherein said interferometer further comprises a stepped etalon, wherein a stepped etalon may be used in conjuction with said stepped mirror.

49. The method of claim 44, wherein said spatial delay change for all positions across said beam can be incremented versus time to produce an incremented delay change, wherein the average delay for a given exposure of said detector can be made different than said average delay for a later exposure, wherein an incremented delay change is optimally an even fraction of a wave such as one quarter wave or one third wave, wherein this is called phase stepping, wherein the total travel of a sequence of incremented phase changes is optimally an integer number of waves.

50. The method of claim 42, wherein said spatial delay change, for all positions across said beam, can be incremented versus time, wherein an average delay for a given exposure of a detector can be made different than said average delay for a later exposure, wherein said increment is optimally an even fraction of a wave such as one quarter wave or one third wave, wherein this is called phase stepping, wherein the total travel of a sequence of said increments is optimally an integer number of waves.

51. The method of claim 42, wherein said spatial delay change varies spatially less than half a wave across said beam, wherein said fringe is said to be taller than the beam and spatially unresolved, wherein said phase and said amplitude of said fringe for a given wavelength channel of said independent channels is determined using two or more phase stepping exposures and an assumed sinusoidal dependence of said fringe intensity with phase stepping phase.

52. The method of claim 42, wherein said spatial delay change varies spatially by at least one half a wave across said beam, wherein said phase and said amplitude of said fringe for a given wavelength channel of said independent channels can be determined from its spatial variation across said beam for a single exposure.

53. The method of claim 52, wherein additional phase stepping exposures improve the determination of fringe phase and amplitude for a given wavelength channel apart from common mode errors, by assuming said fringe phase varies sinusoidally with phase stepping phase and assuming common mode errors are stationary with respect to phase stepping phase.

54. The method of claim 42, wherein the step for dispersing comprises a disperser having a spectral resolution, wherein said means for interfering comprises an interferometer having a spectral comb, wherein said spectral resolution of said disperser is sufficient to resolve said spectral comb of said interferometer, wherein said interferometer has a periodicity along the dispersion axis of λ^2/(delay).

55. The method of claim 42, wherein the step for interfering comprises an interferometer having a spectral comb, wherein said vector spectrum is numerically blurred to diminish said spectral comb and enhance Moire fringes between said spectral comb and a target spectrum.

56. The method of claim 42, wherein the spectral resolution of said disperser is insufficient to resolve the spectral comb of said interferometer, which has a periodicity along the dispersion axis of λ^2/(delay).

57. The method of claim 42, wherein the sum bandwidth of said method is wide enough to allow fringes on separate wavelength channels that differ by at least 90 degrees.

58. The method of claim 42, further including a spectral reference which is recorded together with a target beam so that said vector spectrum contains components of both target and reference.

59. The method of claim 56, wherein said spectral reference is an absorption spectrum, such as provided by an iodine vapor cell.

60. The method of claim 56, wherein said spectral reference has an emission spectrum.

61. The method of claim 58, wherein said emission spectrum comprises a thorium lamp.

62. The method of claim 42, further comprising at least one additional interferometers in series with said beam, wherein each interferometer of said at least one additional interferometers imprints additional components in said vector spectrum.

63. The method of claim 42, wherein said step for interfering comprises an interferometer, wherein said interferometer is a Michelson interferometer, wherein an input beam is split into two paths which are interfered to produce an output.

64. The method of claim 63, wherein said Michelson is a superimposing interferometer, wherein rays of said two paths superimpose in said output.

65. The method of claim 42, wherein said means for interfering comprises an interferometer, wherein said interferometer is a Fabry-Perot interferometer, wherein an input beam enters into a recirculating path, which effectively interferes an infinite series of copies of said input beam having geometrically decreasing amplitudes.

66. The method of claim 65, wherein Fabry-Perot comprises partially reflective mirrors having a reflectance that produces fringes that are approximately sinusoidal.

67. The method of claim 66, wherein said fringes comprise a nonsinusoidal component, wherein said nonsinusoidal components of said fringes are discriminated against by sampling said fringes at four or less discrete places per period.

68. The method of claim 42, wherein a dot product operation between said vector spectrum and an assumed component of said vector spectrum yields a rotational position and magnitude of an actual vector spectrum.

69. The method of claim 68, wherein said dot product operation includes for each wavelength channel a dot product between spatial components

of said vector spectrum and said vector component, to form a channelized dot product.

70. The method of claim 69, wherein said dot product operation includes summing or averaging said channelized dot product over groups of wavelength channels to produce a generalized dot product.

71. The method of claim 39, wherein said vector spectrum is expressed as a linear combination of assumed vector spectrum components, wherein rotation and magnitude of said vector spectrum components are solved for by applying dot products between linear combination and individual assumed vector spectrum components.

72. The method of claim 42, further comprising applying a Fourier transform operation to said vector spectrum to produce an interferogram segment, wherein said interferogram segment can be shifted in delay-space by an amount equal to said interferometer delay to produce an adjusted interferogram segment, wherein said adjusted interferogram segment represents a measurement of a portion of a theoretical interferogram of the vector spectrum to invert the instrument behavior that generates Moire fringes in said vector spectrum from said input spectrum.

73. The method of claim 72, wherein said adjusted interferogram segment can be concatenated with other interferogram segments which have different delay values to produce a concatenated interferogram, wherein said concatenated interferogram represents a measurement of a theoretical interferogram of said vector spectrum, wherein said concatenation process produces a more accurate representation of said theoretical interferogram.

74. The method of claim 42, wherein the step for interfering comprises an interferometer, wherein said interferometer is formed by a long baseline interferometer, wherein light from a target is collected at two places separated by a baseline distance, wherein changes in angular position of said target relative to said baseline produce changes in arrival times between two said beams at a beamsplitter of said interferometer, wherein said changes in arrival time are equivalent to changes in the delay of said interferometer, wherein changes in angular position of a target can be inferred from corresponding changes in phase of said vector spectrum.

75. The method of claim 42, wherein a multiplicative spectral reference is inserted into the optical path of said beam at a place where it imprints a spectrum of both said beams by the same said spectral reference, after said beamsplitter and at said separate collection places if two identical references are used.

76. The method of claim 75, wherein said multiplicative spectral reference is an absorptive spectral reference, wherein said reference

spectrum has many narrow spectral features having stable center wavelengths.

77. The method of claim 76, wherein said absorptive spectral reference comprises an iodine vapor cell.

78. The method of claim 42, wherein the illumination from additional targets collected passed through said interferometer along a common path with said beam produce a plurality of vector spectrums each containing several components corresponding to each said additional targets, wherein relative changes in phase of said components represent relative changes in angular position of targets, wherein this can be inferred independent of detailed knowledge of said optical path lengths between said collection ports which effect all said target light in common.

79. The apparatus of claim 4, wherein said apparatus comprises a total bandwidth that is wide enough to allow fringes on separate wavelength channels that differ by at least 90°.

80. The apparatus of claim 4, wherein said means for interfering comprises an interferometer having a spectral comb, wherein said vector spectrum is numerically blurred to diminish said spectral comb and enhance Moire fringes between said spectral comb and a target spectrum.

Part 7
Examples in the Scientific Literature

Articles in the scientific literature demonstrating or further describing the patented technologies include the following abstracts, with excerpted Figures.

I. WHITE LIGHT VELOCITY INTERFEROMETRY

Involves measuring the velocity of an external target by active illumination, where the illumination is from an inexpensive incoherent white light source rather than a coherent laser as in the prior art. The coherence properties of the illumination is altered by passing it through a preparatory interferometer. See pages 1-11, 1-15, and 1-19 of 5,642,194, and 5-30 of 6,115,121.

1. D. J. Erskine & N. C. Holmes, "White Light Velocimetry", Nature **377**, 317-320 (1995).

Abstract We demonstrate with white light from an incandescent lamp a generic method for using broadband incoherent radiation in a Doppler velocity interferometer (Fig. 1). Laser illumination is no longer required. The principle is applicable to any wave phenomenon for which interferometers can be constructed, such as light, sound, and microwaves. Two interferometers are used in series, with the reflecting target illuminated by light passing through the first interferometer. When the interferometer delays match within a coherence length of the illumination, partial fringes are produced which shift with target velocity similarly to previous monochromatic systems. Benefits include absolute velocity determination (lack of fringe skip), unambiguous multiple velocity detection, the ability to use low cost illumination sources, independence from illumination wavelength including the use of chirped lasers, and the use of pulsed lasers normally lacking sufficient coherence.

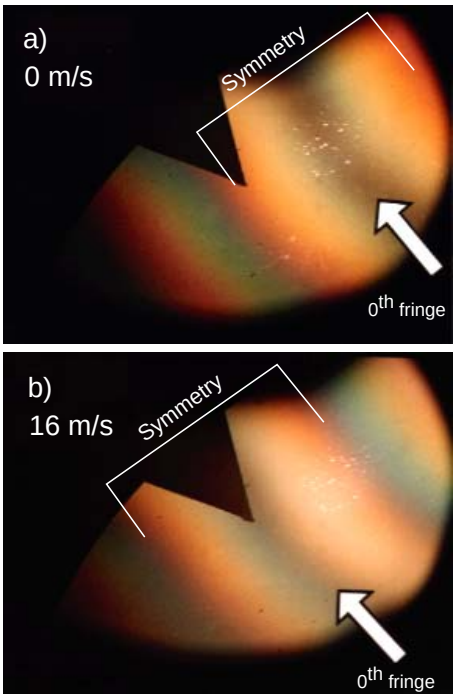

FIG. 1: Illustration from Ref. 1. Fringe shift between (a) and (b) demonstrates measurement of 16 m/s motion of a fan blade using incoherent broadband light from an incandescent lamp.

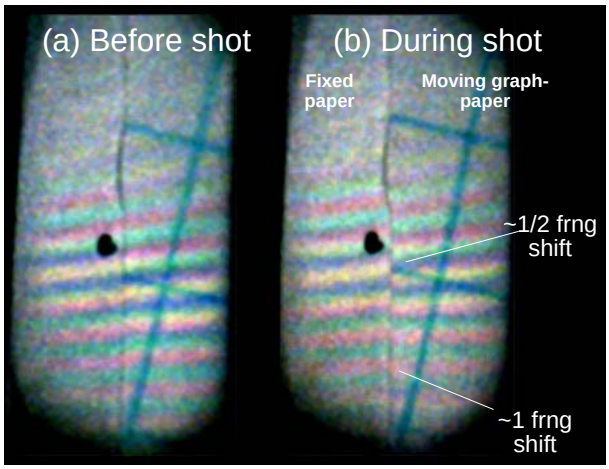

FIG. 2: Illustration from Ref. 2. Color photograph of multi-color fringes produced by the white light velocimeter prior (a) and during (b) a shot. The fringes were recorded on Kodak Royal 1000 color negative film. The illumination source was a consumer grade camera flash, of 20 μs duration. The target was a stationary piece of white paper (left side with dot) overlapping non-uniformly moving graph paper behind it (right side with blue grid lines). The fringes on the graph paper side have shifted vertically due to velocity. The shift varies with position (top to bottom) because of a velocity gradient.

2. D. J. Erskine & N. C. Holmes, "Imaging White Light VISAR", in SPIE Conf. Proc. **2869**, *High Speed Photography and Photonics*, ed. D. Paisley, 1080-1083 (1997).

Abstract An imaging white light velocimeter consisting of two image superimposing Michelson interferometers in series with the target interposed is demonstrated. Interferometrically measured 2-dimensional velocity maps can be made of moving surfaces using unlimited bandwidth incoherent and extended area sources. Short pulse and broadband chirped pulse lasers can be used to provide temporal resolution not possible with monochromatic illumination. A ∼20 m/s per fringe imaging velocimeter is demonstrated using an ordinary camera flash for illumination (Fig. 2). Radial and transverse velocity components can be measured when the illuminating and viewing beams are non-parallel.

II. DISPERSIVE INTERFEROMETRY (ASTRONOMICAL VELOCIMETRY)

Involves measuring the Doppler velocity of an external source (such as a star) through its own emitted light rather than active illumination (the source must have spectral features). An interferometer is added in series to the traditional diffraction grating. The technology improves upon the prior art by allowing much smaller instruments which are more robust to instrumental noise. See pages 6-1 through 6-15 of 6,351,307.

3. D. J. Erskine, "An Externally Dispersed Interferometer Prototype for Sensitive Radial Velocimetry: Theory and Demonstration on Sunlight", Publ. Astron. Soc. Pacific. **115**, 255-269 (2003).

Abstract A new analytical theory of operation of a wideband interferometric Doppler spectroscopy technique, called Externally Dispersed Interferometry (EDI), is presented. The first EDI prototype was tested on sunlight and detected the 12 m/s amplitude lunar signature in Earth's motion (Fig. 3). The hybrid instrument is an undispersed Michelson interferometer having fixed delay of about 1 cm, in series with an external spectrograph of about 20000 resolution. The Michelson provides the Doppler shift discrimination, while the external spectrograph boosts net white light fringe visibility by reducing crosstalk from adjacent continuum channels. A Moiré effect between the sinusoidal interferometer transmission and the input spectrum heterodynes high spectral details to broad Moiré patterns, which carry the Doppler information in its phase. These broad patterns survive the blurring of the spectrograph, which can have several times lower resolution than grating-only spectrographs typically used now for the Doppler planet search. This enables the net instrument to be dramatically smaller in size (∼ 1 m) and cost. The EDI behavior is compared and contrasted with a previous kind of hybrid, and to the conventional grating-only technique. The inclusion of a light efficient interferometer is shown to improve the net photon signal to noise ratio,

when the nonfringing and fringing velocity information are combined. The fringing Doppler information alone can be competitive with or larger than the nonfringing component, depending on the spatial size of the source relative to the slit, and on the bandwidths utilized. The EDI is theoretically shown to be dramatically less sensitive to PSF shape and centroid variations. This could allow use of wider bandwidth spectral fiducial sources and gratings optimized for highest diffraction efficiency.

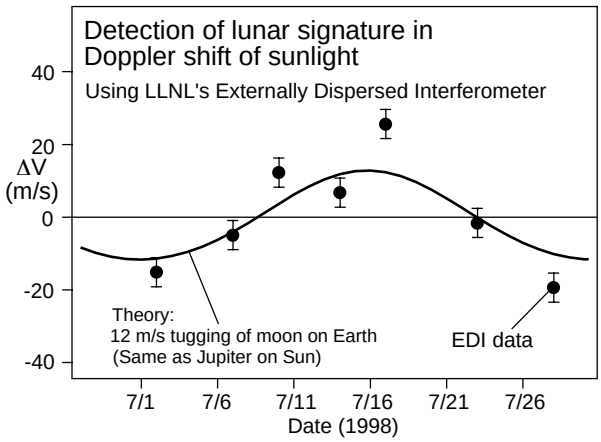

FIG. 3: Illustration from Ref. 3. The early EDI prototype detected the 12 m/s amplitude Doppler signature of the moon tugging the Earth. Sunlight fringing spectra were measured and the effects of the Earth's orbit and daily rotation subtracted, leaving the wobble caused by the moon's gravitational pull. This is the same size effect as a Jupiter-like planet pulling a star. The 8 m/s scatter is believed due to pointing error of the rooftop heliostat against the 4000 m/s velocity gradient of the solar disk. The estimated ±4 m/s long term instrument error is based on bromine-iodine tests under similar configuration.

III. DISPERSIVE INTERFEROMETRY (ANGULAR MEASUREMENT)

Involves spectrally dispersing the output of a long baseline interferometer, detecting a sinusoidal variation vs wavelength, and assigning the periodicity to the angle of the source. Improves upon the prior art by adding significant spectral dispersion, which allows use on multiple sources and hence use in a differential mode. The latter allows accurate measurements in spite of drifts in the optical path length of the baseline, a major engineering problem for the prior art. See pages 6-17 through 6-19 of 6,351,307.

4. D. J. Erskine & J. Edelstein, "Spectral Astrometry Mission for Planets Detection", in SPIE Proc. **4852**, *Interferometry in Space*, ed. M. Shao, 695-706 (2003).

Abstract The Spectral Astrometry Mission is a space-mission concept that uses simultaneous, multiple-star differential astrometry to measure exo-solar planet masses. The goal of SAM is to measure the reflex motions of hundreds of nearby (∼50 pc) F, G and K stars, relative to adjacent stars, with a resolution of 2.5 μ-arcsec. SAM is a new application of Spectral Interferometry (SI), also called Externally Dispersed Interferometry (EDI), that can simultaneously measure the angular difference between the target and multiple reference stars. SI has demonstrated the ability to measure a $\lambda/20,000$ white-light fringe shift with only $\lambda/3$ baseline control. SAM's structural stability and compensation requirements are therefore dramatically reduced compared to existing long-arm balanced-arm interferometric astrometry methods. We describe the SAM's mission concept, long-baseline SI astrometry method, and technical challenges to achieving the mission.

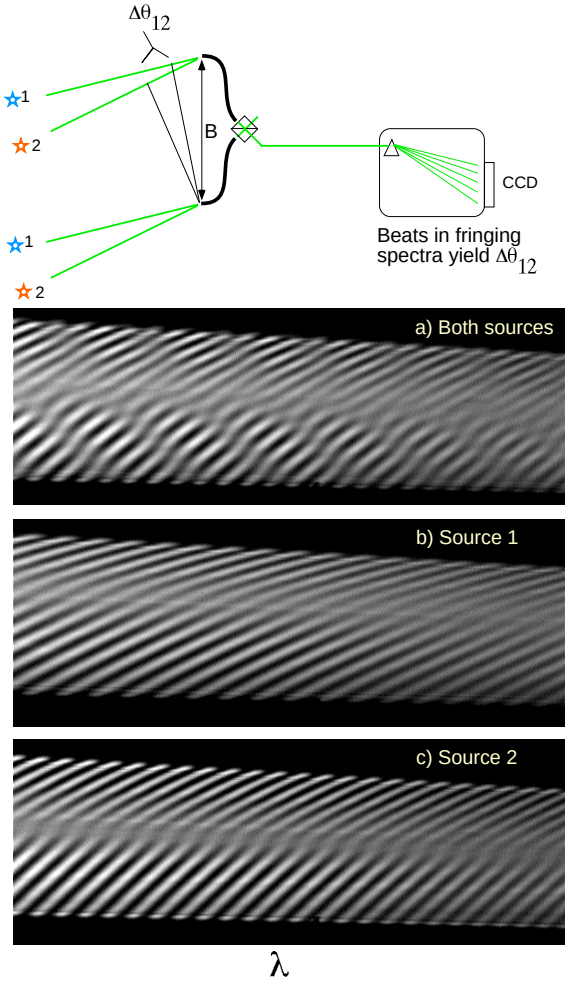

FIG. 4: Illustration from Ref. 4. Laboratory data demonstration of a multi-object long baseline spectral interferometer (SI). Two stars observed by the spectral interferometer each would produce a unique fringe pattern, which manifests beats when summed at the detector. The white light fringe patterns shown were obtained using the prototype SI modified to have a baseline B, and two white light pinhole sources simulating stars, both together (#a with beats) and separately (#b, #c). Pinholes were separated by 0.5° with B=6 mm and spectrum bandwidth was 350 Å over 5400 Å.

IV. DISPERSIVE INTERFEROMETRY (HIGH RESOLUTION SPECTROSCOPY)

Involves inserting a small interferometer in series with a conventional spectrograph, recording the moire patterns produced in the spectrum, and numerically processing these to recover high resolution spectral information otherwise not detectable by the spectrograph alone. Improves upon the prior art by dramatically reducing the spectrograph size needed to achieve a given resolution. Relative to Fourier Transform Spectrometers it improves the photon limited signal to noise ratio by 1 or 2 orders of magnitude. See pages 6-19 through 6-21 of 6,351,307.

5. D. J. Erskine, J. Edelstein, W. M. Feuerstein & B. Welsh, "High Resolution Broadband Spectroscopy using an Externally Dispersed Interferometer", ApJ **592**, L103-L106 (2003).

Abstract An externally dispersed interferometer (EDI) is a series combination of a fixed delay interferometer and an external grating spectrograph. We describe how the EDI interferometer can boost the effective resolving power of an echelle or linear grating spectrograph by a factor of 2-3 or more over the spectrograph's full-bandwidth. The interferometer produces spectral fringes over the entire spectrograph bandwidth. The fringes heterodyne with spectral features to provide a low spatial-frequency moiré pattern. The heterodyning is numerically reversed to recover highly detailed spectral information that would otherwise be unattainable by the spectrograph alone. We demonstrate resolution boosting for stellar and solar measurements of 2d echelle and linear grating spectra. Effective spectral resolution of ∼100,000 has

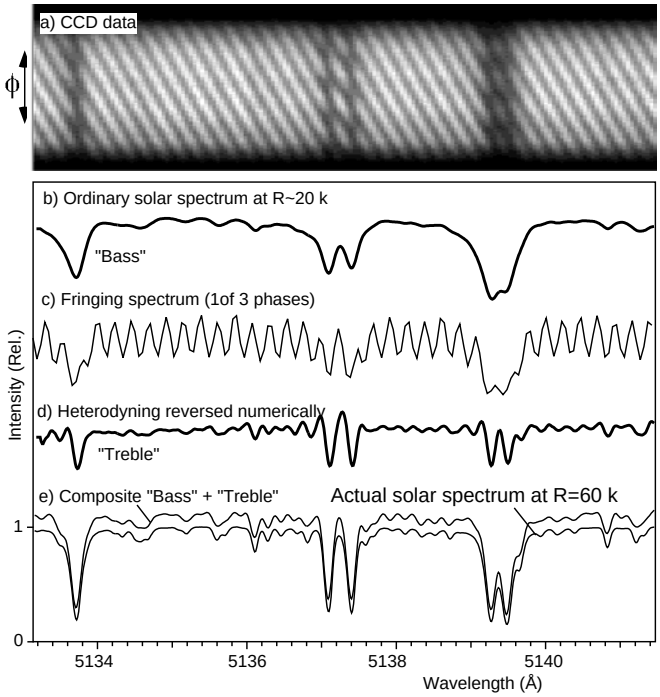

FIG. 5: Illustration from Ref. 5. Demonstration of EDI 2.5× resolution boosting for the solar spectrum using a R∼20,000 linear grating spectrograph and τ= 1.1 cm interferometer delay. (a) CCD recording of an EDI fringing spectrum where ϕ varies transversely to dispersion (multi-phase recording). (b) The ordinary spectrum $B_{ord}(\lambda)$ derived from a histogram of (a). (c) A fringing spectrum phase exposure B_{ϕ},from a lineout of (a) is used to obtain (d), the fringing spectrum $B_{edi}(\lambda)$. (e) The EDI composite spectrum(upper curve), after equalization using iodine calibration spectra, is nearly identical to a reference Kitt Peak FTS solar spectrum (lower curve) artificially blurred to R=60,000. Data was taken June 16, 1998 at Lawrence Livermore Nat. Lab. Intensities are relative and have been offset.

been obtained from the ∼50,000 resolution Lick Observatory 2d echelle spectrograph, and of ∼50,000 from a ∼20,000 linear grating spectrograph (Fig. 5).